BioMed Research International

Circadian System Development and Plasticity

Guest Editors: Martin Fredensborg Rath, Yoav Gothilf, Mario Guido, and Estela Muñoz

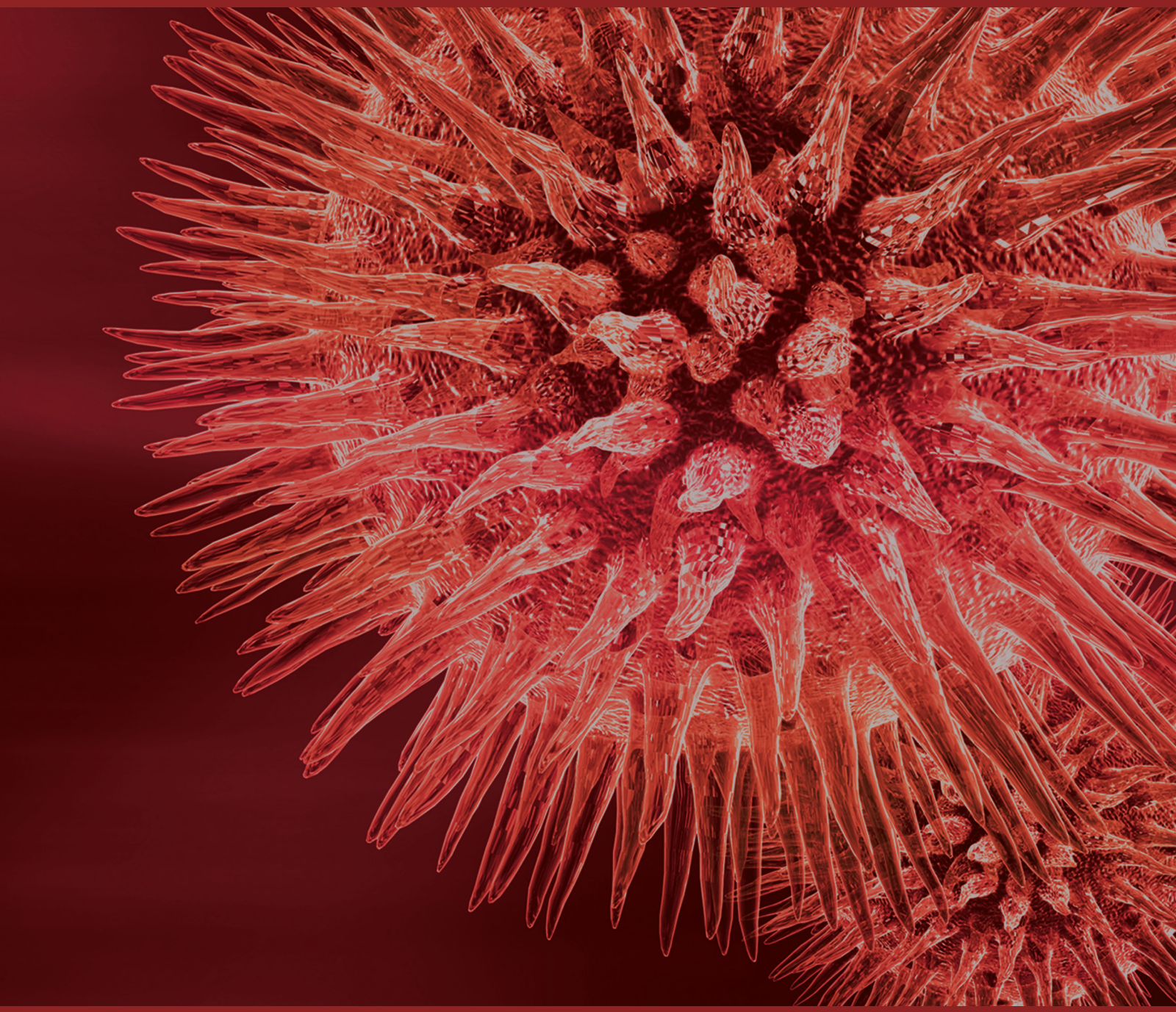

Circadian System Development and Plasticity

BioMed Research International

Circadian System Development and Plasticity

Guest Editors: Martin Fredensborg Rath, Yoav Gothilf, Mario Guido, and Estela Muñoz

Contents

Hindawi Publishing Corporation
BioMed Research International
Volume 2014, Article ID 436760, 2 pages
http://dx.doi.org/10.1155/2014/436760

Editorial

Circadian System Development and Plasticity

Martin Fredensborg Rath,[1] Yoav Gothilf,[2] Mario Guido,[3] and Estela Muñoz[4]

[1] *Department of Neuroscience and Pharmacology, Faculty of Health and Medical Sciences, University of Copenhagen, Rigshospitalet 6102, Blegdamsvej 9, 2100 Copenhagen, Denmark*
[2] *Department of Neurobiology, The George S. Wise Faculty of Life Sciences and Sagol School of Neuroscience, Tel-Aviv University, Sherman Building, Room 405, 69978 Tel Aviv, Israel*
[3] *CIQUIBIC (CONICET), Departamento de Química Biológica, Facultad de Ciencias Químicas, Universidad Nacional de Córdoba, Haya de la Torre s/n, Ciudad Universitaria, 5000 Córdoba, Argentina*
[4] *Laboratorio de Cronobiología, IHEM-CONICET, ANPCyT, Facultad de Ciencias Médicas, UNCuyo, CC 56, Parque Gral. San Martín, 5500 Mendoza, Argentina*

Correspondence should be addressed to Estela Muñoz; munoz.estela@fcm.uncu.edu.ar

Received 22 May 2014; Accepted 22 May 2014; Published 16 June 2014

Circadian clocks drive 24 h oscillations in physiology and behavior from algae to humans, using light/dark cycles as the main synchronizing input. The questions of where, when, and how these rhythms take place have inspired amazing advances in the field of circadian biology, resulting in the discovery of the major players that compose, regulate, and fine-tune a precise molecular clock mechanism. Nevertheless, how the whole circadian system is developed and what allows this system to be plastic and adaptive, along with precision, are questions that are still unclear. It is therefore of special interest to continue the efforts to understand the cellular, molecular, and genetic mechanisms behind the ontogeny and plasticity of circadian clocks. This special issue includes ten original articles and reviews. These contributions address different developmental and dynamic aspects of the circadian timing system from molecular and cellular mechanisms to synchronization of physiology and behavior, in diverse models such as zebrafish, *Xenopus laevis*, chicken, rodents, and primates, including humans. This diversity of species clearly reflects the evolutionary conservation of basic circadian mechanisms.

Starting with zebrafish, Z. Ben-Moshe et al. reviewed the group contributions and general knowledge about the maturation of the circadian clock in the fish pineal gland, finishing the manuscript with an open-ended question related to the influence of this and other peripheral oscillators in the physiology and behavior of the intact animal. They propose that the light-induced onset of the zebrafish pineal gland circadian clock is dependent upon entrainment of asynchronous cellular oscillators by light. Investigation and analysis of the light-regulated transcriptome and miRNome, among other approaches, suggest a complex mechanism with some similarities with those present in peripheral clocks.

The advantages of the zebrafish as a model species in the field of chronobiology are further emphasized by the study of K. Lahiri et al. These authors developed a reporter transgenic line which expresses luciferase under the control of the *Per1b* promoter. This reporter line and other molecular markers were then used to demonstrate that the zebrafish clock can be entrained by temperature cycles, as well as by light/dark cycles. They further show shifts in the developmental maturation of the response to temperature, which is an important step towards understanding the mechanism of temperature entrainment, and possibly temperature compensation. Future work is necessary to confront the mechanisms of entrainment induced by both *zeitgebers*, temperature and light.

M. N. de C. M. Moraes et al. investigated the effect of α-MSH and the nocturnal signal melatonin, on the expression of the clock gene *Per1* and nonvisual photopigments (melanopsins: *Opn4x* and *Opn4m*) in photosensitive

melanophores of *Xenopus laevis*. It is known that light and α-MSH exert a dispersing effect on pigment granule distribution while melatonin facilitates their aggregation. Remarkably, *Per1* showed temporal oscillations regardless of the presence of either α-MSH or melatonin. On the contrary, the expression of *Opn4x* and *Opn4m* was differentially affected by these hormones: α-MSH increased melanopsin expression while melatonin effects depended on the time when it was applied, dramatically abolishing their temporal oscillations and decreasing their expression levels during the light phase.

Using the chicken as a model, N. M. Díaz et al. provide evidence that during early development, retinal melanopsinergic horizontal cells and ganglion cells express a number of core clock genes as well as the melatonin rhythm-generating enzyme AANAT. Their findings indicate that these circadian molecular features comprise a characteristic of melanopsinergic neurons of the developing inner retina which facilitates the development of the retinal circadian timing system.

D. S. Pereira et al. used the *Per3* knockout mouse to analyze the role of the clock gene *Per3* in the circadian rhythm of behavioral responsiveness. Their data show that upon transition to long days synchronization to the new light regime is delayed in the knockout mice, thus suggesting that *Per3* is required for efficient circadian synchronization to the changing environment.

K. Rohde et al. present their current understanding of the role of homeobox genes, not only as phenotype determinants in the rodent pineal gland but also as regulators of adult pineal gland function, specifically of the melatonin rhythm generation. They introduced a new working model with the transcriptional factor CRX facilitating tissue specificity and daily changes in *Aanat* expression, the gene that encodes the rate-limiting enzyme of melatonin synthesis.

In the rat SCN, J. Alamilla et al. used perforated or whole cell patch clamp techniques to investigate the temporal (day versus night) and regional (dorsal versus ventral) GABAergic neurotransmission. Their results suggest an excitatory role for GABA in the SCN and further demonstrate both daily and topographic modulations of GABAergic postsynaptic currents in the central clock.

Liver is one clear example of a peripheral oscillator in which other synchronizing signals besides the light/dark cycle, such as food availability or daytime restricted feeding (DRF), are able to adjust daily rhythms. D. D. Ita-Pérez et al. show that DRF influences the daily variations of hepatic mRNA levels, stability, and enzymatic activity of GABA transaminase (GABA-T), thus suggesting that the liver GABAergic system responds to the metabolic challenges imposed by DRF and denoting the presence of a food-entrained oscillator.

In a study on primates, R. C. G. J. Engelberth et al. evaluated the influence of senescence on the relative neuronal and glial SCN populations in female marmosets. Neuronal loss and astrocyte increase are reported in the aged marmosets. The authors speculate that these changes might be related with rhythmic pattern variations in the aging central clock.

Finally, in a study on human material, M. Møller et al. show the presence of classical neuropeptidergic NPY-immunoreactive nerve fibers in fetal (around 4th month of gestation) and adult pineal gland, which are likely to modulate pineal function. According to the location in both the pineal stalk and pineal follicles, this NPYergic innervation might represent an independent nonsympathetic central regulatory pathway. The authors discuss and present possible origins for these fibers and the significance of their studies. Further investigations are required to understand NPY roles in pineal gland ontogeny and function.

Authors' Contribution

The four Guest Editors contributed equally to this special issue.

Martin Fredensborg Rath
Yoav Gothilf
Mario Guido
Estela Muñoz

Hindawi Publishing Corporation
BioMed Research International
Volume 2014, Article ID 243825, 10 pages
http://dx.doi.org/10.1155/2014/243825

Research Article

Morphological Changes in the Suprachiasmatic Nucleus of Aging Female Marmosets (*Callithrix jacchus*)

Rovena Clara G. J. Engelberth,[1] Kayo Diogenes de A. Silva,[1] Carolina V. de M. Azevedo,[2] Elaine Cristina Gavioli,[3] Jose Ronaldo dos Santos,[4] Joacil Germano Soares,[5] Expedito S. Nascimento Junior,[5] Judney C. Cavalcante,[5] Miriam Stela M. O. Costa,[5] and Jeferson S. Cavalcante[1]

[1] *Laboratory of Neurochemical Studies, Physiology Department, Biosciences Center, Federal University of Rio Grande do Norte, Natal, RN, Brazil*
[2] *Laboratory of Chronobiology, Physiology Department, Biosciences Center, Federal University of Rio Grande do Norte, Natal, RN, Brazil*
[3] *Behavioral Pharmacology Laboratory, Department of Biophysics and Pharmacology, Federal University of Rio Grande do Norte, Natal, RN, Brazil*
[4] *Biology Department, Federal University of Sergipe, Aracaju, SE, Brazil*
[5] *Laboratory of Neuroanatomy, Morphology Department, Biosciences Center, Federal University of Rio Grande do Norte, Natal, RN, Brazil*

Correspondence should be addressed to Jeferson S. Cavalcante; jefsc@uol.com.br

Received 26 December 2013; Revised 4 April 2014; Accepted 18 April 2014; Published 2 June 2014

Academic Editor: Estela Muñoz

The suprachiasmatic nuclei (SCN) are pointed to as the mammals central circadian pacemaker. Aged animals show internal time disruption possibly caused by morphological and neurochemical changes in SCN components. Some studies reported changes of neuronal cells and neuroglia in the SCN of rats and nonhuman primates during aging. The effects of senescence on morphological aspects in SCN are important for understanding some alterations in biological rhythms expression. Therefore, our aim was to perform a comparative study of the morphological aspects of SCN in adult and aged female marmoset. Morphometric analysis of SCN was performed using Nissl staining, NeuN-IR, GFAP-IR, and CB-IR. A significant decrease in the SCN cells staining with Nissl, NeuN, and CB were observed in aged female marmosets compared to adults, while a significant increase in glial cells was found in aged marmosets, thus suggesting compensatory process due to neuronal loss evoked by aging.

1. Introduction

The suprachiasmatic nuclei (SCN) are a pair of neurons located in the anterior hypothalamus above the optic chiasma, [1, 2] and it is constituted of about 8,000 to 10,000 neurons [3–5]. Since the 1970's, the SCN has been considered the central pacemaker [6, 7] that controls physiological and behavioral rhythmic oscillations in mammals [8]. Approximately 10% of SCN neurons express VIP in the core subdivision, while around 20% (which means about 2,100 neurons) of SCN in the shell part express VP [9]. Other neurotransmitters, besides VIP and VP, have been described in terminals and perikarya in the SCN, such as neuropeptide Y [10–12], 5-HT [13] and calbindin (CB) [10].

In humans, many factors attempt to explain the aging process; among them, mitochondrial dysfunction [14] and oxidative stress [15] appear to be strong candidates able to promote alterations in aged organisms. Aging process alters structural complexity of the central nervous system, resulting in neurotransmitters alterations [16], atrophy of total gray matter [17], and soma size and dendrites [18].

During aging, changes in morphological, neurochemical, and circadian rhythms can be observed [19]. The effects of aging on circadian rhythm range from simple alterations in physiological functions to impairment of cognitive performance [20]. However, neonatal SCN tissue transplantation in old hamsters increased life span and restored normal rhythms in many physiological mechanisms [21]. Thus, it supports that longevity appears to be correlated with regulated circadian rhythm activity.

In mammals, changes in basic parameters of circadian rhythms have been showed, such as alterations in length period, besides reduction of amplitude and phase duration [22, 23]. These alterations in circadian rhythms can be caused by changes in neurochemical and morphological aspects during aging. Some studies have reported contradictory results with regard to the decrease in neuronal cells in the SCN in rodents and primates [24–26]. In female aged rodents, there were no reported alterations in the SCN neuron numbers, whereas Roberts et al. [25] showed reductions in SCN neurons in aged female Rhesus monkey. Besides, *post mortem* studies in human beings showed that neurodegenerative processes occur in the SCN during senescence, suggesting progressive deterioration of the circadian pacemaker [27, 28].

Considering that neuronal nuclear protein (NeuN) has been widely used as a neuronal marker, while, in marmosets, CB is used as an important cell marker of the SCN [10, 29], in the present study we aimed to assess in the *Callithrix jacchus* a new world primate, the number of neurons in the SCN in aged female. To this aim, a morphometric analysis using Nissl staining and the immunoreactivity of SCN cells to NeuN, CB, and glial fibrillary acidic protein (GFAP—the main intermediate filament protein in mature astrocytes [30]) were performed in adult and aged female animals.

2. Material and Methods

2.1. Experimental Animals. Four young adult female marmosets and four aged female marmosets (see Table 1 for animals details) from the Primatology Center of the Federal University Rio Grande do Norte, Natal, Brazil, were used in this study. The use of the animals was approved by the Brazilian Environmental Protection Agency (IBAMA Register number 1/24/92/0039-00). The animals were kept in cages measuring 2,00 × 1,00 × 2,00 m and housed under natural conditions of temperature and humidity in a light-dark cycle, with food and water being freely available. The experimental procedures were in accordance with the Brazilian law number 11.794/2008 for animal experimental use. All experiments were approved by the local ethic committee for animal use (CEUA-UFRN number 026/2010).

2.2. Anaesthesia and Perfusion. The procedure perfusions in all animals were performed between 9–11 am. The animals were given tramadol hydrochloride and xylazine as preanaesthetic medication, both at the dose of 5 mg/kg intramuscularly and maintained on inhalation anaesthesia with isoflurane and 100% oxygen administered by a mask.

Table 1: Summary of subjects used in the present study.

Animal	Age (years)	Weight (g)
Marmoset 2	6.3	321
Marmoset cnq6	4.0	302
Marmoset s.15	4.9	299
Marmoset s.19	3.6	260
Aged marmoset 3	11.8	357
Aged marmoset 4	12.11	322
Aged marmoset 5	9.11	367
Aged marmoset 6	11.6	355

After the administration of the anaesthetic drugs, animals were perfused transcardially with 400 mL phosphate-buffered saline (PBS), pH 7.4, containing 500 IU heparin (Liquemin, Roche, São Paulo, Brazil), followed by 700 mL 4% paraformaldehyde in 0.1 M phosphate buffer, pH 7.4. Brains were removed from the skull, postfixed in the same fixative solution for 2–4 h, and transferred to a solution containing 30% sucrose in 0.1 M PBS, pH 7.4. Each brain was serially cut in the coronal plane into 30 mm thick sections with a freezing sliding microtome. The sections were placed sequentially in six compartments (one section per compartment), with the distance between one section and the next in the same compartment being approximately 180 μm. All sections in the six compartments were stored in antifreezing solution. Each compartment was then individually processed to reveal one of the following substances: NeuN, CB, and GFAP. In all cases, one of the compartments was processed by the Nissl technique with thionin dye (for technique details see [31]).

2.3. Tissue Processing and Data Acquisition. For immunostaining, free-floating sections of the one compartment were washed in phosphate buffer and incubated with the primary antibodies to NeuN (mouse anti-NeuN, Chemicon Internat. Inc., Temecula, CA, USA, Lot number LV1457494, dilution 1 : 1000), CB (mouse anti-CB, Sigma-Aldrich, Saint Louis, MO, USA, Lot number 031M4859, dilution 1 : 1000), and GFAP (mouse anti-GFAP, Sigma-Aldrich, Sain Louis, MO, USA, lot number 037K4759, dilution 1 : 1000) for 18–24 h at room temperature, containing 2% normal donkey serum in 0.3% Triton X-100 and 0.1 M phosphate buffer, pH 7.4. Next, the sections were incubated with the biotinylated secondary antibody (rabbit anti-mouse IgG; Sigma-Aldrich, Saint Louis, MO, USA, Lot number 072K4876, dilution 1 : 1000), for 90 min, followed by incubation with the avidin-biotin peroxidase solution (ABC Elite kit, Vector Labs, Burlingame, CA, USA) for 90 min. The reaction was developed by the addition of diaminobenzidine tetrahydrochloride (Sigma, St. Louis, MO, USA) and 0.01% H_2O_2 in 0.1 M phosphate buffer, pH 7.4. The sections were washed (5x, 5 min) with 0.1 M phosphate buffer, pH 7.4, between each step and at the end of the procedure. The sections were then dried, dehydrated in a graded alcohol series, cleared in xylene, and coverslipped with neutral mounting medium (DPX; Sigma). Sections in which the primary antibodies were omitted and replaced with normal serum from the same species served as controls.

Under these conditions, staining was completely abolished. All the immunostainings, for specific substance, were performed concomitantly, minimizing possible differences in background between the animals.

The sections were examined under bright field illumination on a light microscope (Olympus BX-41) and images were captured using a CCD camera (Nikon DXM-1200).

2.4. Morphometric Analysis. In order to estimate the number of SCN cells, six images (objective 40x) of each animal, aged and adult, were selected: one at the rostral level, three at medium level, and two at caudal level, representative of the rostrocaudal extension of area of interest. For all solutions used as cell markers, we use only the right side of each hemisphere to the cell count. A rectangle measuring 125 um × 100 um, corresponding to 52% of the total area of the SCN, was extracted of every image and the number of cells found in this area was counted. All images (adults and aged) were randomly renamed so that the counter did not know which animal belonged to the image, featuring a blind count. Thus, it minimized the suggestive effects of knowing the sample. Some histological characteristics presented by neurons in the thionine dye were used as selection criteria in the cell counting, for example, rounded shape, strong staining, and evident nucleolus.

Additionally, GFAP levels in the SCN were assessed by analyzing relative optical densitometry (ROD) of images using the software Image J (Version 1.46i, NIH). Six representative sections of the rostrocaudal extension of SCN were chosen. In each section, fields bypassing throughout the SCN were analyzed. The medium pixels in the target area were subtracted from de medium values of a control region (areas that should not have specific GFAP staining) of the same tissue (optic chiasma). Finally, all values were normalized considering the control group, in order to evaluate proportional alterations.

2.5. Data Analysis. To confirm whether there are differences between the animal groups, the nonparametric Mann-Whitney test was applied. Correlations between age of animals and morphometric values were performed using the Spearman test (r). The level of significance was set at $P < 0.05$.

3. Results

In SCN sections Nissl-stained (Figures 1(a) and 1(a′)), or marked to NeuN-IR (Figures 1(b) and 1(b′)) and CB-IR (Figures 1(c) and 1(c′)), a decrease in the number of cells was observed in aged marmosets when compared with adult animals. In aged animals, sections stained with Nissl (Figure 1(a′)) and NeuN (Figure 1(b′)) revealed many whitish areas throughout the SCN. However, these whitish areas were not observed in adult animals, which suggest the occurrence of neurodegeneration (Figures 1(a) and 1(b)). For immunostaining to CB, it is also possible to qualitatively observe a decrease in the number of cells available in the SCN of aged marmosets (Figure 1(c′)) compared to adult animals (Figure 1(c)).

These qualitative decreases in the number of cells in SCN sections observed in photomicrographs (Figure 1(c′) versus Figure 1(c)) were quantitatively documented. Mann-Whitney test revealed a significant decrease in the number of cells in the SCN stained by Nissl technique in aged compared to adult marmosets (adult marmoset: 110.0 (133.37–87.81); aged marmoset: 51.8 (55.62–49.64); data are represented as median (interquartile range q3–q1); $P = 0.0209$; Figure 2(a)) and NeuN (adult marmoset: 92.8 (108.06–75.12); aged marmoset: 37.4 (42.68–32.5); data are represented as median (interquartile ranges q3–q1); $P = 0.0294$; Figure 2(b)).

Mann-Whitney test showed a significant decrease in the number of neurons CB-stained in the SCN of aged female marmoset compared to adult female marmosets (adult marmoset: 84.3 (85.31–74.62); aged marmoset: 36.4 (43.68–30.25); data are represented as median (interquartile ranges q3–q1); $P = 0.0143$; Figure 2(c)). Using Spearman test, a significant negative correlation between age and counting of Nissl-stained and CB-IR in SCN neuronal cells was found, respectively ($r = -0.881$, $P = 0.007$, Figure 3(a); $r = -0.866$, $P = 0.004$, Figure 3(c)). Additionally, a marginal negative correlation between age and counting of NeuN-IR SCN cells was observed ($r = -0.706$, $P = 0.057$, Figure 3(b)).

Considering GFAP immunoreactivity in the SCN, Mann-Whitney test revealed a significant increase in GFAP expression in aged marmosets compared with adult animals (adult marmoset: 2745.8 (4737.7–1339.1); aged marmoset: 12880.1 (14877.3–11807.3; $P = 0.0209$; Figure 4(b)). A significant positive correlation between age and GFAP immunoreactivity expression was found ($r = 0.857$; $P = 0.010$; Figure 4(c)).

4. Discussion

NeuN immunoreactivity has become an excellent marker for neuronal phenotypes that along with the traditional Nissl technique provides a new framework to structural and morphological studies [32], including the SCN [33]. The expression of NeuN has been shown in studies which verify neuronal death associated to age [34], since it has been proposed that immunoreactivity to NeuN depends on the phosphorylation state of protein [35], and aging could alter levels of cellular protein phosphorylation, resulting in neuronal loss [36].

Some papers reported that senescence influences the brain volume, showing that some regions are more susceptible to age-related plasticity than others [37, 38]. Regarding SCN, stereological studies have shown a decrease in the number of neurons in the SCN in humans with neurodegenerative diseases, such as Alzheimer's, and in aged people [39, 40]. A study in aged rodents of both gender without any neurodegenerative disease showed a decrease in the number of SCN cells, with a significant reduction of total neuronal volume [26]. A recent study with nonhuman primates (rhesus monkey) showed neurodegeneration in adult males and aged females [25]. Aged marmosets that served as the sample for cell counting in our results were all females with advanced ages (10–13 years) within the period of reproductive senescence [41, 42]. These aged marmosets

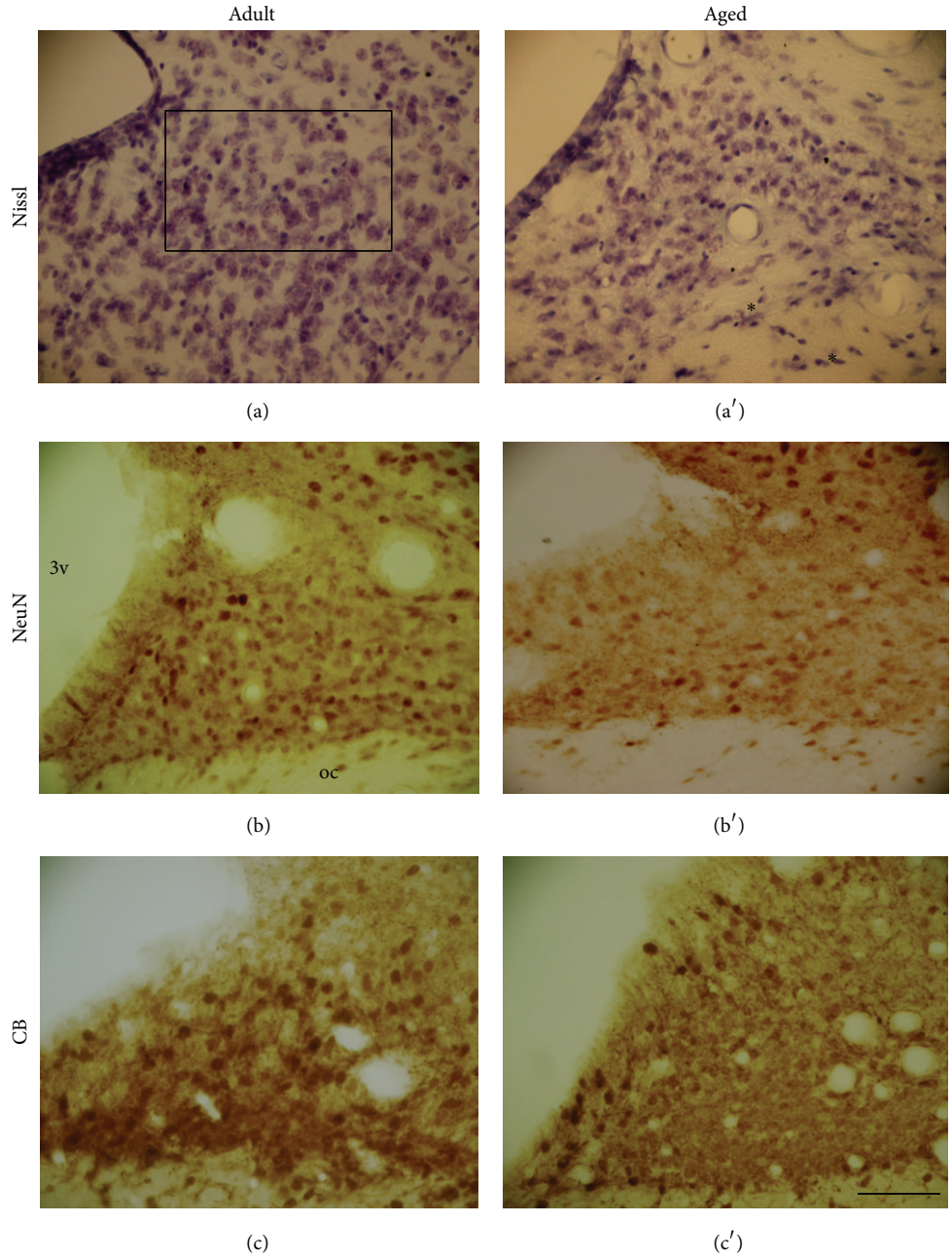

Figure 1: The suprachiasmatic nucleus. Digital images of coronal sections at hypothalamic level of the marmoset brain showing SCN at Nissl stained sections in adult (a) and aged (a′) animals; ((b) and (b′)) NeuN-immunostained; and ((c) and (c′)) CB-immunostained. Asterisk (*) shows degenerative areas and the rectangle in the figure represents the count area. CB: Calbindin; 3v: third ventricle; oc: optic chiasm. Scale bar: 50 μm.

showed a significant neuronal loss in the SCN, in which cell counting was performed by Nissl staining procedure and NeuN immunoreactivity. Similar results were reported in other studies using aged females rat and rhesus monkeys [25, 26].

Studies have suggested a possible role for progesterone in protecting neurons against neurodegeneration mainly during the senescent period in which hormone levels remain high in females [43]. Progesterone is a gonadal hormone synthesized in large proportion by the ovary in females and, in lesser amounts, by the testicles and adrenal cortex in rats [44]. Progesterone has been shown to exert significant protective effects in a variety of experimental model factors that mimic brain dysfunction seen with old age or neurodegenerative diseases related to age, such as in Alzheimer's disease [44]. Furthermore, it has been shown that progesterone decreases neuronal death resulting from global ischemic episode [45]; it may induce a remyelination of nerve fibers [46], and it increases hippocampal synapses [47].

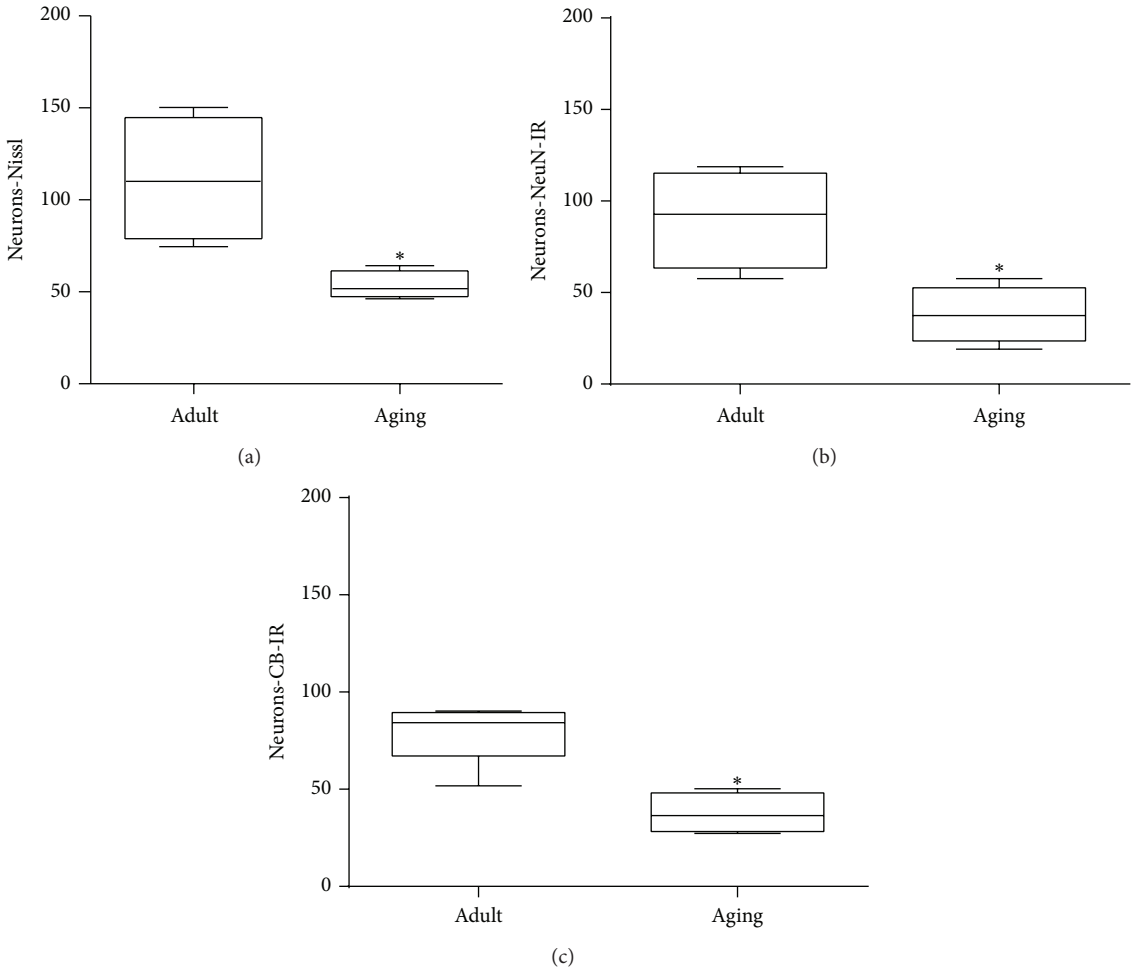

Figure 2: Effects of age on the number of neurons in the suprachiasmatic nucleus (SCN) of the marmoset *Callithrix jacchus:* (a) number of neurons for Nissl, (b) NeuN, and (c) CB-IR (Calbindin immunoreactivity). Mann-Whitney test revealed statistically significant difference between groups (Adult and Aged) for all stained. Data are expressed as median and interquartile intervals (q3–q1). $^{*}P < 0.05$ compared to adult group.

The calcium-binding protein (CaBP) CB is shown as an excellent marker of SCN cells in marmosets [10, 11]. CB is part of a group of CaBPs termed EF-hand of low molecular weight, and it is associated with the reduction and the control of cytoplasmic Ca^{2+} concentration, therefore being called "buffering" [48]. In our study, we found a significant decrease in the number of CB-IR cells in the SCN of aged marmosets compared to adult animals. This reduction of CB-IR neurons may be related to circadian behavioral changes seen in some aged animals, such as the rhythm of locomotor activity in rodents [49] and primates [50]. Moreover, studies have shown that the decrease of intracellular CB may result in increased vulnerability to degeneration of central and peripheral neurons [51, 52].

The labeling pattern of CB in the SCN cells of adult marmosets is characterized by nucleus almost completely stained [53], thus resembling the pattern found in hamsters and *Arvicanthis* [54]. However, in lemurs (*Microcebus murinus*), a nonhuman primate also, there is found a CB marking mainly concentrated in the central region of the nucleus [53]. In aged marmosets, the labeling pattern of CB in the SCN cells keeps appearing (i.e., nucleus almost completely stained); however, a substantial reduction of CB-IR neurons was evident. Areas without cells were more frequently found in the SCN of aged marmosets. The reduction of CB-IR neurons observed in aged animals was quite similar to what is seen in sections of aged SCN to NeuN-IR and histological Nissl staining. Thus, these findings contribute to hypothesis that neurodegeneration is occurring in the SCN of aged marmosets.

The ability of CB binds to the Ca^{2+} seems to confer protection against agents that promote cell death [55]; for example, neuronal CB-IR in the hippocampus has been shown to be resistant to induced neurodegeneration by a hiperactivation of excitatory amino acids, as well as by hypoxia/ischemia, both greatly increasing intracellular Ca^{2+} levels [56]. Therefore, the decrease of CB-IR in the SCN in aged marmosets may contribute to the reduction of cells observed with the use of other staining techniques, such as Nissl and NeuN.

Wu et al. [55] in a study using senior marmosets found a substantial reduction in regional CB-IR neurons in

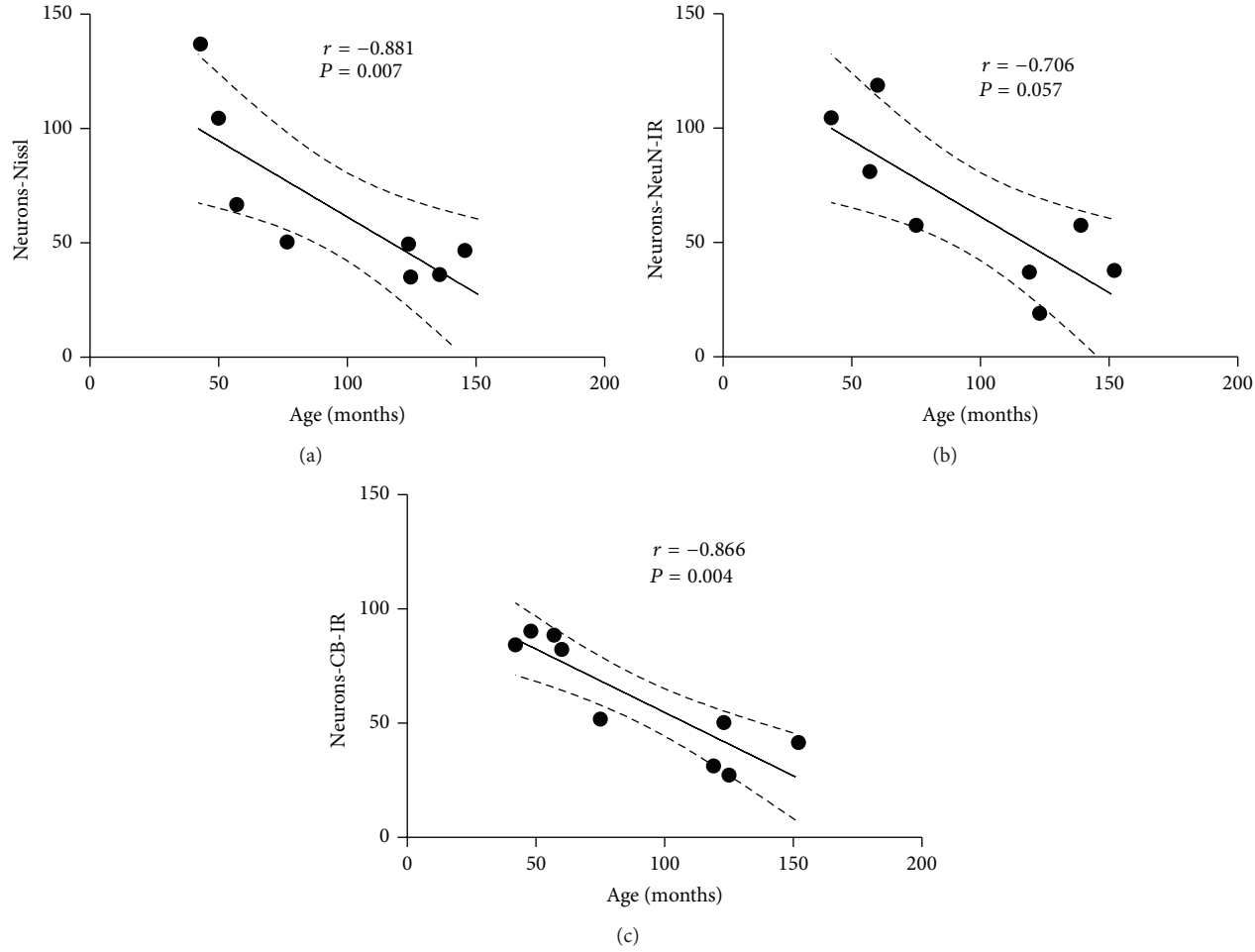

Figure 3: Correlation between cellular count and age in marmoset (*Calllithrix jacchus*) suprachiasmatic nucleus (SCN). Significant correlations (Spearman correlation—R) when $^{*}P < 0.05$.

the cholinergic basal forebrain (BFCN). In this study, authors classified animals as seniors when they were six years old. However, according to Geula et al. [57], the appearance of senile plaques in the cerebral cortex of marmosets starts to occur at seven years of age. It is important to mention that our animals were judged aged nine years old, while at six years old, they were considered adults. However, when we analyzed our correlation data, we found a marmoset of 6 years and 3 months of age (the eldest adult), which shows discrepant cells reduction compared to other adult animals, thus resembling the morphological aspects of aged marmosets. This pattern was evident in all marks used, such as CB-IR, NeuN-IR, and also Nissl-stained cells. Two recently published studies, Tardif et al. [42] and Ross et al. [58], actually showed aspects of senescence in animals from six years of age.

Lesions of CB-IR cells in the SCN lead to a failure in the circadian rhythm regulation of body temperature, heart rate, melatonin, and cortisol, suggesting that CB is required to support circadian rhythm functioning [59]. In a study with hamster, a partial lesion restricted to the central portion of the SCN produces a decrease in the circadian rhythm activity. Interestingly, in hamsters this central portion of SCN is characterized by a rich subnucleus of CB-IR neurons. Moreover, transplantation of CB-positive cells in the injured area restored rhythm, indicating that this subregion is essential for the maintenance of locomotor activity [59] and thus may result in large changes in locomotor activity seen in aged animals [49]. Although the study of the circadian rhythm pattern of aged marmosets is still being developed, we believe that the marmoset presents the same behavior activity alterations seen in other primates [50, 53] and rodents [20, 49].

We suggest that the loss associated with the CB-IR neurons in SCN of aged marmosets may increase the vulnerability of these neurons to degenerative processes that occur in aging, such as those involving increased intracellular Ca^{2+}, favoring neuronal death.

ROD analysis showed a significative increase of GFAP expression in SCN of aged marmosets compared to adults. The increase of glial expression in response to neuronal decrease is a recognized pathophysiological reaction, which is mainly seen in neurodegenerative diseases, such as Alzheimer's disease and other neurological disorders [60].

Measurements of gliogenesis rate have been used to estimate the regional overproduction of glia in response

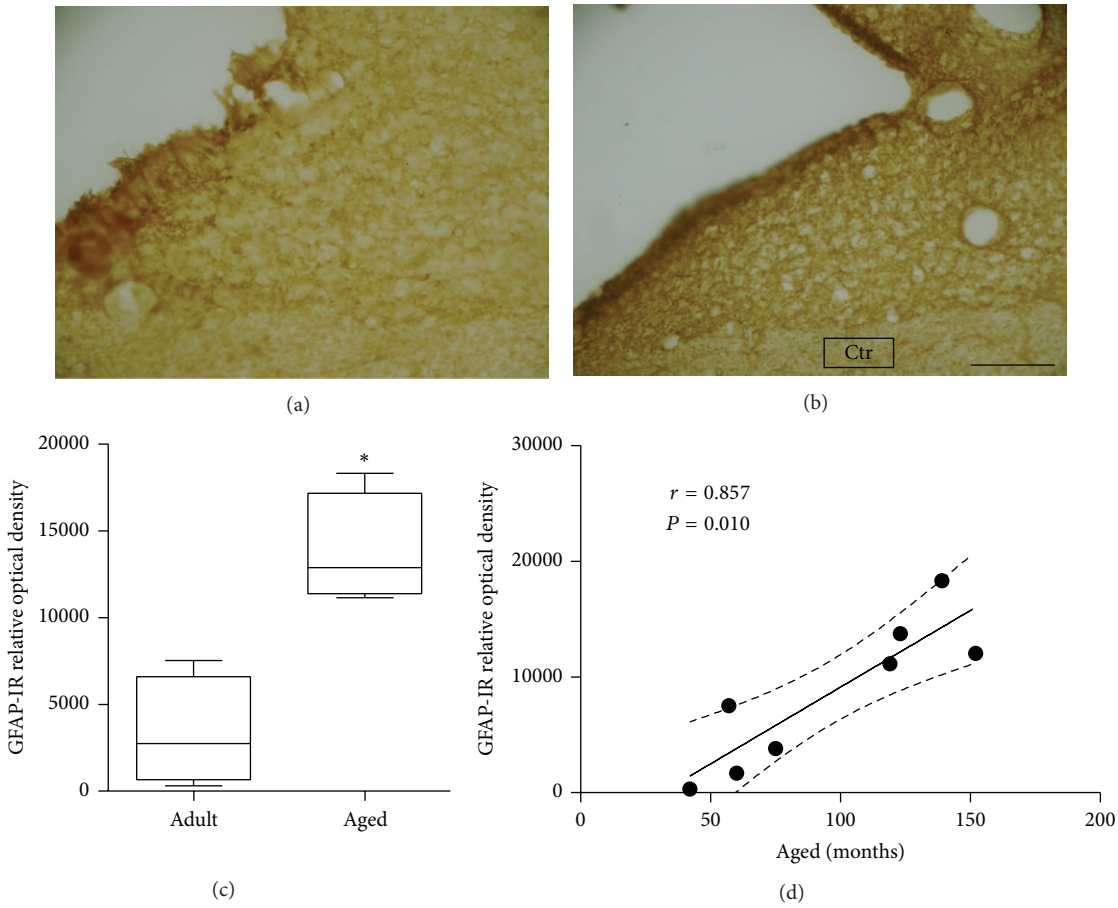

Figure 4: GFAP expression in SCN. Digital image of coronal section showing GFAP expression in adult SCN (a) and aged (b). Relative optical density measured showed a significant increase of GFAP expression in aged SCN compared to adult marmoset (c). Besides, Spearman test pointed to a significant positive correlation between GFAP-IR and age. Significant correlations (Spearman correlation—R) when $^{*}P < 0.05$. ctr: control area. Scale bar: 50 μm.

to regional decrease of neurons in a variety of disease conditions, as well as during normal aging [61, 62]. It has been suggested that the increased expression of GFAP during aging occurs due to an increase in protein damage due to oxidative processes, in all biological tissues, including the nervous system [61]. In this study, we observed a gliogenesis in response to neuronal decline in aged SCN, different from what is shown in rat and rhesus monkey, in which no changes in glial expression were found [25, 26]. Some studies reported that aged female mice showed an increase of approximately 20% of GFAP (protein) and 25% GFAP mRNA in hypothalamus and thalamus [63] and hippocampus [64] in response to neurodegeneration. Therefore, it is possible that the same effect might occur in our older animals, including in the SCN, supporting the idea that there might be a compensatory process between neuronal death (neurodegeneration) and gliogenesis in the aged marmosets SCN.

5. Conclusions

A morphometric analysis of SCN in aged female marmosets compared with adult animals showed a significant decrease in the number of neurons stained with Nissl and labeled immunohistochemically for NeuN, a specific marker for neurons. Other two protein markers, CB which is used as an excellent marker for SCN cells in marmoset, and GFAP were observed. This neuronal decline in aged animals may be responsible for changes seen in the pattern of expression of biological rhythms in animals during the aging process.

Conflict of Interests

The authors declare that there is no conflict of interests regarding the publication of this paper.

Authors' Contribution

Dr. Rovena Clara G. J. Engelberth, Dr. Jeferson Souza Cavalcante, and Dr. Carolina V. de M. Azevedo defined experimental design, performed experiments, and analyzed histological sections; besides, they prepared the first version of the paper; Dr. Jose Ronaldo dos Santos and Dr. Elaine Cristina Gavioli gave some suggestions in the final version of the paper; Kayo Diogenes de A. Silva, Dr. Judney C. Cavalcante,

Dr. Miriam Stela M. O. Costa, and Dr. Expedito S. Nascimento Júnior worked on histochemical and immunohistochemical markers used for processing histological sections; they also founded part of the research.

Acknowledgments

The authors thank CAPES, FAPERN, and CNPq for financial support.

References

[1] R. Lydic, H. E. Albers, B. Tepper, and M. C. Moore-Ede, "Three dimensional structure of the mammalian suprachiasmatic nuclei: a comparative study of five species," *The Journal of Comparative Neurology*, vol. 204, no. 3, pp. 225–237, 1982.

[2] V. A. Rocha, R. Frazão, L. M. G. Campos et al., "Intrinsic organization of the suprachiasmatic nucleus in the capuchin monkey," *Brain Research*, vol. 1543, pp. 65–72, 2014.

[3] R. Y. Moore, J. C. Speh, and R. K. Leak, "Suprachiasmatic nucleus organization," *Cell & Tissue Research*, vol. 309, no. 1, pp. 89–98, 2002.

[4] E. E. Abrahamson and R. Y. Moore, "Suprachiasmatic nucleus in the mouse: retinal innervation, intrinsic organization and efferent projections," *Brain Research*, vol. 916, no. 1-2, pp. 172–191, 2001.

[5] A. N. Van den Pol, "The hypothalamic suprachiasmatic nucleus of rat: intrinsic anatomy," *The Journal of Comparative Neurology*, vol. 191, no. 4, pp. 661–702, 1980.

[6] A. E. Hendrickson, N. Wagoner, and W. M. Cowan, "An autoradiographic and electron microscopic study of retino-hypothalamic connections," *Zeitschrift für Zellforschung und mikroskopische Anatomie*, vol. 135, no. 1, pp. 1–26, 1972.

[7] R. Y. Moore and N. J. Lenn, "A retinohypothalamic projection in the rat," *The Journal of Comparative Neurology*, vol. 146, no. 1, pp. 1–14, 1972.

[8] S. Koinuma, T. Asakawa, M. Nagano et al., "Regional circadian period difference in the suprachiasmatic nucleus of the mammalian circadian center," *European Journal of Neuroscience*, vol. 38, no. 6, pp. 2832–2841, 2013.

[9] D. K. Welsh, J. S. Takahashi, and S. A. Kay, "Suprachiasmatic nucleus: cell autonomy and network properties," *Annual Review of Physiology*, vol. 72, pp. 551–577, 2010.

[10] J. S. Cavalcante, L. R. G. Britto, C. A. B. Toledo et al., "Calcium-binding proteins in the circadian centers of the common marmoset (*Callithrix jacchus*) and the rock cavy (*Kerodon rupestris*) brains," *Brain Research Bulletin*, vol. 76, no. 4, pp. 354–360, 2008.

[11] M. S. M. O. Costa, L. F. Moreira, V. Alones et al., "Characterization of the circadian system in a Brazilian species of monkey (*Callithrix jacchus*): immunohistochemical analysis and retinal projections," *Biological Rhythm Research*, vol. 29, no. 5, pp. 510–520, 1998.

[12] L. Pinato, R. Frazão, R. J. Cruz-Rizzolo, J. S. Cavalcante, and M. I. Nogueira, "Immunocytochemical characterization of the pregeniculate nucleus and distribution of retinal and neuropeptide Y terminals in the suprachiasmatic nucleus of the *Cebus* monkey," *Journal of Chemical Neuroanatomy*, vol. 37, no. 4, pp. 207–213, 2009.

[13] J. S. Cavalcante, A. S. Alves, M. S. M. O. Costa, and L. R. G. Britto, "Differential distribution of afferents containing serotonin and neuropeptide Y within the marmoset suprachiasmatic nucleus," *Brain Research*, vol. 927, no. 2, pp. 200–203, 2002.

[14] N. A. Bishop, T. Lu, and B. A. Yankner, "Neural mechanisms of ageing and cognitive decline," *Nature*, vol. 464, no. 7288, pp. 529–535, 2010.

[15] F. L. Muller, M. S. Lustgarten, Y. Jang, A. Richardson, and H. Van Remmen, "Trends in oxidative aging theories," *Free Radical Biology & Medicine*, vol. 43, no. 4, pp. 477–503, 2007.

[16] P. R. Hof and J. H. Morrison, "The aging brain: morphomolecular senescence of cortical circuits," *Trends in Neurosciences*, vol. 27, no. 10, pp. 607–613, 2004.

[17] H. Oh, C. Madison, S. Villeneuve, C. Markley, and W. J. Jagust, "Association of gray matter atrophy with age, β-amyloid, and cognition in aging," *Cerebral Cortex*, vol. 24, no. 6, pp. 1609–1618, 2014.

[18] H. Duan, S. L. Wearne, A. B. Rocher, A. Macedo, J. H. Morrison, and P. R. Hof, "Age-related dendritic and spine changes in corticocortically projecting neurons in macaque monkeys," *Cerebral Cortex*, vol. 13, no. 9, pp. 950–961, 2003.

[19] R. C. G. J. Engelberth, A. L. B. Pontes, F. P. Fiuza et al., "Changes in the suprachiasmatic nucleus during aging: implications for biological rhythms," *Psychology & Neuroscience*, vol. 6, no. 3, pp. 287–297, 2013.

[20] E. A. Antoniadis, C. H. Ko, M. R. Ralph, and R. J. McDonald, "Circadian rhythms, aging and memory," *Behavioural Brain Research*, vol. 114, no. 1-2, pp. 221–233, 2000.

[21] M. W. Hurd and M. R. Ralph, "The significance of circadian organization for longevity in the golden hamster," *Journal of Biological Rhythms*, vol. 13, no. 5, pp. 430–436, 1998.

[22] E. Satinoff, H. Li, T. K. Tcheng et al., "Do the suprachiasmatic nuclei oscillate in old rats as they do in young ones?" *American Journal of Physiology: Regulatory Integrative and Comparative Physiology*, vol. 265, no. 5, pp. R1216–R1222, 1993.

[23] A. Watanabe, S. Shibata, and S. Watanabe, "Circadian rhythm of spontaneous neuronal activity in the suprachiasmatic nucleus of old hamster in vitro," *Brain Research*, vol. 695, no. 2, pp. 237–239, 1995.

[24] M. D. Madeira, N. Sousa, R. M. Santer, M. M. Paula-Barbosa, and H. J. G. Gundersen, "Age and sex do not affect the volume, cell numbers, or cell size of the suprachiasmatic nucleus of the rat: an unbiased stereological study," *The Journal of Comparative Neurology*, vol. 361, no. 4, pp. 585–601, 1995.

[25] D. E. Roberts, R. J. Killiany, and D. L. Rosene, "Neuron numbers in the hypothalamus of the normal aging rhesus monkey: stability across the adult lifespan and between the sexes," *The Journal of Comparative Neurology*, vol. 520, no. 6, pp. 1181–1197, 2012.

[26] S. Tsukahara, S. Tanaka, K. Ishida, N. Hoshi, and H. Kitagawa, "Age-related change and its sex differences in histoarchitecture of the hypothalamic suprachiasmatic nucleus of F344/N rats," *Experimental Gerontology*, vol. 40, no. 3, pp. 147–155, 2005.

[27] M. A. Hofman and D. F. Swaab, "Living by the clock: the circadian pacemaker in older people," *Ageing Research Reviews*, vol. 5, no. 1, pp. 33–51, 2006.

[28] J.-N. Zhou and D. F. Swaab, "Activation and degeneration during aging: a morphometric study of the human hypothalamus," *Microscopy Research & Technique*, vol. 44, no. 1, pp. 36–48, 1999.

[29] M. S. M. O. Costa and L. R. G. Britto, "Calbindin immunoreactivity delineates the circadian visual centers of the brain of the common marmoset (*Callithrix jacchus*)," *Brain Research Bulletin*, vol. 43, no. 4, pp. 369–373, 1997.

[30] J. Middeldorp and E. M. Hol, "GFAP in health and disease," *Progress in Neurobiology*, vol. 93, no. 3, pp. 421–443, 2011.

[31] G. Clark, "Tissue preparation and basic staining techniques," in *Neuroanatomical Research Techniques*, R. T. Robertson, Ed., pp. 25–45, Academic Press, New York, NY, USA, 1978.

[32] R. J. Mullen, C. R. Buck, and A. M. Smith, "NeuN, a neuronal specific nuclear protein in vertebrates," *Development*, vol. 116, no. 1, pp. 201–211, 1992.

[33] R. B. Nascimento, J. S. Borda, R. C. G. J. Engelberth et al., "The presence of neuronal-specific nuclear protein (NeuN) in the circadian timing system of the capuchin monkey (*Cebus apella*)," *Sleep Science*, vol. 3, no. 1, pp. 36–39, 2010.

[34] E. L. Portiansky, C. G. Barbeito, E. J. Gimeno, G. O. Zuccolilli, and R. G. Goya, "Loss of NeuN immunoreactivity in rat spinal cord neurons during aging," *Experimental Neurology*, vol. 202, no. 2, pp. 519–521, 2006.

[35] D. Lind, S. Franken, J. Kappler, J. Jankowski, and K. Schilling, "Characterization of the neuronal marker NeuN as a multiply phosphorylated antigen with discrete subcellular localization," *Journal of Neuroscience Research*, vol. 79, no. 3, pp. 295–302, 2005.

[36] K. Iqbal and I. Grundke-Iqbal, "Metabolic/signal transduction hypothesis of Alzheimer's disease and other tauopathies," *Acta Neuropathologica*, vol. 109, no. 1, pp. 25–31, 2005.

[37] A. M. Fjell and K. B. Walhovd, "Structural brain changes in aging: courses, causes and cognitive consequences," *Reviews in the Neurosciences*, vol. 21, no. 3, pp. 187–221, 2010.

[38] Y. Huang, R. Potter, W. Sigurdson et al., "Effects of age and amyloid deposition on Aβ dynamics in the human central nervous system," *Archives of Neurology*, vol. 69, no. 1, pp. 51–58, 2012.

[39] D. G. Harper, E. G. Stopa, V. Kuo-Leblanc et al., "Dorsomedial SCN neuronal subpopulations subserve different functions in human dementia," *Brain*, vol. 131, no. 6, pp. 1609–1617, 2008.

[40] E. G. Stopa, L. Volicer, V. Kuo-Leblanc et al., "Pathologic evaluation of the human suprachiasmatic nucleus in severe dementia," *Journal of Neuropathology & Experimental Neurology*, vol. 58, no. 1, pp. 29–39, 1999.

[41] D. H. Abbott, D. K. Barnett, R. J. Colman, M. E. Yamamoto, and N. J. Schultz-Darken, "Aspects of common marmoset basic biology and life history important for biomedical research," *Comparative Medicine*, vol. 53, no. 4, pp. 339–350, 2003.

[42] S. D. Tardif, K. G. Mansfield, R. Ratnam, C. N. Ross, and T. E. Ziegler, "The marmoset as a model of aging and age-related diseases," *ILAR Journal*, vol. 52, no. 1, pp. 54–65, 2011.

[43] M. Singh and C. Su, "Progesterone-induced neuroprotection: factors that may predict therapeutic efficacy," *Brain Research*, vol. 1514, pp. 98–106, 2013.

[44] M. Singh and C. Su, "Progesterone and neuroprotection," *Hormones and Behavior*, vol. 63, no. 2, pp. 284–290, 2013.

[45] M. Cervantes, M. D. González-Vidal, R. Ruelas, A. Escobar, and G. Moralí, "Neuroprotective effects of progesterone on damage elicited by acute global cerebral ischemia in neurons of the caudate nucleus," *Archives of Medical Research*, vol. 33, no. 1, pp. 6–14, 2002.

[46] C. Ibanez, S. A. Shields, M. El-Etr et al., "Steroids and the reversal of age-associated changes in myelination and remyelination," *Progress in Neurobiology*, vol. 71, no. 1, pp. 49–56, 2003.

[47] Y. Zhao, J. Wang, C. Liu, C. Jiang, C. Zhao, and Z. Zhu, "Progesterone influences postischemic synaptogenesis in the CA1 region of the hippocampus in rats," *Synapse*, vol. 65, no. 9, pp. 880–891, 2011.

[48] P. R. Hof, I. I. Glezer, F. Condé et al., "Cellular distribution of the calcium-binding proteins parvalbumin, calbindin, and calretinin in the neocortex of mammals: phylogenetic and developmental patterns," *Journal of Chemical Neuroanatomy*, vol. 16, no. 2, pp. 77–116, 1999.

[49] V. S. Valentinuzzi, K. Scarbrough, J. S. Takahashi, and F. W. Turek, "Effects of aging on the circadian rhythm of wheel running activity in C57BL/6 mice," *American Journal Physiology: Regulatory, Integrative and Comparative Physiology*, vol. 273, no. 6, part 2, pp. R1957–R1964, 1997.

[50] I. V. Zhdanova, K. Masuda, C. Quasarano-Kourkoulis, D. L. Rosene, R. J. Killiany, and S. Wang, "Aging of intrinsic circadian rhythms and sleep in a diurnal nonhuman primate, *Macaca mulatta*," *Journal of Biological Rhythms*, vol. 26, no. 2, pp. 149–159, 2011.

[51] C. D'Orlando, B. Fellay, B. Schwaller et al., "Calretinin and calbindin D-28k delay the onset of cell death after excitotoxic stimulation in transfected P19 cells," *Brain Research*, vol. 909, no. 1-2, pp. 145–158, 2001.

[52] D. Riascos, D. de Leon, A. Baker-Nigh et al., "Age-related loss of calcium buffering and selective neuronal vulnerability in Alzheimer's disease," *Acta Neuropathologica*, vol. 122, no. 5, pp. 565–576, 2011.

[53] F. Cayetanot, J. Deprez, and F. Aujard, "Calbindin D_{28K} protein cells in a primate suprachiasmatic nucleus: localization, daily rhythm and age-related changes," *European Journal of Neuroscience*, vol. 26, no. 7, pp. 2025–2032, 2007.

[54] R. Silver, M.-T. Romero, H. R. Besmer, R. Leak, J. M. Nunez, and J. LeSauter, "Calbindin-D28k cells in the hamster SCN express light-induced Fos," *Neuroreport*, vol. 7, no. 6, pp. 1224–1228, 1996.

[55] C. K. Wu, N. Nagykery, L. B. Hersh, L. F. Scinto, and C. Geula, "Selective age-related loss of calbindin-D_{28k} from basal forebrain cholinergic neurons in the common marmoset (*Callithrix jacchus*)," *Neuroscience*, vol. 120, no. 1, pp. 249–259, 2003.

[56] R. G. Phillips, T. J. Meier, L. C. Giuli, J. R. McLaughlin, D. Y. Ho, and R. M. Sapolsky, "Calbindin D_{28K} gene transfer via herpes simplex virus amplicon vector decreases hippocampal damage in vivo following neurotoxic insults," *Journal of Neurochemistry*, vol. 73, no. 3, pp. 1200–1205, 1999.

[57] C. Geula, N. Nagykery, and C.-K. Wu, "Amyloid-β deposits in the cerebral cortex of the aged common marmoset (*Callithrix jacchus*): incidence and chemical composition," *Acta Neuropathologica*, vol. 103, no. 1, pp. 48–58, 2002.

[58] C. N. Ross, K. Davis, G. Dobek, and S. D. Tardif, "Aging phenotypes of common marmosets (*Callithrix jacchus*)," *Journal of Aging Research*, vol. 2012, Article ID 567143, 6 pages, 2012.

[59] L. J. Kriegsfeld, J. LeSauter, and R. Silver, "Targeted microlesions reveal novel organization of the hamster suprachiasmatic nucleus," *The Journal of Neuroscience*, vol. 24, no. 10, pp. 2449–2457, 2004.

[60] M. D. Smyth, D. D. Limbrick Jr., J. G. Ojemann et al., "Outcome following surgery for temporal lobe epilepsy with hippocampal involvement in preadolescent children: emphasis on mesial temporal sclerosis," *Journal of Neurosurgery*, vol. 106, no. 3, pp. 205–210, 2007.

[61] F. Cerbai, D. Lana, D. Nosi et al., "The neuron-astrocyte-microglia triad in normal brain ageing and in a model of neuroinflammation in the rat hippocampus," *PLoS ONE*, vol. 7, no. 9, Article ID e45250, 2012.

[62] T. S. Roy, V. Sharma, F. J. Seidler, and T. A. Slotkin, "Quantitative morphological assessment reveals neuronal and glial deficits in

hippocampus after a brief subtoxic exposure to chlorpyrifos in neonatal rats," *Developmental Brain Research*, vol. 155, no. 1, pp. 71–80, 2005.

[63] S. G. Kohama, J. R. Goss, C. E. Finch, and T. H. Mcneill, "Increases of glial fibrillary acidic protein in the aging female mouse brain," *Neurobiology of Aging*, vol. 16, no. 1, pp. 59–67, 1995.

[64] P. R. Mouton, J. M. Long, D.-L. Lei et al., "Age and gender effects on microglia and astrocyte numbers in brains of mice," *Brain Research*, vol. 956, no. 1, pp. 30–35, 2002.

Hindawi Publishing Corporation
BioMed Research International
Volume 2014, Article ID 646847, 9 pages
http://dx.doi.org/10.1155/2014/646847

Research Article

Early Appearance of Nonvisual and Circadian Markers in the Developing Inner Retinal Cells of Chicken

Nicolás M. Díaz, Luis P. Morera, Daniela M. Verra, María A. Contin, and Mario E. Guido

CIQUIBIC (CONICET), Departamento de Química Biológica, Facultad de Ciencias Químicas, Universidad Nacional de Córdoba, Ciudad Universitaria, 5000 Córdoba, Argentina

Correspondence should be addressed to Mario E. Guido; mguido@fcq.unc.edu.ar

Received 27 January 2014; Revised 7 April 2014; Accepted 23 April 2014; Published 20 May 2014

Academic Editor: Martin Fredensborg Rath

The retina is a key component of the vertebrate circadian system; it is responsible for detecting and transmitting the environmental illumination conditions (day/night cycles) to the brain that synchronize the circadian clock located in the suprachiasmatic nucleus (SCN). For this, retinal ganglion cells (RGCs) project to the SCN and other nonvisual areas. In the chicken, intrinsically photosensitive RGCs (ipRGCs) expressing the photopigment melanopsin (Opn4) transmit photic information and regulate diverse nonvisual tasks. In nonmammalian vertebrates, two genes encode *Opn4*: the *Xenopus* (*Opn4x*) and the mammalian (*Opn4m*) orthologs. RGCs express both *Opn4* genes but are not the only inner retinal cells expressing *Opn4x*: horizontal cells (HCs) also do so. Here, we further characterize primary cultures of both populations of inner retinal cells (RGCs and HCs) expressing *Opn4x*. The expression of this nonvisual photopigment, as well as that for different circadian markers such as the clock genes *Bmal1*, *Clock*, *Per2*, and *Cry1*, and the key melatonin synthesizing enzyme, arylalkylamine *N*-acetyltransferase (AA-NAT), appears very early in development in both cell populations. The results clearly suggest that nonvisual Opn4 photoreceptors and endogenous clocks converge all together in these inner retinal cells at early developmental stages.

1. Introduction

The circadian system of vertebrates that controls most physiological and behavioral rhythms includes the retina, the pineal gland, and the hypothalamic suprachiasmatic nucleus (SCN) together with a number of peripheral oscillators distributed throughout the body [1, 2]. Light is the main synchronizer of the circadian system while the retina is responsible for sensing the environmental lighting conditions which change along the day/night cycles, by more than six orders of magnitude, to adjust endogenous clocks located in the brain. The retina contains the autonomous clock machinery that generates a variety of self-sustained biochemical and cellular rhythms, allowing it to measure time and predict the 24 h changes in the ambient light conditions [1, 3, 4]. Embryonic retinal cells maintained in culture and different retinal cell populations display robust circadian rhythms in a number of molecular and biochemical aspects and express circadian-based clock genes [5–10]. In this respect, photoreceptor cells (PRCs) synthesize melatonin almost exclusively in the retina of different vertebrate species with the highest levels at night [1, 8, 11–13]; by contrast, retinal ganglion cells (RGCs) in the chicken synthesize small amounts of melatonin rhythmically with higher levels during the day, in clear antiphase to the nocturnal PRC profiles [1, 8, 11–13].

Briefly, the molecular clock that also operates in the vertebrate retina consists of a transcriptional/translational feedback circuitry that generates circadian patterns of gene expression by means of the action of positive elements such as Clock, Bmal1, and NPAS2. These latter interact with the negative elements Periods (Per) 1 and 2 and cryptochrome (Cry) 1 and 2, in which the casein kinases CKI and CKIδ set the circadian period by phosphorylating PER proteins to regulate their degradation and nuclear localization [1, 14].

In the last decades, two major discoveries have had an extraordinary impact in the field of vision and chronobiology: the identification of a novel photopigment named melanopsin (Opn4) which is only expressed in a subpopulation of RGCs in mammals [15] and the demonstration that these Opn4 (+) RGCs were intrinsically photosensitive cells

(ipRGCs) [16]. Working with nonmammalian vertebrates, we were the first to demonstrate that a subpopulation of RGCs in the chicken retina was ipRGCs acting through a photocascade similar to that of rhabdomeric photoreceptors of invertebrates involving the activation of phospholipase C and Ca^{2+} mobilization [17, 18]. Moreover, we and other laboratories have shown that the two genes for Opn4, the Xenopus (*Opn4x*) and the mammalian (*Opn4m*) orthologs, are expressed in chicken retina at the level of mRNA [5, 6, 17, 19, 20] and protein [7, 21]. Moreover, the expression of Opn4 proteins was reported to vary during development [21]. In fact, Opn4m was shown to be restricted exclusively to the ganglion cell layer (GCL) all through development, whereas Opn4x was limited to the formation of GCL and optic nerve at early embryonic days (E8), though by E15 its expression was mostly in Prox1 (+) horizontal cells (HCs) [21]. Concomitantly with HC birth and migration between E10–15, Opn4x (+) immunoreactivity appeared in the cell somas of Prox1 (+) HC and displayed prominent labelling of the lower outer plexiform layer (OPL). Indeed, these Opn4x cells resembled typical HCs: morphologically, some are axonless candelabrum-shaped HCs shown to mainly connect to cone pedicles [22, 23]. Based on a number of specification markers, horizontal and amacrine cells in the inner retina could be considered sister cells of ipRGCs derived from a common ancestor photoreceptor progenitor [24].

In this work, we further characterize primary cultures of RGCs and HCs obtained from embryonic retinas at early stages in development by different procedures of purification; strikingly, both retinal cell populations express the nonvisual photopigment Opn4 (*Opn4m* and/or *Opn4x*) as well as components of the clock machinery needed to measure time to temporally adjust retinal physiology. To this end, the aim of this work was to investigate whether nonvisual Opn4 photoreceptors and endogenous clocks converge in specific cell populations of the chicken inner retina.

2. Materials and Methods

2.1. Materials. All reagents were of analytical grade. The secondary antibodies used for immunocytochemistry (ICC) and immunohistochemistry (IHC) were Alexa Fluor 488 goat anti-rabbit and Alexa Fluor 546 goat anti-mouse IgG (dilution 1 : 1000; Invitrogen-Molecular Probes, Eugene, OR, USA), Prox-1 Polyclonal Antibody, anti-rabbit (dilution 1/2500, Millipore, Temecula, CA, USA) NeuN monoclonal antibody, mouse (1/100, Millipore, Temecula, CA); glutamine synthetase (GS) monoclonal antibody, mouse (1/500, Millipore, Temecula, CA, USA); GABA polyclonal antibody, rabbit (1/500, Abcam Cambridge MA, USA); anti-mouse Cry1 cat CRY11-A (1/100 Alpha Diagnostic Intl. inc), anti-mouse Per2 cat PER21-A (1/100 Alpha Diagnostic Intl. Inc.), and anti-BMAL1 AB2298 (1/100 Millipore Temecula California). α-Tubulin (α-Tub) was detected by the mouse monoclonal DM1A antibody (Sigma Aldrich, 1 : 1000 for WB). The primary antibody against chicken *Opn4x* was raised in rabbit using the specific *Opn4x* peptide 1: RQKRDLLPDSYSCSEE [21]. The antibody against the chicken *Opn4m* was raised in rat and generated with the specific *Opn4m* peptide: CKHGNRELQKQYHR (Bio-Synthesis Inc., Lewisville, TX, USA) [21]. Preparation of anti-chicken Thy-1 sera was performed by Bio-Synthesis, Inc. (Bio-Synthesis Inc., Lewisville, TX, USA), by using the NH2-KNITVIKDKLEKC-OH peptide sequence conjugated with KLH [17].

Propidium iodide (PI), DAPI, protease inhibitor, papain suspension in 0.05 M sodium acetate, and laminin were from Sigma Aldrich (St. Louis, MO). Aqueous mounting medium (FluorSave) was from Calbiochem (San Diego, CA). B-27 supplement 50 was from Invitrogen-Gibco (Grand Island, NY), Leibovitz's (L-15) from Life Technologies, Invitrogen GIBCO (Carlsbad, CA).

2.2. Animal Handling. For studies involving immunochemistry, we used 10-day-old chickens (*Gallus gallus domesticus*). Chickens were anesthetized with 2.5 mL/Kg Equitesin (426 mg chloral hydrate, 96 mg pentobarbital, 212 mg $MgSO_4$, 3.5 mL propylene glycol, and 1 mL ethanol, final volume 10 mL) and sacrificed by decapitation.

All experiments were performed in accordance with the Use of Animals in Ophthalmic and Vision Research of ARVO, approved by the local animal care committee (School of Chemistry, Universidad Nacional de Córdoba; Exp. 15-99-39796).

2.3. Primary Cultures of Embryonic RGCs. RGCs were purified from embryonic day 8 (E8); neural chicken retinas were dissected in ice-cold Ca^{+2}- Mg^{+2} free Tyrode's buffer containing 25 mM glucose as previously reported [9, 25]. Briefly, cells were trypsin-treated and rinsed with soybean trypsin inhibitor and Dulbecco's modified Eagle's medium (DMEM). After dissociation, the cell suspension from 30 to 60 retinas was poured into petri dishes pretreated with 2.5 μg/mL protein A followed by incubation at 37°C for 30 min with an anti-chicken Thy-1 polyclonal antibody. After being washed exhaustively, identical aliquots of the remaining bound RGCs were harvested in DMEM containing B27 (Life Technologies, Invitrogen, GIBCO, Carlsbad, CA; dilution: 1/500 v/v) and seeded in petri dishes previously treated with 10 μg/mL polylysine and 5 μg/mL laminin. The RGC cultures were incubated at 37°C under constant 5% CO_2-air flow in a humid atmosphere [17, 18, 21]. In an alternative procedure, the cell suspension from 20 to 40 retinas was poured into petri dishes pretreated with 2.5 μg/mL protein A followed by incubation at 37°C for 30 min with an anti-chicken *Opn4x* polyclonal antibody (Bio-Synthesis Inc., Lewisville, TX, USA). After exhaustive washing, similar aliquots of the remaining bound cells were harvested in DMEM containing B27 (Life Technologies, Invitrogen, GIBCO, Carlsbad, CA; dilution: 1/50 v/v), forskolin from *Coleus forskohlii* (Sigma Aldrich, St. Louis, MO, 4.25 μg/mL in DMSO), and Recombinant Human BDNF (R&D Systems, Minneapolis, MN, 50 μg/mL) and seeded in petri dishes previously treated with 10 μg/mL polylysine and 5 μg/mL laminin. Primary cell cultures were incubated at 37°C under constant 5% CO_2-air flow in a humid atmosphere for 3 days and further characterized with specific retinal cell type markers by immunochemistry.

2.4. Primary Cultures of Embryonic Horizontal Cells (HCs). HCs were purified from the chicken neural retinas at embryonic day 15 (E15) as previously reported [26]. Briefly, eyes were dissected out from the head and sectioned in ice-cold Ca^{+2}- Mg^{+2} free Hank's buffered saline solution containing 25 mM glucose (CMF-HBSS) at the level of the ora serrata, the vitreous body was removed, and the retina was peeled from the eyecup by gentle shaking in order to avoid detachment of the pigment epithelium. The retina was cut into 6–8 pieces and incubated with CMF containing 3 U/mL of papain for 25 min at 37°C and then kept on ice until use.

In order to isolate HCs, cells were dissociated from the retinal tissue by a mechanical triturating procedure with a fire-polished Pasteur pipette. After dissociation, the cell suspension was subjected to a bovine serum albumin (BSA) discontinuous gradient of concentrations ranging from 1 to 4%. After dissociation, cells were centrifuged at 300 rpm for 15 min and different phases were collected and cultured for 4 days in L15 containing B27 (Life Technologies, Invitrogen, GIBCO, Carlsbad, CA; dilution: 1/500 v/v) in order to allow neurite outgrowth and morphological differentiation. Cultures were incubated over 4 days at 37°C in a humid atmosphere containing 5% CO_2. Characterization of harvested cells was performed by immunostaining with different HC and other retinal cell type markers. The cell cultures were highly enriched in HCs (≥75%) as previously shown [26].

2.5. Immunocytochemistry (ICC). Cultured cells were fixed for 30 minutes in 4% paraformaldehyde in phosphate buffer saline (PBS) and cover slips were washed in PBS, treated with blocking buffer (PBS supplemented with 0.1% BSA, 0.1% Tween 20, and 0.1% $NaNO_3$), and incubated with the respective antibodies as described [18, 26]. They were then rinsed in PBS and incubated with goat anti-rabbit IgG Alexa Fluor 488 or goat anti-mouse IgG Alexa Fluor 546 (monoclonal antibodies) (1 : 1000) for 1 h at room temperature (RT). In some experiments, samples were incubated with propidium iodide (PI) (0.05 mg/mL). Cover slips were finally washed thoroughly and visualized by confocal microscopy (FV1000; Olympus, Tokyo, Japan).

2.6. RNA Isolation and RT-PCR. Total RNA from RGC or HC primary cultures was extracted following the method of Chomczynski and Sacchi using the TRIzol kit for RNA isolation (Invitrogen) as previously described [17]. RNA integrity was checked in 1.5% agarose gel and quantified by UV spectrophotometry (Gene Quant spectrophotometer, Amersham Biosciences). Finally, 1-2 μg of total RNA was treated with DNAse (Promega) to eliminate contaminating genomic DNA. cDNA was synthesized with M-MLV (Promega) using oligo (dT).

The oligonucleotide sequences used for RT-PCR from the *Gallus gallus* sequences were as follows [27]:

Bmal1
Forward: 5′ TGAGGAGTCGCTGGTTCAGTTTCA 3′
Reverse: 5′ ACGCTGTCCATGCTATGTGGAGAA 3′

GAPDH
Forward: 5′ AGG CGA GAT GGT GAA AGT CG 3′
Reverse: 5′ TCT GCC CAT TTG ATG TTG CT 3′

Cry 1
Forward: 5′ AGAGAGTGTCCAGAAGGCTGCAAA 3′
Reverse: 5′ ACTGTTGCAAGAAGACCCAGTCCT 3′

Cry 2
Forward: 5′ CCA AGT GCA TCA TTG GAG TGG 3′
Reverse: 5′ CTT CAG TGC ACA GCT CTT CTG CTC 3′

AA-NAT
Forward: 5′ ACAGGCACCTTTACAGCACGAGA 3′
Reverse: 5′ CTGCTTCACGACAAACCAAGGCAT 3′

Clock
Forward: 5′ ACGGTCAAGGACTGCAGATGTTCT 3′
Reverse: 5′ CTGCAAAGGCTGTTGCTGGATCAT 3′

Per 2
Forward: 5′ TGGTCACCGTCAGACACTTCACAA 3′
Reverse: 5′ TTTCCCGAGTCTGGCAGCTGATTA 3′

NPAS2
Forward: 5′ CCAGGGCAAATTGCATCTCCACAA 3′
Reverse: 5′ AGGATGTGGGCATCATAGGCTGAA 3′

2.7. Polymerase Chain Reaction (PCR). PCR reactions were carried out according to [17] with an initial denaturation step of 3 min at 95°C followed by 36 cycles of denaturation at 95°C for 15 sec, annealing at 60°C for 30 sec, extension at 72°C for 30 sec, and a final 5 min elongation step at 72°C. Amplification products were separated by agarose gel electrophoresis and visualized by ethidium bromide staining.

2.8. Inositol Phosphates (IPs) Assessment. RGC cultures were metabolically labeled with 2 μCi·mL^{-1} of myo-[2-^{3}H(N)] inositol (PerkinElmer Life and Analytical Sciences) during 48 h. The cells were then stimulated with cool white fluorescence light (1200 lux) during different times according to conditions used to depolarize ipRGCs in mammals [28], in the presence of 10 mM LiCl. The lipids were recovered by TCA extraction methods [29–31] and the inositol phosphates (IPs) were recovered from the protein/membrane pellets [32]. IPs were then separated by Dowex AG1-X8 columns and eluted with increasing concentrations of ammonium formate and formic acid as described [29, 30]. The radiolabeled IP content was determined in a scintillation counter.

2.9. Statistics. Statistical analyses involved a one-way analysis of variance (ANOVA) with Duncan post hoc tests or Student's *t*-tests, when appropriate (significance at $P < 0.05$).

3. Results and Discussion

We first examined the expression of Opn4 and a number of retinal cell type markers in primary cultures of RGCs obtained either by Thy-1-(Figure 1(a)) or *Opn4x*-antibody immunopurifications (Figure 1(b)) at embryonic day 8 (E8).

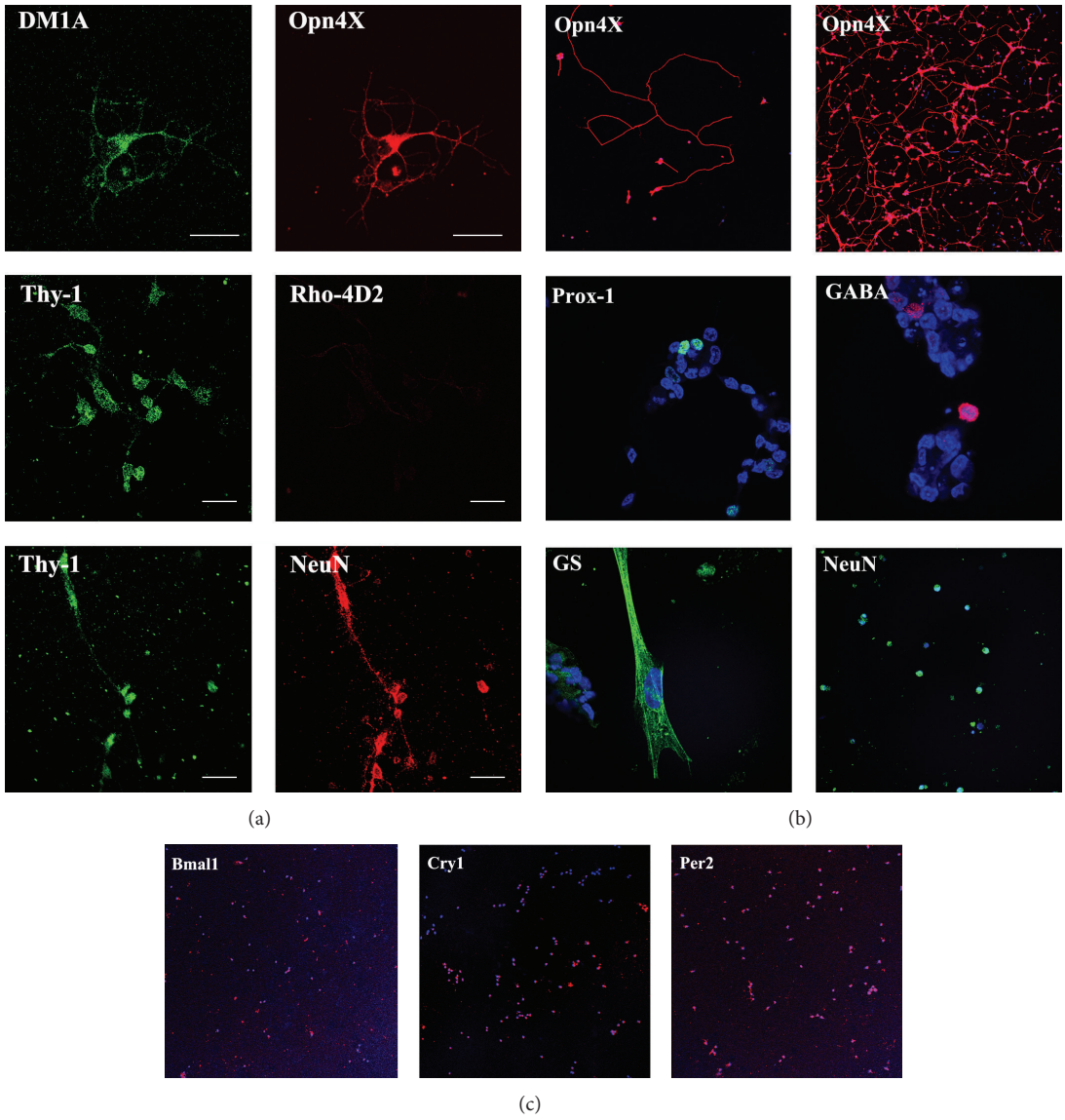

Figure 1: Immunocytochemistry for immunopurified RGC primary cultures at embryonic day 8 (E8) by Thy-1 (a), Opn4x (b) antibody purifications, and clock genes of RGC Opn4x cultures. (a) Primary cultures of embryonic RGCs purified by Thy-1 antibody immunopanning and maintained for 48–72 h were immunolabeled for DM1A, Opn4x, Thy-1, Rhod-4D2, and NeuN. (b) Immunocytochemistry for Opn4x- Prox-1, GABA, glutamine synthetase (GS), and NeuN, with DAPI staining in purified RGC cultures at E8 by Opn4x- antibody immunopurification. Primary cultures were visualized by confocal microscopy with specific primary antibodies as described in Section 2. Scale bar = 20 μm. (c) Primary cultures of RGC's immunopurified by Opn4x-antibody immunolabeled with anti-Bmal1, Cry1, and Per2.4.

Primary cell cultures were obtained by Thy-1 immunopanning, expressed Opn4x (Figures 1(a) and 2) and Opn4m (Figure 2), and exhibited a positive immunoreactivity for the RGC markers NeuN and Thy-1 in most cells but not for rhodopsin, a typical PRC marker (Figure 1(a)). When the primary RGC cultures were prepared by Opn4x immunopurification at E8, most cells expressed Opn4x and NeuN while only a very few (<10%) exhibited positive immunostaining for HC markers such as Prox-1 or GABA or for the glial cell marker GS (Figure 1(b)). In addition, the immunoreactivity associated with Opn4x clearly labeled all RGC neurite processes, even the longest ones (see stained individual cells in upper panel of Figures 1(a) and 1(b)). Moreover, Opn4x (+) RGC cultures were also found to express different clock proteins such as the Bmal1, Cry1, and Per2 (Figure 1(c)). To further characterize the expression of both Opn4 proteins in RGC primary cultures obtained by Thy-1 antibody immunopurification at E8 and their photic responsiveness, we carried out a series of new experiments shown in Figure 2. RGC cultures displayed a positive immunoreactivity associated with Opn4x or Opn4m in approximately 11% and 22% of total cells, respectively, in agreement with observations previously reported [18]. In addition, we further investigated the intrinsic light responsiveness of the primary RGC cultures shown in Figure 2 by assessing the formation of different radiolabeled inositol phosphates (IPs) (IP, IP_2, IP_3, IP_4, and

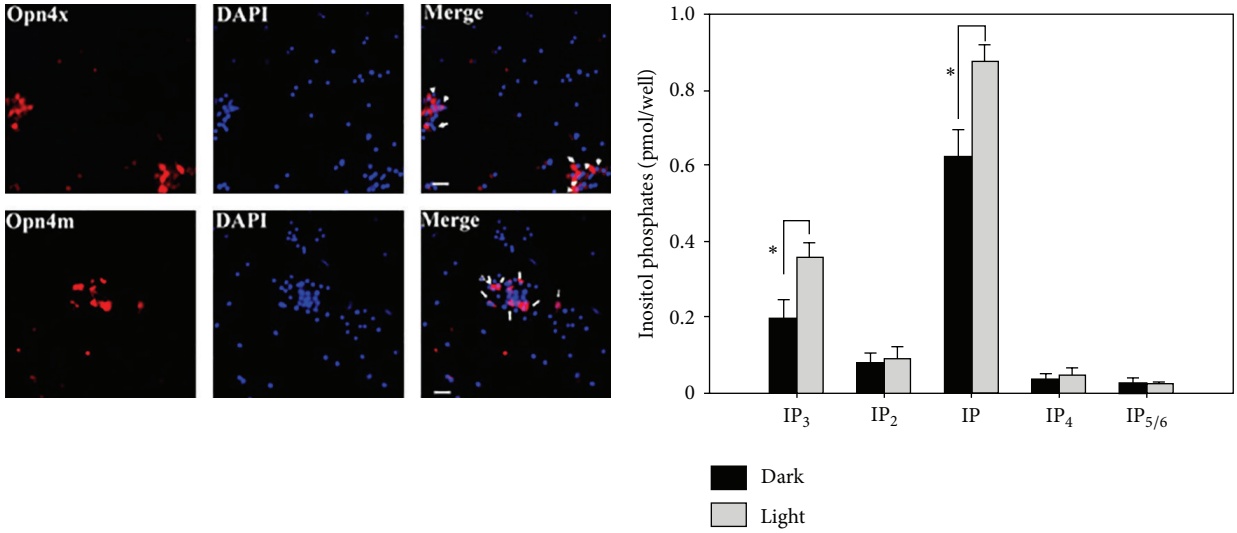

FIGURE 2: Melanopsin expression and light responses in RGC cultures. (a) Primary cultures of embryonic RGCs maintained for 48–72 h were immunolabeled for Opn4x or Opn4m with specific antibodies and DAPI (nuclei staining). The white arrows identify clusters of Opn4 (+) cells present in RGC cultures observed at 40X. (b) Content of inositol phosphates (IPs) in primary cultures of RGCs maintained in the dark (black squares) or stimulated by light (gray squares). Cultures previously incubated with myo-^{3}H inositol for 48 h were light-stimulated during 90 sec to investigate the generation of different IP derivatives directly in RGCs. IP production was evaluated after bright light stimuli and control cells were maintained in the dark as described in the text. Significant increases in radiolabeled IP_3 and IP were seen in cultures exposed to bright white light as compared with dark controls ($P < 0.04$). On the contrary, no significant light-dark differences were found in the content of other IPs determined such as IP_2, IP_4, and $IP_{5/6}$. See text for further details.

$IP_{5/6}$) after light stimulation and comparing it with cultures kept in the dark. A very rapid generation of radiolabeled IPs occurred in the light by activation of the phospholipase C (PLC) which was previously shown to be involved in the RGC phototransduction cascade [17, 18]. In this connection, RGC cultures previously incubated with myo-^{3}H inositol were light-stimulated during 90 sec or maintained in the dark (controls) in the presence of LiCl (20 mM), a well-known inositol monophosphate phosphatase inhibitor, in order to assess levels of different IPs under both light conditions. We found a significant increase in labeled IP_3 and IP in cultures exposed to bright white light as compared with controls kept in the dark (Figure 2(b)); this increase represents a 70% and 40% rise in IP content, respectively, compared to basal levels ($P < 0.04$). By contrast, no significant light-dark differences were found in the content of other IPs determined such as IP_2, IP_4, and $IP_{5/6}$, likely reflecting the very fast metabolism of these particular IP derivatives.

Opn4x-like protein was strongly visualized in the OPL of the chicken retina at a later developmental/postnatal stage. Moreover, Opn4x was strongly expressed in Prox-1(+) cells localized in the inner nuclear layer of the avian retina [21]. More recently, we described a protocol using a BSA gradient to obtain primary cultures highly enriched in HCs at embryonic day 15 [26]. By means of this purification procedure, in this paper, we have further characterized the 2.5% phase containing HCs. As shown in Figure 3, primary cultures highly enriched in HCs exhibiting positive immunoreactivity for Prox-1, a typical nuclear HC marker, colocalized with the fluorescence for Opn4x. Interestingly, *Opn4x* labeling was concentrated in both soma and neurites of cultured cells; these observations are in clear agreement with the immunostaining observed in our previous observations [21] at E15 and posthatch days. In addition, this figure also shows colocalization of Tubulin with Prox-1 to clearly denote the typical HC morphology.

We then investigated the expression of clock genes and circadian markers in primary cultures of RGCs and HCs and compared it with expression of markers in the whole mature retina. RGC cultures immunopurified by Opn4x-antibody purification at a very early embryonic day (E8) express the transcripts for positive elements of the molecular clock such as *Bmal1* and *Clock* but not for *NPAS2*, which are strongly present in the whole retina (Figure 4); Opn4 (+) RGCs also express the negative elements of the molecular clock such as *Per2* and *Cry1* as well as the mRNA for *AA-NAT*, the key enzyme for melatonin biosynthesis (Figure 4).

In addition, highly enriched primary cultures of HCs, prepared with the 2.5% phase of the BSA gradient, clearly expressed the clock genes *Bmal1*, *Cry1*, and *Per2* as well as *AA-NAT* (Figure 4). By contrast, the transcripts for *NPAS2* and *Clock* were not detected in the cultures, although they were clearly visualized in the positive controls (the whole mature chicken retina). These findings demonstrate the presence of some clock and clock-related genes in the cultures, allowing us to infer that Opn4x and components of the molecular clock are present in the same cell population. Although it has been previously reported that embryonic retinal cell cultures

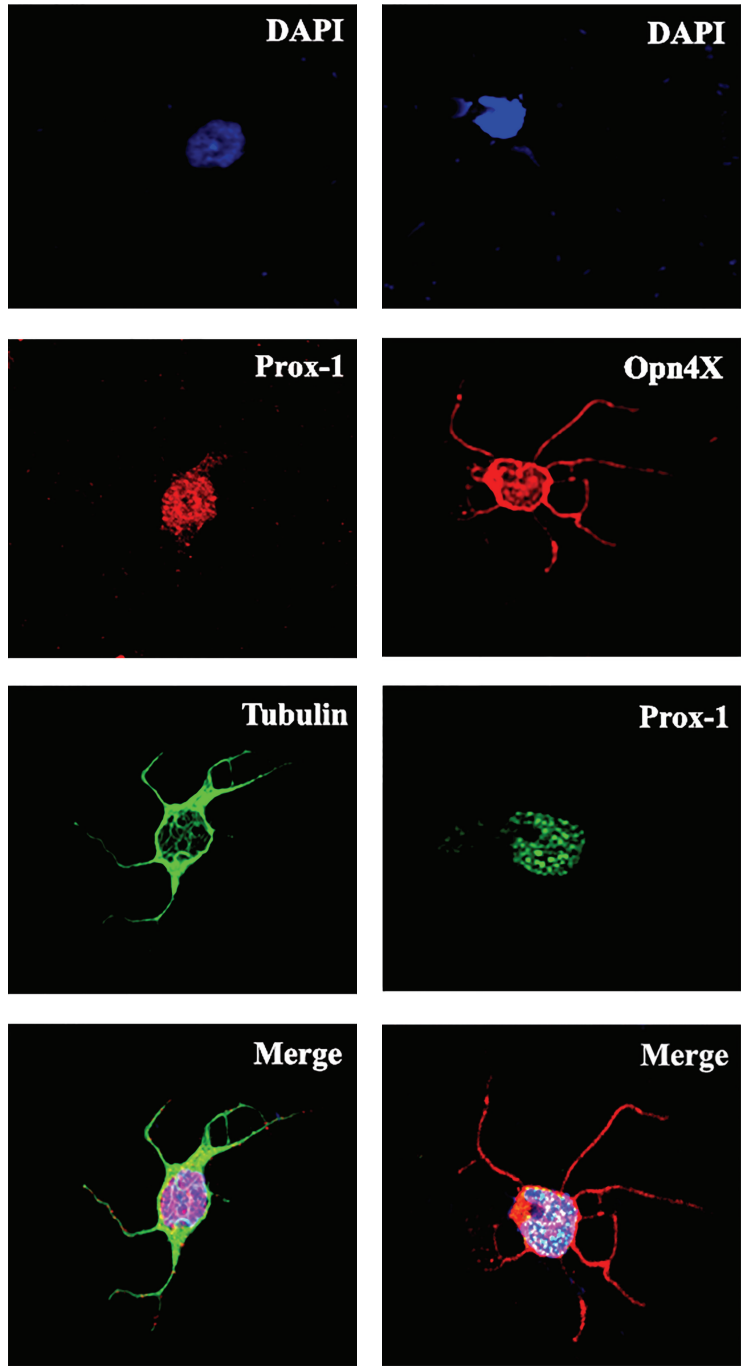

Figure 3: Immunocytochemistry for Prox-1, Opn4x, and α-Tubulin proteins staining and merge in HC cultures at E15. Individual cells from primary cultures of HCs were obtained by the 2.5% phase of a bovine albumin serum (BSA) gradientpurification, maintained for 48–72 h, immunolabeled for Opn4x-like protein ((b) red), α-Tubulin (DM1A) ((a) green), Prox-1 ((a) red; (b) green), and nuclei staining by DAPI (blue), and then visualized by confocal microscopy as described in Section 2.

in the chicken express clock genes [7], this is the first time that the presence of clock genes and AA-NAT together has been shown in primary cultures of both Opn4x (+) RGCs and isolated HCs in the developing retina when PRCs are not yet functional [33]. Based on these observations we may infer that inner retinal cells (RGCs and HCs) contain components of the molecular and genetic machinery for endogenous rhythm generation. Moreover, highly enriched preparations of inner retinal cells containing HCs, among other cells, from mature lyophilized retinas, display detectable levels of AA-NAT activity (data not shown) with values closely related to those found in RGCs [8]. In addition, it has

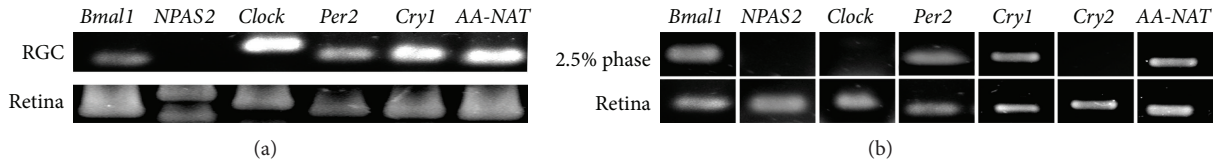

Figure 4: Analysis of mRNA expression in primary cultures of chicken RGCs at E8 (a) and of HCs at E15 (b) and in the whole postnatal chicken retina. (a) Chicken embryonic retinas were dissected out at E8 and RGCs were purified and cultured. Expression of clock genes cryptochrome 1 (*Cry 1*), *Clock*, *Bmal1*, *NPAS2*, and *Per 2* and clock-outputs: the melatonin synthesizing enzyme, arylalkylamine *N*-acetyltransferase (AA-NAT) mRNA was assessed by the reverse transcription- (RT-) polymerase chain reaction (PCR). *Cry 1*, *Per2 Clock*, *Bmal1*, and *AA-NAT* PCR products were found in RGC cultures whereas no detectable amplification was found for the *NPAS2* transcript. (b) Chicken embryonic retinas were dissected out at E15, and HCs were purified and cultured. mRNA expression for clock genes cryptochromes 1 (*Cry 1*) and 2 (*Cry 2*), *Bmal 1*, and *Clock* and for the clock-outputs AA-NAT was assessed by RT-PCR from HCs at E15 (phase 2.5%) and samples from the whole postnatal retina (positive control). Positive amplification was found for the mRNAs of *Cry 1*, *Per2*, *Bmal1*, and *AANAT* whereas *Cry2*, *NPAS2*, and *Clock* amplifications products were not found in HC cultures.

been reported that AA-NAT levels can vary along with variation of the intracellular Ca^{+2} content [34]. In this respect, *Opn4x* expressed in chicken HCs, if functionally photoactive, could be implicated in the putative mechanism of AA-NAT variation likely triggered by light stimulation. Nevertheless, further studies will be required to demonstrate the intrinsic photoreceptive capacity of these cells in the chicken retina.

Remarkably, visual photoreceptor cells (cones and rods) and ipRGCs in the vertebrate retina together with oscillators located in the pineal gland of nonmammalian vertebrates are all photoreceptive and capable of producing melatonin in a circadian fashion [1]. Although HCs express the photopigment *Opn4x* and exhibit detectable levels of clock genes and *AA-NAT* mRNAs and appreciable levels of enzyme activity were found in inner retinal preparations of postnatal retinas (data not shown), future research will address the potential capacity of HCs to synthesize acetylserotonin and/or more complex methoxyindoles as well as their potential intrinsic responsiveness to light.

4. Conclusions

In this work, we have further characterized primary cultures of two different populations of inner retinal cells (RGCs and HCs) at early developmental stages (E8–E15) that express the nonvisual photopigment Opn4x. Opn4 has been shown to confer intrinsic photosensitivity on nonretinal cells [35, 36] and to be responsible for light detection, regulating a number of nonvisual activities (synchronization of biological rhythms, suppression of pineal melatonin, sleep, etc) in mammals [37] and nonmammalian vertebrates [1]. Overall, the expression of this novel opsin as well as that for different circadian markers such as the clock genes *Bmal1*, *Per*, and *Cry* and the key melatonin synthesizing enzyme, AA-NAT, appears very early in development in RGCs and HCs, even before any sign of formal vision takes place. Inner retinal cells may therefore acquire the capacity to both sense ambient light conditions and measure time very early in development, which may help to improve the adjustment of retinal clock physiology. In this context, melatonin can act as the nocturnal circadian marker in the outer retina and together with dopamine as a diurnal signal in the inner retina regulating the function of local circuits [1]. Our observations clearly suggest that nonvisual Opn4 photoreceptors and endogenous clocks may converge in these inner retinal cell populations to further support the circadian timing system and to improve the temporal regulation of physiology.

Conflict of Interests

The authors declare that there is no conflict of interests regarding the publication of this paper.

Authors' contribution

Nicolás M. Díaz, Luis P. Morera, and Daniela M. Verra contributed equally to this work.

Acknowledgments

This work has been supported by Agencia Nacional de Promoción Científica y Técnica (FONCyT, PICT 2010 N° 647 and PICT 2012 N° 0364), Consejo Nacional de Investigaciones Científicas y Tecnológicas de la República Argentina (CONICET), Secretaría de Ciencia y Tecnología de la Universidad Nacional de Córdoba (SeCyT-UNC), and Ministry of Science and Technology of Córdoba (MinCyT-Cba).

References

[1] M. E. Guido, E. Garbarino-Pico, M. A. Contin et al., "Inner retinal circadian clocks and non-visual photoreceptors: novel players in the circadian system," *Progress in Neurobiology*, vol. 92, no. 4, pp. 484–504, 2010.

[2] J. C. Dunlap, J. J. Loros, and P. J. DeCoursey, *Chronobiology : Biological Timekeeping*, Sinauer Associates, Sunderland, Mass, USA, 2004.

[3] P. M. Iuvone, "Development of melatonin synthesis in chicken retina: regulation of serotonin N-acetyltransferase activity by light, circadian oscillators, and cyclic AMP," *Journal of Neurochemistry*, vol. 54, no. 5, pp. 1562–1568, 1990.

[4] C. T. Steele, G. Tosini, T. Siopes, and H. Underwood, "Time keeping by the quail's eye: circadian regulation of melatonin production," *General and Comparative Endocrinology*, vol. 145, no. 3, pp. 232–236, 2006.

[5] M. J. Bailey, P. D. Beremand, R. Hammer, E. Reidel, T. L. Thomas, and V. M. Cassone, "Transcriptional profiling of circadian patterns of mRNA expression in the chick retina," *The Journal of Biological Chemistry*, vol. 279, no. 50, pp. 52247–52254, 2004.

[6] S. S. Chaurasia, M. D. Rollag, G. Jiang et al., "Molecular cloning, localization and circadian expression of chicken melanopsin (Opn4): differential regulation of expression in pineal and retinal cell types," *Journal of Neurochemistry*, vol. 92, no. 1, pp. 158–170, 2005.

[7] L. H. R. G. De Lima, K. P. Dos Santos, and A. M. De Lauro Castrucci, "Clock genes, melanopsins, melatonin, and dopamine key enzymes and their modulation by light and glutamate in chicken embryonic retinal cells," *Chronobiology International*, vol. 28, no. 2, pp. 89–100, 2011.

[8] E. Garbarino-Pico, A. R. Carpentieri, M. A. Contin et al., "Retinal ganglion cells are autonomous circadian oscillators synthesizing *N*-acetylserotonin during the day," *The Journal of Biological Chemistry*, vol. 279, no. 49, pp. 51172–51181, 2004.

[9] E. Garbarino-Pico, A. R. Carpentieri, P. I. Castagnet et al., "Synthesis of retinal ganglion cell phospholipids is under control of an endogenious circadian clock: daily variations in phospholipid-synthesizing enzyme activities," *Journal of Neuroscience Research*, vol. 76, no. 5, pp. 642–652, 2004.

[10] R. Haque, S. S. Chaurasia, J. H. Wessel III, and P. M. Iuvone, "Dual regulation of cryptochrome I mRNA expression in chicken retina by light and circadian oscillators," *NeuroReport*, vol. 13, no. 17, pp. 2247–2251, 2002.

[11] P. M. Iuvone, M. Bernard, A. Alonso-Gomez, P. Greve, V. M. Cassone, and D. C. Klein, "Cellular and molecular regulation of serotonin N-acetyltransferase activity in chicken retinal photoreceptors," *Biol Signals*, vol. 6, no. 4-6, pp. 217–224, 1997.

[12] P. M. Iuvone, G. Tosini, N. Pozdeyev, R. Haque, D. C. Klein, and S. S. Chaurasia, "Circadian clocks, clock networks, arylalkylamine *N*-acetyltransferase, and melatonin in the retina," *Progress in Retinal and Eye Research*, vol. 24, no. 4, pp. 433–456, 2005.

[13] G. Tosini, K. Baba, C. K. Hwang, and P. M. Iuvone, "Melatonin: an underappreciated player in retinal physiology and pathophysiology," *Experimental Eye Research*, vol. 103, pp. 82–89, 2012.

[14] J. A. Mohawk, C. B. Green, and J. S. Takahashi, "Central and peripheral circadian clocks in mammals," *Annual Review of Neuroscience*, vol. 35, pp. 445–462, 2012.

[15] I. Provencio, I. R. Rodriguez, G. Jiang, W. P. Hayes, E. F. Moreira, and M. D. Rollag, "A novel human opsin in the inner retina," *Journal of Neuroscience*, vol. 20, no. 2, pp. 600–605, 2000.

[16] D. M. Berson, F. A. Dunn, and M. Takao, "Phototransduction by retinal ganglion cells that set the circadian clock," *Science*, vol. 295, no. 5557, pp. 1070–1073, 2002.

[17] M. A. Contin, D. M. Verra, and M. E. Guido, "An invertebrate-like phototransduction cascade mediates light detection in the chicken retinal ganglion cells," *The FASEB Journal: Official Publication of the Federation of American Societies for Experimental Biology*, vol. 20, no. 14, pp. 2648–2650, 2006.

[18] M. A. Contín, D. M. Verra, G. Salvador, M. Ilincheta, N. M. Giusto, and M. E. Guido, "Light activation of the phosphoinositide cycle in intrinsically photosensitive chicken retinal ganglion cells," *Investigative Ophthalmology and Visual Science*, vol. 51, no. 11, pp. 5491–5498, 2010.

[19] M. J. Bailey and V. M. Cassone, "Melanopsin expression in the chick retina and pineal gland," *Molecular Brain Research*, vol. 134, no. 2, pp. 345–348, 2005.

[20] S. Tomonari, A. Takagi, S. Akamatsu, S. Noji, and H. Ohuchi, "A non-canonical photopigment, melanopsin, is expressed in the differentiating ganglion, horizontal, and bipolar cells of the chicken retina," *Developmental Dynamics*, vol. 234, no. 3, pp. 783–790, 2005.

[21] D. M. Verra, M. A. Contín, D. Hicks, and M. E. Guido, "Early onset and differential temporospatial expression of melanopsin isoforms in the developing chicken retina," *Investigative Ophthalmology and Visual Science*, vol. 52, no. 8, pp. 5111–5120, 2011.

[22] M. Araki and H. Kimura, "GABA-like immunoreactivity in the developing chick retina: differentiation of GABAergic horizontal cell and its possible contacts with photoreceptors," *Journal of Neurocytology*, vol. 20, no. 5, pp. 345–355, 1991.

[23] R. A. Poché and B. E. Reese, "Retinal horizontal cells: challenging paradigms of neural development and cancer biology," *Development*, vol. 136, no. 13, pp. 2141–2151, 2009.

[24] D. Arendt, "Evolution of eyes and photoreceptor cell types," *International Journal of Developmental Biology*, vol. 47, no. 7-8, pp. 563–571, 2003.

[25] M. A. Brocco and P. Panzetta, "Survival and process regrowth of purified chick retinal ganglion cells cultured in a growth factor lacking medium at low density. Modulation by extracellular matrix proteins," *Developmental Brain Research*, vol. 118, no. 1-2, pp. 23–32, 1999.

[26] L. P. Morera, N. M. Diaz, and M. E. Guido, "A novel method to prepare highly enriched primary cultures of chicken retinal horizontal cells," *Experimental Eye Research*, vol. 101, pp. 44–48, 2012.

[27] S. S. Chaurasia, R. Haque, N. Pozdeyev, C. R. Jackson, and P. M. Iuvone, "Temporal coupling of cyclic AMP and Ca^{2+}/calmodulin-stimulated adenylyl cyclase to the circadian clock in chick retinal photoreceptor cells," *Journal of Neurochemistry*, vol. 99, no. 4, pp. 1142–1150, 2006.

[28] D. M. Berson, "Strange vision: ganglion cells as circadian photoreceptors," *Trends in Neurosciences*, vol. 26, no. 6, pp. 314–320, 2003.

[29] I. M. Bird, "Phosphoinositidase C activation assay. I. Cell labeling, stimulation, and recovery of cellular [3H]phosphoinositides and [3H]phosphoinositols," *Methods in Molecular Biology*, vol. 105, pp. 1–9, 1998.

[30] I. M. Bird, "Phosphoinositidase C activation assay. II. Simple analysis of recovered cellular phosphoinositides and phosphoinositols," *Methods in Molecular Biology*, vol. 105, pp. 11–23, 1998.

[31] I. M. Bird, "Preparation of [3H]phosphoinositol standards and conversion of [3H]phosphoinositides to [3H]phosphoinositols," *Methods in Molecular Biology*, vol. 105, pp. 65–76, 1998.

[32] E. G. Bligh and W. J. Dyer, "A rapid method of total lipid extraction and purification," *Canadian journal of biochemistry and physiology*, vol. 37, no. 8, pp. 911–917, 1959.

[33] S. Thanos and J. Mey, "Development of the visual system of the chick II. Mechanisms of axonal guidance," *Brain Research Reviews*, vol. 35, no. 3, pp. 205–245, 2001.

[34] T. N. Ivanova and P. M. Iuvone, "Melatonin synthesis in retina: circadian regulation of arylalkylamine *N*-acetyltransferase activity in cultured photoreceptor cells of embryonic chicken retina," *Brain Research*, vol. 973, no. 1, pp. 56–63, 2003.

[35] Z. Melyan, E. E. Tarttelin, J. Bellingham, R. J. Lucas, and M. W. Hankins, "Addition of human melanopsin renders mammalian

cells photoresponsive," *Nature*, vol. 433, no. 7027, pp. 741–745, 2005.

[36] X. Qiu, T. Kumbalasiri, S. M. Carlson et al., "Induction of photosensitivity by heterologous expression of melanopsin," *Nature*, vol. 433, no. 7027, pp. 745–749, 2005.

[37] R. J. Lucas, "Mammalian inner retinal photoreception," *Current Biology*, vol. 23, no. 3, pp. R125–R133, 2013.

Hindawi Publishing Corporation
BioMed Research International
Volume 2014, Article ID 424982, 15 pages
http://dx.doi.org/10.1155/2014/424982

Research Article

Circadian Modulation of the Cl^- Equilibrium Potential in the Rat Suprachiasmatic Nuclei

Javier Alamilla,[1,2] Azucena Perez-Burgos,[1,3] Daniel Quinto,[1] and Raúl Aguilar-Roblero[1]

[1] *División de Neurociencias, Instituto de Fisiología Celular, Universidad Nacional Autónoma de México, Apartado Postal 70-253, 04510 México, DF, Mexico*
[2] *Department of Psychology, Neuroscience & Behaviour, McMaster University, Hamilton, ON, Canada L8S 4K1*
[3] *McMaster Brain-Body Institute, St Joseph's Healthcare, Hamilton, ON, Canada L8N 4A6*

Correspondence should be addressed to Raúl Aguilar-Roblero; raguilar@ifc.unam.mx

Received 27 January 2014; Revised 23 March 2014; Accepted 27 March 2014; Published 18 May 2014

Academic Editor: Mario Guido

The suprachiasmatic nuclei (SCN) constitute a circadian clock in mammals, where γ-amino-butyric acid (GABA) neurotransmission prevails and participates in different aspects of circadian regulation. Evidence suggests that GABA has an excitatory function in the SCN in addition to its typical inhibitory role. To examine this possibility further, we determined the equilibrium potential of GABAergic postsynaptic currents (E_{GABA}) at different times of the day and in different regions of the SCN, using either perforated or whole cell patch clamp. Our results indicate that during the day most neurons in the dorsal SCN have an E_{GABA} close to −30 mV while in the ventral SCN they have an E_{GABA} close to −60 mV; this difference reverses during the night, in the dorsal SCN neurons have an E_{GABA} of −60 mV and in the ventral SCN they have an E_{GABA} of −30 mV. The depolarized equilibrium potential can be attributed to the activity of the Na(+)-K(+)-2Cl(−) (NKCC) cotransporter since the equilibrium potential becomes more negative following addition of the NKCC blocker bumetanide. Our results suggest an excitatory role for GABA in the SCN and further indicate both time (day versus night) and regional (dorsal versus ventral) modulation of E_{GABA} in the SCN.

1. Introduction

The main pacemakers implicated in the regulation of circadian rhythms in mammals are the suprachiasmatic nuclei (SCN) [1]. The SCN is divided into two distinct anatomical and functional subdivisions: the ventrolateral SCN or core, which receives most of the afferent inputs to the SCN from the retina, the median raphe nucleus, and the intergeniculate leaflet and has been implicated in entrainment to external cycles, and the dorsomedial SCN, or shell, which has been implicated in the pacemaker function and in the output of the circadian clock to the rest of the brain [2–4]. A molecular oscillator, involving translation-transcription loops of specific clock genes in SCN neurons, generates circadian overt rhythms from the pacemaker neurons as the spontaneous firing rate (SFR), metabolic activity, and synthesis and secretion of neurotransmitters and neuropeptides [5].

The most widespread neurotransmitter in the SCN is GABA, which colocalizes with different peptides in specific regions of the SCN. For example, vasopressin colocalizes with GABA in the dorsomedial region and vasoactive intestinal polypeptide colocalizes with GABA in the ventromedial region [6, 7]. The GABA synthesizing enzyme L-glutamic acid decarboxylase (GAD) and the concentration of GABA itself have distinct circadian rhythmicity in SCN neurons [8]. There is also circadian rhythmicity in the frequency of spontaneous inhibitory GABAergic postsynaptic currents [9, 10]. Furthermore, several studies indicate that GABA plays an important role in the entrainment of the circadian rhythms [11–13]; it also seems to couple the dorsal and ventral SCN in order to function as an integrated oscillator [14].

Wagner et al. [15] first described excitatory effects of GABA in SCN during daytime, which created some controversy about the role of GABA as a neurotransmitter in SCN neurons. Some studies indicate that GABA has its usual inhibitory functions [16–18], whereas others support excitatory actions of GABA in the SCN nuclei [19, 20]. Additionally, de Jeu and Pennartz [21] found excitatory effects of GABA during the night, Albus et al. [14] demonstrated excitatory actions of GABA in the dorsal part of the SCN

during the day and night, Choi et al. [22] reported excitatory actions during the night in the dorsal SCN attributable to the Cl^- cotransporter NKCC1, and Irwin and Allen [23] found that GABA elicits opposite effects on SCN neuronal Ca^{2+} responses and that excitatory responses involve the NKCC1 cotransporter. In order to contribute to resolving this controversy, we characterized E_{GABA} in the two main topographical regions of the SCN (dorsal and ventral) at two different times of the day (around midday or midnight), using perforated and whole cell patch clamp recordings in coronal brain slices.

2. Materials and Methods

2.1. Animals and General Conditions. Male Wistar rats (35–45 days old, 100–120 g) were housed under 12 : 12 h light : dark cycle (lights on at 6:00, 400 lux; 22°+/−1°C) in a sound attenuated room for a week before the experiments. For experiments during the night, animals were maintained in a reversed 12 : 12 h light : dark cycle (lights on at 22:00 h, 400 lux) for 3 weeks before the experiments. Animals had food and water *ad libitum*. All the procedures were conducted according to the guidelines for use of experimental animals from the Universidad Nacional Autónoma de México in accordance with national laws (NOM-062-200-1999) and the guidelines from the Society for Neuroscience.

2.2. Slice Preparation. Rats were deeply anaesthetized with isoflurane 3 h after lights on (ZT 3) and their brains were quickly removed and placed in an ice cold low Ca^{2+} artificial cerebrospinal fluid (aCSF) containing (in mM): 126 NaCl, 2.5 KCl, 1.2 NaH_2PO_4, 4 $MgCl_2$, 0.5 $CaCl_2$, 26 $NaHCO_3$, and 10 glucose, pH 7.38, 330 mOsm/L, oxygenated with 95% O_2/5% CO_2. For night recording, to avoid phase shifts induced by light, the brain extraction was done 1 h before lights off (ZT 11). Coronal slices (250–300 μm) containing the SCN were cut on a vibratome (Vibratome, St. Louis, MO, USA) and transferred to a recovery chamber with fresh low Ca^{2+} aCSF at RT until use (at least 1 hour of recovery). The slices were then placed in the recording chamber and continuously perfused (2.5–5 mL/min) with oxygenated aCSF. The recording chamber solution was the same as the extraction solution except that $CaCl_2$ was increased to 2.4 mM and $MgCl_2$ reduced to 1.3 mM. SCN neurons were viewed and the recording electrodes were positioned by infrared Nomarski microscopy at 60x using a Nikon Eclipse 600 (Nikon, Melville, NY, USA) with a Dage MTI video camera and monitor.

2.3. Patch Clamp Recordings. Voltage clamp recordings were performed with either perforated or whole cell patch clamp techniques at RT (20–25°C). Recordings were made either between 5 and 10 h after lights on (ZT 5–10, day) or between 5 and 10 h after lights off (ZT 17–22, night). For perforated patch recordings, borosilicate electrodes (tip diameter, 1.0–1.5 μm; 3–5 MΩ, WPI, Sarasota, FL, USA) were filled with intracellular solution containing (in mM): 143 K-gluconate, 2 KCl, 10 HEPES, and 0.5 EGTA, pH 7.38, adjusted with KOH, 275 mOsml/L. The antibiotic gramicidin was used in order to maintain the intracellular Cl^- concentration $[Cl^-]_i$ [24]. Gramicidin was dissolved in dimethyl sulfoxide (DMSO) and was prepared as a stock solution on the day of the experiment (10 mg/mL). The intracellular solution plus gramicidin (50 μg/mL) was not filtered. The recording electrodes were backfilled with the gramicidin-containing solution and the tip of the electrode was filled with gramicidin-free solution. It usually took between 5 and 10 min to perforate the membrane and between 15 and 30 min to obtain a stable series resistance. Capacitance and series resistance were compensated by a minimum of 80%, and the seal was monitored throughout each experiment. Cells were discarded if input resistance was lower than 150 MΩ and/or access resistance exceeded 45 MΩ or changed more than 15%. Access resistance was usually ≤35 MΩ.

Two intracellular solutions were used for whole cell recordings. The first had a calculated E_{Cl^-} of −30 mV (at 25°C) and contained (in mM): 72 KH_2PO_4, 36 KCl, 2 $MgCl_2$, 10 HEPES, 1.1 EGTA, 0.2 Na_2ATP, and 0.2 Na_2GTP, pH 7.38 adjusted with KOH, 275 mOsmol/L. The other intracellular solution had a calculated E_{Cl^-} of −60 mV (at 25°C) and contained (in mM): 111 KH_2PO_4, 12 KCl, 2 $MgCl_2$, 10 HEPES, 1.1 EGTA, 0.2 Na_2ATP, and 0.2 Na_2GTP, pH 7.2, adjusted with KOH, 275 mOsmol/L. Pipettes had a tip diameter of 1.0–1.5 μm and a resistance of 3–5 MΩ. Once a good seal was obtained (above 2 GΩ) between the recording electrode and the neuron, the membrane was disrupted by a gentle suction. Capacitance and series resistance were compensated and the seal was monitored similarly to perforated patch experiments. Neurons were discarded if input resistance was <150 MΩ and/ or if access resistances were >25 MΩ or changed more than 15% during the experiment. The average access resistance was less than 15 MΩ.

Recordings were made with an Axopatch 200B amplifier (Axon instruments, Foster City, CA, USA). Online data was collected with a custom made program in the LabView environment through a digital acquisition board (DAQ, National Instruments, Austin, TX, USA). Recordings were sampled at 10 kHz and filtered at 5 kHz.

2.4. Postsynaptic Currents. To examine spontaneous postsynaptic currents (sPSCs) at different membrane holding potentials (from −100 mV to +80 mV), QX-314 (5 mM) was added into the recording pipette solution in order to block Na^+ currents. Pharmacological isolation of GABAergic sPSCs was accomplished by adding DL-2-amino-5-phosphonopentanoic acid (APV, 50 μM) and 6,7-dinitroquinoxaline-2,3(1H,4H)-dione (DNQX, 10 μM) into the recording aCSF. Bicuculline methiodide (10 μM) was applied to abolish all the spontaneous synaptic inputs and to confirm that GABA produced the sPSCs. Bumetanide (10 μM) was used to block NKCC1 in order to determine its contribution to E_{GABA}. All drugs were purchased from Sigma (St. Louis, MO, USA).

2.5. Localization of Recorded Neurons in the Dorsal or Ventral Regions of the SCN. The neurons recorded were visualized using a 10x objective water immersion lens (Nikon) and

Table 1: Descriptive statistics from GABAergic sPSCs equilibrium potentials (E_{GABA} in mV) recorded from SCN neurons in perforated patch configuration.

Variable	Group	n	min	max	median
	All neurons	97	−9	−87	−51
Region	Dorsal	62	−9	−87	−49.5
	Ventral	35	−18	−81	−51
Time	Day	59	−9	−87	−50
	Night	38	−9	−81	−51

marked in a representative drawing of the SCN (previously prepared) with the third ventricle at the center and the optic chiasm at the bottom, which resembles the coronal slice with the two SCN. When the experiment was finished, the schematic drawing was analyzed by an independent observer and neurons were categorized as ventral or dorsal according to Abrahamson and Moore [2].

2.6. Electrophysiological Data Analysis. Analysis of the synaptic currents was done with Mini Analysis 6.0.3 (Synaptosoft, Decatur, GA, USA). The E_{GABA} was estimated as follows: (1) for the average E_{GABA} obtained from the neurons at each group (SCN region/time of recording). The E_{GABA} in each neuron was calculated by the interception of zero current with its corresponding voltage value (mV). To calculate the zero current, we fitted a third order polynomial curve to the I-V plot using Origin 8 (Origin Lab, Northampton, MA, USA) and (2) by the interception of the zero current and its corresponding voltage (mV) obtained by the I-V curves shown in the figures. Each dot indicates the mean ± SEM current that was obtained from the neurons in the corresponding category (SCN region/time of recording). The line represents a third order polynomial curve fit to all data in the I-V. There were only minor discrepancies in the E_{GABA} data obtained by the two methods.

2.7. Statistical Analysis. The values are reported in text and tables as the range from the minimum to the maximal individual values, median, and mean ± SEM for each group. Normality tests (Shapiro-Wilk) were applied to the different samples (E_{GABA} sorted by the SCN region/time of recording) for perforated patch and whole cell recordings. The groups were not normally distributed ($P < 0.05$). Gaussian curves were fitted to the data graphed in frequency histograms. "Best fit" analyses suggested the presence of more than one population in the sample (χ^2, R^2). −50 mV was chosen to divide the samples for two reasons: (1) this value split the Gaussian curves (the tails of the curves overlapped around this point) and (2) the median for all the samples was equal or very close to −50 mV (Table 1).

Statistical analysis was done using GraphPad Prism 4.0 (GraphPad Sowftware, La Joya, CA, USA), Origin 8, and SPSS (IBM Corporation, Armonk, NY). Statistical tests were nonparametric (Wilcoxon test for matched pairs) unless otherwise stated. Kruskal-Wallis for independent samples was performed in those data that represent the predominant part of the sample (above or below −50 mV) for the experiments in perforated patch configuration. The α level was set at 0.05.

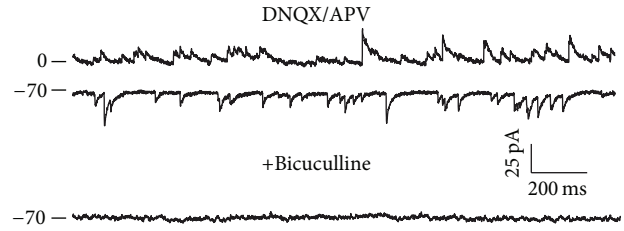

Figure 1: Spontaneous GABAergic postsynaptic currents in the suprachiasmatic nucleus. GABA sPSCs were pharmacologically isolated by administration of the ionotropic glutamate receptor antagonists, DNQX (10 μM) and APV (50 μM). Recordings at 0 mV and −70 mV are shown. Subsequent bicuculline administration (10 μM) completely abolished the sPSCs at all membrane holding potentials. Example recordings obtained in a dorsal SCN neuron during the day period in perforated patch configuration.

3. Results

A total of 178 SCN neurons were recorded; 97 neurons were recorded in perforated patch configuration and the remaining 81 in whole cell configuration. All experiments were carried out in the presence of DNQX and APV in order to isolate the GABAergic synaptic currents. At least 100 sPSCs were analyzed at each holding potential from −100 mV to +80 mV (20 mV steps). The GABAergic nature of the sPSCs was confirmed if they were completely abolished by bicuculline administration (Figure 1).

3.1. Perforated Patch Clamp Recordings. The descriptive statistics of the equilibrium potential of sPSCs from all 97 neurons are shown in Table 1. No differences were found when the data was sorted by either SCN location (dorsal versus ventral, Figure 3(a)) or time of recording (subjective day versus subjective night, Figure 3(b)). Nevertheless, inspection of the frequency histogram of sPSCs equilibrium potential suggests the presence of more than one population, one above and one below −50 mV. This was examined further by fitting the frequency histogram to a two-peak Gaussian model; the results demonstrate a $\chi^2 = 9.8$ and a $R^2 = 0.88$ (Figure 2(a)). Arrangement of the data by SCN location or time of recording showed in all cases a similar pattern of two partially overlapped Gaussian distributions around −50 mV as shown in Figures 2(b)–2(e).

Inspection of the histograms revealed asymmetric patterns of the E_{GABA} between dorsal and ventral SCN and between neurons recorded during the day and those recorded during the night; therefore, we reanalyzed the data by grouping the neurons according to the SCN region and time of recording and whether the equilibrium potential was above or below −50 mV (Figure 3(c)). Of 45 neurons recorded during the day in the dorsal SCN, the E_{GABA} was −64 ± 3 mV in 19 neurons (42.2%) and −36 ± 2 mV in 26

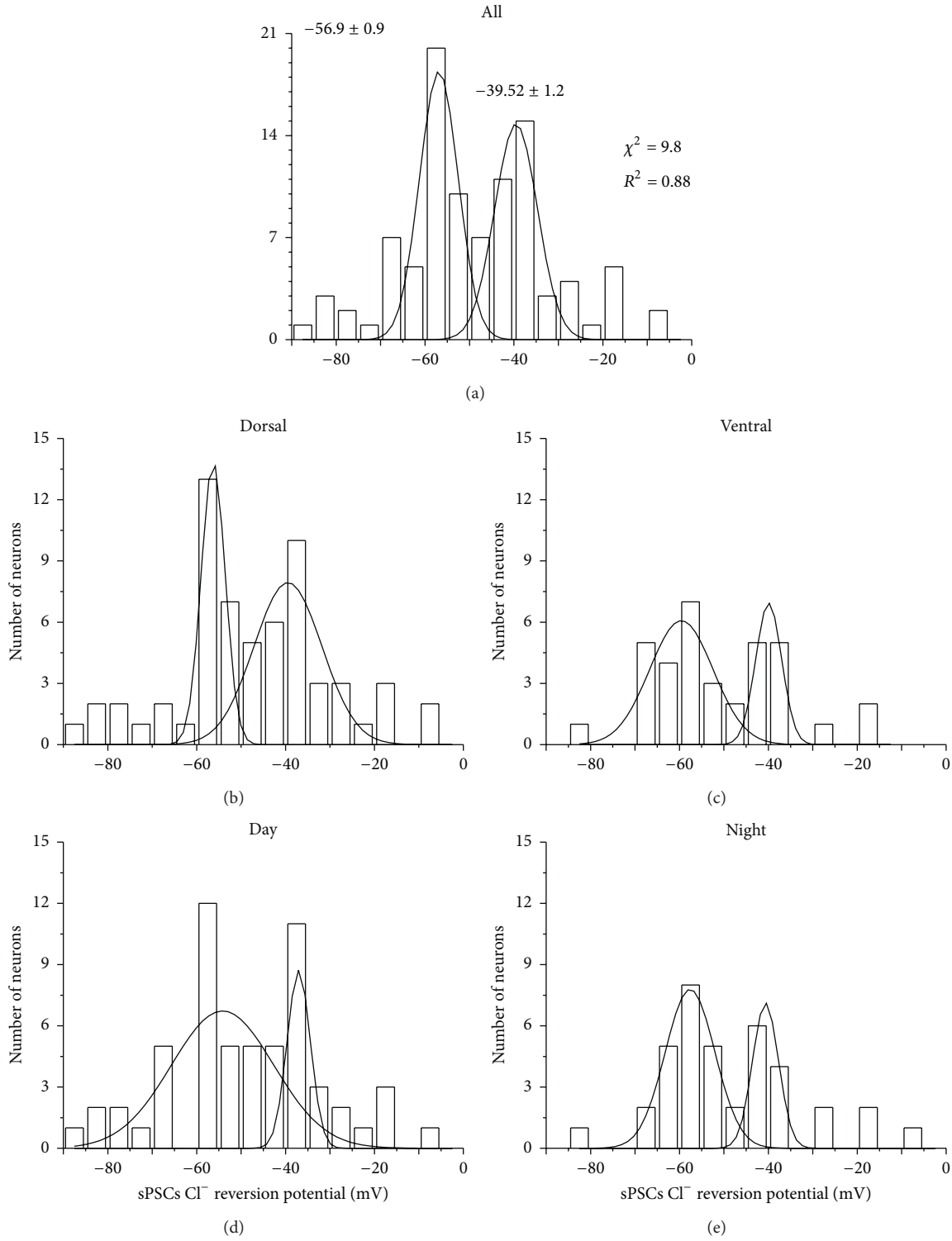

FIGURE 2: Frequency histograms of E_{GABA} obtained using perforated patch recordings. Gaussian fitting analyses revealed two populations in E_{GABA} distribution, belonging to (a) all the neurons recorded in different ZT and SCN regions, (b, c) E_{GABA} sorted by dorsal and ventral SCN regions, and (d, e) E_{GABA} grouped by ZT of recording.

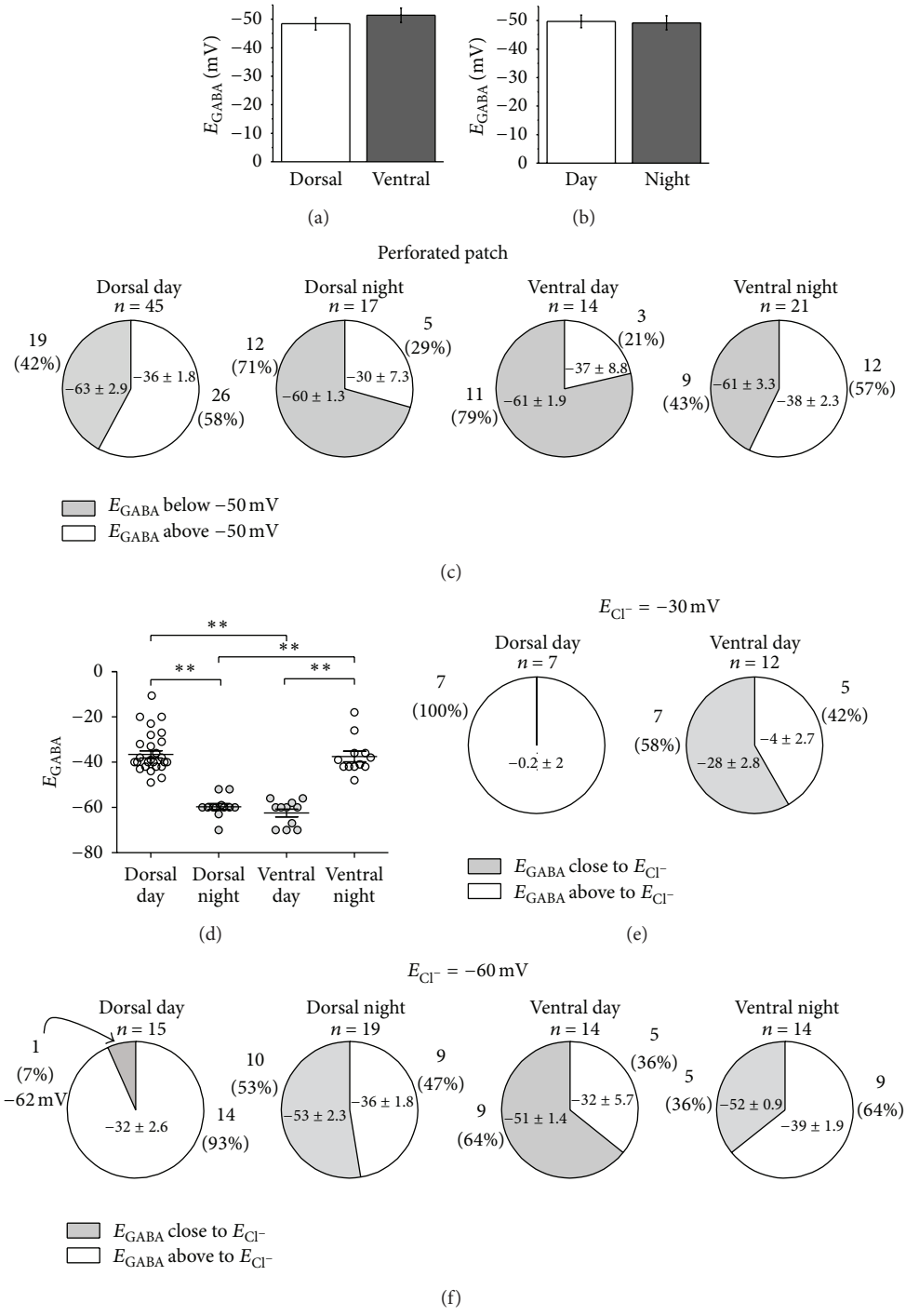

FIGURE 3: E_{GABA} distributions in the SCN. Comparison of all E_{GABA} values recorded in perforated patch configuration, grouped by SCN region (a) or ZT of recording (b). Values are shown in mean ± SEM. (c) Distribution of E_{GABA} separated by SCN region and ZT of recording. Experiments obtained in perforated patch configuration. (d) Statistically significant differences were found with Kruskal-Wallis test (H = 42.4, $P < 0.0001$). Analysis was performed with the prevailing part of the groups depicted in (c). Dunn's multiple comparison test indicated significant differences between the groups ($P < 0.05$). Distribution of E_{GABA} in neurons recorded in whole cell configuration with a theoretical E_{Cl^-} of −30 mV (e) and E_{Cl^-} of −60 mV (f).

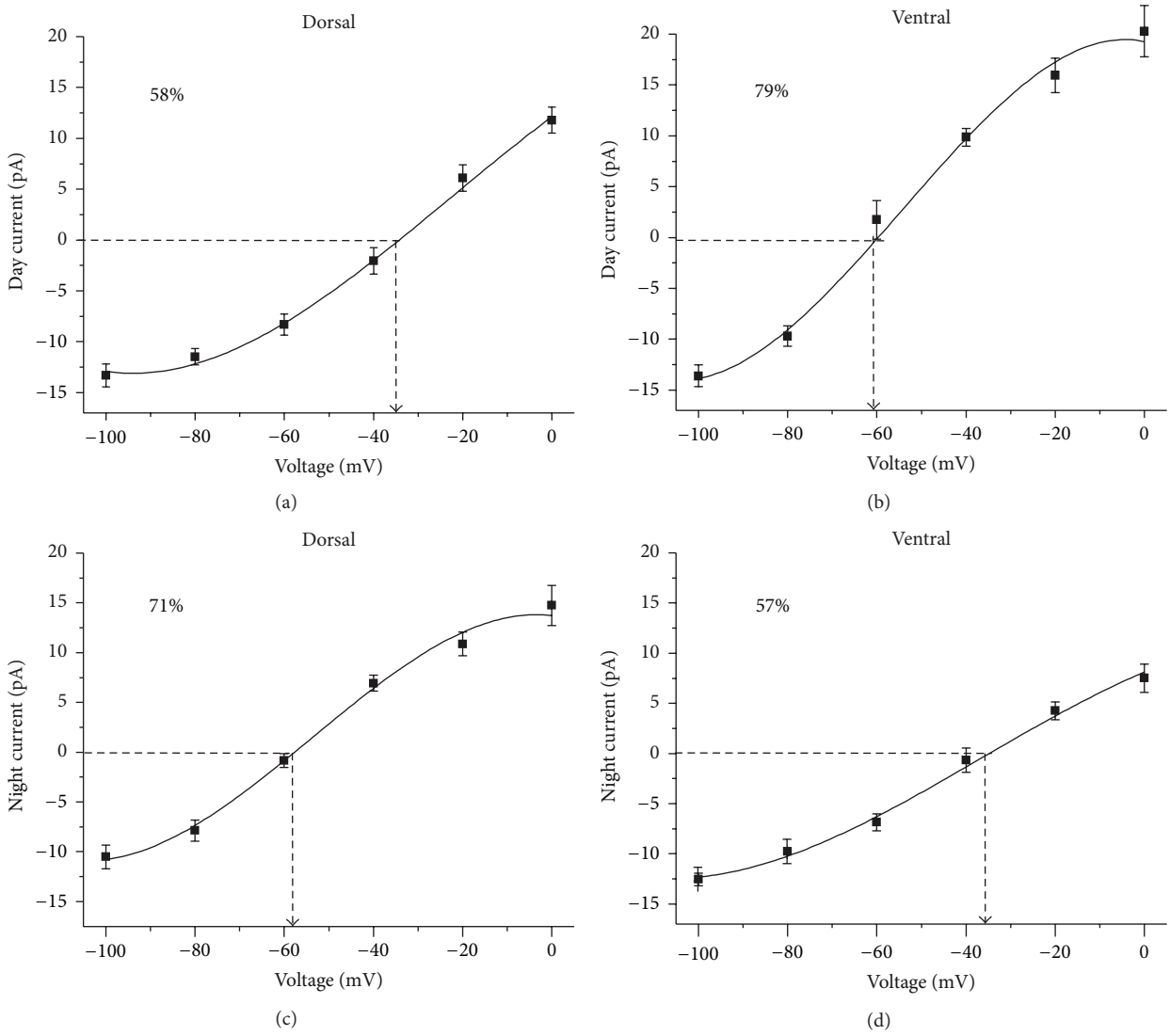

FIGURE 4: Diurnal and regional modulation of E_{GABA} from neurons recorded using perforated patch. During the day, the predominant equilibrium potential from the dorsal SCN neurons is −37 ± 2 mV (a) and in the ventral SCN is −61 ± 2 mV (b); during the night, the pattern reverses so that the predominant equilibrium potential from the dorsal SCN is −60 ± 1 mV (c) and in the ventral SCN is −38 ± 2 mV (d). Each panel shows the percentage of neurons contributing to each *I*-*V* curve.

neurons (57.8%; Figures 3(c), 4(a), and 5(a)), whereas, of 17 neurons recorded during the night in the same SCN region, the E_{GABA} was −60 ± 1 mV in 12 neurons (70.6%; Figures 3(c), 4(c), and 5(b)) and −30 ± 8 mV only in 5 neurons (29.4%). Conversely, in the ventral SCN, of 14 neurons recorded during the day, 11 (78.6%) had an E_{GABA} of −61 ± 2 mV (Figures 3(c), 4(b), and 6(a)) and 3 (21.4%) had an E_{GABA} of −37 ± 9 mV, whereas, of 21 neurons recorded in the ventral SCN region during the night, 9 (42.9%) had an E_{GABA} of −61 ± 3 mV and 12 neurons (57.1%) had an E_{GABA} of −38 ± 2 mV (Figures 3(c), 4(d), and 6(b)). These results suggest a differential regulation in $[Cl^-]_i$ depending on the region of the nucleus and ZT of recording. A Kruskal-Wallis test carried out on the data that represented the majority of each group (above or below −50 mV, Figure 3(c)) demonstrated a statistically significant difference between the groups ($H = 42.4$, $P < 0.0001$). A Dunn's multiple comparison test indicated significant differences between dorsal day versus dorsal night, dorsal day versus ventral day, dorsal night versus ventral night, and ventral day versus ventral night. ($P < 0.05$; Figure 3(d)).

As we previously stated, different research groups have identified an excitatory role of the inhibitory classical neurotransmitter in the SCN and other areas of the brain during development [25]. The most likely candidates to control $[Cl^-]_i$ are the Cl^- cotransporters. In the SCN several lines of evidence indicate that the NKCC1 cotransporter is the most important for $[Cl^-]_i$ regulation [22, 23]. In order to test the participation of the NKCC1 cotransporter in $[Cl^-]_i$ regulation, we used the selective blocker bumetanide (10 μM). Bumetanide was added to a subpopulation of the experimental groups mentioned above. In those neurons

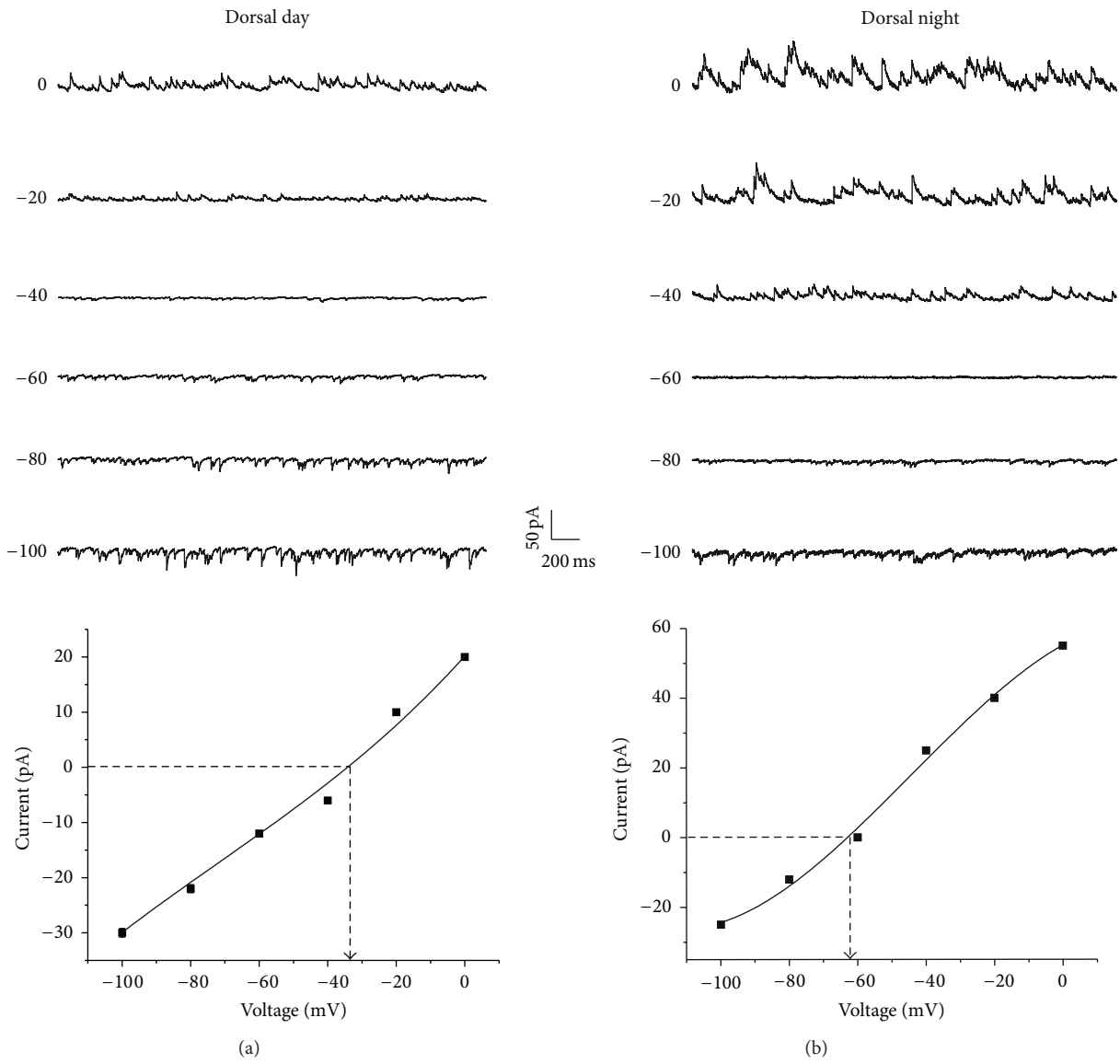

FIGURE 5: E_{GABA} in dorsal SCN region. (a) Perforated patch recording in a dorsal SCN neuron obtained during the day. E_{GABA} for this neuron was −33 mV, as shown in the *I-V* curve below. (b) Recording performed using perforated patch in a dorsal SCN neuron during the nocturnal ZT. The E_{GABA} for this example was −62 mV (*I-V* curve below).

that E_{GABA} was hyperpolarized (below −50 mV) bumetanide administration did not have any effect on the reversal potential (data not shown). In contrast with those neurons with a depolarized E_{GABA} (above −50 mV), bumetanide adding shifted the values to more negative than −50 mV ($W = 28$, $P = 0.01$, Wilcoxon test). The results are summarized in Table 2. These results are in agreement with the participation of the NKCC1 cotransporter in regulating $[Cl^-]_i$, as previously proposed [22, 23].

3.2. Whole Cell Patch Clamp Recordings. In whole cell patch clamp configuration, there is dialysis of the ions contained in the patch pipette into the intracellular space, as well as washout of elements required for neuronal functions. However, since GABAergic sPSCs depend on E_{Cl^-} we can attempt to use whole cell configuration to control (clamp) the intracellular concentration of ions and test whether SCN neurons could have a different E_{GABA} than the one predicted by the Nernst equation [26, 27]. To answer this question, we used two intracellular solutions with different Cl^- concentrations, one with an $E_{Cl^-} = -30$ mV and another with the $E_{Cl^-} = -60$ mV. We analyzed E_{GABA} in 81 SCN neurons recorded in whole cell patch clamp configuration (Figures 3(e)–3(f)). In 19 neurons recorded during the day (7 dorsal and 12 ventral) we used the internal solution with an E_{Cl^-} of −30 mV. In all dorsal SCN

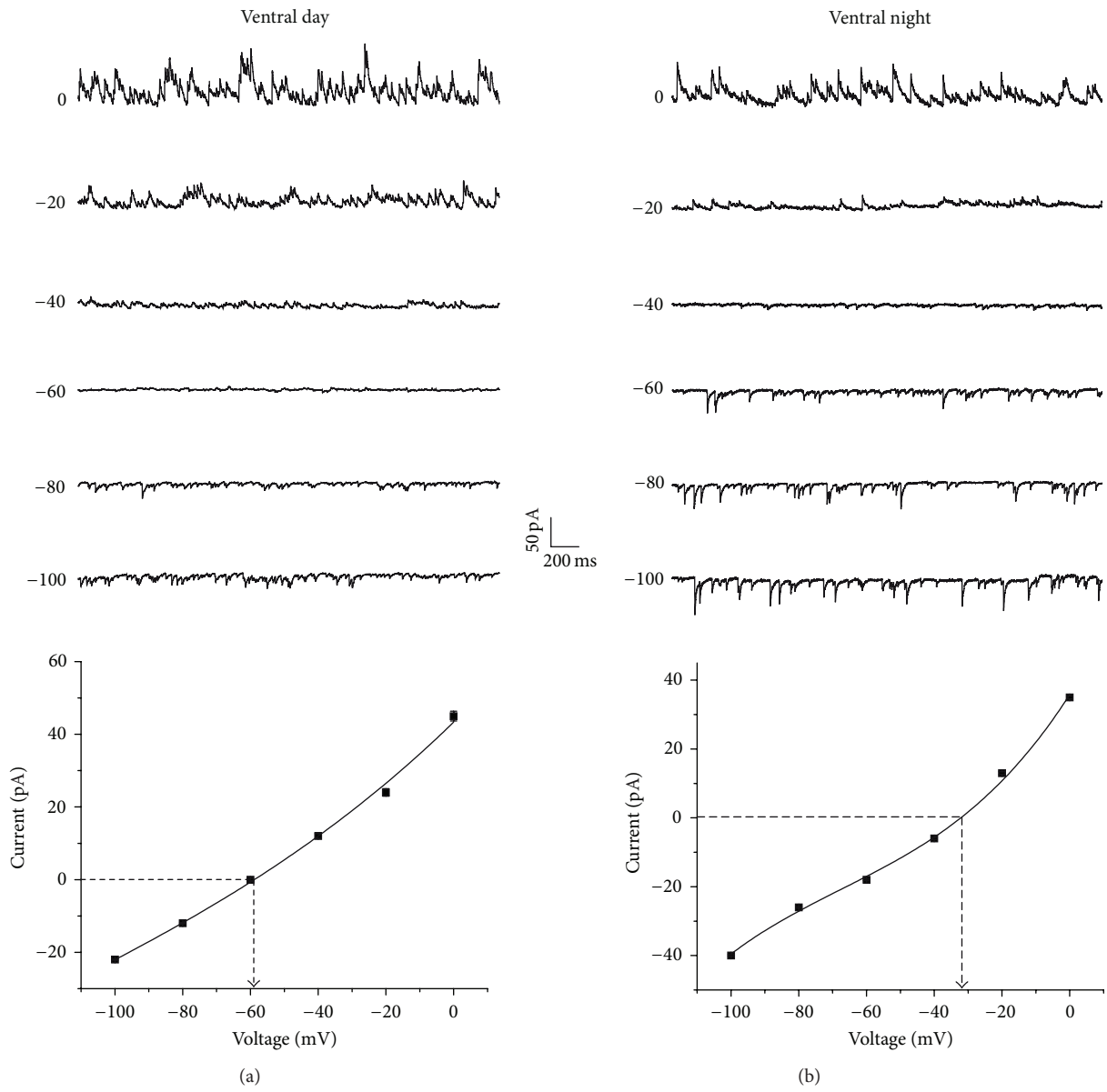

Figure 6: E_{GABA} in ventral SCN region. (a) Neuron recorded in perforated patch in a ventral SCN neuron during the day. E_{GABA} for this neuron was −58 mV (*I-V* curve below). (b) Perforated patch recording performed during the night period in a ventral SCN neuron. E_{GABA} for this cell was −33 mV (*I-V* curve below).

neurons the E_{GABA} was 0.2±2 mV, which is above the expected E_{Cl^-} (Figures 3(e) and 7(a)). In contrast, in 7 of 12 neurons in the ventral SCN (58.3%) E_{GABA} was −28 ± 2.8 mV (close to the calculated E_{Cl^-}) (Figures 3(e) and 7(b)), and in the remaining 5 neurons (41.7%) the E_{GABA} was −4 ± 2.7 mV (nearly 30 mV above the E_{Cl^-}).

We used the second intracellular solution with an E_{Cl^-} of −60 mV to record from 66 SCN neurons. In 14 of 15 dorsal SCN neurons recorded during midday the E_{GABA} was −32 ± 2.6 mV, nearly 30 mV above the E_{Cl^-} (Figures 3(f), 7(c), and 8(a)); the remaining neuron had an E_{GABA} of −62 mV, close to the expected E_{Cl^-}. In contrast, 10 of 19 neurons (52.6%) recorded from the dorsal SCN during the night showed an E_{GABA} of −53 ± 2.3 mV, close to the E_{Cl^-} (Figures 3(f) and 7(e)), whereas in the remaining 9 neurons (47.4%) the E_{GABA} was −36 ± 1.8 mV, about 30 mV above the E_{Cl^-}. In the ventral SCN, of 14 neurons recorded during midday 9 (64.3%) had an E_{GABA} of −51 ± 1.4 mV, close to the E_{Cl^-} (Figures 3(f), 7(d), and 8(b)), whereas the remaining 5 (35.7%) had an E_{GABA} of −32 ± 5.7 mV, about 30 mV above the E_{Cl^-}. Of 14 neurons recorded in the ventral SCN during the night, only 5 (35.7%) had an E_{GABA} of −52 ± 0.9 mV which is close to the E_{Cl^-}, whereas the remaining 9 neurons (64.3%) had an E_{GABA} of −39 ± 2 mV (Figures 3(f) and 7(f)). The different distribution of neurons according to the E_{GABA} in whole cell experiments (E_{Cl^-} = −60 mV; Figure 3(f)) was similar to

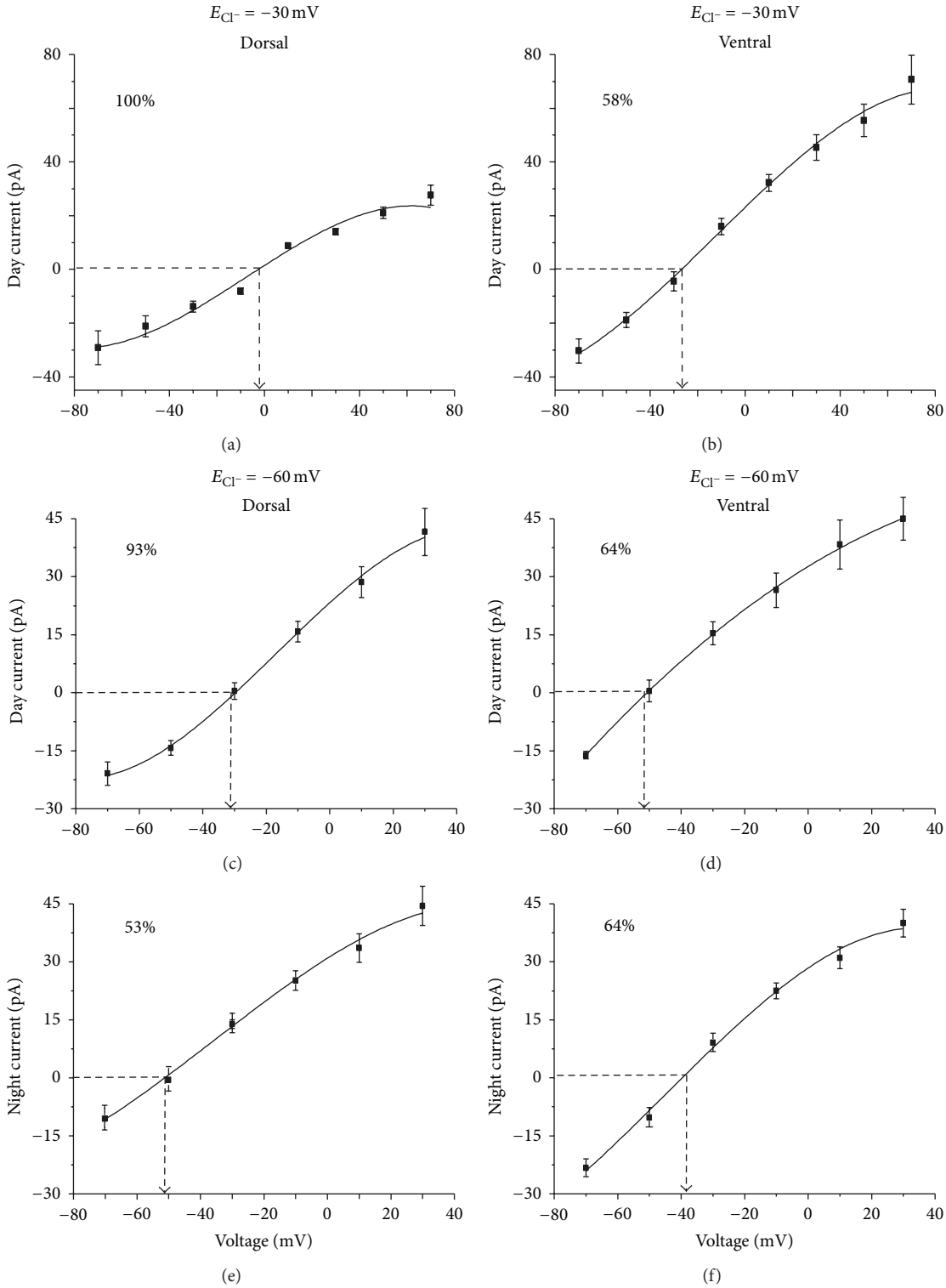

FIGURE 7: E_{GABA} is shifted from the E_{Cl^-} estimated from the Nernst equation in subpopulations of the SCN neurons recorded in whole cell configuration. At an estimated E_{Cl^-} of −30 mV, the dorsal SCN neurons recorded during the day showed an E_{GABA} of 0 ± 2 mV (a), while in ventral SCN the predominant E_{GABA} is −28 ± 3 mV (b), close to the hypothetical equilibrium potential. At an estimated E_{Cl^-} of −60 mV, when recorded during day, the predominant GABAergic sPSCs equilibrium potential in the dorsal SCN was −32 ± 2.6 mV (c), while in the ventral SCN was −51 ± 1.4 mV (d). Conversely, during the night, the predominant equilibrium potential in the dorsal SCN was −53 ± 2.3 mV (e) and in the ventral SCN was −39 ± 1.9 mV (f).

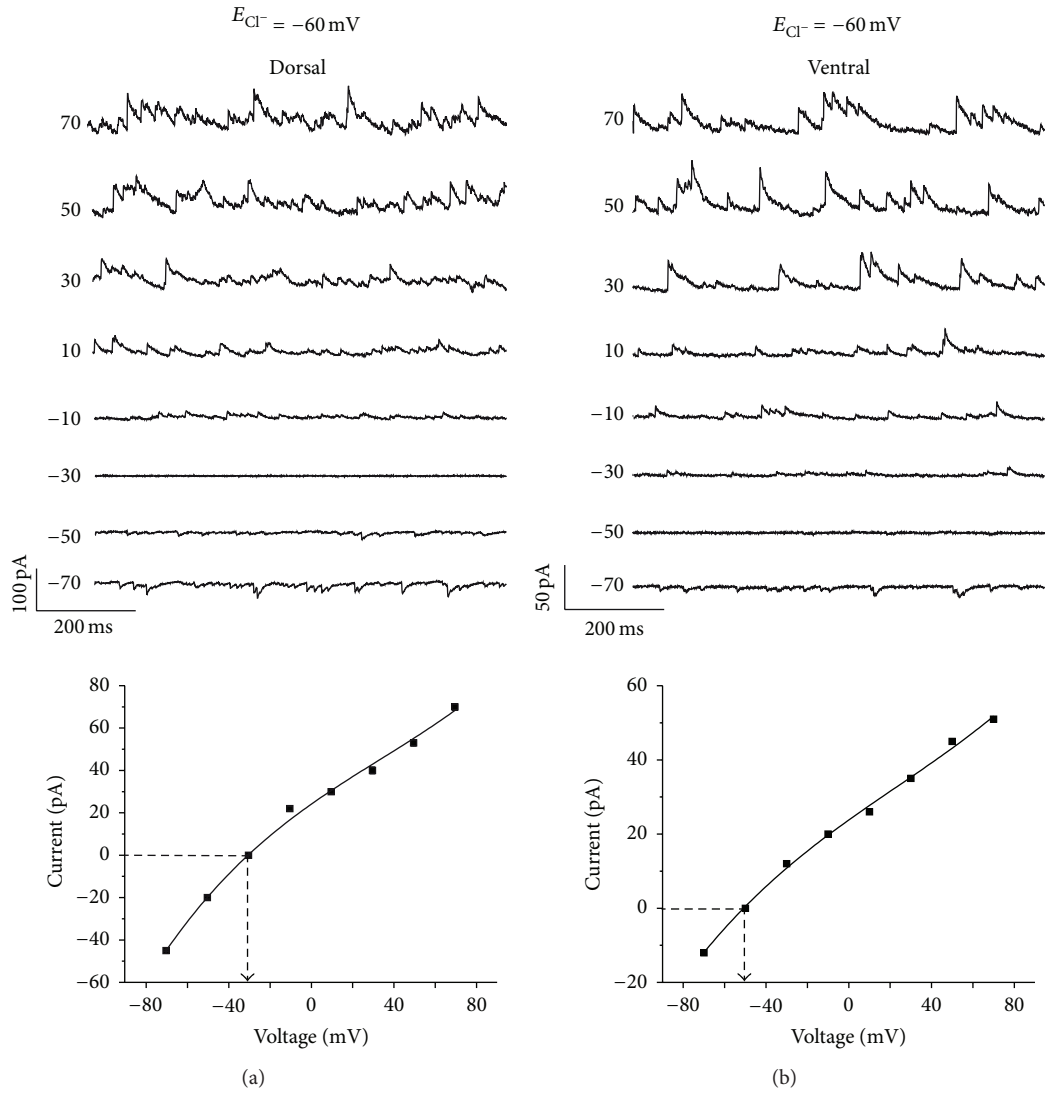

Figure 8: Regional differences in E_{GABA} obtained in whole cell configuration. (a) Dorsal SCN neuron recorded during the day in whole cell. E_{GABA} for this neuron was −30 mV (*I-V* curve below). (b) Ventral SCN neuron recorded during the day in whole cell configuration. E_{GABA} for this neuron was −50 mV (*I-V* curve below). Theoretical E_{Cl^-} = −60 mV.

Table 2: SCN neurons show two E_{GABA} depending on the region and time of recording, as shown by the relative distribution of the equilibrium potential around −50 mV. Blockade of Cl^- transporter NKCCl by bumetanide affected only the potential above −50 mV (W = 28, P = 0.01, Wilcoxon test).

Region	Time	Control		+Bumetanide	
		n	Mean ± SEM	*n*	Mean ± SEM
Dorsal	Day	26	−35.5 ± 1.8	11	−58.5 ± 3.9
	Night	5	−30.2 ± 7.3	5	−53.4 ± 3.7
Ventral	Day	3	−36.7 ± 8.8	3	−56.7 ± 3.6
	Night	12	−37.5 ± 2.3	5	−65.1 ± 8.2

the distribution found using perforated patch recording (Figure 3(c)). Together, these results suggest that the SCN neurons have autonomous mechanisms to increase $[Cl^-]_i$ that can be increased by the exogenous Cl^- concentrations contained in the recording pipette.

4. Discussion

In the majority of the mature neurons, GABA acts as an inhibitory neurotransmitter because $[Cl^-]_i$ is lower (~5 mM) than $[Cl^-]_o$ (~140 mM) which leads in most neurons to an E_{Cl^-} hyperpolarized in comparison to the resting membrane potential (E_m). Synaptic inhibition occurs when the activation of GABA or glycine receptors causes an inward flux of Cl^- ions, which in turn hyperpolarizes the neuronal E_m. $[Cl^-]_i$ is regulated by different cotransporters: the NKCCl cotransporter pumps Cl^- into the neuron, whereas the K^+

and Cl^- cotransporters (KCC2 and KCC4) pump Cl^- out of the neuron. Thus, upregulation of NKCC1 activity or downregulation of KCC2 or KCC4 activity increases $[Cl^-]_i$ which depolarizes the E_{Cl^-} with respect to the E_m, which leads GABA to produce excitatory postsynaptic responses.

4.1. Perforated Patch Experiments. In this study we analyzed the E_{GABA} in the SCN using the perforated patch clamp technique. We found at least 2 populations of SCN neurons: 53% showed an E_{GABA} close to the typical E_{Cl^-} in the adult brain, whereas 47% showed an E_{GABA} depolarized by about 30 mV as compared to the typical E_{Cl^-}. Since in the second set of neurons the E_{GABA} is depolarized with respect to −45 mV, typical E_m of SCN neurons [28], activation of $GABA_A$ receptors (R) leads to an outward flux of chloride ions following its driving force, which depolarizes SCN neurons as previously reported [14, 15, 20–23].

We also found that the relative proportion of SCN neurons expressing each E_{GABA} change with time in each of the two studied regions. Thus in dorsal part of the SCN about 58% of neurons is distributed around an E_{GABA} of -36.2 ± 2 mV during the day and decreased to 29% during the night, while in the ventral part such a depolarized value was found only in 21% of neurons recorded during the day and increased up to 57% during the night. These changes suggest that the neuronal subsets found according to the E_{GABA} represent functional states from a general neuronal population. This hypothesis may conciliate seeming discrepancies among previous reports of excitatory effects of GABA in SCN neurons either during the day [14, 15, 19], or during the night [21–23].

4.2. Cl^- Cotransporter in SCN Neurons. The depolarizing shift in the E_{GABA} in SCN neurons is mainly due to NKCC1, as indicated by the shift back to the typical E_{GABA} after administration of its specific blocker bumetanide. These results corroborate previous observations on the participation of NKCC1 in the regulation of $[Cl^-]_i$ [22, 23]. However, we cannot exclude the participation of other chloride cotransporters since NKCC1, KCC2, and KCC4 are all present in SCN neurons [29].

4.3. Whole Cell Experiments. Although in whole cell the intracellular messengers could wash out and blunt SFR circadian rhythms [30], there is no evidence that they have major effects on transporters and ionotropic receptors in SCN neurons. Hence we further test the effect of shifting $[Cl^-]_i$ from its usual value in the SCN by the use of two different internal solutions in whole cell configuration to "clamp" E_{Cl^-} to predicted values of −30 mV and −60 mV and to compare them with the actual E_{GABA}. In these experiments we found two populations of neurons distributed around E_{GABA} values, one similar to the E_{Cl^-} predicted from the internal solution composition and the other depolarized about 30 mV (~0 mV and ~ −30 mV) from the value expected from the internal solution (−30 mV and −60 mV). These results suggest an autonomous mechanism in SCN neurons that increases $[Cl^-]_i$. Given the results obtained with bumetanide application in our perforated patch experiments and previous evidence in the field [22, 23], it is likely that the mechanisms that increase $[Cl^-]_i$ in SCN neurons are associated with the NKCC1 cotransporter. Comparable results have been found by different laboratories (using whole cell recordings), where the actual E_{Cl^-} differs from the calculated one for $[Cl^-]_i$ and $[Cl^-]_o$ [26, 27]. We hypothesize that $[Cl^-]_i$ (near $GABA_A$ R) was even more increased than the Cl^- concentration provided by the pipette recording, as a result of local mechanisms as NKCC1 cotransporter.

An interesting finding is that in the experiments with an estimated E_{Cl^-} of −60 mV the SCN neurons populations showed relative distributions and dynamics regarding time and region which resemble the ones found in the perforated patch recordings. The similarity in the distribution of E_{GABA} in these two experimental configurations allows us to recognize a common process that is present despite the dissimilarity of the experimental conditions and the fact that the process is independently regulated in time at different SCN regions.

4.4. Debate about Excitatory GABA Actions. There has been debate about the role of GABA in the SCN for almost the last two decades. The majority of the studies deal with this topic in reference to the effects of agonists and antagonists of $GABA_A$ R or GABA administration on the SFR of SCN neurons. The study of GABA effects on SFR allows inferring about its role on the neuronal network; however, in SCN neurons, SFR is a physiological process much more intricate than E_{GABA} or E_{Cl^-}. SFR involves activation of several types of different voltage-activated channels by phosphorylation and dephosphorylation that can mask the function of GABA. E_{GABA} itself might be a more accurate indicator of GABA actions during different times of the circadian cycle as well as SCN regions.

Wagner et al. [15] found excitatory actions of GABA during the day, through $GABA_A$ R activation, whereas opposite result is found during the night period. Synaptic noise analysis (in whole cell experiments) indicates a higher $[Cl^-]_i$ during the day in comparison to the night. However, the authors do not describe the region of the SCN that was recorded from, which could be the reason of discrepancy between the excitation and inhibition they find in the same circadian time of SCN neurons. In this study we found excitatory actions of GABA during the day in the dorsal SCN, whereas inhibitory actions in the night period in the same area, which is consistent with the conclusions of Wagner et al. Additionally, we calculated $[Cl^-]_i$ in the perforated patch experiments using E_{GABA} and the Nernst equation [31]. In the dorsal SCN, during the day $[Cl^-]_i$ is ~32 mM (58%; Figure 3(c)), whereas during the night it is ~12 mM (71%; Figure 3(c)). These calculated $[Cl^-]_i$ are comparable to the $[Cl^-]_i$ that Wagner et al. found.

Liu and Reppert [12] state the role of GABA as a synchronizer in the SCN. Even though the authors report inhibitory actions of GABA at all times explored, they describe that GABA pulses induce phase shifts in the circadian rhythm of

the extracellular SFR (through the activation of $GABA_A$ R) of single SCN neurons, in cultured slices. The phase shifts induced by GABA are similar (Liu and Reppert, Figure 3) to the ones that result from the photic stimulation in behavioral experiments or the phase shifts that result by the administration of glutamate on the SFR of SCN neurons [32], which suggest excitatory actions of GABA on the SCN neurons. These results are consistent with our present findings regarding a depolarized E_{GABA} in ventral SCN neurons during the night period. As we have mentioned before, ventral SCN neurons are mainly responsible for the synchronization of external signals as light, and they transmit the phase shift information to the rest of the SCN network. We hypothesize that the putative excitatory GABA actions enforce the information communicated by light through the activation of ionotropic glutamate receptors.

In contrast to our findings, de Jeu and Pennartz [21] describe a more depolarized E_{GABA} (~ -59 mV) during the night than during the day period (~ -70 mV), in recordings obtained with perforated patch in acute SCN slices. The authors do not provide any indication about the area of the SCN where the recordings were performed. Though our results differ from these, it is interesting to notice the variability that E_{GABA} has during both periods of the circadian time (day and night) and the size of the samples ($N = 17$ day/$N = 18$ night). We hypothesize that with a bigger population in the results of de Jeu and Pennartz there would be more than one group in the day and night periods.

Shimura et al. [31] report a rhythmical $[Cl^-]_i$ that peaks in the middle of the day, calculated by E_{GABA} in perforated patch clamp experiments carried out in acutely dissociated SCN neurons. $[Cl^-]_i$ proposed by these authors (~23 mM) and the time of its peak (middle of the day) are comparable to the results found in the present work, given that we calculated a putative $[Cl^-]_i$ of ~32 mM during the day and ~12 mM during the night in dorsal SCN neurons. Shimura et al. describe also a lower $[Cl^-]_i$ (~10 mM) at other times of recording that also is in agreement with the present results.

Extracellular recordings (after several days in dissociated SCN neurons culture) show that bicuculline administration decreases the SFR during the period of higher activity (day) whereas it increases the SFR during the period of lower activity (night). These results are relevant because they indicate that the same SCN neuron can regulate GABA actions depending on the circadian time [19]. Analogous results are reported by Ikeda et al. [33] where the $GABA_A$ agonist (muscimol) increases $[Ca^{2+}]_i$ during the day in dorsomedial SCN neurons in a higher proportion than during the night. These results are found in postnatal ages beyond P6 (P9–14), whereas at P6 and younger there are no differences between day and night. These results indicate ontogenic changes that modulate circadian GABA actions. These two studies are in accordance with the present results.

Choi et al. [22] demonstrated excitatory GABA actions mainly during the night, on the SFR that was monitored after the exogenous administration of GABA and the $GABA_A$ antagonist bicuculline. However, there is evidence that relates bicuculline to the blocking of Ca^{2+}-activated K^+ channels that directly regulate the spike generation [34]. Moreover, Choi et al. found that E_{GABA} is more depolarized in the dorsal part of the SCN during the night period than at any other time/SCN region. These last experiments were obtained in perforated patch configuration of SCN slices. The results described by Choi et al. are in contrast with the present results. An interesting fact is that Choi et al. found excitatory GABA actions at all SCN regions explored and at all times of the circadian cycle (Figure 3(c)) [22], which is comparable to our results, though the proportion of excitatory GABA actions (regarding SCN region/time) are different from those found in the present results. We ignore how E_{GABA} could be integrated in the neural activity as the SFR or the excitatory postsynaptic potentials are. As we have previously stated the SFR is a more complex process than E_{GABA}, where E_{GABA} is just one term in the equation. We can infer that E_{GABA} could have an influence on SFR, especially when spike properties of rhythmic SFR are silent or downregulated.

Irwin and Allen [23] found using Ca^{2+} imaging that GABA increases the intracellular Ca^{2+} concentration $[Ca^{2+}]_i$ at all circadian times and in all regions of the SCN (dorsal/ventral); however, this Ca^{2+} increase is higher in the dorsal part during the night. The increase in $[Ca^{2+}]_i$ that is reported in the ventral SCN during the night in comparison to the day period in the same area (Figure 4(e) Irwin and Allen [23]) is comparable with the results of this study (more depolarized E_{GABA} during the night in the ventral SCN) but is inconsistent with the fact that $[Ca^{2+}]_i$ increases even more in the night period in dorsal SCN. $[Ca^{2+}]_i$ could be taken as an indirect method of E_{GABA}, given that it is expected that the Cl^- efflux depolarizes E_m and induces activation of voltage-gated Ca^{2+} channels. Excitatory actions induced by GABA have been reported by many laboratories using different approaches. Our observations have the advantage that they were obtained in acute slices (over dissociated neurons), with a direct method to estimate GABA actions (E_{GABA}), through measurement of spontaneous GABA release rather than through administration of exogenous GABA or other $GABA_A$ agonists, which may have undesirable effects on other proteins (such as $GABA_B$ R, transporters, and voltage-activated channels). Moreover, our recordings were obtained with two different patch clamp configurations.

Our present results demonstrate dynamical GABA modulation which depends on the time of the day and the location of the neuron within the SCN. These results may be due to circadian modulation of NKCC or other Cl^- cotransporters but further studies are still necessary. Present findings suggest excitatory actions of GABA during the day in the dorsal region that might be important for the output signal of the SCN neurons to other projecting areas, especially in those neurons that have a downregulated SFR. During the night, the excitatory GABA actions are centered in the ventral SCN that could conciliate the reports that indicate phase shifts induced by GABA at a cellular level as well as behavioral level, with those indicating that light phase shifts involve NMDA receptors activation in the ventral SCN.

In conclusion, we propose the model depicted in Figure 9, where, during the day, in dorsal SCN, there would be more

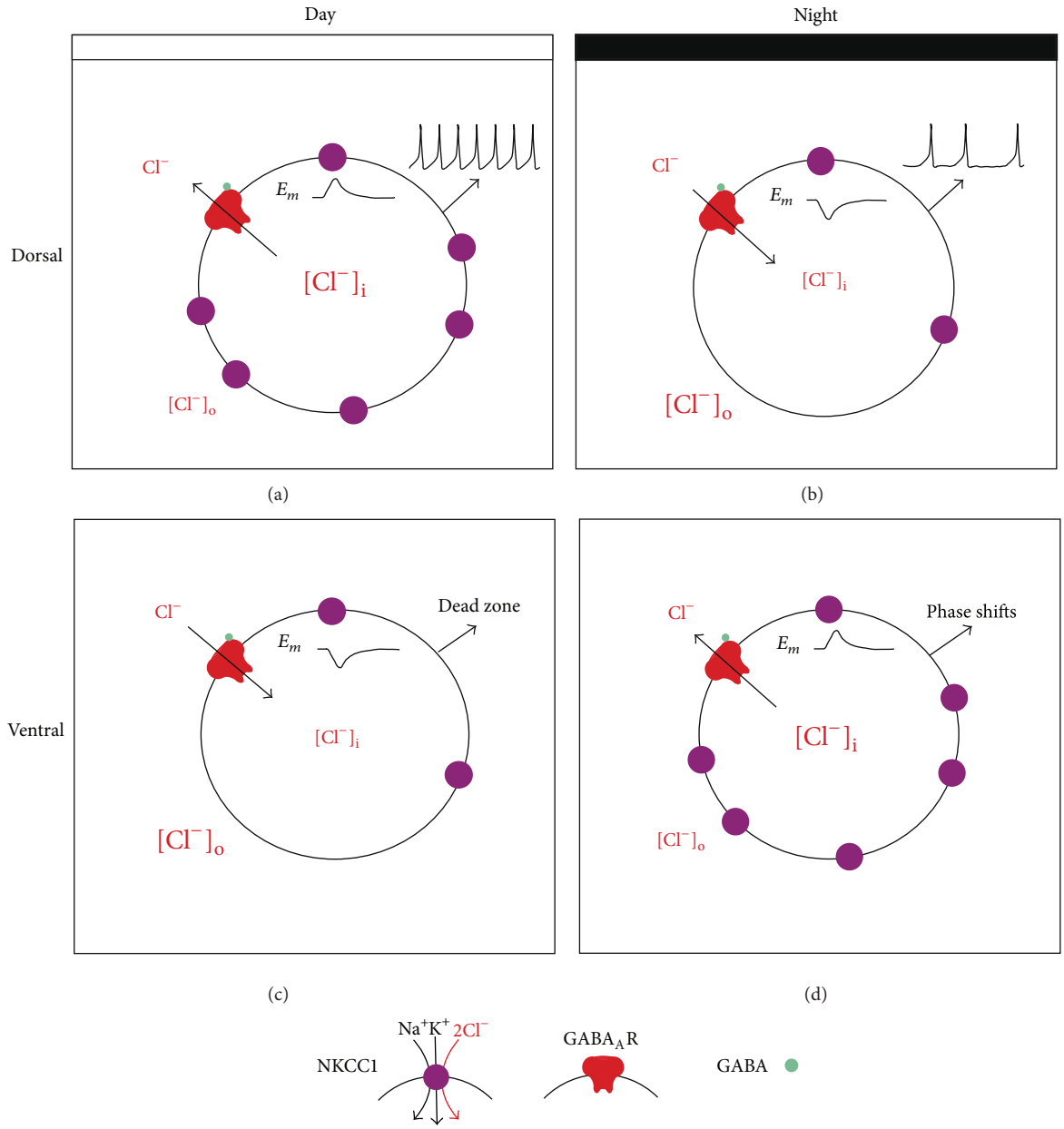

Figure 9: Integrative model of excitatory GABA actions depending on SCN region and circadian time. (a) Dorsal day SCN neurons. High expression of NKCC1 cotransporters increases the $[Cl^-]_i$. $GABA_A$ R activation induces Cl^- efflux, which depolarizes the E_m. Depolarized E_m increases the probability of action potentials that strengthens the SFR during the day. (b) Dorsal night. Low expression of NKCC1 decreases the $[Cl^-]_i$. GABA binding induces Cl^- influx, which hyperpolarizes the E_m. More negative E_m decreases the probability of spikes that reduces the SFR during the night. (c) Ventral day. Diminished NKCC1 expression reduces $[Cl^-]_i$, and $GABA_A$ R activation hyperpolarizes E_m. Less excitability in ventral neurons decreases the probability of phase shifts. (d) Ventral night. Upregulated NKCC1 expression generates high $[Cl^-]_i$ that shifts the E_m close to the spike threshold. More excitability in ventral SCN neurons during the night enhances the probability of phase shifts by GABA.

NKCC1 transporters in the cellular membrane of the SCN neuron that increase $[Cl^-]_i$. As result of this, $GABA_A$ R activation induces an efflux of Cl^- that depolarizes the E_m. This process may enforce the high SFR mechanisms of SCN neurons. At the same time in ventral SCN neurons E_{GABA} is hyperpolarized, probably due to low expression of NKCC1. This would reinforce the lack of response to light pulses during the death zone of the phase response curve. During the night, E_{GABA} is depolarized in the ventral SCN due to higher expression of NKCC1. When $GABA_A$ R are activated, Cl^- is expelled from the neuron, depolarizing the E_m, which is important to accomplishing the synchronization process that takes place during the subjective night. During the same period in the dorsal SCN, NKCC1 expression is

downregulated, which induces a low $[Cl^-]_i$. When $GABA_A$ R are activated, Cl^- enters into the neuron, hyperpolarizing the E_m. This situation helps with the low levels of SFR that the SCN neurons have during the night.

Abbreviations

(E_{Cl^-}): Chloride equilibrium potential
(DNQX): Dinitroquinoxaline-2,3(1H,4H)-dione
(APV): DL-2-Amino-5-phosphonopentanoic acid
(E_{GABA}): Equilibrium potential of GABAergic postsynaptic currents
$[Cl^-]_o$: Extracellular Cl^- concentration
$[Ca^{2+}]_i$: Intracellular Ca^{2+} concentration
$[Cl^-]_i$: Intracellular Cl^- concentration
(KCC): K^+ and Cl^- cotransporters
(GAD): L-Glutamic acid decarboxylase
(E_m): Membrane potential
(NKCC): Na^+, K^+, and Cl^- cotransporters
(SFR): Spontaneous firing rate
(sPSCs): Spontaneous postsynaptic currents
(SCN): Suprachiasmatic nucleus
(ZT): Zeitgeber time
(GABA): γ-Aminobutyric acid.

Conflict of Interests

The authors declare that there is no conflict of interests regarding the publication of this paper.

Acknowledgments

The authors thank Jose Luis Chávez-Juárez, Victor Saenger, and Ana-María Escalante for the skillful technical assistance and Dr. Dan Case for the comments about the grammar. This work was partially supported by Grants from PAPIIT-DGAPA IN204811 and CONACyT 12858.

References

[1] D. C. Klein, R. Y. Moore, and S. M. Reppert, *Suprachiasmatic Nucleus: The Mind's Clock*, Oxford University Press, New York, NY, USA, 1991.

[2] E. E. Abrahamson and R. Y. Moore, "Suprachiasmatic nucleus in the mouse: retinal innervation, intrinsic organization and efferent projections," *Brain Research*, vol. 916, no. 1-2, pp. 172–191, 2001.

[3] J. LeSauter, L. J. Kriegsfeld, J. Hon, and R. Silver, "Calbindin-D28K cells selectively contact intra-SCN neurons," *Neuroscience*, vol. 111, no. 3, pp. 575–585, 2002.

[4] L. P. Morin, K.-Y. Shivers, J. H. Blanchard, and L. Muscat, "Complex organization of mouse and rat suprachiasmatic nucleus," *Neuroscience*, vol. 137, no. 4, pp. 1285–1297, 2006.

[5] S. M. Reppert and D. R. Weaver, "Coordination of circadian timing in mammals," *Nature*, vol. 418, no. 6901, pp. 935–941, 2002.

[6] R. Y. Moore and J. C. Speh, "GABA is the principal neurotransmitter of the circadian system," *Neuroscience Letters*, vol. 150, no. 1, pp. 112–116, 1993.

[7] M. Castel and J. F. Morris, "Morphological heterogeneity of the GABAergic network in the suprachiasmatic nucleus, the brain's circadian pacemaker," *Journal of Anatomy*, vol. 196, no. 1, pp. 1–13, 2000.

[8] R. Aguilar-Roblero, L. Verduzco-Carbajal, C. Rodriguez, J. Mendez-Franco, J. Moran, and M. Perez de la Mora, "Circadian rhythmicity in the GABAergic system in the suprachiasmatic nuclei of the rat," *Neuroscience Letters*, vol. 157, no. 2, pp. 199–202, 1993.

[9] J. Itri and C. S. Colwell, "Regulation of inhibitory synaptic transmission by vasoactive intestinal peptide (VIP) in the mouse suprachiasmatic nucleus," *Journal of Neurophysiology*, vol. 90, no. 3, pp. 1589–1597, 2003.

[10] J. Itri, S. Michel, J. A. Waschek, and C. S. Colwell, "Circadian rhythm in inhibitory synaptic transmission in the mouse suprachiasmatic nucleus," *Journal of Neurophysiology*, vol. 92, no. 1, pp. 311–319, 2004.

[11] C. F. Gillespie, E. M. Mintz, C. L. Marvel, K. L. Huhman, and H. E. Albers, "GABA(A) and GABA(B) agonists and antagonists alter the phase-shifting effects of light when microinjected into the suprachiasmatic region," *Brain Research*, vol. 759, no. 2, pp. 181–189, 1997.

[12] C. Liu and S. M. Reppert, "GABA synchronizes clock cells within the suprachiasmatic circadian clock," *Neuron*, vol. 25, no. 1, pp. 123–128, 2000.

[13] E. M. Mintz, A. M. Jasnow, C. F. Gillespie, K. L. Huhman, and H. E. Albers, "GABA interacts with photic signaling in the suprachiasmatic nucleus to regulate circadian phase shifts," *Neuroscience*, vol. 109, no. 4, pp. 773–778, 2002.

[14] H. Albus, M. J. Vansteensel, S. Michel, G. D. Block, and J. H. Meijer, "A GABAergic mechanism is necessary for coupling dissociable ventral and dorsal regional oscillators within the circadian clock," *Current Biology*, vol. 15, no. 10, pp. 886–893, 2005.

[15] S. Wagner, M. Castel, H. Gainer, and Y. Yarom, "GABA in the mammalian suprachiasmatic nucleus and its role in diurnal rhythmicity," *Nature*, vol. 387, no. 6633, pp. 598–603, 1997.

[16] V. K. Gribkoff, R. L. Pieschl, T. A. Wisialowski et al., "A reexamination of the role of GABA in the mammalian suprachiasmatic nucleus," *Journal of Biological Rhythms*, vol. 14, no. 2, pp. 126–130, 1999.

[17] V. K. Gribkoff, R. L. Pieschl, and F. E. Dudek, "GABA receptor-mediated inhibition of neuronal activity in rat SCN in vitro: pharmacology and influence of circadian phase," *Journal of Neurophysiology*, vol. 90, no. 3, pp. 1438–1448, 2003.

[18] N. I. Kononenko and F. E. Dudek, "Mechanism of irregular firing of suprachiasmatic nucleus neurons in rat hypothalamic slices," *Journal of Neurophysiology*, vol. 91, no. 1, pp. 267–273, 2004.

[19] T. Shirakawa, S. Honma, Y. Katsuno, H. Oguchi, and K.-I. Honma, "Synchronization of circadian firing rhythms in cultured rat suprachiasmatic neurons," *European Journal of Neuroscience*, vol. 12, no. 8, pp. 2833–2838, 2000.

[20] S. Wagner, N. Sagiv, and Y. Yarom, "GABA-induced current and circadian regulation of chloride in neurones of the rat suprachiasmatic nucleus," *Journal of Physiology*, vol. 537, no. 3, pp. 853–869, 2001.

[21] M. de Jeu and C. Pennartz, "Circadian modulation of GABA function in the rat suprachiasmatic nucleus: excitatory effects during the night phase," *Journal of Neurophysiology*, vol. 87, no. 2, pp. 834–844, 2002.

[22] H. J. Choi, C. J. Lee, A. Schroeder et al., "Excitatory actions of GABA in the suprachiasmatic nucleus," *Journal of Neuroscience*, vol. 28, no. 21, pp. 5450–5459, 2008.

[23] R. P. Irwin and C. N. Allen, "GABAergic signaling induces divergent neuronal Ca^{2+} responses in the suprachiasmatic nucleus network," *European Journal of Neuroscience*, vol. 30, no. 8, pp. 1462–1475, 2009.

[24] A. Kyrozis and D. B. Reichling, "Perforated-patch recording with gramicidin avoids artifactual changes in intracellular chloride concentration," *Journal of Neuroscience Methods*, vol. 57, no. 1, pp. 27–35, 1995.

[25] Y. Ben-Ari, "Excitatory actions of GABA during development: the nature of the nurture," *Nature Reviews Neuroscience*, vol. 3, no. 9, pp. 728–739, 2002.

[26] D. E. Ehrlich, S. J. Ryan, R. Hazra, J. D. Guo, and D. G. Rainnie, "Postnatal maturation of GABAergic transmission in the rat basolateral amygdala," *Journal of Neurophysiology*, vol. 110, pp. 926–941, 2013.

[27] C. Gonzalez-Islas, N. Chub, and P. Wenner, "NKCC1 and AE3 appear to accumulate chloride in embryonic motoneurons," *Journal of Neurophysiology*, vol. 101, no. 2, pp. 507–518, 2009.

[28] R. Aguilar-Roblero, C. Mercado, J. Alamilla, A. Laville, and M. Díaz-Muñoz, "Ryanodine receptor Ca^{2+}-release channels are an output pathway for the circadian clock in the rat suprachiasmatic nuclei," *European Journal of Neuroscience*, vol. 26, no. 3, pp. 575–582, 2007.

[29] M. A. Belenky, P. J. Sollars, D. B. Mount, S. L. Alper, Y. Yarom, and G. E. Pickard, "Cell-type specific distribution of chloride transporters in the rat suprachiasmatic nucleus," *Neuroscience*, vol. 165, no. 4, pp. 1519–1537, 2010.

[30] J. Schaap, N. P. A. Bos, M. T. G. de Jeu, A. M. S. Geurtsen, J. H. Meijer, and C. M. A. Pennartz, "Neurons of the rat suprachiasmatic nucleus show a circadian rhythm in membrane properties that is lost during prolonged whole-cell recording," *Brain Research*, vol. 815, no. 1, pp. 154–166, 1999.

[31] M. Shimura, N. Akaike, and N. Harata, "Circadian rhythm in intracellular Cl^- activity of acutely dissociated neurons of suprachiasmatic nucleus," *American Journal of Physiology: Cell Physiology*, vol. 282, no. 2, pp. C366–C373, 2002.

[32] J. M. Ding, D. Chen, E. T. Weber, L. E. Faiman, M. A. Rea, and M. U. Gillette, "Resetting the biological clock: mediation of nocturnal circadian shifts by glutamate and NO," *Science*, vol. 266, no. 5191, pp. 1713–1717, 1994.

[33] M. Ikeda, T. Yoshioka, and C. N. Allen, "Developmental and circadian changes in Ca^{2+} mobilization mediated by GABAA and NMDA receptors in the suprachiasmatic nucleus," *European Journal of Neuroscience*, vol. 17, no. 1, pp. 58–70, 2003.

[34] F. Debarbieux, J. Brunton, and S. Charpak, "Effect of bicuculline on thalamic activity: a direct blockade of I(AHP) in reticularis neurons," *Journal of Neurophysiology*, vol. 79, no. 6, pp. 2911–2918, 1998.

Hindawi Publishing Corporation
BioMed Research International
Volume 2014, Article ID 654710, 10 pages
http://dx.doi.org/10.1155/2014/654710

Research Article

Regulation of Melanopsins and *Per1* by α-MSH and Melatonin in Photosensitive *Xenopus laevis* Melanophores

Maria Nathália de Carvalho Magalhães Moraes,[1] Luciane Rogéria dos Santos,[1] Nathana Mezzalira,[1] Maristela Oliveira Poletini,[2] and Ana Maria de Lauro Castrucci[1]

[1] *Department of Physiology, Institute of Biosciences, University of São Paulo, R. do Matão, Travessera 14, No. 101, 05508-900 São Paulo, SP, Brazil*
[2] *Department of Physiology, Institute of Biological Sciences, Federal University of Minas Gerais, 31270-901 Belo Horizonte, MG, Brazil*

Correspondence should be addressed to Ana Maria de Lauro Castrucci; amdlcast@ib.usp.br

Received 26 January 2014; Revised 27 March 2014; Accepted 30 March 2014; Published 13 May 2014

Academic Editor: Mario Guido

α-MSH and light exert a dispersing effect on pigment granules of *Xenopus laevis* melanophores; however, the intracellular signaling pathways are different. Melatonin, a hormone that functions as an internal signal of darkness for the organism, has opposite effects, aggregating the melanin granules. Because light functions as an important synchronizing signal for circadian rhythms, we further investigated the effects of both hormones on genes related to the circadian system, namely, *Per1* (one of the clock genes) and the melanopsins, *Opn4x* and *Opn4m* (photopigments). *Per1* showed temporal oscillations, regardless of the presence of melatonin or α-MSH, which slightly inhibited its expression. Melatonin effects on melanopsins depend on the time of application: if applied in the photophase it dramatically decreased *Opn4x* and *Opn4m* expressions, and abolished their temporal oscillations, opposite to α-MSH, which increased the melanopsins' expressions. Our results demonstrate that unlike what has been reported for other peripheral clocks and cultured cells, medium changes or hormones do not play a major role in synchronizing the *Xenopus* melanophore population. This difference is probably due to the fact that *X. laevis* melanophores possess functional photopigments (melanopsins) that enable these cells to primarily respond to light, which triggers melanin dispersion and modulates gene expression.

1. Introduction

Color change is an important strategy for animals' camouflages, which allows them to match their body color with the environment [1]. In ectothermic vertebrates, pigment granule aggregation or dispersion, within the cytoplasm of cutaneous pigment cells, are responsible for the physiological color changes resulting in skin lightening or darkening, respectively [2, 3]. Notably, pigment translocation can be induced by light [4–7] and by several neurohumoral signals [7, 8].

α-Melanocyte stimulating hormone (α-MSH), which is produced in the pars intermedia of the pituitary gland, is a darkening agent in all vertebrates. It induces a very rapid dispersion in dermal melanophores of ectothermic vertebrates [9–13], and it also plays a role in skin, fur, and feather darkening [14, 15], in cell proliferation, in cell differentiation [16], and immune activity [17, 18] of endothermic animals. Human α-MSH is produced in sites other than the pituitary, such as the skin itself and its systemic action promotes melanin production by the human skin in response to UV light [19]. In addition, α-MSH is produced in the mammalian hypothalamus affecting behaviors such as food intake and lordosis [20, 21]. Melatonin (5-methoxy-N-acetyl tryptamine) is an indoleamine synthesized by the pineal gland and released at night. Contrary to α-MSH, melatonin aggregates melanin granules acting as a lightening hormone [7, 22]. Many ectothermic vertebrates exhibit a circadian rhythm of color change, a night paling related with melatonin secretion [23, 24]. Melatonin integrates the endocrine system and the external environment, translating the photoperiod information into hormone signal, thus synchronizing various aspects of physiology and neuroendocrine functions with light-dark cycles [25]. This hormone plays a crucial role in the regulation

of circadian and seasonal changes, influencing reproductive functions through the hypothalamic-pituitary-gonadal (HPG) axis [26]. In addition, melatonin may also act as an antioxidant agent [27], some of its antioxidative activities being exerted by its metabolite, cyclic 3-hydroxymelatonin, which completely prevents the cytochrome C degradation by hydrogen peroxide [28].

Studies on the photoresponses of *Xenopus laevis* melanophores led to the discovery of the photopigment melanopsin, which is present in the retina of all vertebrates, including humans [29, 30]. In mammals, melanopsin is present in a subpopulation of photosensitive ganglion cells [31], which convey light information to the hypothalamic suprachiasmatic nuclei (SCN) [32, 33], the master biological clock. In addition to adjusting the biological clock to light-dark cycles, these cells mediate nonvisual photic responses, such as pupillary constriction and melatonin suppression [34, 35]. In 2006, Bellingham and coworkers [36] demonstrated the existence of two *Opn4* genes, encoding melanopsins in nonmammalian vertebrates. The second melanopsin, *Opn4m*, presents a much higher homology with the mammalian than with the *X. laevis* melanopsin, which was then named *Opn4x*. Despite the presence of melanopsins in nonmammalian retinas, their function as a photoentrainment pigment has yet to be defined.

The molecular basis for endogenous biological rhythm is a loop of transcriptional/translation of clock proteins. In general, CLOCK and BMAL1 dimers acting through E-box elements increase the transcription of *Per*, *Cry*, *Reverb-α,* and *Ror* which after being translated inhibit CLOCK/BMAL1 effect [37]. Additionally, CLOCK/BMAL1 dimers regulate other genes known as clock controlled genes [38–40]. Tyrosinase, a rate-limiting enzyme for melanin production, has E-box motif in its promoter, suggesting that it can be a clock-controlled gene [41].

Although α-MSH and melatonin have opposite effects on pigment translocation, both mediate light responses, that is, α-MSH disperses melanin granules in the same manner as light does, whereas melatonin is the messenger of the darkness. α-MSH and light have the same effect on pigment translocation within *X. laevis* melanophores; however, the intracellular signaling pathways are different [42, 43], which may indicate plasticity in this response. α-MSH acts through MC1R receptor coupled to a Gs-protein, triggering the activation of the cAMP pathway [44], whereas light stimulates melanopsin leading to phospholipid hydrolysis and increase of cytosolic calcium [42]. On the other hand, melatonin triggers *X. laevis* melanin aggregation through the activation of Mel 1c receptor, which is coupled to a Gi-protein, thus leading to a decrease in cAMP [22].

X. laevis melanophores incorporate all components of a circadian system, as they express clock genes and photopigments. In addition, *Per1* expression increases in response to a blue light stimulus, indicating the mediation of a blue sensitive pigment [45]. The fact that both hormones, α-MSH and melatonin, signal external environmental light conditions to the organisms in an opposite manner, and that light is an important zeitgeber in *X. laevis* melanophores, we hypothesized that these hormones may differentially affect the melanopsins *Opn4x* and *Opn4m* (blue sensitive photopigments) as well as *Per1* expression.

2. Material and Methods

Immortalized cultures of embryonic *X. laevis* melanophores (a kind gift of Professor Mark Rollag, University of New Mexico, USA) were kept in 60% L-15 medium, supplemented with 5 mg/mL insulin/transferrin/selenium, 2X hypoxanthine/thymidine, 1% antibiotic/fungicide solution (10,000 U/mL penicillin/10,000 μg/mL streptomycin/25 μg/mL amphotericin B), and 10% non-inactivated fetal calf serum (all from Life Technologies, Carlsbad, CA, USA) at pH 7.5 and 25°C [46]. The culture medium was changed weekly and when the cells reached 80% confluence, they were removed with 60% Tyrode/EDTA solution and transferred to new flasks (the cells from one flask were split into 3 flasks).

For the experiments, the cells were plated 2×10^6 per 25 cm^2 flask, the serum was reduced to 2%, and 2×10^{-7} M retinaldehyde was added. Cells were manipulated in the dark using Konex illuminator with a 7 W red light (~5 lux) and a Safe-Light GBX-2 filter (Kodak, SP, Brazil). Each experiment was repeated 2 to 3 times with duplicate flasks of cells (*n* number presented in the graphs).

The protocols described below were based on the fact that *Xenopus* melanophores aggregate the melanin granules in DD, or in response to melatonin, and disperses pigment granules in response to light or to α-MSH. Therefore, α-MSH was employed to mimic light signal in aggregated cells, that is, in DD, whereas melatonin was applied on already dispersed cells; there is LD.

2.1. Protocol 1: α-MSH Treatment. Cells were kept under constant darkness for 5 days. At 8:00 h of the fifth day, the flasks were divided into two groups: (1) cells were subject to a medium change without hormone (control); (2) cells were subject to a medium change containing 10^{-9} M α-MSH (Sigma-Aldrich, St. Louis, MO, USA). Twelve hours later, both groups received a new medium change without hormone. At 8:00 h of the sixth day (24 hours after the beginning of the treatment) total RNA was extracted every 4 hours (0, 4, 8, 12, 16, and 20 ZT).

2.2. Protocol 2: Melatonin Treatment. Cells were kept in 12 : 12 LD for 5 days and then treated for 6 hours with 10^{-9} M melatonin (Sigma-Aldrich, St. Louis, MO, USA) in one of the following conditions: (a) beginning of the light phase of the 6th day and (b) beginning of the dark phase of the 6th day. Control cells were kept in the absence of the hormone but were subject to similar light conditions and medium changes. Twenty-four hours after beginning of the treatment, total RNA was extracted every 4 hours (0, 4, 8, 12, 16, and 20 ZT). During the light phase, the flasks received irradiance of 87.85 μw/cm^2 (600 lux, 2.5×10^{14} photons·s^{-1}·cm^{-2}, full spectrum, 8-W cool white fluorescent tube, T5-8W, SCT, São Paulo, Brazil).

Table 1: Primers and probes used for qPCR assays.

18S RNA	Forward: 5′-CGGCTACCACATCCAAGGAA-3′
	Backward: 5′-GCTGGAATTACCGCGGCT-3′
	Probe: 5′-5-TexRd-TGCTGGCACCAGACTTGCCCTC-BHQ_2-3′
Opn4x NM_00108564.1	Forward: 5′-ATTATTGTCCTTGTCTGGATGTATTCA-3′
	Backward: 5′-AAGCCCTCTGGCACATAGGAA-3′
	Probe: 5′-6-FAM-AATGTGGAGCTTGGCACCATTACTTGGC-BHQ_1-3′
Opn4m DQ_384639.1	Forward: 5′-AGGGCAGTGCTAATCCTTTCAGGT-3′
	Backward: 5′-AATCCCAGGTGCAGGATGTCAGAA-3′
Per1 NM_001085703.2	Forward: 5′-TGAAGGCCCTTAAAGAGCTAAAGA-3′
	Backward: 5′-TTGCCAGTGTGCCAGACTTG-3′
	Probe: 5′-/5Cy5/TCGGCTCCCATCAGAGAAGAG GCTAAAAG/3BHQ_2/3′

2.3. RNA Extraction, RT-PCR and Quantitative PCR. Total RNA was extracted with TRIzol reagent; the RNA pellet was then resuspended in DEPC water and treated with DNase (*turbo-DNA-free*), according to the manufacturer's instructions (all reagents from Life Technologies, Carlsbad, CA, USA). RNA concentration was determined with a spectrophotometer (Nanodrop, Willmington, DE, USA) and 1 μg was used in reverse transcription reaction with SuperScript III and random primers (Life Technologies, Carlsbad, CA, USA).

Quantitative PCR reactions were carried out with primers and probes specific for the genes of interest or ribosomal 18S, designed with *Primer Express* (Life Technologies, CA, USA) based on Genbank sequences (http://www.ncbi.nlm.nih.gov/PubMed/) and synthesized by IDT (Coralville, IA, USA) (Table 1). Multiplex quantification was performed for *Opn4x* and 18S RNA and *Per1* and 18S RNA; the solutions contained 1 μL of cDNA, primers (300 nM for each gene,50 nM for 18S RNA), probes (200 nM for each gene, 50 nM for 18S RNA), Platinum Supermix (Life Technologies, Carlsbad, CA, USA) supplemented to final concentrations of 6 mM $MgCl_2$, 0.4 mM dNTPS, 0.1 U/μL Platinum Taq DNA polymerase.

To normalize the results, 18S ribosomal RNA was used, as recommended for mammalian and nonmammalian species [47–51]. The efficiency of each pair of primers was calculated and varied between 80 and 104%. The assays were performed in i5 thermocycler (BioRad Laboratories, Hercules, CA, USA), with the following conditions: 7 min at 95°C, followed by 40 cycles of 30 s at 95°C and 30 s at 55°C.

2.4. Statistical Analyses. The results were analyzed using the ΔΔCT method [52]. The threshold was established by the thermocycler software and crossed the amplification curves to determine the number of cycles, the CT. The difference between the CTs for 18S RNA and the CT for each gene at the same time point is the ΔCT. The maximal ΔCT was then subtracted from each ΔCT value to obtain ΔΔCT, used as a negative exponential of base 2 ($2^{-\Delta\Delta CT}$). The log values (at least four flasks of cells, from two independent experiments) were averaged and graphed as mean ± SEM relative to the minimal value expression for each protocol. The levels of significance of differences among time points were determined comparing the log data by one-way ANOVA, followed by Tukey; between time points in different protocols, as well as control versus hormone-stimulated groups, the log data were compared by two-way ANOVA followed by Bonferroni's test (significant at $P < 0.05$).

3. Results and Discussion

The vertebrate circadian system consists of an element that detects environmental light, an internal oscillator, and one or more output signals. The internal oscillator is comprised by a central clock and several peripheral clocks which, when in synchrony, display a time-accurate output [53]. Notably, the central clock remains rhythmic when in culture [54], whereas peripheral clocks lose this ability due to the loss of coupling among cells [55, 56].

Per1 expression in *X. laevis* melanophores kept in constant dark (DD) did not statistically vary throughout ZTs after medium changes (Figure 1(a)). Several data from literature have shown that a single medium change, serum shock [57, 58], phorbol esters (TPA) [59], or glucocorticoids [60] act as coupling factor in a variety of cultured cell types leading to a synchronization of clock genes. Unlike the literature reports, our data have shown that medium changes were unable to induce *Per1* temporal oscillation in *X. laevis* melanophores in DD, similarly to previous results in cells which were kept undisturbed in DD, that is, did not receive medium changes [45, 61]. However, when these cells were kept in light-dark cycles (12 : 12 LD) and subject to medium changes, *Per1* mRNA showed a temporal oscillation. Higher levels of mRNA were found at ZT4 comparing to all other ZTs (Figure 1(b), $P < 0.001$), and at ZT8 when was compared to ZT12 and ZT20 (Figure 1(b), $P < 0.01$). *Per1* mRNA has also been reported to increase in undisturbed *X. laevis* melanophores in LD 14 : 10 [61] or LD 12 : 12 [45] cycles. The results of the present study together with previous data suggest a major role for light in the clock gene expression changes in these cells, as it had already been demonstrated in *X. laevis* eye [62].

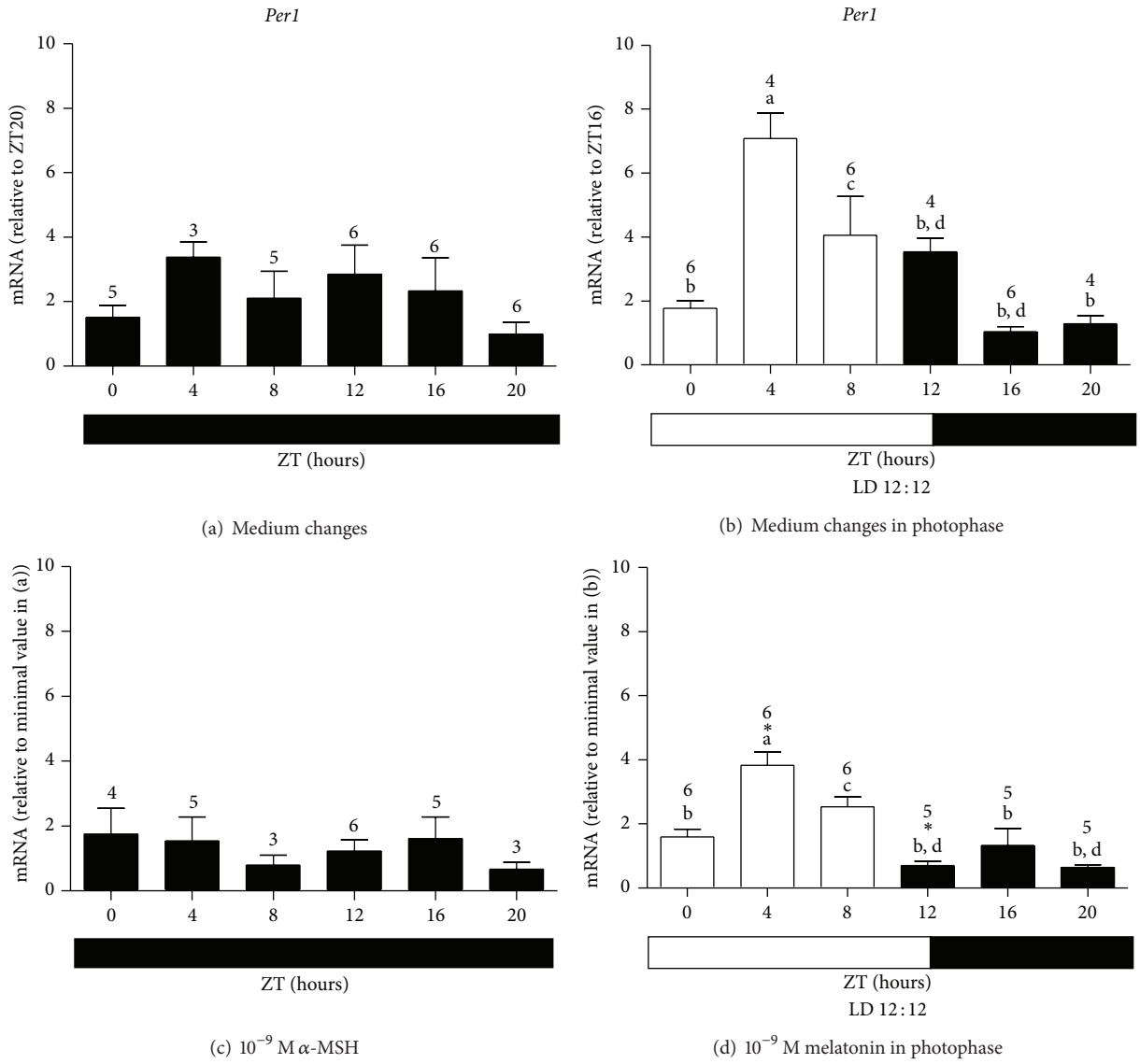

Figure 1: Quantitative PCR of *Per1* in *X. laevis* melanophores after 2 medium changes in DD (a); 2 medium changes in LD 12 : 12 (b); 10^{-9} M α-MSH in DD (c); and 10^{-9} M melatonin in the photophase of LD 12 : 12 (d). Each bar represents the mean, ± SE, mRNA relative to the noted ZT. (a) Significantly different from (b); (c) significantly different from (d) by one-way ANOVA, Tukey's post-test; ∗ means significantly different from the respective control at the same ZT, by two-way ANOVA and Bonferroni's post-test. *n* number shown on top of each bar in this and the following figures.

Because of the similar effects of light and of α-MSH on melanin granule dispersion, we evaluated the action of this hormone on one of the clock genes, *Per1*, as well as the effects of melatonin, an internal dark messenger for the organism. Melatonin was applied at the beginning of the photophase for 6 hours, whereas α-MSH was applied for 12 hours at the beginning of the subjective photophase in DD, thus mimicking the presence of light in causing melanin dispersion. One-way ANOVA analyses showed that there was no temporal variation in either 10^{-9} M α-MSH treated cells or in cells subject to medium changes in DD. On the other hand, two-way ANOVA showed that the hormone treatment considerably affected the results ($F_{(1,45)} = 10.19$, $P = 0.0026$, Figures 1(a) and 1(c)), though no effects were seen when each time-point comparison was analyzed by Bonferroni's post-test.

The temporal oscillations of *Per1* expression seen in control cells persisted after melatonin treatment. Higher levels of *Per1* mRNA were seen at ZT4 when compared to ZT0, ZT12, ZT16, and ZT20 ($P < 0.001$, Figure 1(d)), and at ZT8 as compared to ZT12 and ZT20 ($P < 0.01$, Figure 1(d)). Melatonin and time exerted strong influences on the results, as shown by two-way ANOVA ($F_{(1,52)} = 20.06$, $P < 0.0001$ and $F_{(5,52)} = 19.74$, $P < 0.0001$, resp.). Bonferroni's post-test analysis of each time point indicated that *Per1* mRNA levels were 2 times lower at ZT4 ($P < 0.001$) and ZT12

($P < 0.01$) after 10^{-9} M melatonin treatment in the photophase (Figure 1(d)) than the control group (Figure 1(b)). Interestingly, the temporal oscillation of *Per1* expression seen in the control was maintained. Bluhm and coworkers [61] found that 1 hour melatonin treatment of *X. laevis* melanophores, kept in DD, did not affect *Per1* expression, except for an increase at 3 hours. In mammals, entrainment mechanisms involve light stimulation of melanopsin positive ganglion cells that release glutamate/PACAP in the SCN cells, ultimately increasing *Per1* expression [63]. In undisturbed *X. laevis* melanophores, light at 460 nm wavelength, which maximally stimulates the melanopsins (or one of them) [42], also leads to enhancement of *Per1* expression [45]. These results point to a role of a blue light sensitive pigment in the light entrainment mechanism of *X. laevis* melanophores. Thus, we hypothesized that melatonin decreasing effects on the amplitude of *Per1* expression found here could be due to melatonin-induced reduction of the photopigment expression. In fact, 10^{-9} M melatonin treatment in the photophase dramatically decreased *Opn4x* and *Opn4m* expression during the light period, as compared to cells only subject to medium changes (Figures 2(a) and 2(b); Figures 3(a) and 3(b)) as described below.

Melatonin treatment in the photophase considerably affected *Opn4x* ($F_{(1,73)} = 16.49$, $P < 0.0001$ and $F_{(5,73)} = 2.84$, $P = 0.0214$ resp.) and *Opn4m* ($F_{(1,74)} = 21.48$, $P < 0.0001$ and $F_{(5,74)} = 3.64$, $P = 0.0053$ resp.) expressions. In addition, the temporal oscillation of *Opn4x* and *Opn4m* seen after medium changes in the photophase (Figures 2(a) and 3(a)) was abolished by the hormone treatment (Figures 2(b) and 3(b)). This reduction was statistically significant as shown by Bonferroni post-test for *Opn4x* and *Opn4m* at ZT0 ($P < 0.05$, $P < 0.001$ resp.) and ZT4 ($P < 0.001$). Therefore, melatonin is affecting the sensitivity of *X. laevis* melanophores to an important light-wavelength (460–480 nm), which we believe is the entrainment factor in this model. Melatonin *per se* does not seem to participate in the entrainment mechanism of the biological clock, as demonstrated by its lack of effect on *Per1* expression when applied either in the photophase (Figure 1(d)), or in the scotophase (data notshown).

If medium changes were performed in the photophase, *Opn4x* and *Opn4m,* showed a temporal profile with higher expression throughout the light period(Figures 2(a) and 3(a)). *Opn4x* expression was higher at ZT0 as compared to ZT16 ($P < 0.05$) and at ZT4 as compared to ZT12, ZT16, and ZT20 ($P < 0.01$). *Opn4m* expression was higher at ZT0 ($P < 0.05$) and at ZT4 ($P < 0.01$) than at ZT12, 16 and 20. When medium changes were performed in the scotophase, the highest levels of *Opn4x* and *Opn4m* mRNA were found at ZT8 ($P < 0.01$ and $P < 0.05$ resp.), that is, at the end of the light period (Figures 2(c) and 3(c)). The profile seen for *Opn4x* (Figure 2(a)) did not differ from what has been reported by Moraes and coworkers in *X. laevis* melanophores subject to 12 : 12 LD without further manipulation, whereas for *Opn4m,* LD cycles were not sufficient to induce temporal changes (unpublished data). So, *Opn4m* requires LD cycles plus medium changes to display a temporal oscillation as shown here (Figure 3(a)). Therefore, light seems to be the important *zeitgeber* for *Opn4x*, since it already showed an oscillatory pattern, which was not affected by medium changes, similarly to what was observed in *Per1* expression.

Melatonin applied in the scotophase strongly affected *Opn4x* and *Opn4m* expressions throughout the time points ($F_{(5,35)} = 60.7$, $P < 0.0001$ and $F_{(5,32)} = 10.96$, $P < 0.0001$ resp.), which implied an altered temporal profile of both melanopsins. *Opn4x* mRNA levels decreased at ZT0 ($P < 0.05$) and increased at ZT4 ($P < 0.001$, Figure 2(d)), as compared to cells only subject to medium changes in the scotophase (Figure 2(c)). *Opn4m* mRNA levels increased at ZT4 ($P < 0.05$, Figure 3(d)), as compared to cells in control group (Figure 3(c)). Melatonin seems to exert permissive actions on gene expression, allowing *Opn4x* and *Opn4m* to resume a smoother time-course variation (Figures 2(d) and 3(d)). In control cells subject to medium changes in LD, *Opn4x* mRNA levels were higher at ZT8 compared to all other ZTs ($P < 0.001$), and *Opn4m* mRNA levels were higher at ZT8 compared to ZT0, ZT4, and ZT16 ($P < 0.05$). After melatonin treatment, both melanopsin expressions gradually increased during the photophase.

Melatonin administration during the scotophase mimics pineal melatonin secretion in physiological conditions, so one would expect a more relevant effect of melatonin. However, this hormone was incapable of significantly altering melanopsin temporal oscillations. Both diurnal and nocturnal animals release pineal gland melatonin at night, indicating the duration of the dark phase of the day, thus melatonin is a crucial compound that sets circadian temporal system [64]. During the photophase, melatonin seems to promote a disruption of the light sensor —melanopsins in this model— represented by the dramatic inhibition of both photopigment expressions and loss of changes in the temporal profile (Figures 2(a), 2(b), 3(a), and 3(b)). This inhibitory effect of melatonin on gene expression was also seen after only 1 hour melatonin treatment of *X. laevis* melanophores in DD [61]. *X. laevis* melanophores, therefore, is an interesting model to study melatonin regulation of the circadian peripheral systems.

α-MSH exerts opposite effect on *Opn4x* expression when compared to melatonin, as it does on pigment translocation. After 10^{-9} M α-MSH treatment, *Opn4x* expression increased 3-4 times at ZT0 ($P < 0.05$) and ZT16 ($P < 0.05$). The stimulatory effect of α-MSH on the overall expression was considered very significant ($F_{(1,51)} = 7.7$, $P = 0.0077$) (Figures 2(e) and 2(f)). *Opn4m*, on the other hand, was less affected by α-MSH; its mRNA levels decreased at ZT4 ($P < 0.05$) and increased at ZT12 ($P < 0.001$) as compared to the control group (Figures 3(e) and 3(f)). After α-MSH or medium changes, both *Opn4x* and *Opn4m* showed temporal oscillation. In DD after medium changes, similar levels of *Opn4x* mRNA were found at ZT0, ZT4, and ZT16, compared to ZT8, ZT12, and ZT20 ($P < 0.05$) (Figure 2(e)); but higher levels were seen at ZT0 and ZT16 compared to ZT20 after α-MSH treatment ($P < 0.05$, Figure 2(f)). In DD after medium changes, *Opn4m* expression was higher at ZT4 as compared to ZT0, ZT8, ZT12, and ZT20 ($P < 0.05$) and

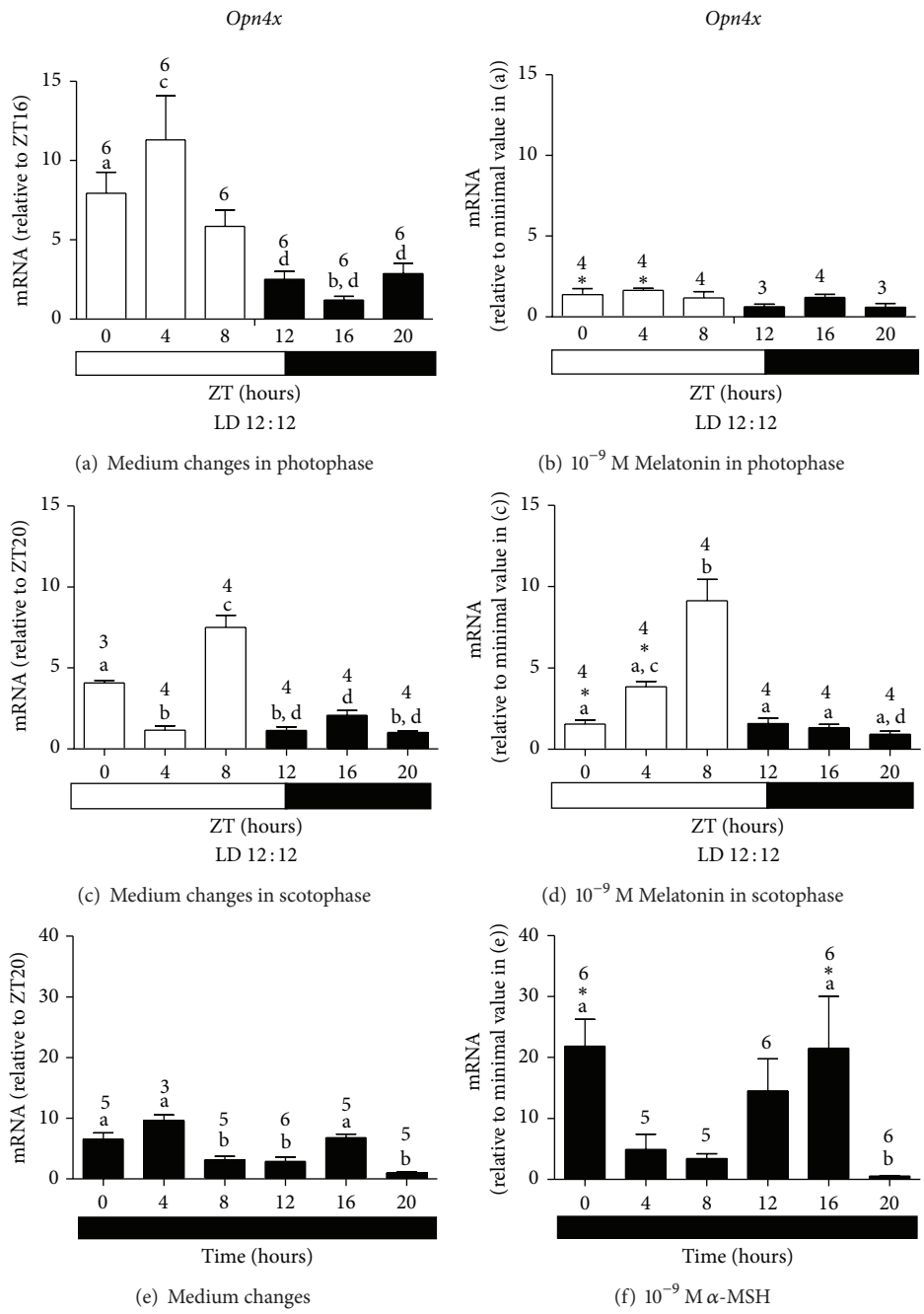

Figure 2: Quantitative PCR of *Opn4x* in *X. laevis* melanophores after 2 medium changes in the photophase of LD 12 : 12 (a); 10^{-9} M melatonin in the photophase of LD 12 : 12 (b); 2 medium changes in the scotophase of LD 12 : 12 (c); 10^{-9} M melatonin in the scotophase of LD 12 : 12 (d); 2 medium changes in DD (e); 10^{-9} M α-MSH in DD (f). Each bar represents the mean, ± SE, mRNA relative to the noted ZT. (a) Significantly different from (b); (c) significantly different from (d), except in 2 C where (a) is different from (b) and (c) is different from (a) and (d) by one-way ANOVA and Tukey's post-test; ∗ means significantly different from the respective control at the same ZT, by two-way ANOVA and Bonferroni's post-test.

lower at ZT8 as compared to ZT16 (Figure 3(e)); after α-MSH treatment, its expression was higher at ZT12 as compared to ZT8 and ZT20 ($P < 0.01$) (Figure 3(f)). Therefore α-MSH effects on melanopsins expressions do not seem to involve the molecular clock machinery, since the hormone did not affect *Per1* expression except for a sporadic modulation throughout the day.

In fact, the opposite effects of α-MSH and melatonin seem to be conserved, because they have previously been described in other groups of animals [65, 66]. This may be explained by the opposite actions of these hormones on cAMP production in *X. laevis* melanophores: α-MSH increases the nucleotide concentration [43], whereas melatonin reverses melanosome dispersion through the inhibition of adenylyl cyclase [67].

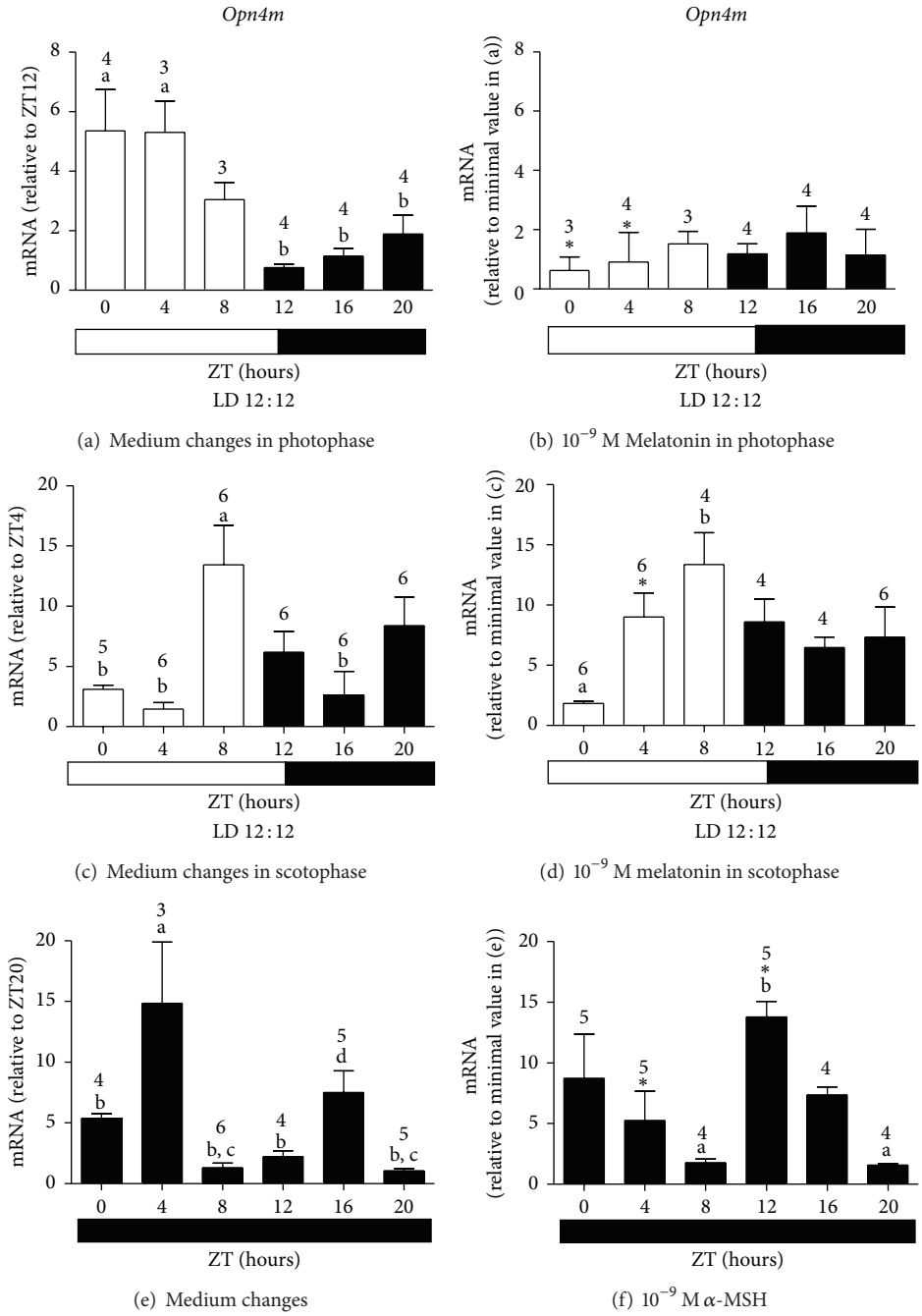

Figure 3: Quantitative PCR of *Opn4m* in *X. laevis* melanophores after to 2 medium changes in the photophase of LD 12 : 12 (a); 10^{-9} M melatonin in the photophase of LD 12 : 12 (b); 2 medium changes in the scotophase of LD 12 : 12 (c); 10^{-9} M melatonin in the scotophase of LD 12 : 12 (d); 2 medium changes in DD (e); 10^{-9} M α-MSH in DD (f). Each bar represents the mean, ± SE, mRNA relative to the noted ZT. (a) Significantly different from (b); (c) significantly different from (d), by one-way ANOVAandTukey's post-test; ∗ means significantly different from the respective control at the same ZT, by two-way ANOVA and Bonferroni's post-test.

We would expect similar effects of α-MSH (Figures 2(f) and 3(f)) and light (Figures 2(a) and 3(a)) on *Opn4x* and *Opn4m* expression; however, unlike the hormone, light was able to induce temporal variation in both melanopsin expressions. This may be explained by the fact that the signaling pathway leading to light-stimulated responses of gene expression and pigment dispersion is distinct from the one triggering melanin dispersion by α-MSH. In fact, light stimulates PKC pathway leading to an increase of cytosolic Ca^{2+} and cGMP [42], whereas α-MSH promotes an increase of cAMP [43]. This response is decreased by preexposure of melanophores to light, because light-induced Ca^{2+} rise inhibits adenylyl cyclase [43]. Although mammalian *Per1* promoter is known to possess cAMP responsive element

[68], little is known about *X. laevis Per1* promoter. In *Danio rerio* embryonic cells, we and others have demonstrated that the light-stimulated pathway increases both *Per1* and *Per2* expressions, what is blocked by MAP kinase inhibitors [69–71], whereas there is controversial evidence of cAMP involvement [71]. In NIH-3T3 fibroblasts, it has been shown that the circadian oscillation of clock gene expression is abolished by a MEK inhibitor [59], suggesting that transcription factors other than CREB may be the activators of *Per1* promoter in vertebrate peripheral clocks.

In summary, *Per1* is sensitive to light-dark cycles, regardless of the presence of melatonin or α-MSH, which slightly inhibited its expression. It is worth to mention, however, that the hormones may be affecting the expression of other clock genes, such as *Per2* or *Bmal1*, or even exerting a posttranslational effect. Melatonin effects on melanopsins depend on the time of application. Melatonin applied in the photophase dramatically decreases *Opn4x* and *Opn4m* expressions and abolishes its temporal oscillation, opposite to α-MSH which increases the melanopsin expressions. Our results demonstrate that unlike what has been reported for other peripheral clocks and cultured cells, medium changes or hormones do not play a major role in synchronizing *Xenopus* melanophore cell population. This difference is most probably due to the fact that *X. laevis* melanophores possess functional photopigments, the melanopsins, enabling these cells to respond primarily to light, which triggers melanin dispersion and modulation of gene expression.

Conflict of Interests

The authors declare that there is no conflict of interests regarding the publication of this paper.

Authors' Contribution

Maristela Oliveira Poletini and Ana Maria de Lauro Castrucci contributed equally to this work.

Acknowledgments

The authors acknowledge Fundação de Amparo à Pesquisa do Estado de São Paulo (FAPESP) and Conselho Nacional de Desenvolvimento Tecnológico e Científico (CNPq) Grants. Maria Nathália de Carvalho Magalhães Moraes is a fellow of FAPESP, Nathana Mezzalira is a fellow of CAPES, and Luciane Rogéria dos Santos was a fellow of FAPESP.

References

[1] D. Stuart-Fox and A. Moussalli, "Camouflage, communication and thermoregulation: lessons from colour changing organisms," *Philosophical Transactions of the Royal Society B: Biological Sciences*, vol. 364, no. 1516, pp. 463–470, 2009.

[2] J. T. Bagnara and M. E. Hadley, *Chromatophores and Color Change: The Comparative Physiology of Animal Pigmentation*, Prentice-Hall, Englewood Cliffs, NJ, USA, 1973.

[3] H. Nilsson-Sköld, S. Aspengren, and M. Wallin, "Rapid color change in fish and amphibians—function, regulation, and emerging applications," *Pigment Cell Melanoma Research*, vol. 26, no. 1, pp. 29–38, 2013.

[4] J. T. Bagnara, "Hypophysectomy and the tail darkening reaction in *Xenopus*," *Proceedings of the Society for Experimental Biology and Medicine*, vol. 94, no. 3, pp. 572–575, 1957.

[5] T. Iga and I. Takabatake, "Melanophores of *Zacco temmincki* (Teleostei) are light sensitive," *Journal of Experimental Zoology*, vol. 227, no. 1, pp. 9–14, 1983.

[6] M. D. Rollag, "Pertussis toxin sensitive photoaggregation of pigment in isolated Xenopus tail-fin melanophores," *Photochemistry and Photobiology*, vol. 57, no. 5, pp. 862–866, 1993.

[7] R. Fujii, "The regulation of motile activity in fish chromatophores," *Pigment Cell Research*, vol. 13, no. 5, pp. 300–319, 2000.

[8] L. E. M. Nery and A. M. D. L. Castrucci, "Pigment cell signalling for physiological color change," *Comparative Biochemistry and Physiology A: Physiology*, vol. 118, no. 4, pp. 1135–1144, 1997.

[9] R. Fujii and Y. Miyashita, "Receptor mechanisms in fish chromatophores V. MSH disperses melanosomes in both dermal and epidermal melanophores of a catfish (*Parasilurus asotus*)," *Comparative Biochemistry and Physiology C: Pharmacology Toxicology and Endocrinology*, vol. 71, no. 1, pp. 1–6, 1982.

[10] L. A. M. De Castrucci, E. Hadley Mac, and V. J. Hruby, "Melanotropin bioassays: in vitro and in vivo comparisons," *General and Comparative Endocrinology*, vol. 55, no. 1, pp. 104–111, 1984.

[11] W. C. Sherbrooke, M. E. Hadley, and A. M. L. Castrucci, "Melanotropic peptides and receptors: an evolutionary perspective in vertebrate physiological color change," in *The Melanotropic Peptides*, M. E. Hadley, Ed., vol. 2, pp. 175–190, CRC Press, Washington, DC, USA, 1988.

[12] H. Vaudry, N. Chartrel, L. Desrues et al., "The pituitary-skin connection in amphibians. Reciprocal regulation of melanotrope cells and dermal melanocytes," *Annals of the New York Academy of Sciences*, vol. 885, pp. 41–56, 1999.

[13] C. R. Camargo, M. A. Visconti, and A. M. L. Castrucci, "Physiological color change in the bullfrog, *Rana catesbeiana*," *Journal of Experimental Zoology*, vol. 283, pp. 160–169, 1999.

[14] W. C. Chou, M. Takeo, P. Rabbani et al., "Direct migration of follicular melanocyte stem cells to the epidermis after wounding or UVB irradiation is dependent on Mc1r signaling," *Nature Medicine*, vol. 19, no. 7, pp. 924–929, 2013.

[15] X. H. Zhang, Y. Z. Pang, S. J. Zhao et al., "The relationship of plumage colours with MC1R (Melanocortin 1 Receptor) and ASIP (Agouti Signaling Protein) in Japanese quail (*Coturnix coturnix japonica*)," *British Poultry Science*, vol. 54, no. 3, pp. 306–311, 2013.

[16] A. Slominski and J. Wortsman, "Neuroendocrinology of the skin," *Endocrine Reviews*, vol. 21, no. 5, pp. 457–487, 2000.

[17] T. Brzoska, M. Böhm, A. Lügering, K. Loser, and T. A. Luger, "Terminal signal: anti-inflammatory effects of α-melanocyte-stimulating hormone related peptides beyond the pharmacophore," *Advances in Experimental Medicine and Biology*, vol. 681, pp. 107–116, 2010.

[18] W. Chen, J. Li, H. Qu et al., "The melanocortin 1 receptor (MC1R) inhibits the inflammatory response in Raw 264.7 cells and atopic dermatitis (AD) mouse model," *Molecular Biology Reports*, vol. 40, no. 2, pp. 1987–1996, 2013.

[19] B. Iyengar, "The melanocyte photosensory system in the human skin," *SpringerPlus*, vol. 1, pp. 158–188, 2013.

[20] A. Bertolini, R. Tacchi, and A. V. Vergoni, "Brain effects of melanocortins," *Pharmacological Research*, vol. 59, no. 1, pp. 13–47, 2009.

[21] E. Keen-Rhinehart, K. Ondek, and J. E. Schneider, "Neuroendocrine regulation of appetitive ingestive behavior," *Frontiers in Neuroscience*, vol. 7, pp. 213–243, 2013.

[22] D. Sugden, K. Davidson, K. A. Hough, and M.-T. Teh, "Melatonin, melatonin receptors and melanophores: a moving story," *Pigment Cell Research*, vol. 17, no. 5, pp. 454–460, 2004.

[23] S. Binkley, *Pineal: Endocrine and Nonendocrine Function*, Prentice-Hall, Englewood Cliffs, NJ, USA, 1988.

[24] A. M. C. Filadelfi and A. M. D. L. Castrucci, "Comparative aspects of the pineal/melatonin system of poikilothermic vertebrates," *Journal of Pineal Research*, vol. 20, no. 4, pp. 175–186, 1996.

[25] D. Hazlerigg, "The evolutionary physiology of photoperiodism in vertebrates," *Progress in Brain Research*, vol. 199, pp. 413–422, 2012.

[26] L. Shi, N. Li, L. Bo, and Z. Xu, "Melatonin and hypothalamic-pituitary-gonadal axis," *Current Medicinal Chemistry*, vol. 20, no. 15, pp. 2017–2031, 2013.

[27] D.-X. Tan, L. C. Manchester, M. P. Terron, L. J. Flores, and R. J. Reiter, "One molecule, many derivatives: a never-ending interaction of melatonin with reactive oxygen and nitrogen species?" *Journal of Pineal Research*, vol. 42, no. 1, pp. 28–42, 2007.

[28] D. X. Tan, R. Hardeland, L. C. Manchester, A. Galano, and R. J. Reiter, "Cyclic-3-hydroxymelatonin (C3HOM), a potent antioxidant, scavenges free radicals and suppresses oxidative reactions," *Current Medicinal Chemistry*, vol. 21, no. 13, pp. 1557–1565, 2014.

[29] I. Provencio, G. Jiang, W. J. De Grip, W. Pär Hayes, and M. D. Rollag, "Melanopsin: an opsin in melanophores, brain, and eye," *Proceedings of the National Academy of Sciences of the United States of America*, vol. 95, no. 1, pp. 340–345, 1998.

[30] I. Provencio, I. R. Rodriguez, G. Jiang, W. P. Hayes, E. F. Moreira, and M. D. Rollag, "A novel human opsin in the inner retina," *Journal of Neuroscience*, vol. 20, no. 2, pp. 600–605, 2000.

[31] I. Provencio, M. D. Rollag, and A. M. Castrucci, "Photoreceptive net in the mammalian retina. This mesh of cells may explain how some blind mice can still tell day from night," *Nature*, vol. 415, no. 6871, p. 493, 2002.

[32] D. M. Berson, F. A. Dunn, and M. Takao, "Phototransduction by retinal ganglion cells that set the circadian clock," *Science*, vol. 295, no. 5557, pp. 1070–1073, 2002.

[33] S. Hattar, H.-W. Liao, M. Takao, D. M. Berson, and K.-W. Yau, "Melanopsin-containing retinal ganglion cells: architecture, projections, and intrinsic photosensitivity," *Science*, vol. 295, no. 5557, pp. 1065–1070, 2002.

[34] S. Panda, T. K. Sato, A. M. Castrucci et al., "Melanopsin (Opn4) requirement for normal light-induced circadian phase shifting," *Science*, vol. 298, no. 5601, pp. 2213–2216, 2002.

[35] S. Panda, I. Provencio, D. C. Tu et al., "Melanopsin is required for non-image-forming photic responses in blind mice," *Science*, vol. 301, no. 5632, pp. 525–527, 2003.

[36] J. Bellingham, S. S. Chaurasia, Z. Melyan et al., "Evolution of melanopsin photoreceptors: discovery and characterization of a new melanopsin in nonmammalian vertebrates," *PLoS Biology*, vol. 4, no. 8, article e254, 2006.

[37] U. Albrecht, "Timing to perfection: the biology of central and peripheral circadian clocks," *Neuron*, vol. 74, no. 2, pp. 246–260, 2012.

[38] S. Panda, M. P. Antoch, B. H. Miller et al., "Coordinated transcription of key pathways in the mouse by the circadian clock," *Cell*, vol. 109, no. 3, pp. 307–320, 2002.

[39] K.-F. Storch, O. Lipan, I. Leykin et al., "Extensive and divergent circadian gene expression in liver and heart," *Nature*, vol. 417, pp. 78–83, 2002.

[40] B. E. McIntosh, J. B. Hogenesch, and C. A. Bradfield, "Mammalian Per-Arnt-Sim proteins in environmental adaptation," *Annual Review of Physiology*, vol. 72, pp. 625–645, 2010.

[41] C. Murre, P. Schonleber McCaw, H. Vaessin et al., "Interactions between heterologous helix-loop-helix proteins generate complexes that bind specifically to a common DNA sequence," *Cell*, vol. 58, no. 3, pp. 537–544, 1989.

[42] M. C. Isoldi, M. D. Rollag, A. M. De Lauro Castrucci, and I. Provencio, "Rhabdomeric phototransduction initiated by the vertebrate photopigment melanopsin," *Proceedings of the National Academy of Sciences of the United States of America*, vol. 102, no. 4, pp. 1217–1221, 2005.

[43] M. C. Isoldi, I. Provencio, and A. M. D. L. Castrucci, "Light modulates the melanophore response to α-MSH in *Xenopus laevis*: an analysis of the signal transduction crosstalk mechanisms involved," *General and Comparative Endocrinology*, vol. 165, no. 1, pp. 104–110, 2010.

[44] F. Rouzaud, A. L. Kadekaro, Z. A. Abdel-Malek, and V. J. Hearing, "MC1R and the response of melanocytes to ultraviolet radiation," *Mutation Research: Fundamental and Molecular Mechanisms of Mutagenesis*, vol. 571, no. 1-2, pp. 133–152, 2005.

[45] M. N. C. M. Moraes, M. O. Poletini, B. C. R. Ramos, L. H. R. G. Lima, and A. M. L. Castrucci, "Effect of light on expression of clock genes in *Xenopus laevis* melanophores," *Photochemistry and Photobiology*, 2013.

[46] M. D. Rollag, I. Provencio, D. Sugden, and C. B. Green, "Cultured amphibian melanophores: a model system to study melanopsin photobiology," *Methods in Enzymology*, vol. 316, pp. 291–309, 2000.

[47] J. L. Aerts, M. I. Gonzales, and S. L. Topalian, "Selection of appropriate control genes to assess expression of tumor antigens using real-time RT-PCR," *BioTechniques*, vol. 36, no. 1, pp. 84–91, 2004.

[48] D. Goidin, A. Mamessier, M.-J. Staquet, D. Schmitt, and O. Berthier-Vergnes, "Ribosomal 18S RNA prevails over glyceraldehyde-3-phosphate dehydrogenase and β-actin genes as internal standard for quantitative comparison of mRNA levels in invasive and noninvasive human melanoma cell subpopulations," *Analytical Biochemistry*, vol. 295, no. 1, pp. 17–21, 2001.

[49] A. T. McCurley and G. V. Callard, "Characterization of housekeeping genes in zebrafish: male-female differences and effects of tissue type, developmental stage and chemical treatment," *BMC Molecular Biology*, vol. 9, pp. 102–119, 2008.

[50] H. Schmid, C. D. Cohen, A. Henger, S. Irrgang, D. Schlöndorff, and M. Kretzler, "Validation of endogenous controls for gene expression analysis in microdissected human renal biopsies," *Kidney International*, vol. 64, no. 1, pp. 356–360, 2003.

[51] L.-J. Zhu and S. W. Altmann, "mRNA and 18S-RNA coapplication-reverse transcription for quantitative gene expression analysis," *Analytical Biochemistry*, vol. 345, no. 1, pp. 102–109, 2005.

[52] K. J. Livak and T. D. Schmittgen, "Analysis of relative gene expression data using real-time quantitative PCR and the 2-$\Delta\Delta$CT method," *Methods*, vol. 25, no. 4, pp. 402–408, 2001.

[53] D. A. Golombek and R. E. Rosenstein, "Physiology of circadian entrainment," *Physiological Reviews*, vol. 90, no. 3, pp. 1063–1102, 2010.

[54] S. Liu, Y. Cai, R. B. Sothern, Y. Guan, and P. Chan, "Chronobiological analysis of circadian patterns in transcription of seven key clock genes in six peripheral tissues in mice," *Chronobiology International*, vol. 24, no. 5, pp. 793–820, 2007.

[55] A.-J. F. Carr and D. Whitmore, "Imaging of single light-responsive clock cells reveals fluctuating free-running periods," *Nature Cell Biology*, vol. 7, no. 3, pp. 319–321, 2005.

[56] D. K. Welsh, T. Imaizumi, and S. A. Kay, "Real-time reporting of circadian-regulated gene expression by luciferase imaging in plants and mammalian cells," *Methods in Enzymology*, vol. 393, article 11, pp. 269–288, 2005.

[57] A. Balsalobre, F. Damiola, and U. Schibler, "A serum shock induces circadian gene expression in mammalian tissue culture cells," *Cell*, vol. 93, no. 6, pp. 929–937, 1998.

[58] S. Yamazaki, R. Numano, M. Abe et al., "Resetting central and peripheral circadian oscillators in transgenic rats," *Science*, vol. 288, no. 5466, pp. 682–685, 2000.

[59] M. Akashi and E. Nishida, "Involvement of the MAP kinase cascade in resetting of the mammalian circadian clock," *Genes and Development*, vol. 14, no. 6, pp. 645–649, 2000.

[60] A. Balsalobre, S. A. Brown, L. Marcacci et al., "Resetting of circadian time in peripheral tissues by glucocorticoid signaling," *Science*, vol. 289, no. 5488, pp. 2344–2347, 2000.

[61] A. P. C. Bluhm, N. N. Obeid, A. M. L. Castrucci, and M. A. Visconti, "The expression of melanopsin and clock genes in *Xenopus laevis* melanophores and their modulation by melatonin," *Brazilian Journal of Medical and Biological Research*, vol. 45, pp. 730–736, 2012.

[62] M. Zhuang, Y. Wang, B. M. Steenhard, and J. C. Besharse, "Differential regulation of two period genes in the *Xenopus* eye," *Molecular Brain Research*, vol. 82, no. 1-2, pp. 52–64, 2000.

[63] S. M. Reppert and D. R. Weaver, "Coordination of circadian timing in mammals," *Nature*, vol. 418, no. 6901, pp. 935–941, 2002.

[64] R. J. Reiter, "The pineal gland: an intermediary between the environment and the endocrine system," *Psychoneuroendocrinology*, vol. 8, no. 1, pp. 31–40, 1983.

[65] A. M. C. Filadelfi and A. M. L. Castrucci, "Melatonin desensitizing effects on the *in vitro* responses to MCH, alpha-MSH, isoproterenol and melatonin in pigment cells of a fish (*S. marmoratus*), a toad (*B. ictericus*), a frog (*R. pipiens*), and a lizard (*A. carolinensis*), exposed to varying photoperiodic regimens," *Comparative Biochemistry and Physiology A: Physiology*, vol. 109, no. 4, pp. 1027–1037, 1994.

[66] A. L. Kadekaro, L. N. S. Andrade, L. M. Floeter-Winter et al., "MT-1 melatonin receptor expression increases the antiproliferative effect of melatonin on S-91 murine melanoma cells," *Journal of Pineal Research*, vol. 36, no. 3, pp. 204–211, 2004.

[67] B. H. White, R. D. Sekura, and M. D. Rollag, "Pertussis toxin blocks melatonin-induced pigment aggregation in *Xenopus* dermal melanophores," *Journal of Comparative Physiology B: Biochemical, Systemic, and Environmental Physiology*, vol. 157, no. 2, pp. 153–159, 1987.

[68] S. A. Tischkau, J. W. Mitchell, S.-H. Tyan, G. F. Buchanan, and M. U. Gillette, "Ca^{2+}/cAMP response element-binding protein (CREB)-dependent activation of *Per1* is required for light-induced signaling in the suprachiasmatic nucleus circadian clock," *Journal of Biological Chemistry*, vol. 278, no. 2, pp. 718–723, 2003.

[69] N. Cermakian, M. P. Pando, C. L. Thompson et al., "Light induction of a vertebrate clock gene involves signaling through blue-light receptors and MAP kinases," *Current Biology*, vol. 12, no. 10, pp. 844–848, 2002.

[70] J. Hirayama, L. Cardone, M. Doi, and P. Sassone-Corsi, "Common pathways in circadian and cell cycle clocks: light-dependent activation of Fos/AP-1 in zebrafish controls CRY-1a and WEE-1," *Proceedings of the National Academy of Sciences of the United States of America*, vol. 102, no. 29, pp. 10194–10199, 2005.

[71] N. Cermakian, M. P. Pando, C. L. Thompson et al., "Light induction of a vertebrate clock gene involves signaling through blue-light receptors and MAP kinases," *Current Biology*, vol. 12, no. 10, pp. 844–848, 2002.

Hindawi Publishing Corporation
BioMed Research International
Volume 2014, Article ID 170795, 5 pages
http://dx.doi.org/10.1155/2014/170795

Research Article

The Effect of Different Photoperiods in Circadian Rhythms of *Per3* Knockout Mice

D. S. Pereira,[1] D. R. van der Veen,[2] B. S. B. Gonçalves,[3,4] S. Tufik,[1] M. von Schantz,[2] S. N. Archer,[2] and M. Pedrazzoli[5]

[1] *Departamento de Psicobiologia, Universidade Federal de São Paulo (UNIFESP), Rua Napoleão de Barros 925, 3ºAndar, 04024-002 São Paulo, SP, Brazil*
[2] *Faculty of Health and Medical Science, University of Surrey, Guildford, UK*
[3] *Departamento de Fisiologia, Universidade Federal do Rio Grande do Norte (UFRN), Natal, RN, Brazil*
[4] *Instituto Federal Sudeste de Minas Gerais, Campus Barbacena, Barbacena, MG, Brazil*
[5] *Escola de Artes, Ciências e Humanidades, Universidade de São Paulo (USP), São Paulo, SP, Brazil*

Correspondence should be addressed to D. S. Pereira; danyellap@gmail.com

Received 26 January 2014; Revised 24 March 2014; Accepted 19 April 2014; Published 8 May 2014

Academic Editor: Martin Fredensborg Rath

The aim of this study was to analyse the circadian behavioural responses of mice carrying a functional knockout of the *Per3* gene ($Per3^{-/-}$) to different light : dark (L : D) cycles. Male adult wild-type (WT) and $Per3^{-/-}$ mice were kept under 12-hour light : 12-hour dark conditions (12L : 12D) and then transferred to either a short or long photoperiod and subsequently released into total darkness. All mice were exposed to both conditions, and behavioural activity data were acquired through running wheel activity and analysed for circadian characteristics during these conditions. We observed that, during the transition from 12L : 12D to 16L : 8D, $Per3^{-/-}$ mice take approximately one additional day to synchronise to the new L : D cycle compared to WT mice. Under these long photoperiod conditions, $Per3^{-/-}$ mice were more active in the light phase. Our results suggest that $Per3^{-/-}$ mice are less sensitive to light. The data presented here provides further evidence that *Per3* is involved in the suppression of behavioural activity in direct response to light.

1. Introduction

Circadian (~24-hour) rhythms are driven by internal clocks, which are entrained by external timing cues (Zeitgebers). One of the most important Zeitgebers is the environmental light : dark (L : D) cycle. Photic signals entrain the circadian clock in the suprachiasmatic nuclei (SCN) of the hypothalamus, and the entrained signal is distributed to the hierarchical network of clocks in peripheral tissues [1].

In the last four decades, substantial progress has been made in the understanding of the molecular basis of circadian rhythmicity. Several clock genes have been identified in mammals (for review, [2]). Studies using functional clock gene knockout mice have shown alterations in the endogenous circadian period length, loss of persistence of circadian rhythms, and disturbed sleep-wake cycles [3, 4].

Among the so-called clock genes, reports on the function of *Per3* have been the most inconclusive. While studies in animals suggest that the *Per3* gene is not critical for regulating circadian rhythms based on the small changes found in the free-running period and the lack of differential responses to light pulses in functional knockout animals [3, 4], human studies have shown that this gene is strongly associated with chronotypes, circadian dysfunction, and the homeostatic regulation of sleep [5–9]. More recently, the absence of *Per3* has been shown to differentially affect peripheral oscillators [10].

Our understanding of the function of *Per3* was improved by the finding that functional *Per3* knockout mice ($Per3^{-/-}$) are characterised by altered sensitivity to light [11] and altered sleep homeostatic responses to sleep deprivation [9]. It has also been proposed that, in humans, the *PER3* gene could

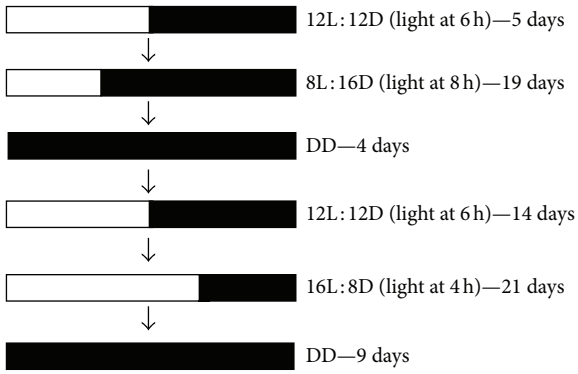

Figure 1: Schematic representation of the experimental protocol. All mice were submitted to this protocol in the same sequence. L : D = light : dark, DD = dark : dark.

be involved in the entrainment to differential seasonal light signals created by latitude [7, 12]. Based on the previous finding that the *Per3* gene plays a role in circadian light sensitivity, the aim of this study was to analyse whether *Per3*$^{-/-}$ mice respond differently to different photoperiods.

2. Materials and Methods

2.1. Animals. C57BL/6 *Per3*$^{-/-}$ mice were generated as previously described [4, 11]. Six wild-type (WT) mice and six *mPer3*$^{-/-}$ mice, originating from heterozygous backcrosses on a C57Bl/6 background and 3 months of age, were housed in running wheel cages in light-tight, sound-attenuated cabinets, and activity was recorded in 1 min bins (Clocklab, Actimetrics, Wilmette, IL). The light intensity was 800 +/− 13 mW/m^2 (mean +/− SEM) in the light phase. The temperature was maintained at 19 to 22°C and relative humidity at 55% ± 10%. The animals were provided with food (transgenic mouse diet, B & K Universal Ltd, Hull, UK) and water *ad libitum*.

The experiments had previously received a favourable opinion from the University of Surrey Animal Ethics Committee and were carried out under UK Home Office License in accordance with the Declaration of Helsinki.

2.2. Light Entrainment. Mice were entrained to 12L : 12D for 5 days and then exposed to the following sequential L : D schemes: 8L : 16D for 19 days, 4 days in constant dark (DD), 12L : 12D for 14 days, 16L : 8D for 22 days, and 9 days in DD (Figure 1).

2.3. Behavioural and Statistic Analysis. Behavioural (periodogram) analysis [13]) and graphical output (actograms) were produced using the *El Temps* software (A. Díez-Noguera, University of Barcelona, 1999), and statistical significance was tested using Statistica software (StatSoft Inc., 1984–2007, Tulsa, OK). The Kolmogorov-Smirnov test was used to test for normality of distribution. Normally distributed data were compared between groups using Student's *t* test, and data that were not normally distributed were compared using the Mann-Whitney test. The significance level was set at $P < 0.05$.

The phase angle of entrainment was calculated under all light conditions and defined as the difference in minutes between the onset of darkness and the activity onset. Positive phase angles indicate that the animal became active after lights off, and negative phase angles indicate that the animal became active before the light was turned off. For behavioural phase determination, we smoothed the data using a boxcar smoothing approach with a 2-hour window. For each day, we determined for the first instance that the activity level of the smoothed activity exceeded (onset) the 24-hour average. To filter out any fluctuations (e.g., the typical late night "dip" in behavioural activity observed in C57Bl/6 mice), we set an additional requirement that any onset was valid only when the activity in the 2 hours preceding this onset was lower than 10 running wheel revolutions and at least 50 revolutions in the 2 hours after the onset.

We visually determined the number of days (transients) required to resynchronise after L : D cycle change for each animal. We considered that transients were fully completed at the new L : D condition when activity onset stabilised at a time point and remained at the same point at least for two consecutive days.

The amount of running wheel activity during the light and dark phase was expressed in centimeters ($2\pi R$ of the running wheel, where R is the radius of the wheel); total amount of activity per animal per L : D schedule was calculated and then averaged by group. Transients of light transitions were excluded in each light or dark phase to calculate the amount of running wheel activity.

3. Results

Periodogram analysis (all individual periodograms are included in the supplementary material) showed that mice of both genotypes were entrained to a near 24 h period (no significant difference in period length).

Figures 2 and 3 show representative examples of activity plots for a WT (Animal 8 in Supplementary Material available online at http://dx.doi.org/10.1155/2014/170795) and *Per3*$^{-/-}$ (Animal 2 in Supplementary Material) animal, respectively. In the transition from 12L : 12D to 8L : 16D, we observed no difference between WT and *Per3*$^{-/-}$ mice in terms of behavioural reentrainment. The average transient for both groups was 5.5 days (±1.6 and ±2.9 SD, WT and *Per3*$^{-/-}$, resp.). By contrast, for the transition from 12L : 12D to 16L : 8D, *Per3*$^{-/-}$ mice took on average 2.0 ± 0.8 (±SD) days to synchronise while WT mice responded rapidly to the new light stimulus ($Z_{\text{adjusted}} = -2.3$, $P = 0.02$). Mice quickly synchronised to the long photoperiod, suggesting that behavioural activity in what is now the light phase is, in fact, predominantly masked by light. When mice were released to DD after 16L : 8D, they did not retain activity patterns seen in 16L : 8D, but, after a few transients, they seemed to return to the same phase where they were in the previous 12L : 12D cycles.

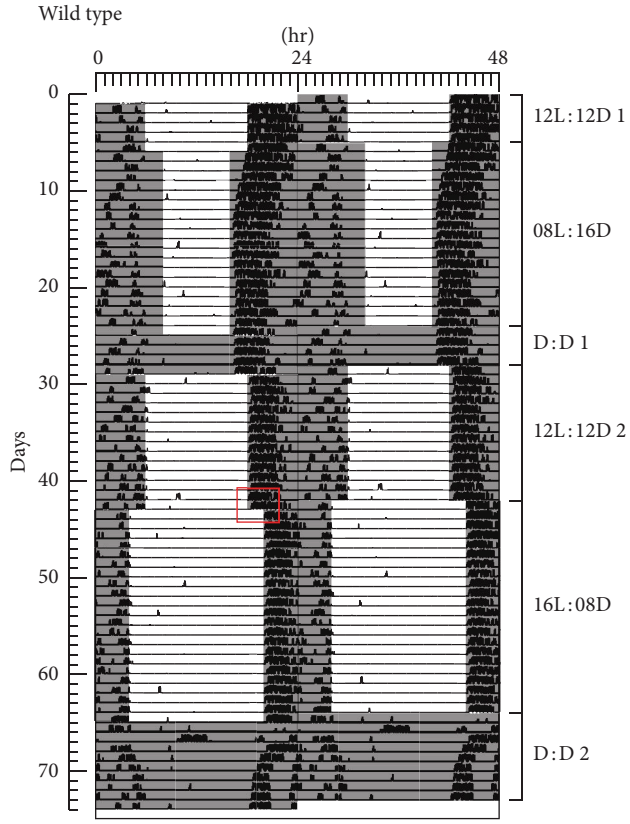

Figure 2: A representative double-plot actogram of one WT mouse. Mice were entrained to the following light : dark conditions: 12L : 12D for 5 days; 8L : 16D for 19 days; constant dark (DD) for 4 days; 12L : 12D for 14 days; 16L : 8D for 22 days and DD for 9 days. The red rectangle depicts the transition from 12L : 12D to 16L : 8D.

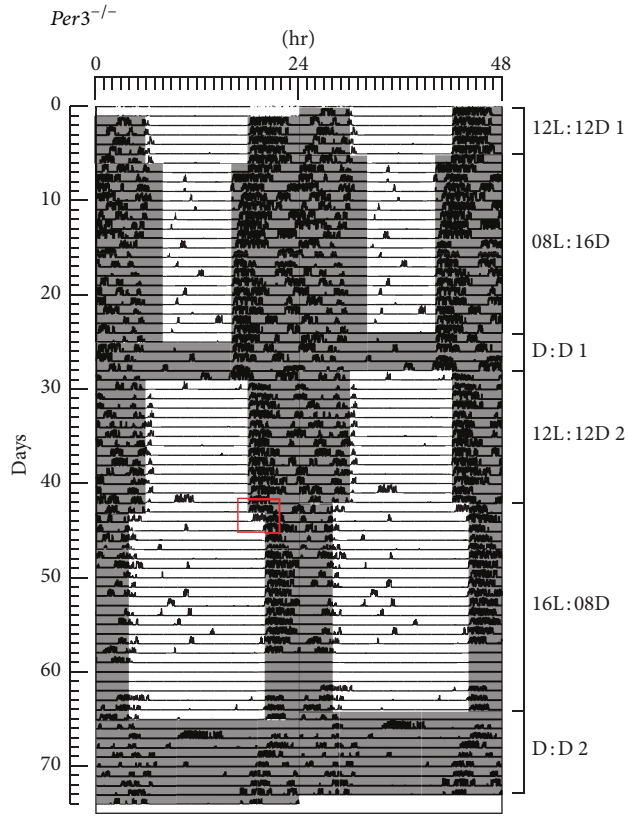

Figure 3: A representative double-plot actogram of one *mPer3*$^{-/-}$ mouse. Mice were entrained to the following light : dark conditions : 12L : 12D for 5 days; 8L : 16D for 19 days; constant dark (DD) for 4 days; 12L : 12D for 14 days; 16L : 8D for 22 days and DD for 9 days. The red rectangle depicts the transition from 12L : 12D to 16L : 8D.

In agreement with previous data [9], *Per3*$^{-/-}$ mice were overall more active than WT mice. Although increased activity can be observed in the light phase during all L : D conditions, this increase reached statistical significance during the longer photoperiod cycles ($Z_{\text{adjusted}} = -2.24$, $P = 0.02$, Figure 4).

We compared the phase angle of entrainment between WT and *Per3*$^{-/-}$ mice in all photoperiods analysed (Figure 5). No significant difference between groups was observed, but we did notice a tendency to a shorter phase angle in *Per3*$^{-/-}$ mice in 12L : 12D 1 and 16L : 8D (t value = −2, 16, $P = 0.056$ and t value = −1, 89, $P = 0.088$, resp.).

4. Discussion

Based on the actograms and analysis of phase angles of entrainment, we observed that *Per3*$^{-/-}$ mice appeared to need more days to synchronise to the long photoperiod (16L : 8D) than WT mice and show more activity than WT mice in the light phase in 16L : 8D. When mice were released into DD after 16L : 8D, after a few transients in the cases of some animals, the onset of activity shifted to a phase similar to that in the preceding 12L : 12D period, suggesting that the main effect of lacking *Per3* is not a strong direct shift of the phase of the circadian clock (phase of entrainment) but is instead more likely related to a preponderant masking effect of light on the activity behaviour.

In fact, the light signal may be considered a Zeitgeber as well as a masking agent. These roles of light on activity patterns are inseparable during light dark entrainment [14, 15]. Although we did not use a classical protocol to distinguish between masking and entrainment [14], our results are indicative of masking and corroborate a more elaborate protocol applied in our previous work [11]. The fact that the animals, when released into constant darkness after the 16L : 8D cycles, adopted rest-activity rhythms with an onset phase similar to their former 12L : 12D cycle (instead of maintaining the rest-activity profile they displayed in their previous 16L : 8D) supports the interpretation that their activity in 16L : 8D cycles was in fact preponderantly masked.

Studies of *Per3*$^{-/-}$ mice have reported none or only subtle behavioural changes in circadian properties [3, 4, 16–18]. However, these studies used short light pulses as the stimulus. In the present study, the stimulus was chronic light : dark conditions, and the observed behavioural differences between

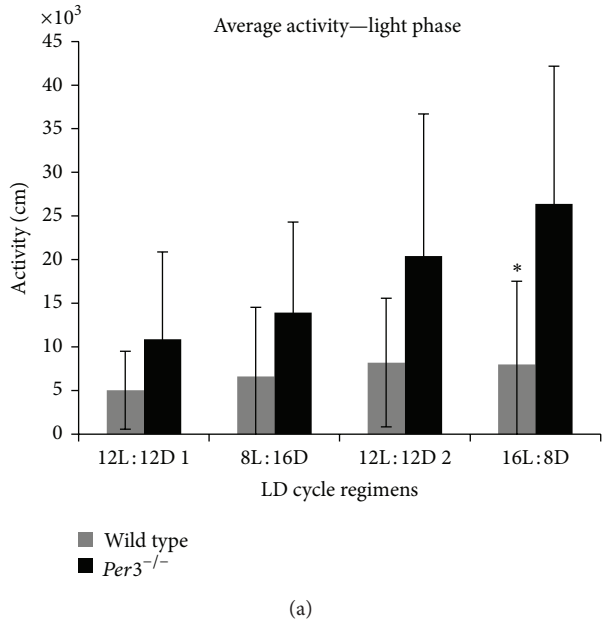

(a)

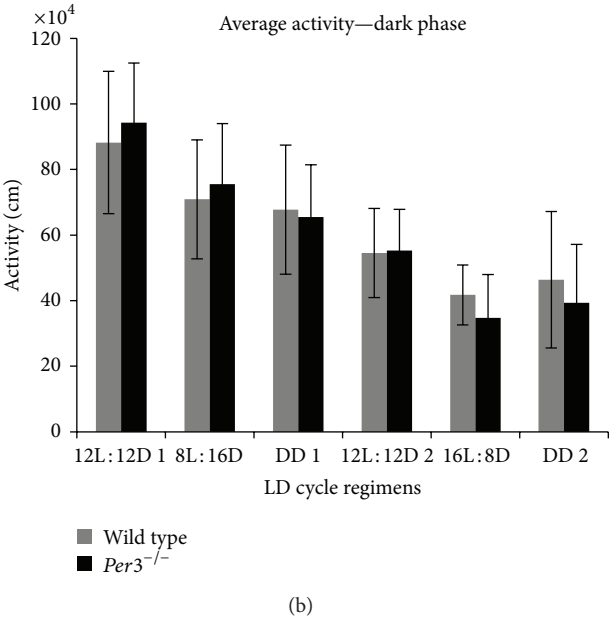

(b)

Figure 4: Total activity in light (a) and dark (b) phases. Values are represented as mean ± SD. Gray bars represent wild-type mice, and black bars show $mPer3^{-/-}$ mice. *Statistically significant $P < 0.05$.

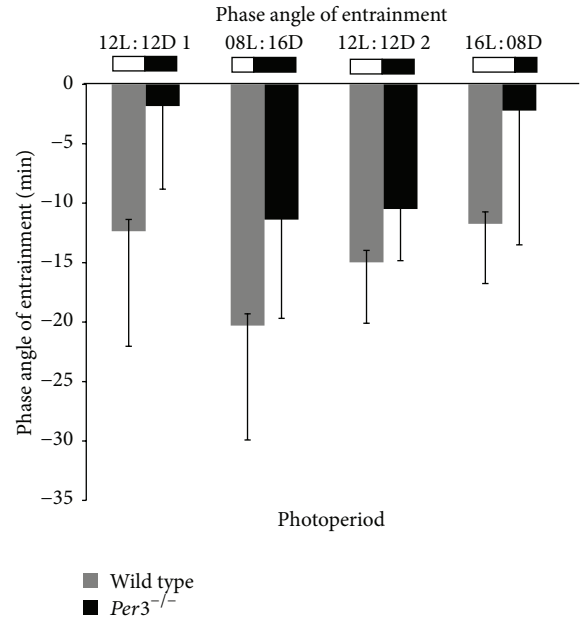

Figure 5: Phase angle of entrainment of WT and $Per3^{-/-}$ mice in all photoperiods analysed. Values are represented as mean ± SD. Gray bars represent wild-type mice, and black bars show $mPer3^{-/-}$ mice.

$Per3^{-/-}$ and WT mice, especially following long light exposure, suggest that *mPer3* is somehow importantly related to the sensitivity of light.

Thus, it seems that *Per3* is not involved in the processing of acute responses to light, but when animals are exposed to chronic light regimens, changes in behaviour appear. Our results strengthen the hypothesis that $Per3^{-/-}$ mice are less sensitive to light and corroborate reports showing that constant light affected the length of the endogenous period of $Per3^{-/-}$ differentially compared to WT and that the masking effect of light was attenuated or nonexistent in $mPer3^{-/-}$ animals [11].

Studies investigating *Per3* mRNA expression in suprachiasmatic nuclei are consistent with this; that is, the expression is not responsive to light pulses [16, 17]. However, in animals submitted to different photoperiods, (short photoperiod 10L : 14D and long photoperiod 14L : 10D), changes in *Per3* expression are the most prominent among all clock genes [19].

Our study has some limitations; the number of animals used and the natural individual variability in motor activity limit the power of the analyses and may account for the borderline significance for the phase angle of entrainment in 12L : 12D and 16L : 8D cycles. In addition, we may not exclude an effect of order of the sequence of L : D cycles on behavioural parameters observed.

Studies on humans [6–8], a recent study on $mPer3^{-/-}$ mice [11], and the present study indicate that the *Per3* gene is most likely involved in masking responses and thus may be associated with the interaction between the circadian clock and the motivational drive of behavioural activity in response to light-dark cycle.

Conflict of Interests

The authors declare that there is no conflict of interests regarding the publication of this paper.

Acknowledgments

This work was supported by Biotechnology and Biological Sciences Research Council (BBSRC; BB/E003672/1; Simon N Archer), Royal Society (Malcolm von Schantz), Fundação de Amparo à Pesquisa do Estado de São Paulo—FAPESP (Processo n° 2007/05037-9, CEPID 98/14303-3, Mario Pedrazzoli,

Danyella S Pereira, Sergio Tufik), Associação Fundo de Incentivo à Pesquisa (AFIP, Sergio Tufik), and Conselho Nacional de Desenvolvimento Científico e Tecnológico (CNPq, Sergio Tufik).

References

[1] J. S. Takahashi, H.-K. Hong, C. H. Ko, and E. L. McDearmon, "The genetics of mammalian circadian order and disorder: implications for physiology and disease," *Nature Reviews Genetics*, vol. 9, no. 10, pp. 764–775, 2008.

[2] M. von Schantz, "Phenotypic effects of genetic variability in human clock genes on circadian and sleep parameters," *Journal of Genetics*, vol. 87, no. 5, pp. 513–519, 2008.

[3] K. Bae, X. Jin, E. S. Maywood, M. H. Hastings, S. M. Reppert, and D. R. Weaver, "Differential functions of mPer1, mPer2, and mPer3 in the SCN circadian clock," *Neuron*, vol. 30, no. 2, pp. 525–536, 2001.

[4] L. P. Shearman, X. Jin, C. Lee, S. M. Reppert, and D. R. Weaver, "Targeted disruption of the mPer3 gene: subtle effects on circadian clock function," *Molecular and Cellular Biology*, vol. 20, no. 17, pp. 6269–6275, 2000.

[5] T. Ebisawa, M. Uchiyama, N. Kajimura et al., "Association of structural polymorphisms in the human period3 gene with delayed sleep phase syndrome," *EMBO Reports*, vol. 2, no. 4, pp. 342–346, 2001.

[6] S. N. Archer, D. L. Robilliard, D. J. Skene et al., "A length polymorphism in the circadian clock gene Per3 is linked to delayed sleep phase syndrome and extreme diurnal preference," *Sleep*, vol. 26, no. 4, pp. 413–415, 2003.

[7] D. S. Pereira, S. Tufik, F. M. Louzada et al., "Association of the length polymorphism in the human Per3 gene with the delayed sleep-phase syndrome: does latitude have an influence upon it?" *Sleep*, vol. 28, no. 1, pp. 29–32, 2005.

[8] A. U. Viola, S. N. Archer, L. James et al., "PER3 polymorphism predicts sleep structure and waking performance," *Current Biology*, vol. 17, no. 7, pp. 613–618, 2007.

[9] S. Hasan, D. R. van der Veen, R. Winsky-Sommerer, D.-J. Dijk, and S. N. Archer, "Altered sleep and behavioral activity phenotypes in PER3-deficient mice," *American Journal of Physiology—Regulatory Integrative and Comparative Physiology*, vol. 301, no. 6, pp. R1821–R1830, 2011.

[10] J. S. Pendergast, K. D. Niswender, and S. Yamazaki, "Tissue-specific function of period3 in circadian rhythmicity," *PLoS ONE*, vol. 7, no. 1, Article ID e30254, 2012.

[11] D. R. Van der Veen and S. N. Archer, "Light-dependent behavioral phenotypes in PER3-deficient mice," *Journal of Biological Rhythms*, vol. 25, no. 1, pp. 3–8, 2010.

[12] N. A. Nadkarni, M. E. Weale, M. Von Schantz, and M. G. Thomas, "Evolution of a length polymorphism in the human PER3 gene, a component of the circadian system," *Journal of Biological Rhythms*, vol. 20, no. 6, pp. 490–499, 2005.

[13] P. G. Sokolove and W. N. Bushell, "The chi square periodogram: its utility for analysis of circadian rhythms," *Journal of Theoretical Biology*, vol. 72, no. 1, pp. 131–160, 1978.

[14] U. Redlin and N. Mrosovsky, "Masking of locomotor activity in hamsters," *Journal of Comparative Physiology A*, vol. 184, no. 4, pp. 429–437, 1999.

[15] M. D. Marques and J. M. Waterhouse, "Masking and the evolution of circadian rhythmicity," *Chronobiology International*, vol. 11, no. 3, pp. 146–155, 1994.

[16] M. J. Zylka, L. P. Shearman, D. R. Weaver, and S. M. Reppert, "Three period homologs in mammals: differential light responses in the suprachiasmatic circadian clock and oscillating transcripts outside of brain," *Neuron*, vol. 20, no. 6, pp. 1103–1110, 1998.

[17] T. Takumi, K. Taguchi, S. Miyake et al., "A light-independent oscillatory gene mPer3 in mouse SCN and OVLT," *The EMBO Journal*, vol. 17, no. 16, pp. 4753–4759, 1998.

[18] J. S. Pendergast, R. C. Friday, and S. Yamazaki, "Photic entrainment of period mutant mice is predicted from their phase response curves," *Journal of Neuroscience*, vol. 30, no. 36, pp. 12179–12184, 2010.

[19] B. B. Tournier, J. S. Menet, H. Dardente et al., "Photoperiod differentially regulates clock genes' expression in the suprachiasmatic nucleus of Syrian hamster," *Neuroscience*, vol. 118, no. 2, pp. 317–322, 2003.

Hindawi Publishing Corporation
BioMed Research International
Volume 2014, Article ID 946075, 8 pages
http://dx.doi.org/10.1155/2014/946075

Review Article

Homeobox Genes and Melatonin Synthesis: Regulatory Roles of the Cone-Rod Homeobox Transcription Factor in the Rodent Pineal Gland

Kristian Rohde, Morten Møller, and Martin Fredensborg Rath

Department of Neuroscience and Pharmacology, Faculty of Health and Medical Sciences, University of Copenhagen, Rigshospitalet 6102, Blegdamsvej 9, 2100 Copenhagen, Denmark

Correspondence should be addressed to Kristian Rohde; rohde@sund.ku.dk

Received 26 January 2014; Accepted 7 April 2014; Published 30 April 2014

Academic Editor: Yoav Gothilf

Nocturnal synthesis of melatonin in the pineal gland is controlled by a circadian rhythm in arylalkylamine N-acetyltransferase (AANAT) enzyme activity. In the rodent, *Aanat* gene expression displays a marked circadian rhythm; release of norepinephrine in the gland at night causes a cAMP-based induction of *Aanat* transcription. However, additional transcriptional control mechanisms exist. Homeobox genes, which are generally known to encode transcription factors controlling developmental processes, are also expressed in the mature rodent pineal gland. Among these, the cone-rod homeobox (CRX) transcription factor is believed to control pineal-specific *Aanat* expression. Based on recent advances in our understanding of *Crx* in the rodent pineal gland, we here suggest that homeobox genes play a role in adult pineal physiology both by ensuring pineal-specific *Aanat* expression and by facilitating cAMP response element-based circadian melatonin production.

1. Introduction

Homeobox genes encode a large group of transcription factors involved in developmental processes throughout the animal kingdom [1]. The homeobox genes are molecularly characterized by the presence of a 180-nucleotide sequence element, the homeobox, which encodes a 60-amino acid structural motif, the homeodomain. The homeodomain recognizes specific DNA binding sites and thereby enables the homeodomain proteins to function as transcription factors [2–6]. In the pineal gland, a number of homeobox genes control developmental processes. However, certain homeobox genes predominantly exert their function in mature pinealocytes [7]. Among these, the cone-rod homeobox (*Crx*) gene seems to play an important role in transcriptional regulation of arylalkylamine N-acetyltransferase (*Aanat*) encoding the enzyme that controls the huge nocturnal peak in pineal melatonin synthesis [8].

In this paper, we review recent progress in our understanding of the biology of the CRX homeodomain transcription factor in the rodent pineal gland and propose a revised working model for the function of homeodomain transcription factors in regulation of rodent pineal *Aanat* transcription.

2. Homeobox Genes Regulate Pineal Gland Development

The mammalian pineal gland develops as a dorsal evagination from the most caudal part of the diencephalic roof [9]. As in other parts of the brain, timely and spatially controlled expression of a specific set of homeobox genes is essential for development of the pineal gland [7]. Gene knockout studies have identified a limited number of homeobox genes that are required for normal development of the rodent pineal gland; these include orthodenticle homeobox 2 (*Otx2*) [10], paired box 6 (*Pax6*) [11], brain specific homeobox (*Bsx*) [12], and LIM homeobox 9 (*Lhx9*) [13]. In line with a role of this set of homeobox genes in the immature developing pinealocyte, that is, the principal melatonin-producing cell type of the pineal gland, *in situ* hybridization analyses have revealed that these homeobox genes are highly expressed during early stages in rodent pineal gland development before the

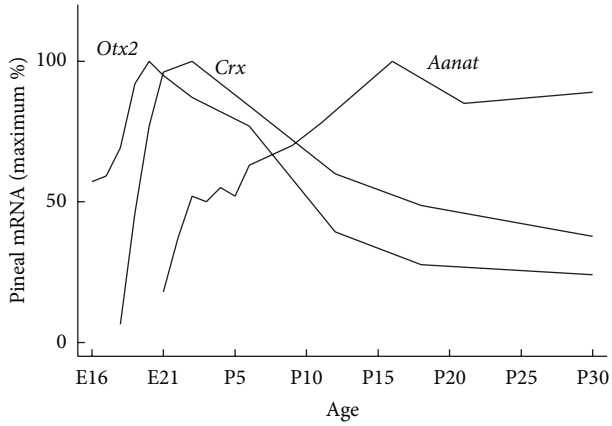

Figure 1: Appearance of *Otx2*, *Crx,* and *Aanat* transcripts in the developing rat pineal gland. *Otx2* and *Crx* expression peak around birth [14], at which time *Aanat* expression is initiated [19]. The spatial and temporal correlation between peaks in expression of *Otx2* and *Crx* and the start of *Aanat* expression supports that the OTX2 and CRX homeodomain transcription factors induce *Aanat* transcription [7]. E, embryonic day; P, postnatal day.

appearance of pineal melatonin synthesis [13–17]. However, pineal expression of homeobox genes is not restricted to prenatal stages (Figure 1); expression of homeobox genes involved in pineal development may persist into adulthood (e.g., *Otx2*) [14], expression may start at perinatal stages just prior to the onset of melatonin synthesis (e.g., *Crx* and retina and anterior neural fold homeobox (*Rax*)) [14, 18], or expression levels may start to increase even after or concomitant with the ontogenetic onset of melatonin synthesis (e.g., *Pax4* and *Lhx4*) [13, 15]. Thus, another set of homeobox genes, including *Crx*, predominantly exert their function in the mature melatonin-producing pinealocyte.

3. Circadian Regulation of Melatonin Synthesis in the Mammalian Pineal Gland

The mammalian melatonin rhythm generating system transforms the ambient lighting conditions into the internal hormonal message of melatonin, which is restricted to night time. The system is comprised of three parts: the suprachiasmatic nucleus (SCN) of the hypothalamus, the retina, and the pineal gland [20] as opposed to the melatonin rhythm generating system in nonmammalian vertebrate species, in which the three elements are integrated into one cell [21] (see below). The SCN of mammals generates a circadian rhythm. This rhythm is established by a cellular clock mechanism that comprises interacting transcriptional feedback loops [22]. The clock mechanism of the SCN is then synchronized with the successions of day and night via specific retinal photoreceptors projecting light information to the SCN via the retinohypothalamic tract [23]. Interestingly, a subset of retinal ganglion cells contains the photopigment melanopsin, which equips the cells with light-sensing properties. These irradiance detectors integrate their information on the surrounding lighting condition with signals from rod and cone photoreceptors to photoentrain the endogenous rhythm of the SCN [24]. The circadian clock of the SCN controls the pineal gland through a multisynaptic pathway [25]. The last neuron in the pathway, which has its soma situated in the superior cervical ganglion of the sympathetic nervous system, releases norepinephrine (NE) in the perivascular spaces of the pineal gland at night. NE binds to adrenergic receptors on the membrane of the pinealocyte and activates intracellular signaling pathways; this results in nocturnal melatonin synthesis [20, 26].

The enzymes AANAT and acetylserotonin O-methyltransferase (ASMT) catalyze the conversion of serotonin to melatonin. Nocturnal increase in AANAT enzymatic activity, as a result of NE release, determines the circadian melatonin production of the pineal gland. In the rodent, a marked nightly increase of *Aanat* transcription and posttranslational modifications of the AANAT protein account for the increase in AANAT enzymatic activity [8, 27, 28]. In other mammalian species, the dynamics of the AANAT enzymatic activity is effectuated through mechanisms other than transcriptional regulation of the *Aanat* gene. For instance, in sheep, monkey, and human, pineal *Aanat* transcript levels do not oscillate on a circadian basis. However, in all mammalian species, the rhythm of pineal gland melatonin production is reliant on the nocturnal release of NE in the gland [29–31]. In the rodent, the release of NE from the sympathetic nerve endings binds and activates adrenergic receptors on the pinealocyte, which results in an increased intracellular cAMP level. cAMP-activated protein kinase A phosphorylates the cAMP response element binding protein (CREB), which binds cAMP responsive element (CRE) *cis*-regulatory elements in the *Aanat* promoter and induces transcription [32, 33]. Thus, in the rodent, transcriptional regulation of *Aanat* is of special importance for melatonin to function as the hormonal messenger of darkness.

Because cAMP does not elevate the level of *Aanat* mRNA in cells other than the pinealocytes and to some extent retinal photoreceptors [34] (see below), additional regulatory mechanisms of *Aanat* expression must exist. These are thought to play a permissive or regulatory role in ensuring tissue-specific *Aanat* expression in addition to the cAMP/CRE-based transcriptional control [7, 35]. As mentioned above, several homeobox genes have been shown to be expressed in the developing and adult pineal gland of the rodent and some have also been shown to bind photoreceptor conserved elements (PCEs) that are present in the *Aanat* promoter region and to influence *Aanat* transcription.

4. Local Control of *Aanat* Rhythms in Photoreceptor Cells

Melatonin is also synthesized in the mammalian retina [36, 37]. Whereas circadian biology of the mammalian pineal gland is controlled by the circadian clock of the SCN, the existence of an endogenous circadian clock within the mammalian retina is evident from the persistence of the retinal melatonin rhythm in cultured retinae [38] and SCN-lesioned rats [39]. The endogenous retinal pacemaker appears to be located in photoreceptor cells [40].

Retinal *Aanat* expression is also present in photoreceptors [41, 42] and exhibits a day-night rhythm [43]. Contrary to the regulation of *Aanat* in the pineal gland, retinal *Aanat* transcription is driven directly by clock gene products; that is, the dimer consisting of circadian locomotor output cycles kaput (CLOCK) and aryl hydrocarbon receptor nuclear translocator-like (ARNTL), which are encoded by core clock genes, binds directly to *cis*-regulatory elements, so-called E-boxes, in the *Aanat* promoter to drive circadian gene expression [44, 45]. As reviewed below, a set of homeobox genes predominantly expressed in the pinealocyte and the retinal photoreceptor seems to control tissue-specific *Aanat* expression; however, certain E-box sequences have also been shown to confer tissue specificity presumably by silencing ectopic *Aanat* expression [46]. Retinal melatonin appears to play a paracrine role in dark-adaptation processes [34] and retinal AANAT further acts to counteract light-induced retinal degeneration [47].

A close relationship between photoreception and melatonin synthesis is also seen in pineal organs of nonmammalian vertebrates, which contain cells endowed with light-sensing properties [48, 49], an endogenous circadian clock [50–52], and nocturnal melatonin production guided by daily oscillations in AANAT activity [53, 54]. From an evolutionary point of view, a common ancestral photoreceptor cell appears to have evolved into the retinal photoreceptor of the lateral eyes and the pinealocyte of the mammalian pineal gland [55, 56] which presently share both nocturnal melatonin production and the molecular characteristic of expression of a common set of homeobox genes, including *Crx*.

5. *Crx* Expression in the Rodent Pineal Gland

The *Crx* gene is expressed specifically in the photoreceptors of the retina and the pinealocytes of the pineal gland in the adult rodent [7, 14, 57–59]. During development, *Crx* is expressed in the rat pineal gland from embryonic day (E) 18 onwards with a peak around birth (Figure 1), suggesting that the role of *Crx* is not at the earliest of pineal gland developmental stages, but rather later on when the pinealocytes become differentiated [14]. Around the same embryonic stage, *Crx* expression has been reported in rat retinal photoreceptor cells [57]. Therefore, *Crx* seems to be important when differentiation processes occur in both photoreceptors and pinealocytes. *Otx2* is expressed in the fore- and midbrain regions in the developing central nervous system. The total *Otx2*-knockout mouse lacks the forebrain and midbrain regions at embryonic developmental stages. However, in a mouse with conditional *Otx2* gene knockout specifically in the developing photoreceptors and pinealocytes, it has been shown that *Otx2* is essential for development of retinal photoreceptors and pinealocytes [10, 60, 61]. Further, OTX2 transactivates *Crx* expression [10] and this is in accord with the timing of the developmental peak of *Otx2* in both photoreceptors and pinealocytes, which precedes that of *Crx* (Figure 1) [14, 57].

Expression of *Aanat* and *Asmt* in the developing rat pineal gland starts around birth [19, 62]. Interestingly, several homeobox genes display a pineal expression peak around the appearance of *Aanat* and *Asmt* and expression persists into adulthood, suggesting that these homeodomain transcription factors are important for inducing expression of the enzymes required for melatonin synthesis and thereby ensuring a pineal-specific circadian melatonin output (Figure 1). Persistent ontogenetic expression of pineal homeobox genes is seen in the case of *Otx2* and *Crx* (Figure 2) [14], as well as *Rax* [18, 63]. The first *Rax* gene expression is confined to the forebrain and midbrain region of the developing central nervous system, but later becomes progressively restricted to specific brain areas, including the pineal gland and neural retina [64, 65]. Moreover, RAX protein also plays a role in the transcriptional regulation of the *Otx2* gene through a newly discovered *cis*-regulatory enhancer region in the *Otx2* gene that RAX is capable of transactivating in photoreceptor precursors [66]. Notably, this enhancer sequence is also active in the rodent pineal gland at postnatal stages [67]. On the contrary, a classical homeobox gene such as *Pax6* that is widely expressed in the developing central nervous system and is required for a normal development of the pineal gland [11, 68] is nearly undetectable in the pineal gland of the adult rodent [15]. In the mouse retina, PAX6 is a suppressor of *Crx* expression during development, thereby preventing an onset of premature photoreceptor differentiation [69]. The concurrent decline of *Pax6* expression and increase of *Crx* expression in developing rat pinealocytes may reflect a similar functional relationship between these two transcription factors, permitting CRX to exert its control over transcription of the melatonin synthesizing enzymes and pinealocyte differentiation [7]. Complete maturation of pineal physiology with circadian melatonin synthesis occurs in the second postnatal week, at the time when sympathetic innervation of the gland is established and the SCN is capable of exerting its circadian control of the pineal endocrine output [7, 70].

6. Roles of CRX in the Rodent Pineal Gland

Investigations in a *Crx*-knockout mouse have demonstrated a central role of *Crx* in the developing rodent visual system. Elimination of *Crx* causes a lack of photoreceptor outer segments, a reduced expression of several photoreceptor-specific genes accompanied by a disturbed development, and phenotype of different neuronal populations in the primary visual cortex. Further, circadian entrainment is attenuated [73, 74]; temperature and running diurnal rhythms display decreased robustness [75]. The morphology of the pineal gland appears normal [76]; however, the expression of pineal *Aanat* is reduced [73, 75, 76].

The observed influence of *Crx* on expression of several photoreceptor- and pineal-specific genes is in accord with the presence of *cis*-regulatory PCEs in the promoter region of these genes, including the *Aanat* promoter [35]. *In vitro* studies have shown that the CRX protein binds PCEs and causes transactivation of reporter constructs [35, 58, 59, 77, 78]. Notably, the promoter of the neural retina leucine zipper (*Nrl*) gene, which is a basic-leucine zipper (bZIP) transcription factor [79], drives tissue-specific expression in rod photoreceptors and the pineal gland [80]. NRL and CRX have been shown to transactivate the rhodopsin promoter in a

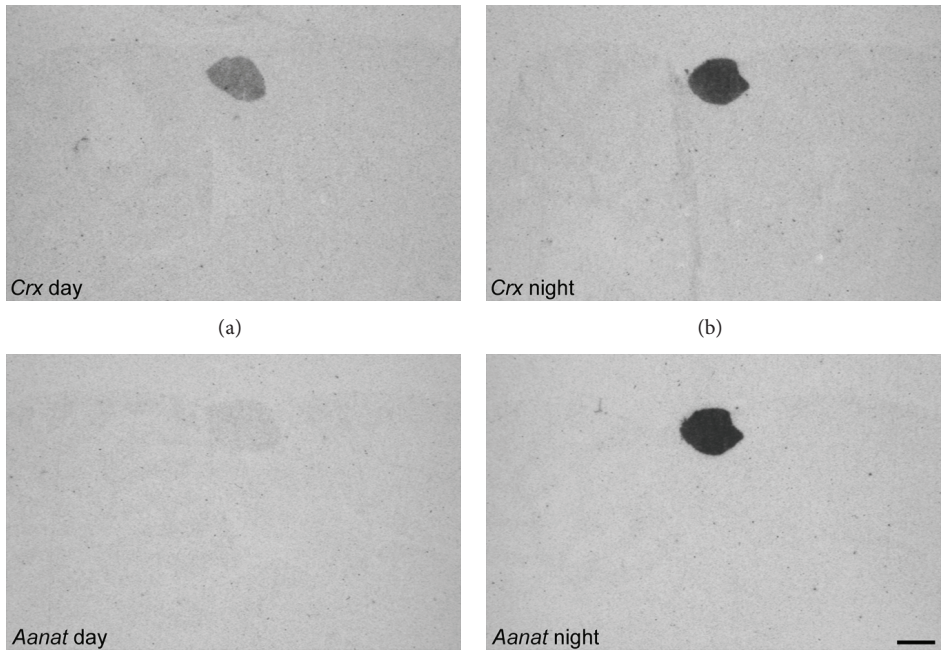

Figure 2: *Crx* and *Aanat* day/night expression in the adult rat pineal gland. Radiochemical *in situ* hybridization autoradiographs of midsagittal brain sections through the pineal gland of rats killed at daytime (Zeitgeber time 6) and nighttime (Zeitgeber time 18). Images are orientated with caudal to the left. *Crx* displays a specific expression in the pineal gland. Studies have shown a diurnal rhythm of *Crx* expression in the rat pineal gland with a night time peak [7, 35, 71]. *Aanat* also exhibits a pineal-specific expression; however, daytime transcript levels are very low. Scale bar, 1 mm. Methodological details have been previously published [14, 71].

synergistic manner, and the rhodopsin gene is also expressed in the mammalian pineal gland [58, 81]. Thus, a similar cooperation between NRL and CRX is possible in the context of transcriptional regulation of *Aanat*, since both the *Aanat* and rhodopsin gene contain the PCE regulatory element in their promoter region [77]. In the adult rat pineal gland, many of the homeobox genes, which show a developmental expression peak around the time of the appearance of *Aanat* and *Asmt* expression, also display a diurnal rhythm of expression, that is, *Rax*, *Otx2,* and *Crx* [7, 18]. During the 24 h period, expression levels of these homeobox genes peak in a sequential manner before the late night expression peak of *Aanat*. That is, *Rax* peaks in the transition from day to night, *Otx2* early in the night, and *Crx* in the middle of the night [7]. The daily expression profiles, existing data on binding of RAX, OTX2, and CRX homeodomain proteins to PCEs and the transactivating property of RAX on *Otx2* transcription and of OTX2 on *Crx* transcription [10, 35, 58, 59, 66, 77, 78, 82], suggest that homeodomain proteins play a role in the expression of genes like *Aanat* that otherwise show a CRE-based circadian rhythm [32]. Thus, the occurrence of the *Crx* expression peaks a few hours before the peak of *Aanat* expression additionally supports the concept that homeodomain proteins act as regulatory factors of the daily expression profile of *Aanat* in the rodent pineal gland with CRX in a central position.

7. *Crx* in the Retinal Photoreceptor and Nonmammalian Pinealocyte

Photoreceptors are present in the retina of all vertebrates and in the pineal gland of most nonmammalian vertebrates [83]. In the retinal photoreceptor, *Crx* is thought to be involved in the process of terminal differentiation of photoreceptors and is essential for formation of photoreceptor outer segments, as evidenced by gene knockout studies [73, 84]. At the molecular level, CRX is centrally placed in a network of transcription factors that regulate photoreceptor gene expression and thereby terminal differentiation of the various photoreceptor subtypes [85, 86]. As in the rodent pineal gland, expression of *Crx* persists in the mature retina [14, 57–59], where CRX seems to positively control expression of a number of genes involved in phototransduction [58, 59, 87, 88]. Many of these genes are also detectable in the mammalian pineal gland, reflecting the common phylogenetic relationship between the retinal photoreceptor and the pinealocyte.

In contrast to the mammalian pineal gland, the zebrafish pineal organ comprises cells that are capable of photodetection, which enable entrainment of the endogenously generated rhythm that controls circadian expression of genes in pinealocytes and hence the nocturnal synthesis of melatonin [89]. In zebrafish, the *Otx5* gene, which is orthologous to the mammalian *Crx* gene, regulates genes that exhibit a circadian pattern of expression in the pineal complex. A lack

of OTX5 protein attenuates the circadian pineal expression of *Aanat2*, which is the homolog of the mammalian *Aanat* gene and thus encodes the rate limiting enzyme in the zebrafish pineal production of melatonin [90]. Similar to the role of CRX in mammals, the action of OTX5 on *Aanat2* in the zebrafish pineal organ is mediated through PCEs [77, 91, 92]. Interestingly, in the zebrafish pineal gland, OTX5, in addition to ensuring pineal-specific expression of *Aanat2*, is also capable of facilitating the circadian expression of *Aanat2*, which, in accordance with the situation in the mammalian retina, is otherwise controlled by the circadian CLOCK/ARNTL-dimer [91].

Like the pinealocyte of the zebrafish, the chicken pinealocytes possess the capability of light perception [48]. It has been shown in chicken that CRX activates transcription of *Asmt* through the interaction with PCEs in the *Asmt* promoter region [93]. A similar relationship has been shown between chicken *Asmt* and OTX2 [94]. Thus, CRX and the related OTX2 seem to exert a highly conserved regulatory role in transcriptional regulation of the enzymes involved in melatonin synthesis between vertebrate species.

8. A Proposed Model for Shaping the Daily *Aanat* Expression Profile

By the use of adenovirus-mediated shRNA knockdown and overexpression of *Crx* mRNA in cultured rat pinealocytes and investigations performed in the *Crx*-knockout mouse, it has been shown that CRX induces *Aanat* transcription in the rodent. At the same time, CRX exhibits a circadian rhythm in the pineal gland driven by the nocturnal release of NE from sympathetic nerve endings in the gland (Rohde K, Rovsing L, Ho AK, Møller M, and Rath MF, in preparation). Based on these findings and existing data on *Aanat* transcription, we here propose an extended working model for the role of homeodomain transcription factors in generation of pineal specificity and circadian output (Figure 3). Thus, in addition to ensuring pineal specificity of *Aanat* expression, mammalian CRX may also facilitate daily changes in *Aanat* expression and therefore act to shape the daily profile of melatonin synthesis.

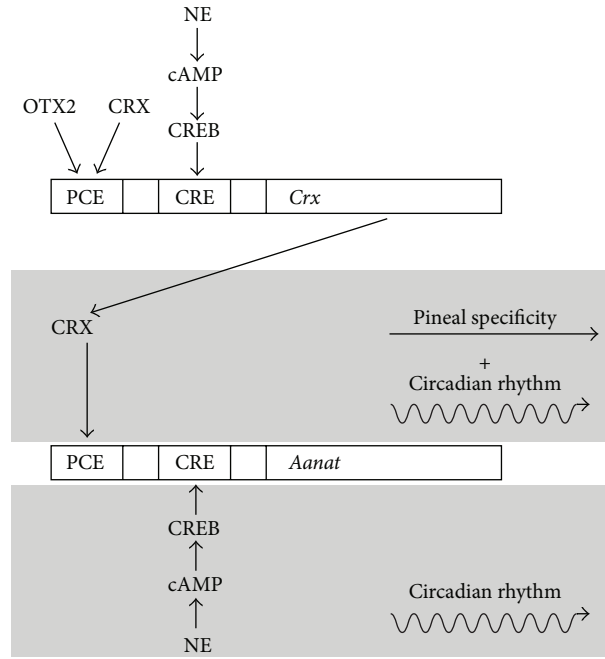

Figure 3: Working model of the role of homeobox genes in generation of pineal specificity and circadian output. CRX and OTX2 homeodomain transcription factors and NE/cAMP/CREB signaling, initiated by NE released from the sympathetic nerve endings at night, act on PCE and CRE *cis*-regulatory elements in the pineal *Crx* promoter region, respectively, to generate tissue-specific circadian expression of *Crx*. CRX protein acts on PCEs in the *Aanat* promoter region and confers a pineal-specific and circadian expression of *Aanat*. The homeodomain transcription factor generated rhythmicity of *Aanat* transcription supports the classical NE/cAMP/CREB-driven circadian rhythm of *Aanat* expression. The *Crx* promoter contains at least one PCE and several CRE *cis*-regulatory elements. In the *Aanat* promoter, several CREs and at least two PCEs exist. Promoter analysis was performed using Genomatix MatInspector software [72]. CRE, cAMP response element; CREB, cAMP response element binding protein; PCE, photoreceptor conserved element.

Abbreviations

Aanat: Arylalkylamine N-acetyltransferase
Arntl: Aryl hydrocarbon receptor nuclear translocator-like
Asmt: Acetylserotonin O-methyltransferase
Bsx: Brain specific homeobox
bZIP: Basic-leucine zipper
Clock: Circadian locomotor output cycles kaput
CRE: cAMP response element
CREB: cAMP response element binding protein
Crx: Cone-rod homeobox
E: Embryonic day
Lhx: LIM homeobox
NE: Norepinephrine
Nrl: Neural retina leucine zipper
Otx: Orthodenticle homeobox
P: Postnatal day
Pax: Paired box
PCE: Photoreceptor conserved element
Rax: Retina and anterior neural fold homeobox
SCN: Suprachiasmatic nucleus.

Conflict of Interests

The authors declare that there is no conflict of interests regarding the publication of this paper.

Acknowledgments

This work was supported by a Ph.D. scholarship from the Faculty of Health and Medical Sciences, University of Copenhagen (to KR), and the Lundbeck Foundation (Grant no. R83-A8083 to MM and R108-A10301 to MFR).

References

[1] M. Mallo and C. R. Alonso, "The regulation of Hox gene expression during animal development," *Development*, vol. 140, no. 19, pp. 3951–3963, 2013.

[2] W. J. Gehring, "The homeobox in perspective," *Trends in Biochemical Sciences*, vol. 17, no. 8, pp. 277–280, 1992.

[3] W. J. Gehring, M. Affolter, and T. Bürglin, "Homeodomain proteins," *Annual Review of Biochemistry*, vol. 63, pp. 487–526, 1994.

[4] W. McGinnis, C. P. Hart, W. J. Gehring, and F. H. Ruddle, "Molecular cloning and chromosome mapping of a mouse DNA sequence homologous to homeotic genes of Drosophila," *Cell*, vol. 38, no. 3, pp. 675–680, 1984.

[5] W. McGinnis, R. L. Garber, J. Wirz, A. Kuroiwa, and W. J. Gehring, "A homologous protein-coding sequence in drosophila homeotic genes and its conservation in other metazoans," *Cell*, vol. 37, no. 2, pp. 403–408, 1984.

[6] M. P. Scott and A. J. Weiner, "Structural relationships among genes that control development: sequence homology between the antennapedia, ultrabithorax, and fushi tarazu loci of Drosophila," *Proceedings of the National Academy of Sciences of the United States of America*, vol. 81, no. 13 I, pp. 4115–4119, 1984.

[7] M. F. Rath, K. Rohde, D. C. Klein, and M. Møller, "Homeobox genes in the rodent pineal gland: roles in development and phenotype maintenance," *Neurochemical Research*, vol. 38, no. 6, pp. 1100–1112, 2013.

[8] D. C. Klein, "Arylalkylamine N-acetyltransferase: 'the timezyme'," *Journal of Biological Chemistry*, vol. 282, no. 7, pp. 4233–4237, 2007.

[9] J. Calvo and J. Boya, "Embryonic development of the rat pineal gland," *Anatomical Record*, vol. 200, no. 4, pp. 491–500, 1981.

[10] A. Nishida, A. Furukawa, C. Koike et al., "Otx2 homeobox gene controls retinal photoreceptor cell fate and pineal gland development," *Nature Neuroscience*, vol. 6, no. 12, pp. 1255–1263, 2003.

[11] G. Estivill-Torrús, T. Vitalis, P. Fernández-Llebrez, and D. J. Price, "The transcription factor Pax6 is required for development of the diencephalic dorsal midline secretory radial glia that form the subcommissural organ," *Mechanisms of Development*, vol. 109, no. 2, pp. 215–224, 2001.

[12] T. McArthur and A. Ohtoshi, "A brain-specific homeobox gene, Bsx, is essential for proper postnatal growth and nursing," *Molecular and Cellular Biology*, vol. 27, no. 14, pp. 5120–5127, 2007.

[13] F. Yamazaki, M. Møller, C. Fu et al., "The Lhx9 homeobox gene controls pineal gland development and prevents postnatal hydrocephalus," *Brain Structure and Function*, 2014.

[14] M. F. Rath, E. Muñoz, S. Ganguly et al., "Expression of the Otx2 homeobox gene in the developing mammalian brain: Embryonic and adult expression in the pineal gland," *Journal of Neurochemistry*, vol. 97, no. 2, pp. 556–566, 2006.

[15] M. F. Rath, M. J. Bailey, J.-S. Kim et al., "Developmental and diurnal dynamics of Pax4 expression in the mammalian pineal gland: Nocturnal down-regulation is mediated by adrenergic-cyclic adenosine 3′,5′-monophosphate signaling," *Endocrinology*, vol. 150, no. 2, pp. 803–811, 2009.

[16] M. Cremona, E. Colombo, M. Andreazzoli, G. Cossu, and V. Broccoli, "Bsx, an evolutionary conserved Brain Specific homeoboX gene expressed in the septum, epiphysis, mammillary bodies and arcuate nucleus," *Gene Expression Patterns*, vol. 4, no. 1, pp. 47–51, 2004.

[17] D. C. Klein, M. A. A. Namboodiri, and D. A. Auerbach, "The melatonin rhythm generating system: developmental aspects," *Life Sciences*, vol. 28, no. 18, pp. 1975–1986, 1981.

[18] K. Rohde, D. C. Klein, M. Mãller, and M. F. Rath, "Rax: Developmental and daily expression patterns in the rat pineal gland and retina," *Journal of Neurochemistry*, vol. 118, no. 6, pp. 999–1007, 2011.

[19] M. Pfeffer and J. H. Stehle, "Ontogeny of a diurnal rhythm in arylalkylamine-N-acetyltransferase mRNA in rat pineal gland," *Neuroscience Letters*, vol. 248, no. 3, pp. 163–166, 1998.

[20] D. C. Klein, M. J. Bailey, D. A. Carter et al., "Pineal function: Impact of microarray analysis," *Molecular and Cellular Endocrinology*, vol. 314, no. 2, pp. 170–183, 2010.

[21] J. Falcón, L. Besseau, M. Fuentès, S. Sauzet, E. Magnanou, and G. Boeuf, "Structural and functional evolution of the pineal melatonin system in vertebrates," *Annals of the New York Academy of Sciences*, vol. 1163, pp. 101–111, 2009.

[22] S. M. Reppert and D. R. Weaver, "Coordination of circadian timing in mammals," *Nature*, vol. 418, no. 6901, pp. 935–941, 2002.

[23] D. C. Klein and R. Y. Moore, "Pineal N-acetyltransferase and hydroxyindole-O-methyltransferase: control by the retinohypothalamic tract and the suprachiasmatic nucleus," *Brain Research*, vol. 174, no. 2, pp. 245–262, 1979.

[24] T. M. Schmidt, M. T. H. Do, D. Dacey, R. Lucas, S. Hattar, and A. Matynia, "Melanopsin-positive intrinsically photosensitive retinal ganglion cells: from form to function," *Journal of Neuroscience*, vol. 31, no. 45, pp. 16094–16101, 2011.

[25] M. Møller and F. M. Baeres, "The anatomy and innervation of the mammalian pineal gland," *Cell and Tissue Research*, vol. 309, no. 1, pp. 139–150, 2002.

[26] M. Møller, "Introduction to mammalian pineal innervation," *Microscopy Research and Technique*, vol. 46, pp. 235–238, 1999.

[27] P. H. Roseboom, S. L. Coon, R. Baler, S. K. Mccune, J. L. Weller, and D. C. Klein, "Melatonin synthesis: analysis of the more than 150-fold nocturnal increase in serotonin N-acetyltransferase messenger ribonucleic acid in the rat pineal gland," *Endocrinology*, vol. 137, no. 7, pp. 3033–3045, 1996.

[28] J. Borjigin, M. M. Wang, and S. H. Snyder, "Diurnal variation in mRNA encoding serotonin N-acetyltransferase in pineal gland," *Nature*, vol. 378, no. 6559, pp. 783–785, 1995.

[29] J. D. Johnston, R. Bashforth, A. Diack, H. Andersson, G. A. Lincoln, and D. G. Hazlerigg, "Rhythmic melatonin secretion does not correlate with the expression of arylalkylamine N-acetyltransferase, inducible cyclic AMP early repressor, Period1 or Cryptochrome1 mRNA in the sheep pineal," *Neuroscience*, vol. 124, no. 4, pp. 789–795, 2004.

[30] S. L. Coon, E. Del Olmo, W. Scott Young III, and D. C. Klein, "Melatonin synthesis enzymes in Macaca mulatta: Focus on arylalkylamine N-acetyltransferase (EC 2.3.1.87)," *Journal of Clinical Endocrinology and Metabolism*, vol. 87, no. 10, pp. 4699–4706, 2002.

[31] K. Ackermann, R. Bux, U. Rüb, H.-W. Korf, G. Kauert, and J. H. Stehle, "Characterization of human melatonin synthesis using autoptic pineal tissue," *Endocrinology*, vol. 147, no. 7, pp. 3235–3242, 2006.

[32] A. K. Ho and C. L. Chik, "Modulation of Aanat gene transcription in the rat pineal gland," *Journal of Neurochemistry*, vol. 112, no. 2, pp. 321–331, 2010.

[33] R. Baler, S. Covington, and D. C. Klein, "The rat arylalkylamine N-acetyltransferase gene promoter. cAMP activation

via a cAMP-responsive element-CCAAT complex," *Journal of Biological Chemistry*, vol. 272, no. 11, pp. 6979–6985, 1997.

[34] P. M. Iuvone, G. Tosini, N. Pozdeyev, R. Haque, D. C. Klein, and S. S. Chaurasia, "Circadian clocks, clock networks, arylalkylamine N-acetyltransferase, and melatonin in the retina," *Progress in Retinal and Eye Research*, vol. 24, no. 4, pp. 433–456, 2005.

[35] X. Li, S. Chen, Q. Wang, D. J. Zack, S. H. Snyder, and J. Borjigin, "A pineal regulatory element (PIRE) mediates transactivation by the pineal/retina-specific transcription factor CRX," *Proceedings of the National Academy of Sciences of the United States of America*, vol. 95, no. 4, pp. 1876–1881, 1998.

[36] S. F. Pang, H. S. Yu, H. C. Suen, and G. M. Brown, "Melatonin in the retina of rats: a diurnal rhythm," *Journal of Endocrinology*, vol. 87, no. 1, pp. 89–93, 1980.

[37] G. Tosini, N. Pozdeyev, K. Sakamoto, and P. M. Iuvone, "The circadian clock system in the mammalian retina," *BioEssays*, vol. 30, no. 7, pp. 624–633, 2008.

[38] G. Tosini and M. Menaker, "Circadian rhythms in cultured mammalian retina," *Science*, vol. 272, no. 5260, pp. 419–421, 1996.

[39] K. Sakamoto, K. Oishi, M. Shiraishi et al., "Two circadian oscillatory mechanisms in the mammalian retina," *NeuroReport*, vol. 11, no. 18, pp. 3995–3997, 2000.

[40] G. Tosini, A. J. Davidson, C. Fukuhara, M. Kasamatsu, and O. Castanon-Cervantes, "Localization of a circadian clock in mammalian photoreceptors," *The FASEB Journal*, vol. 21, no. 14, pp. 3866–3871, 2007.

[41] T. Niki, T. Hamada, M. Ohtomi et al., "The localization of the site of arylalkylamine N-acetyltransferase circadian expression in the photoreceptor cells of mammalian retina," *Biochemical and Biophysical Research Communications*, vol. 248, no. 1, pp. 115–120, 1998.

[42] C. Liu, C. Fukuhara, J. H. Wessel, P. M. Iuvone, and G. Tosini, "Localization of Aa-nat mRNA in the rat retina by flourescence in situ hybridization and laser capture microdissection," *Cell and Tissue Research*, vol. 315, no. 2, pp. 197–201, 2004.

[43] K. Sakamoto and N. Ishida, "Circadian expression of serotonin N-acetyltransferase mRNA in the rat retina," *Neuroscience Letters*, vol. 245, no. 2, pp. 113–116, 1998.

[44] W. Chen and R. Baler, "The rat arylalkylamine N-acetyltransferase E-box: differential use in a master vs. a slave oscillator," *Molecular Brain Research*, vol. 81, no. 1-2, pp. 43–50, 2000.

[45] E. Muñoz, M. Brewer, and R. Baler, "Circadian transcription: thinking outside the E-Box," *Journal of Biological Chemistry*, vol. 277, no. 39, pp. 36009–36017, 2002.

[46] A. Humphries, T. Wells, R. Baler, D. C. Klein, and D. A. Carter, "Rodent Aanat: intronic E-box sequences control tissue specificity but not rhythmic expression in the pineal gland," *Molecular and Cellular Endocrinology*, vol. 270, no. 1-2, pp. 43–49, 2007.

[47] J. Shen, K. Ghai, P. Sompol et al., "N-acetyl serotonin derivatives as potent neuroprotectants for retinas," *Proceedings of the National Academy of Sciences of the United States of America*, vol. 109, no. 9, pp. 3540–3545, 2012.

[48] T. Deguchi, "Rhodopsin-like photosensitivity of isolated chicken pineal gland," *Nature*, vol. 290, no. 5808, pp. 706–707, 1981.

[49] H. Meissl and P. Ekstrom, "Photoreceptor responses to light in the isolated pineal organ of the trout, Salmo gairdneri," *Neuroscience*, vol. 25, no. 3, pp. 1071–1076, 1988.

[50] S. A. Binkley, J. B. Riebman, and K. B. Reilly, "The pineal gland: a biological clock in vitro," *Science*, vol. 202, no. 4373, pp. 1198–1200, 1978.

[51] M. Menaker and S. Wisner, "Temperature-compensated circadian clock in the pineal of Anolis," *Proceedings of the National Academy of Sciences of the United States of America*, vol. 80, no. 19 I, pp. 6119–6121, 1983.

[52] J. Falcon, J. B. Marmillon, B. Claustrat, and J.-P. Collin, "Regulation of melatonin secretion in a photoreceptive pineal organ: an in vitro study in the pike," *Journal of Neuroscience*, vol. 9, no. 6, pp. 1943–1950, 1989.

[53] S. Binkley, J. B. Riebman, and K. B. Reilly, "Timekeeping by the pineal gland," *Science*, vol. 197, no. 4309, pp. 1181–1183, 1977.

[54] J. Falcon, J. F. Guerlotte, P. Voisin, and J.-P. H. Collin, "Rhythmic melatonin biosynthesis in a photoreceptive pineal organ: a study in the pike," *Neuroendocrinology*, vol. 45, no. 6, pp. 479–486, 1987.

[55] D. C. Klein, "The 2004 aschoff/pittendrigh lecture: Theory of the origin of the pineal gland—a tale of conflict and resolution," *Journal of Biological Rhythms*, vol. 19, no. 4, pp. 264–279, 2004.

[56] D. C. Klein, "Evolution of the vertebrate pineal gland: the AANAT hypothesis," *Chronobiology International*, vol. 23, no. 1-2, pp. 5–20, 2006.

[57] M. F. Rath, F. Morin, Q. Shi, D. C. Klein, and M. Møller, "Ontogenetic expression of the Otx2 and Crx homeobox genes in the retina of the rat," *Experimental Eye Research*, vol. 85, no. 1, pp. 65–73, 2007.

[58] S. Chen, Q. L. Wang, Z. Nie et al., "Crx, a novel Otx-like paired-homeodomain protein, binds to and transactivates photoreceptor cell-specific genes," *Neuron*, vol. 19, no. 5, pp. 1017–1030, 1997.

[59] T. Furukawa, E. M. Morrow, and C. L. Cepko, "Crx, a novel otx-like homeobox gene, shows photoreceptor-specific expression and regulates photoreceptor differentiation," *Cell*, vol. 91, no. 4, pp. 531–541, 1997.

[60] A. Simeone, D. Acampora, M. Gulisano, A. Stornaiuolo, and E. Boncinelli, "Nested expression domains of four homeobox genes in developing rostral brain," *Nature*, vol. 358, no. 6388, pp. 687–690, 1992.

[61] D. Acampora, S. Mazan, Y. Lallemand et al., "Forebrain and midbrain regions are deleted in Otx2-/- mutants due to a defective anterior neuroectoderm specification during gastrulation," *Development*, vol. 121, no. 10, pp. 3279–3290, 1995.

[62] C. Ribelayga, F. Gauer, P. Pévet, and V. Simonneaux, "Ontogenesis of hydroxyindole-O-methyltransferase gene expression and activity in the rat pineal gland," *Developmental Brain Research*, vol. 110, no. 2, pp. 235–239, 1998.

[63] C. H. Asbreuk, H. S. van Schaick, J. J. Cox, M. P. Smidt, and J. P. Burbach, "Survey for paired-like homeodomain gene expression in the hypothalamus: restricted expression patterns of Rx, Alx4 and goosecoid," *Neuroscience*, vol. 114, no. 4, pp. 883–889, 2002.

[64] P. H. Mathers, A. Grinberg, K. A. Mahon, and M. Jamrich, "The Rx homeobox gene is essential for vertebrate eye development," *Nature*, vol. 387, no. 6633, pp. 603–607, 1997.

[65] T. Furukawa, C. A. Kozak, and C. L. Cepko, "rax, a novel paired-type homeobox gene, shows expression in the anterior neural fold and developing retina," *Proceedings of the National Academy of Sciences of the United States of America*, vol. 94, no. 7, pp. 3088–3093, 1997.

[66] Y. Muranishi, K. Terada, T. Inoue et al., "An essential role for RAX homeoprotein and NOTCH-HES signaling in Otx2 expression in embryonic retinal photoreceptor cell fate determination," *Journal of Neuroscience*, vol. 31, no. 46, pp. 16792–16807, 2011.

[67] Y. Muranishi, K. Terada, and T. Furukawa, "An essential role for Rax in retina and neuroendocrine system development," *Development Growth and Differentiation*, vol. 54, no. 3, pp. 341–348, 2012.

[68] C. Walther and P. Gruss, "Pax-6, a murine paired box gene, is expressed in the developing CNS," *Development*, vol. 113, no. 4, pp. 1435–1449, 1991.

[69] V. Oron-Karni, C. Farhy, M. Elgart et al., "Dual requirement for Pax6 in retinal progenitor cells," *Development*, vol. 135, no. 24, pp. 4037–4047, 2008.

[70] R. Håkanson, M.-N. Lombard Des Gouttes, and C. Owman, "Activities of tryptophan hydroxylase, DOPA decarboxylase, and monoamine oxidase as correlated with the appearance of monoamines in developing rat pineal gland," *Life Sciences*, vol. 6, no. 24, pp. 2577–2585, 1967.

[71] M. J. Bailey, S. L. Coon, D. A. Carter et al., "Night/day changes in pineal expression of >600 genes: central role of adrenergic/cAMP signaling," *Journal of Biological Chemistry*, vol. 284, no. 12, pp. 7606–7622, 2009.

[72] K. Cartharius, K. Frech, K. Grote et al., "MatInspector and beyond: promoter analysis based on transcription factor binding sites," *Bioinformatics*, vol. 21, no. 13, pp. 2933–2942, 2005.

[73] T. Furukawa, E. M. Morrow, T. Li, F. C. Davis, and C. L. Cepko, "Retinopathy and attenuated circadian entrainment in Crx-deficient mice," *Nature Genetics*, vol. 23, no. 4, pp. 466–470, 1999.

[74] Y. Goldshmit, S. Galley, D. Foo, E. Sernagor, and J. A. Bourne, "Anatomical changes in the primary visual cortex of the congenitally blind Crx-/- mouse," *Neuroscience*, vol. 166, no. 3, pp. 886–898, 2010.

[75] L. Rovsing, M. F. Rath, C. Lund-Andersen, D. C. Klein, and M. Møller, "A neuroanatomical and physiological study of the non-image forming visual system of the cone-rod homeobox gene (Crx) knock out mouse," *Brain Research*, vol. 1343, pp. 54–65, 2010.

[76] L. Rovsing, S. Clokie, D. M. Bustos et al., "Crx broadly modulates the pineal transcriptome," *Journal of Neurochemistry*, vol. 119, no. 2, pp. 262–274, 2011.

[77] L. Appelbaum and Y. Gothilf, "Mechanism of pineal-specific gene expression: the role of E-box and photoreceptor conserved elements," *Molecular and Cellular Endocrinology*, vol. 252, no. 1-2, pp. 27–33, 2006.

[78] A. Kimura, D. Singh, E. F. Wawrousek, M. Kikuchi, M. Nakamura, and T. Shinohara, "Both PCE-1/RX and OTX/CRX interactions are necessary for photoreceptor- specific gene expression," *Journal of Biological Chemistry*, vol. 275, no. 2, pp. 1152–1160, 2000.

[79] A. Swaroop, J. Xu, H. Pawar, A. Jackson, C. Skolnick, and N. Agarwal, "A conserved retina-specific gene encodes a basic motif/leucine zipper domain," *Proceedings of the National Academy of Sciences of the United States of America*, vol. 89, no. 1, pp. 266–270, 1992.

[80] M. Akimoto, H. Cheng, D. Zhu et al., "Targeting of GFP to newborn rods by Nrl promoter and temporal expression profiling of flow-sorted photoreceptors," *Proceedings of the National Academy of Sciences of the United States of America*, vol. 103, no. 10, pp. 3890–3895, 2006.

[81] S. Blackshaw and S. H. Snyder, "Developmental expression pattern of phototransduction components in mammalian pineal implies a light-sensing function," *Journal of Neuroscience*, vol. 17, no. 21, pp. 8074–8082, 1997.

[82] N. Bobola, P. Briata, C. Ilengo et al., "OTX2 homeodomain protein binds a DNA element necessary for interphotoreceptor retinoid binding protein gene expression," *Mechanisms of Development*, vol. 82, no. 1-2, pp. 165–169, 1999.

[83] H.-W. Korf, "Evolution of melatonin-producing pinealocytes," *Advances in Experimental Medicine and Biology*, vol. 460, pp. 17–29, 1999.

[84] A. Swaroop, D. Kim, and D. Forrest, "Transcriptional regulation of photoreceptor development and homeostasis in the mammalian retina," *Nature Reviews Neuroscience*, vol. 11, no. 8, pp. 563–576, 2010.

[85] A. K. Hennig, G.-H. Peng, and S. Chen, "Regulation of photoreceptor gene expression by Crx-associated transcription factor network," *Brain Research*, vol. 1192, pp. 114–133, 2008.

[86] J. C. Corbo, K. A. Lawrence, M. Karlstetter et al., "CRX ChIP-seq reveals the cis-regulatory architecture of mouse photoreceptors," *Genome Research*, vol. 20, no. 11, pp. 1512–1525, 2010.

[87] F. J. Livesey, T. Furukawa, M. A. Steffen, G. M. Church, and C. L. Cepko, "Microarray analysis of the transcriptional network controlled by the photoreceptor homeobox gene Crx," *Current Biology*, vol. 10, no. 6, pp. 301–310, 2000.

[88] S. Blackshaw, R. E. Fraioli, T. Furukawa, and C. L. Cepko, "Comprehensive analysis of photoreceptor gene expression and the identification of candidate retinal disease genes," *Cell*, vol. 107, no. 5, pp. 579–589, 2001.

[89] H. W. Korf, C. Schomerus, and J. H. Stehle, "The pineal organ, its hormone melatonin, and the photoneuroendocrine system," *Advances in Anatomy, Embryology, and Cell Biology*, vol. 146, pp. 1–100, 1998.

[90] J. T. Gamse, Y. C. Shen, C. Thisse et al., "Otx5 regulates genes that show circadian expression in the zebrafish pineal complex," *Nature Genetics*, vol. 30, no. 1, pp. 117–121, 2002.

[91] L. Appelbaum, A. Anzulovich, R. Baler, and Y. Gothilf, "Homeobox-clock protein interaction in zebrafish: a shared mechanism for pineal-specific and circadian gene expression," *Journal of Biological Chemistry*, vol. 280, no. 12, pp. 11544–11551, 2005.

[92] L. Appelbaum, R. Toyama, I. B. Dawid, D. C. Klein, R. Baler, and Y. Gothilf, "Zebrafish serotonin-N-acetyltransferase-2 gene regulation: pineal-restrictive downstream module contains a functional E-box and three photoreceptor conserved elements," *Molecular Endocrinology*, vol. 18, no. 5, pp. 1210–1221, 2004.

[93] M. Bernard, V. Dinet, and P. Voisin, "Transcriptional regulation of the chicken hydroxyindole-O-methyltransferase gene by the cone-rod homeobox-containing protein," *Journal of Neurochemistry*, vol. 79, no. 2, pp. 248–257, 2001.

[94] V. Dinet, N. Girard-Naud, P. Voisin, and M. Bernard, "Melatoninergic differentiation of retinal photoreceptors: activation of the chicken hydroxyindole-O-methyltransferase promoter requires a homeodomain-binding element that interacts with Otx2," *Experimental Eye Research*, vol. 83, no. 2, pp. 276–290, 2006.

Hindawi Publishing Corporation
BioMed Research International
Volume 2014, Article ID 235781, 8 pages
http://dx.doi.org/10.1155/2014/235781

Review Article

Functional Development of the Circadian Clock in the Zebrafish Pineal Gland

Zohar Ben-Moshe,[1] Nicholas S. Foulkes,[2] and Yoav Gothilf[1]

[1] *Department of Neurobiology, George S. Wise Faculty of Life Sciences and Sagol School of Neuroscience, Tel-Aviv University, 69978 Tel-Aviv, Israel*
[2] *Institute of Toxicology and Genetics, Karlsruhe Institute of Technology, 76344 Eggenstein-Leopoldshafen, Germany*

Correspondence should be addressed to Yoav Gothilf; yoavg@tauex.tau.ac.il

Received 26 January 2014; Accepted 13 March 2014; Published 16 April 2014

Academic Editor: Estela Muñoz

The zebrafish constitutes a powerful model organism with unique advantages for investigating the vertebrate circadian timing system and its regulation by light. In particular, the remarkably early and rapid development of the zebrafish circadian system has facilitated exploring the factors that control the onset of circadian clock function during embryogenesis. Here, we review our understanding of the molecular basis underlying functional development of the central clock in the zebrafish pineal gland. Furthermore, we examine how the directly light-entrainable clocks in zebrafish cell lines have facilitated unravelling the general mechanisms underlying light-induced clock gene expression. Finally, we summarize how analysis of the light-induced transcriptome and miRNome of the zebrafish pineal gland has provided insight into the regulation of the circadian system by light, including the involvement of microRNAs in shaping the kinetics of light- and clock-regulated mRNA expression. The relative contributions of the pineal gland central clock and the distributed peripheral oscillators to the synchronization of circadian rhythms at the whole animal level are a crucial question that still remains to be elucidated in the zebrafish model.

1. Introduction

Many aspects of animal behaviour and physiology change significantly over the course of the day-night cycle. This phenomenon confers a selective advantage in relation to changing environmental factors such as food availability, predation risk, temperature, and light [1]. Accordingly, animals have evolved an intrinsic timing mechanism, the circadian clock, which drives day-night rhythms in physiology and behaviour. This clock is reset ("entrained") on a daily basis by environmental signals, primarily light, to ensure synchronization of endogenous rhythms with the 24-hour solar day [2].

Circadian clock research has encompassed essentially all life forms, from the most primitive to the most advanced [3]. Nevertheless, most studies have been conducted in "traditional" genetic models such as the fruit fly and mouse [4, 5]. These studies have revealed the molecular components of the circadian clock, which function essentially in every cell and are coordinated by a master clock that resides in the brain [6]. Amongst vertebrates, the zebrafish represents a powerful model organism with unique advantages for exploring the mechanisms of the circadian clock and its entrainment by light [7]. In particular, as reviewed here, the zebrafish provides access to a circadian timing system that emerges remarkably early during development, a valuable feature for investigation of the functional development of the circadian clock.

2. The Pineal Gland and Rhythmic Melatonin Production

One major output of the vertebrate circadian clock is the rhythmic synthesis and secretion of the pineal gland hormone, melatonin, which constitutes an essential component of the circadian timing system. Being produced at night, melatonin provides a night-time signal and plays

an endocrine role in the regulation of a variety of daily and annual physiological rhythms [8]. Classical examples come from studies in hamsters and sheep, in which the duration of melatonin secretion has been shown to control seasonal changes in reproduction and energy balance via basal hypothalamic sites [9].

The rate of melatonin production is determined by the enzymatic activity of arylalkylamine-*N*-acetyltransferase (AANAT). High melatonin levels at night reflect increased AANAT synthesis and activity, while the termination of melatonin production during the day reflects proteasomal degradation of this enzyme [10, 11]. In nearly all vertebrate species, AANAT activity and melatonin production in the pineal gland are controlled by the circadian clock and modulated by external photic signals. In mammals, the oscillations of AANAT activity and melatonin production are driven by the suprachiasmatic nucleus (SCN) of the hypothalamus [12], which functions as the master clock that coordinates the peripheral cellular oscillators [6]. Neurons of the SCN, which produce a circadian rhythm of firing rate, communicate time and photic information to the pineal gland indirectly through a multisynaptic neural pathway. At night, the SCN stimulates the release of norepinephrine in the pineal gland, generating increased pineal cAMP levels, leading to the phosphorylation of AANAT, which activates AANAT and protects it from proteasomal proteolysis [13, 14]. The suppressive effects of light are achieved by decreased cAMP levels, followed by a rise in dephosphorylated AANAT, leading to its inactivation and rapid proteolytic destruction [15]. In summary, pineal *aanat* has been established as an essential link between the vertebrate circadian clock and its important output signal—melatonin.

3. The Fish Pineal Gland Melatonin System

To date, a homologous structure to the mammalian SCN has not been identified in fish. However, as is the case in other nonmammalian vertebrates, the fish pineal gland (Figure 1) incorporates all the elements required for photic entrainment and circadian rhythm generation: it is photoreceptive and contains an intrinsic circadian oscillator that drives melatonin rhythms [16]. These basic properties are even maintained in culture, when the pineal gland is disconnected from any neuronal input [17]. In some nonmammalian vertebrates, the pineal gland is considered to serve as the master clock organ because its removal results in disruption of rhythmic behaviours such as locomotor activity [18, 19]. Thus, the pineal gland is thought to have evolved from a photoneuroendocrine structure that contains an independent clock, as seen in teleost fish, into an endocrine gland that is driven by SCN neuronal signals in mammals [20].

The roles of the pineal gland and of melatonin in fish have been traditionally investigated by pinealectomy and exogenous administration of melatonin, providing evidence for their role in seasonal reproduction and daily rhythms. However, given the incredible diversity among teleosts, it is not surprising that studies in different fish species have produced conflicting results, ranging from no effect of pinealectomy or melatonin administration to the loss of annual and daily physiological and behavioural rhythms, making it difficult to draw a general conclusion about the role of the pineal gland and melatonin in fish physiology [20, 22, 23]. Moreover, interpretation of the results is challenging. First, in addition to the melatonin-producing photoreceptor cells, the fish pineal gland contains projecting neurons [24–26] that innervate a variety of brain regions [27] and could therefore potentially transmit photic and/or circadian information. Therefore, pinealectomy eliminates both hormonal and neuronal signals. Second, melatonin is also produced in the retina, and although the role of retinal melatonin is considered to be restricted to paracrine effects, this inevitably implies that pinealectomy is an insufficient test of the general role of melatonin. Third, exogenous melatonin administration can be misleading because the effects of melatonin depend on its duration and circadian timing. Hence, further research is required to assess the role of the fish pineal gland and melatonin rhythms in coordinating circadian and annual rhythms of physiology and behaviour.

4. Early Development of the Zebrafish Circadian System

Among the advantages of the zebrafish model for experimental manipulation are its small size and ease of maintenance in large numbers, its short generation time and high fecundity, its external fertilization, and the rapid development of transparent embryos. Furthermore, the zebrafish model offers a plethora of molecular-genetic techniques and bioinformatics tools, including methods for transgenesis, mutagenesis, gene knockdown, and targeted genome modifications, together with advanced genomic annotation.

When it comes to circadian biology, another advantage of the zebrafish, especially for studying the role of melatonin in the regulation of circadian rhythms, is that, like humans, this species is diurnal. The role of the pineal gland and the effects of melatonin on different developmental, physiological, and behavioural processes have been studied in zebrafish by several research groups [28–32]. Among their findings, these studies have shown that exogenous melatonin administration leads to reduced locomotor activity and promotes a sleep-like state [33–35] and acts to schedule the timing of reproduction [28] and feeding [31].

Physiological and behavioural rhythms in zebrafish appear early in life. Circadian rhythms of nocturnal sleep-like behaviour [35] and diurnal locomotor activity [36–38], as well as circadian rhythms of respiration, posture and arousal threshold [35, 39], are established in zebrafish larvae at 4-5 days postfertilization (dpf). In addition, waves of cell cycles in the skin are apparent in zebrafish larvae by 4-5 dpf [40]. In *per3*-luc transgenic zebrafish, rhythmic luciferase activity in the whole body is evident at 5-6 dpf [41]. Importantly, the establishment of all of these behavioural, physiological, and molecular rhythms has been shown to require exposure of the larvae to light-dark cycles. This remarkably early and rapid development of the zebrafish circadian timing system is particularly intriguing and has been instrumental

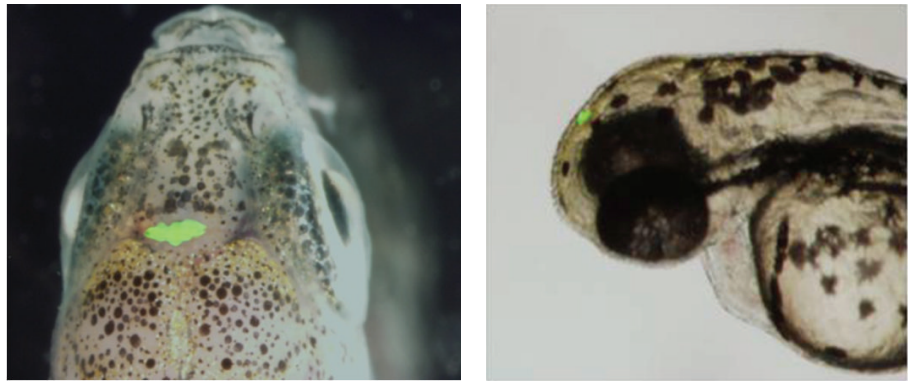

(a) (b)

Figure 1: The zebrafish pineal gland. Transgenic zebrafish expressing enhanced green fluorescent protein (EGFP) in the pineal gland under the control of the pineal-specific *aanat2* promoter [21]. (a) The head region of an adult zebrafish, dorsal view, anterior to the top. (b) The head region of a 72 hpf zebrafish larva, lateral view, anterior to the left.

for the investigation of this system, for example, by enabling functional analyses of genes in intact developing fish.

A circadian rhythm that is established even earlier is that of *aanat2* expression in the pineal gland. The zebrafish, like other teleosts, possesses two *aanat* genes: *aanat1*, which is primarily expressed in the retina, and *aanat2*, which is predominantly expressed in the pineal gland [42, 43]. As in the case of other fish species [44], circadian rhythmicity of AANAT2 activity and melatonin production can be observed in cultured zebrafish pineal glands [45]. In addition, pineal *aanat2* transcription exhibits a robust circadian rhythm that is regulated by the core molecular oscillator, and its enzymatic activity and melatonin production are suppressed in response to light [43, 46–49]. The expression of *aanat2* as well as other pineal gland markers first appears as early as 22 hours postfertilization (hpf), and the circadian rhythms of melatonin production and of *aanat2* transcription begin at 2 dpf, triggered by exposure to light [43, 50–52]. Importantly, this well-documented, robust clock-controlled gene expression and melatonin synthesis in the zebrafish embryonic pineal gland require exposure to a period of light, leading to the hypothesis that light exposure is mandatory for the development of overt clock-controlled rhythms in the pineal gland.

5. Light-Induced Onset of Circadian Rhythms in Zebrafish

What is the molecular mechanism underlying the light-induced onset of the pineal clock? In zebrafish embryos, light exposure induces the expression of *per2* mRNA predominantly in the pineal gland. Pineal gland *per2* mRNA levels increase rapidly following light onset, reaching a peak after 3 hours, while they remain undetectable under constant darkness [48]. Importantly, knockdown of *per2* abolishes *aanat2* mRNA rhythms in the pineal gland, indicating that light-induced *per2* expression is an important event in the developmental maturation of the pineal clock [48].

What are the photopigments that convey photic signals into the pineal gland oscillator? The teleost pineal gland is a classical photoreceptor organ that is evolutionarily and developmentally related to the retina [22] and expresses similar sets of genes, including opsins [42]. In the adult zebrafish, *exo-rhodopsin* is predominantly expressed in the pineal gland photoreceptors, along with several other extraretinal opsins [49, 53–55]. The expression of *exo-rhodopsin* in the zebrafish pineal gland is observed as early as 18 hpf [52] and it displays a daily rhythm, with higher mRNA levels during the night [54]. Furthermore, *exo-rhodopsin* has been shown to be required for high levels of *aanat2* transcription [54]. Therefore, light-induced *per2* expression in the pineal gland is most likely mediated by the early expressed pineal photopigment *exo-rhodopsin*.

Interestingly, light exposure also induces *per2* expression in nonpineal tissues, even at early developmental stages, prior to pineal gland or retina formation, indicating that light induces transcription in embryonic cells that are not considered classical photoreceptor cells [56, 57]. Moreover, exposure to light at these early developmental stages results in overt *aanat2* mRNA rhythms in the pineal gland at later stages, indicating that light-entrainment is preserved throughout proliferation and differentiation [57]. Indeed, it is now widely accepted that the molecular clocks within most zebrafish tissues and even cell lines are entrainable by direct exposure to light, and cell-based assays have been developed and used to study the mechanisms underlying light-induced gene expression [58–60].

The onset of rhythms in the zebrafish pineal gland is considered to represent the earliest essential light-entrainment event. This notion is supported by the observation of intermediate levels of *aanat2* in the pineal gland of arrhythmic embryos that were not exposed to light during development [48]. Thus, in the absence of entraining cues, independent cellular oscillators in the pineal gland are out of phase, generating an overall intermediate level of *aanat2* expression.

The synchronizing effect of light has also been demonstrated in a zebrafish cell line, in which a light pulse entrained the circadian oscillations of *per1b* promoter activity in individual cells and stabilized their 24-hour period, leading to a synchronized, overt rhythm of clock gene expression in the whole cell culture [58, 61]. This was further supported by the finding of asynchronous oscillations of the *per1b* transcript in individual cells of intact embryos raised in constant darkness [62]. Accordingly, in the developing circadian system, light input leads to the synchronization of preexisting cellular oscillators and not to their initial activation, resulting in the emergence of overt rhythms.

6. Mechanisms of Light-Induced Clock Gene Expression in Zebrafish

In order to explore the mechanisms underlying synchronization by light, the regulation of the light-induced zebrafish clock gene, *per2*, has been investigated. The regulation of the zebrafish *per2* promoter was first analyzed *in vivo*, leading to the identification of a minimal promoter fragment that is sufficient to drive *per2* expression and, importantly, regulation by light [63]. The existence of a photoentrainable clock system within zebrafish cells has greatly facilitated the unravelling of the regulatory mechanism underlying the light-induced *per2* expression. These *ex vivo* studies in zebrafish Pac-2 cells revealed a novel molecular mechanism that simultaneously drives clock- and light-regulated transcription [63]. This mechanism is mediated by closely spaced E-box and D-box regulatory elements that are located in proximity to the *per2* transcription start site [63]. The light-induced transcriptional activation was shown to be mediated by the D-box element and a D-box binding transcription factor, *tef-1* [63]. Eleven additional zebrafish D-box-binding factors from the PAR and E4BP4 family have since been cloned and characterized. The expression of nine of these factors is enhanced in the pineal gland and regulated, to varying extents, by the clock and/or by light [64]. Moreover, it was demonstrated that the expression of some of these factors exhibits a somewhat similar clock- or light-driven regulation in zebrafish Pac-2 cells [65]. A systematic functional analysis of the *cry1a* promoter revealed that a single D-box directs light-induced expression of this clock gene and that PAR factors are able to transactivate expression from this D-box element [65]. The D-box-mediated pathway has also been implicated in the regulation of other light-induced genes [66, 67]. Hence, D-box enhancers appear to serve as key elements in light-driven signalling in both the pineal gland and cell lines, pointing towards a somewhat similar mechanism of light-entrainment in the central and peripheral clocks. Interestingly, this differs from the situation in the mammalian circadian timing system, where D-boxes appear to serve as regulatory elements of clock output pathways [68]. The D-box-mediated pathway is probably not the only mechanism underlying light-entrainment of the circadian oscillator in fish. Might a genome-wide approach lead to the identification of parallel mechanisms?

7. Insights from the Light-Induced Transcriptome of the Zebrafish Pineal Gland

Similar to the studies of many other biological processes, circadian clock research has greatly benefited from the availability of technologies for large-scale analysis of transcriptomes, including recent advances in high-throughput RNA sequencing (RNA-seq). These technologies have also been employed for studying the mechanisms underlying light-induced gene expression. In zebrafish, DNA microarray studies of the light-induced transcriptome of embryos [66], larvae, heart, and cell cultures [67] have identified numerous genes belonging to various cellular processes, including transcriptional control and DNA repair, which are directly light-regulated. These studies have expanded the knowledge of light-regulated gene expression in peripheral clock-containing tissues.

With the aim of further exploring the mechanisms by which the central circadian clock is entrained by light, we employed both RNA-seq and microarray technologies to characterize the light-induced coding transcriptome of the zebrafish pineal gland [69], resulting in the identification of multiple light-induced mRNAs. An interesting outcome of this approach was the identification of 14-core clock and clock accessory loop genes as light-induced genes in the pineal gland, including *per2* and *cry1a*, most of which are members of the negative limbs of the molecular oscillator (Figure 2). The finding that a considerable portion of the molecular clock is regulated by light in the central clock structure points to a more complex regulatory mechanism underlying light-entrainment of the circadian clock than previously appreciated. This complexity has been further demonstrated by overexpression analyses of four of these genes, encoding the transcription factors *dec1*, *reverbβ1*, *e4bp4-5,* and *e4bp4-6*, in zebrafish Pac-2 cells. These analyses revealed different effects of the factors on clock and light-regulated promoter activation, demonstrating various mechanisms by which light-induced transcription factors modulate clock gene expression and thereby transmit photic information to the core clock. Moreover, we have shown that *dec1* is important for the light-induced onset of rhythmic locomotor activity in zebrafish larvae. This was achieved by the knockdown of *dec1*, which resulted in the disruption of circadian locomotor activity patterns triggered by a single light pulse, resembling the effect generated by *per2* knockdown. A previous study in *dec1*-deficient mice provided evidence for its role in the resetting of the circadian clock [70]; thus, our data indicate an equivalent role for *dec1* in the process of light-entrainment of the zebrafish clock.

Another intriguing finding was that cellular metabolic pathways are induced by light. Of particular interest is the finding that the expression of *hypoxia-inducible factor 1α* (*hif1α*) and its target *pfkfb4l* are both induced by light, which points to the possibility that the hypoxic pathway is involved in circadian clock entrainment, a hypothesis that requires further investigation.

A common feature of light-induced genes, as well as rhythmic genes, is their transient increase in expression,

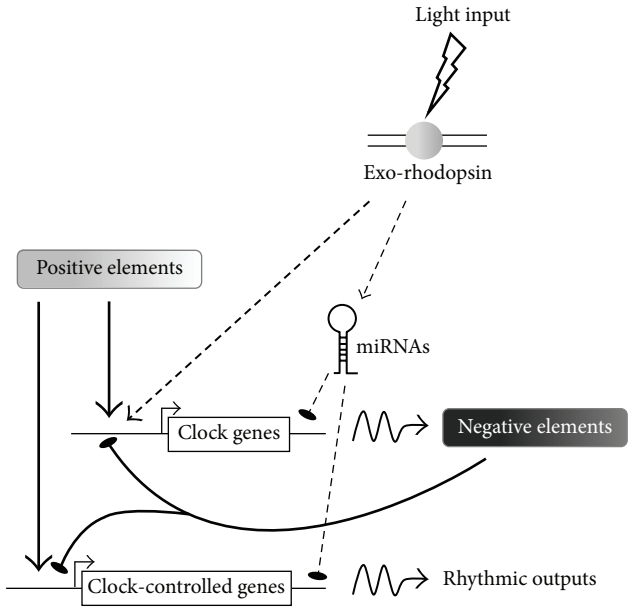

Figure 2: Model of the regulation of the molecular clockwork in the zebrafish pineal gland by light. Light input is perceived by exo-rhodopsin at the cell membrane and relayed to the nucleus by signal transduction pathways. The light signal upregulates the expression of negative elements in the clockwork circuitry. In addition, light-induced miRNAs contribute to the generation of transient expression profiles of clock and clock-controlled target genes. Arrows indicate activation; lines with flat end indicate inhibition.

suggesting the contribution of mechanisms that control mRNA stability, such as regulation by microRNA (miRNA). To search for candidate miRNAs that might play a role in light-entrainment and circadian regulation, we exploited miRNA sequencing (miR-seq) to profile the repertoire of light-induced and abundant miRNAs in the zebrafish pineal gland [69]. This analysis implicated the miR-183/96/182 cluster, the expression of which is both considerably enriched in the pineal gland and upregulated by light, in the regulation of transiently expressed mRNAs. This miRNA cluster has previously been shown to display a daily variation of expression in the mouse retina. Furthermore, it has been suggested to play a role in circadian rhythm regulation via its targeting of *adcy6*, a clock-controlled gene that modulates melatonin synthesis [71]. In a later study, the miR-183/96/182 cluster was found to be regulated by light in the mouse retina and to target the voltage-dependent glutamate transporter *slc1a1* [72]. The miR-183/96/182 cluster has also been shown to be abundantly expressed in the rat retina and pineal gland, in which it exhibits daily dynamics of expression [73]. We have demonstrated that miR-183 downregulates the light-induced *e4bp4-6* and clock-controlled *aanat2* mRNAs via target sites in their 3′UTR regions and, importantly, *in vivo* knockdown analysis indicates that miR-183 contributes to the generation of *aanat2* rhythmic mRNA levels in the pineal gland. Together, these findings imply a conserved function for the miR-183/96/182 cluster in vertebrates and support its involvement in regulating the kinetics of both clock- and light-regulated gene expression (Figure 2). The essential contribution of miRNAs to shaping the transient expression profiles of light- and clock-regulated genes, and their general importance in pineal function, such as fine-tuning the kinetics of rhythmic melatonin production, warrants further investigation.

8. Concluding Remarks

The remarkably early development of the zebrafish circadian clock in the pineal gland has provided a unique opportunity for a thorough investigation of this timing system and has led to the discovery of mechanisms that underlie its maturation. One important conclusion has been that the light-induced onset of the circadian clock is actually a specific case of entrainment of asynchronous cellular oscillators. The analysis of the regulatory mechanisms underlying light-induced clock gene expression in photoentrainable zebrafish cell lines has served as an additional important step towards unravelling the process of circadian clock light-entrainment. Another key step forward in our understanding of these light-regulated mechanisms has been achieved by genome-wide analyses of the light-induced transcriptome in zebrafish embryos, larvae, heart, and cell lines and within the pineal gland. Analysis of the pineal gland light-induced transcriptome indicated that the regulation of the circadian system by light is rather complex, involving multiple factors and pathways. Analysis of the pineal-enhanced and light-induced miRNome has revealed the contribution of miRNAs to light- and clock-regulated expression and to pineal function. There are clear similarities between the central and peripheral clocks in terms of their basic mechanisms and regulation by light. The relative contributions of the pineal gland clock and the distributed peripheral oscillators to synchronizing the physiology and behaviour of the intact animal with the day-night cycle present an important question that still remains to be addressed in the zebrafish model.

Conflict of Interests

The authors declare that there is no conflict of interests regarding the publication of this paper.

Acknowledgments

Yoav Gothilf was supported by Grant 1084/12 from the Israel Science Foundation, Jerusalem, Israel, and Grant 2009/290 from the United States-Israel Binational Science Foundation, Jerusalem, Israel. Nicholas S. Foulkes was supported by the Karlsruhe Institute of Technology (KIT, Germany) through the Helmholtz funding program, BioInterfaces.

References

[1] C. S. Pittendrigh, "Temporal organization: reflections of a Darwinian clock-watcher," *Annual Review of Physiology*, vol. 55, pp. 17–54, 1993.

[2] S. Doyle and M. Menaker, "Circadian photoreception in vertebrates," *Cold Spring Harbor Symposia on Quantitative Biology*, vol. 72, pp. 499–508, 2007.

[3] J. C. Dunlap, "Molecular bases for circadian clocks," *Cell*, vol. 96, no. 2, pp. 271–290, 1999.

[4] N. Peschel and C. Helfrich-Förster, "Setting the clock—by nature: circadian rhythm in the fruitfly *Drosophila melanogaster*," *FEBS Letters*, vol. 585, no. 10, pp. 1435–1442, 2011.

[5] J. A. Ripperger, C. Jud, and U. Albrecht, "The daily rhythm of mice," *FEBS Letters*, vol. 585, no. 10, pp. 1384–1392, 2011.

[6] C. Dibner, U. Schibler, and U. Albrecht, "The mammalian circadian timing system: organization and coordination of central and peripheral clocks," *Annual Review of Physiology*, vol. 72, pp. 517–549, 2010.

[7] G. Vatine, D. Vallone, Y. Gothilf, and N. S. Foulkes, "It's time to swim! Zebrafish and the circadian clock," *FEBS Letters*, vol. 585, no. 10, pp. 1485–1494, 2011.

[8] J. Arendt, "Melatonin and the pineal gland: influence on mammalian seasonal and circadian physiology," *Reviews of Reproduction*, vol. 3, no. 1, pp. 13–22, 1998.

[9] P. J. Morgan and D. G. Hazlerigg, "Photoperiodic signalling through the melatonin receptor turns full circle," *Journal of Neuroendocrinology*, vol. 20, no. 6, pp. 820–826, 2008.

[10] J. Falcón, K. M. Galarneau, J. L. Weller et al., "Regulation of arylalkylamine *N*-acetyltransferase-2 (AANAT2, EC 2.3.1.87) in the fish pineal organ: evidence for a role of proteasomal proteolysis," *Endocrinology*, vol. 142, no. 5, pp. 1804–1813, 2001.

[11] J. A. Gastel, P. H. Roseboom, P. A. Rinaldi, J. L. Weller, and D. C. Klein, "Melatonin production: proteasomal proteolysis in serotonin *N*-acetyltransferase regulation," *Science*, vol. 279, no. 5355, pp. 1358–1360, 1998.

[12] D. C. Klein, S. L. Coon, P. H. Roseboom et al., "The melatonin rhythm-generating enzyme: molecular regulation of serotonin *N*-acetyltransferase in the pineal gland," *Recent Progress in Hormone Research*, vol. 52, pp. 307–358, 1997.

[13] S. Ganguly, S. L. Coon, and D. C. Klein, "Control of melatonin synthesis in the mammalian pineal gland: the critical role of serotonin acetylation," *Cell and Tissue Research*, vol. 309, no. 1, pp. 127–137, 2002.

[14] C. Schomerus, H.-W. Korf, E. Laedtke, J. L. Weller, and D. C. Klein, "Selective adrenergic/cyclic AMP-dependent switch-off of proteasomal proteolysis alone switches on neural signal transduction: an example from the pineal gland," *Journal of Neurochemistry*, vol. 75, no. 5, pp. 2123–2132, 2000.

[15] D. C. Klein, S. Ganguly, S. Coon et al., "14-3-3 proteins and photoneuroendocrine transduction: role in controlling the daily rhythm in melatonin," *Biochemical Society Transactions*, vol. 30, no. 4, pp. 365–373, 2002.

[16] H. W. Korf, C. Schomerus, and J. H. Stehle, "The pineal organ, its hormone melatonin, and the photoneuroendocrine system," *Advances in Anatomy, Embryology, and Cell Biology*, vol. 146, pp. 1–100, 1998.

[17] J. Falcon, J. B. Marmillon, B. Claustrat, and J.-P. Collin, "Regulation of melatonin secretion in a photoreceptive pineal organ: an in vitro study in the pike," *Journal of Neuroscience*, vol. 9, no. 6, pp. 1943–1950, 1989.

[18] E. Gwinner, M. Hau, and S. Heigl, "Melatonin: generation and modulation of avian circadian rhythms," *Brain Research Bulletin*, vol. 44, no. 4, pp. 439–444, 1997.

[19] H. Underwood, "Circadian pacemakers in lizards: phase-response curves and effects of pinealectomy," *American Journal of Physiology*, vol. 244, no. 6, pp. R857–R864, 1983.

[20] J. Falcón, L. Besseau, M. Fuentès, S. Sauzet, E. Magnanou, and G. Boeuf, "Structural and functional evolution of the pineal melatonin system in vertebrates," *Annals of the New York Academy of Sciences*, vol. 1163, pp. 101–111, 2009.

[21] Y. Gothilf, R. Toyama, S. L. Coon, S.-J. Du, I. B. Dawid, and D. C. Klein, "Pineal-specific expression of green fluorescent protein under the control of the serotonin-*N*-acetyltransferase gene regulatory regions in transgenic zebrafish," *Developmental Dynamics*, vol. 225, no. 3, pp. 241–249, 2002.

[22] P. Ekström and H. Meissl, "The pineal organ of teleost fishes," *Reviews in Fish Biology and Fisheries*, vol. 7, no. 2, pp. 199–284, 1997.

[23] J. Falcón, H. Migaud, J. A. Muñoz-Cueto, and M. Carrillo, "Current knowledge on the melatonin system in teleost fish," *General and Comparative Endocrinology*, vol. 165, no. 3, pp. 469–482, 2010.

[24] I. Masai, C.-P. Heisenberg, K. A. Barth, R. Macdonald, S. Adamek, and S. W. Wilson, "Floating head and masterblind regulate neuronal patterning in the roof of the forebrain," *Neuron*, vol. 18, no. 1, pp. 43–57, 1997.

[25] S. W. Wilson and S. S. Easter Jr., "A pioneering growth cone in the embryonic zebrafish brain," *Proceedings of the National Academy of Sciences of the United States of America*, vol. 88, no. 6, pp. 2293–2296, 1991.

[26] S. W. Wilson, L. S. Ross, T. Parrett, and S. S. Easter Jr., "The development of a simple scaffold of axon tracts in the brain of the embryonic zebrafish, *Brachydanio rerio*," *Development*, vol. 108, no. 1, pp. 121–145, 1990.

[27] J. Yáñez, J. Busch, R. Anadón, and H. Meissl, "Pineal projections in the zebrafish (*Danio rerio*): overlap with retinal and cerebellar projections," *Neuroscience*, vol. 164, no. 4, pp. 1712–1720, 2009.

[28] O. Carnevali, G. Gioacchini, F. Maradonna, I. Olivotto, and B. Migliarini, "Melatonin induces follicle maturation in *Danio rerio*," *PLoS ONE*, vol. 6, no. 5, Article ID e19978, 2011.

[29] N. Danilova, V. E. Krupnik, D. Sugden, and I. V. Zhdanova, "Melatonin stimulates cell proliferation in zebrafish embryo and accelerates its development," *The FASEB Journal*, vol. 18, no. 6, pp. 751–753, 2004.

[30] N. H. de Borsetti, B. J. Dean, E. J. Bain, J. A. Clanton, R. W. Taylor, and J. T. Gamse, "Light and melatonin schedule neuronal differentiation in the habenular nuclei," *Developmental Biology*, vol. 358, no. 1, pp. 251–261, 2011.

[31] C. C. Piccinetti, B. Migliarini, I. Olivotto, G. Coletti, A. Amici, and O. Carnevali, "Appetite regulation: the central role of melatonin in *Danio rerio*," *Hormones and Behavior*, vol. 58, no. 5, pp. 780–785, 2010.

[32] O. Rawashdeh, N. H. de Borsetti, G. Roman, and G. M. Cahill, "Melatonin suppresses nighttime memory formation in zebrafish," *Science*, vol. 318, no. 5853, pp. 1144–1146, 2007.

[33] I. V. Zhdanova, "Sleep in zebrafish," *Zebrafish*, vol. 3, no. 2, pp. 215–226, 2006.

[34] I. V. Zhdanova, "Sleep and its regulation in zebrafish," *Reviews in the Neurosciences*, vol. 22, no. 1, pp. 27–36, 2011.

[35] I. V. Zhdanova, S. Y. Wang, O. U. Leclair, and N. P. Danilova, "Melatonin promotes sleep-like state in zebrafish," *Brain Research*, vol. 903, no. 1-2, pp. 263–268, 2001.

[36] G. M. Cahill, "Automated video image analysis of larval zebrafish locomotor rhythms," *Methods in Molecular Biology*, vol. 362, pp. 83–94, 2007.

[37] J. Hirayama, M. Kaneko, L. Cardone, G. Cahill, and P. Sassone-Corsi, "Analysis of circadian rhythms in zebrafish," *Methods in Enzymology*, vol. 393, pp. 186–204, 2005.

[38] M. W. Hurd and G. M. Cahill, "Entraining signals initiate behavioral circadian rhythmicity in larval zebrafish," *Journal of Biological Rhythms*, vol. 17, no. 4, pp. 307–314, 2002.

[39] D. A. Prober, J. Rihel, A. A. Onah, R.-J. Sung, and A. F. Schier, "Hypocretin/orexin overexpression induces an insomnia-like phenotype in zebrafish," *Journal of Neuroscience*, vol. 26, no. 51, pp. 13400–13410, 2006.

[40] M. P. S. Dekens, C. Santoriello, D. Vallone, G. Grassi, D. Whitmore, and N. S. Foulkes, "Light regulates the cell cycle in zebrafish," *Current Biology*, vol. 13, no. 23, pp. 2051–2057, 2003.

[41] M. Kaneko and G. M. Cahill, "Light-dependent development of circadian gene expression in transgenic zebrafish," *PLoS Biology*, vol. 3, no. 2, article e34, 2005.

[42] J. Falcón, Y. Gothilf, S. L. Coon, G. Boeuf, and D. C. Klein, "Genetic, temporal and developmental differences between melatonin rhythm generating systems in the teleost fish pineal organ and retina," *Journal of Neuroendocrinology*, vol. 15, no. 4, pp. 378–382, 2003.

[43] Y. Gothilf, S. L. Coon, R. Toyama, A. Chitnis, M. A. A. Namboodiri, and D. C. Klein, "Zebrafish serotonin *N*-acetyltransferase-2: marker for development of pineal photoreceptors and circadian clock function," *Endocrinology*, vol. 140, no. 10, pp. 4895–4903, 1999.

[44] J. Falcón, "Cellular circadian clocks in the pineal," *Progress in Neurobiology*, vol. 58, no. 2, pp. 121–162, 1999.

[45] G. M. Cahill, "Circadian regulation of melatonin production in cultured zebrafish pineal and retina," *Brain Research*, vol. 708, no. 1-2, pp. 177–181, 1996.

[46] L. Appelbaum, A. Anzulovich, R. Baler, and Y. Gothilf, "Homeobox-clock protein interaction in zebrafish: a shared mechanism for pineal-specific and circadian gene expression," *The Journal of Biological Chemistry*, vol. 280, no. 12, pp. 11544–11551, 2005.

[47] V. Bégay, J. Falcón, G. M. Cahill, D. C. Klein, and S. L. Coon, "Transcripts encoding two melatonin synthesis enzymes in the teleost pineal organ: circadian regulation in pike and zebrafish, but not in trout," *Endocrinology*, vol. 139, no. 3, pp. 905–912, 1998.

[48] L. Ziv, S. Levkovitz, R. Toyama, J. Falcon, and Y. Gothilf, "Functional development of the zebrafish pineal gland: light-induced expression of period2 is required for onset of the circadian clock," *Journal of Neuroendocrinology*, vol. 17, no. 5, pp. 314–320, 2005.

[49] L. Ziv, A. Tovin, D. Strasser, and Y. Gothilf, "Spectral sensitivity of melatonin suppression in the zebrafish pineal gland," *Experimental Eye Research*, vol. 84, no. 1, pp. 92–99, 2007.

[50] J. T. Gamse, Y.-C. Shen, C. Thisse et al., "Otx5 regulates genes that show circadian expression in the zebrafish pineal complex," *Nature Genetics*, vol. 30, no. 1, pp. 117–121, 2002.

[51] N. Kazimi and G. M. Cahill, "Development of a circadian melatonin rhythm in embryonic zebrafish," *Developmental Brain Research*, vol. 117, no. 1, pp. 47–52, 1999.

[52] R. Vuilleumier, L. Besseau, G. Boeuf et al., "Starting the zebrafish pineal circadian clock with a single photic transition," *Endocrinology*, vol. 147, no. 5, pp. 2273–2279, 2006.

[53] H. Mano, D. Kojima, and Y. Fukada, "Exo-rhodopsin: a novel rhodopsin expressed in the zebrafish pineal gland," *Molecular Brain Research*, vol. 73, no. 1-2, pp. 110–118, 1999.

[54] L. X. Pierce, R. R. Noche, O. Ponomareva, C. Chang, and J. O. Liang, "Novel functions for period 3 and Exo-rhodopsin in rhythmic transcription and melatonin biosynthesis within the zebrafish pineal organ," *Brain Research*, vol. 1223, pp. 11–24, 2008.

[55] R. Toyama, X. Chen, N. Jhawar et al., "Transcriptome analysis of the zebrafish pineal gland," *Developmental Dynamics*, vol. 238, no. 7, pp. 1813–1826, 2009.

[56] T. K. Tamai, V. Vardhanabhuti, N. S. Foulkes, and D. Whitmore, "Early embryonic light detection improves survival," *Current Biology*, vol. 14, no. 3, pp. R104–R105, 2004.

[57] L. Ziv and Y. Gothilf, "Circadian time-keeping during early stages of development," *Proceedings of the National Academy of Sciences of the United States of America*, vol. 103, no. 11, pp. 4146–4151, 2006.

[58] A.-J. F. Carr, T. K. Tamai, L. C. Young, V. Ferrer, M. P. Dekens, and D. Whitmore, "Light reaches the very heart of the zebrafish clock," *Chronobiology International*, vol. 23, no. 1-2, pp. 91–100, 2006.

[59] D. Vallone, K. Lahiri, T. Dickmeis, and N. S. Foulkes, "Zebrafish cell clocks feel the heat and see the light!," *Zebrafish*, vol. 2, no. 3, pp. 171–187, 2005.

[60] D. Vallone, C. Santoriello, S. B. Gondi, and N. S. Foulkes, "Basic protocols for zebrafish cell lines: maintenance and transfection," *Methods in Molecular Biology*, vol. 362, pp. 429–441, 2007.

[61] A.-J. F. Carr and D. Whitmore, "Imaging of single light-responsive clock cells reveals fluctuating free-running periods," *Nature Cell Biology*, vol. 7, no. 3, pp. 319–321, 2005.

[62] M. P. S. Dekens and D. Whitmore, "Autonomous onset of the circadian clock in the zebrafish embryo," *The EMBO Journal*, vol. 27, no. 20, pp. 2757–2765, 2008.

[63] G. Vatine, D. Vallone, L. Appelbaum et al., "Light directs zebrafish period2 expression via conserved D and E boxes," *PLoS Biology*, vol. 7, no. 10, Article ID e1000223, 2009.

[64] Z. Ben-Moshe, G. Vatine, S. Alon et al., "Multiple PAR and E4BP4 bZIP transcription factors in zebrafish: diverse spatial and temporal expression patterns," *Chronobiology International*, vol. 27, no. 8, pp. 1509–1531, 2010.

[65] P. Mracek, C. Santoriello, M. L. Idda et al., "Regulation of *per* and *cry* genes reveals a central role for the D-box enhancer in light-dependent gene expression," *PLoS ONE*, vol. 7, no. 12, Article ID e51278, 2012.

[66] D. Gavriouchkina, S. Fischer, T. Ivacevic, J. Stolte, V. Benes, and M. P. S. Dekens, "Thyrotroph embryonic factor regulates light-induced transcription of repair genes in zebrafish embryonic cells," *PLoS ONE*, vol. 5, no. 9, Article ID e12542, 2010.

[67] B. D. Weger, M. Sahinbas, G. W. Otto et al., "The light responsive transcriptome of the zebrafish: function and regulation," *PLoS ONE*, vol. 6, no. 2, Article ID e17080, 2011.

[68] J. A. Ripperger, L. P. Shearman, S. M. Reppert, and U. Schibler, "CLOCK, an essential pacemaker component, controls expression of the circadian transcription factor DBP," *Genes & Development*, vol. 14, no. 6, pp. 679–689, 2000.

[69] Z. Ben-Moshe, S. Alon, P. Mracek et al., "The light-induced transcriptome of the zebrafish pineal gland reveals complex regulation of the circadian clockwork by light," *Nucleic Acids Research*, 2014.

[70] M. J. Rossner, H. Oster, S. P. Wichert et al., "Disturbed clockwork resetting in sharp-1 and sharp-2 single and double mutant mice," *PLoS ONE*, vol. 3, no. 7, Article ID e2762, 2008.

[71] S. Xu, P. D. Witmer, S. Lumayag, B. Kovacs, and D. Valle, "MicroRNA (miRNA) transcriptome of mouse retina and identification of a sensory organ-specific miRNA cluster," *The Journal of Biological Chemistry*, vol. 282, no. 34, pp. 25053–25066, 2007.

[72] J. Krol, V. Busskamp, I. Markiewicz et al., "Characterizing light-regulated retinal microRNAs reveals rapid turnover as a common property of neuronal microRNAs," *Cell*, vol. 141, no. 4, pp. 618–631, 2010.

[73] S. J. Clokie, P. Lau, H. H. Kim, S. L. Coon, and D. C. Klein, "MicroRNAs in the pineal gland: miR-483 regulates melatonin synthesis by targeting arylalkylamine *N*-acetyltransferase," *The Journal of Biological Chemistry*, vol. 287, no. 30, pp. 25312–25324, 2012.

Hindawi Publishing Corporation
BioMed Research International
Volume 2014, Article ID 590581, 8 pages
http://dx.doi.org/10.1155/2014/590581

Research Article

Synchronization by Food Access Modifies the Daily Variations in Expression and Activity of Liver GABA Transaminase

Dalia De Ita-Pérez, Isabel Méndez, Olivia Vázquez-Martínez, Mónica Villalobos-Leal, and Mauricio Díaz-Muñoz

Instituto de Neurobiología, Campus UNAM-Juriquilla, 76230 Querétaro, QRO, Mexico

Correspondence should be addressed to Mauricio Díaz-Muñoz; mdiaz@comunidad.unam.mx

Received 13 December 2013; Revised 3 March 2014; Accepted 11 March 2014; Published 7 April 2014

Academic Editor: Mario Guido

Daytime restricted feeding (DRF) is an experimental protocol that influences the circadian timing system and underlies the expression of a biological clock known as the food entrained oscillator (FEO). Liver is the organ that reacts most rapidly to food restriction by adjusting the functional relationship between the molecular circadian clock and the metabolic networks. γ-Aminobutyric acid (GABA) is a signaling molecule in the liver, and able to modulate the cell cycle and apoptosis. This study was aimed at characterizing the expression and activity of the mostly mitochondrial enzyme GABA transaminase (GABA-T) during DRF/FEO expression. We found that DRF promotes a sustained increase of GABA-T in the liver homogenate and mitochondrial fraction throughout the entire day-night cycle. The higher amount of GABA-T promoted by DRF was not associated to changes in GABA-T mRNA or GABA-T activity. The GABA-T activity in the mitochondrial fraction even tended to decrease during the light period. We concluded that DRF influences the daily variations of GABA-T mRNA levels, stability, and catalytic activity of GABA-T. These data suggest that the liver GABAergic system responds to a metabolic challenge such as DRF and the concomitant appearance of the FEO.

1. Introduction

GABA transaminase (GABA-T; 4-aminobutanoate:2-oxoglutarate aminotransferase, EC 2.6.1.19) is a catabolic enzyme that converts GABA and α-ketoglutarate into succinate semialdehyde and glutamate. Its specificity is not strict since it can also recognize alanine, β-alanine, aspartate, and propanoate as substrates. GABA-T is dependent on pyridoxal-phosphate (PLP) as cofactor, and its catalytic mechanism consists of two coupled half reactions in which the PLP cofactor oscillates between the pyridoxal and the pyridoxamine forms [1]. GABA-T has been found in a large variety of species ranging from microorganisms, plants, invertebrates, and vertebrates. In eukaryotic cells, GABA-T is present, but not exclusively, within the mitochondria [2, 3]. This enzyme has been crystallized from several sources. The structure of GABA-T from brain pig indicates a $\alpha 2$ dimer with 472 residues per subunit; the two monomers are tightly intertwined, and the two PLP cofactors are located close to the subunit interface [4]. The structure of the brain GABA-T also contains a [2Fe-2S] cluster in the vicinity of the PLP cofactors [5]. The maturation process in the synthesis of GABA-T involves a proteolytic cleavage that removes the XRX(∗)XS motif. However, in the liver, GABA-T is further cleaved to a smaller isoform by a second proteolytic step catalyzed by a mitochondrial processing peptidase [6].

GABA is a well-known inhibitory transmitter in the nervous system. However, components of the GABAergic system have also been characterized in a variety of endocrine tissues such as pancreas, testis, and liver [7–9]. Mammalian liver contains GABA at nM levels as well as its specific transporters (GAT2) and receptors (both GABAR-A and GABAR-B) [10]. Liver GABA has been proposed to function as a positive regulator of the cell cycle, with implications in some forms of hepatocellular carcinoma [11]. High GABA-T activity has been reported in hepatic tissue [12], the rationale being that liver GABA-T mainly functions to degrade

the GABA produced by microorganisms in the gastrointestinal tract [13]. In addition, GABA can also be present in the food ingested at mealtime.

Daytime restricted feeding (DRF) is an experimental protocol that influences the circadian timing system by promoting the emergence of an alternate master circadian oscillator that is independent of the suprachiasmatic nucleus (SCN) [14]. The basis for this new form of measuring the "physiological timing" is a circadian entity known as the food entrainable oscillator (FEO), but its anatomical location is still unidentified [15]. The DRF protocol involves the establishment of a catabolic response promoted by limiting the food intake to a few hours (2–4 h) during the light phase of the day-night cycle. The display of an anticipatory behavior is evident before mealtime (food anticipatory activity, FAA) as is a diversity of physiological and metabolic adaptations associated with DRF/FEO expression [16]. During the DRF protocol, some biochemical and structural changes in the liver have been associated with improved mitochondrial function as well as increased apoptotic activity and cell division, resulting in enhanced cellular exchange [17, 18].

To obtain further insights into the modulation of the mitochondrial adaptations of the liver GABA-handling system during the DRF protocol/FEO expression, we analyzed the daily variations of GABA-T mRNA and protein expression and enzymatic activity. The results evidenced under the DRF protocol are as follows: (1) an increased presence of GABA-T in homogenate and mitochondrial fraction, (2) changes in the rhythmic profile of GABA-T activity, and (3) disappearance of an ultradian rhythm of GABA-T mRNA.

2. Materials and Methods

2.1. Animals and Housing. Experiments were carried out with male Wistar rats weighing from 200 to 250 g and maintained under a 12:12 h LD cycle (lights on 08:00 h) at constant temperature (22 ± 1°C). Rats were kept in groups of 4 in transparent acrylic cages (40 × 50 × 20 cm) with free access to Purina Chow and water except during food restriction or fasting conditions. Experimental procedures were conducted in accordance with our Institutional Guide for Care and Use of Experimental Animals (Universidad Nacional Autónoma de México) and with international ethical standards [19].

2.2. Experimental Design. The experimental protocol has been published previously [20]. Briefly, rats were randomly assigned to one of the following feeding conditions for 3 weeks:

(1) control animals fed with *ad libitum* with free access to food and water throughout the 24 h period, AL group;

(2) experimental group with restricted food access (exclusively from 12:00 to 14:00 h), DRF group.

At the end of the 3 weeks, subgroups of animals were sacrificed at 3 h intervals over a complete 24 h cycle, starting at 08:00 h. The protocol was followed until the last day.

In addition, 2 more groups were included to compare the acute fasting and subsequent refeeding response in the DRF group.

(1) Animals fed *ad libitum* were maintained with free food access for 3 weeks; on the last day, food was removed at 14:00 h, and, after 21 h (~1 day) of food deprivation, they were sacrificed (at 11:00 h), F group.

(2) A second group of rats was similarly deprived of food for 21 h, then refed for 2 h (from 12:00 to 14:00), and sacrificed at 14:00 h, F + R group.

2.3. Liver Sampling and Subcellular Fractionation. Rats were beheaded with a guillotine-like instrument. The liver was removed (≈5 g) and immediately placed in an ice-cold isolation medium (1 : 10 wt/vol) containing 250 mM sucrose, 0.1% BSA (fatty acid free), and 0.5 mM EGTA (pH 7.4). The tissue was homogenized in 10 volumes of 10 mM Tris-HCl, pH 7.4, with a Teflon homogenizer (40 rpm for 10 s). Subcellular fractionation was done according to Aguilar-Delfín et al. [21]. Briefly, the homogenate was centrifuged at 1,500 g for 15 min, and the supernatant was centrifuged at 10,000 g for 20 min to sediment the mitochondrial fraction. Protein was measured by the method of Bradford [22].

2.4. GABA-T Activity. GABA-T activity was measured by a coupled enzymatic assay according to the method reported by Jung et al., 1977 [23]. The method involves the conversion of GABA to succinic acid by the consecutive reactions of GABA-T (in the sample) and semialdehyde dehydrogenase (added in the assay). As part of the reactions, NAD^+ is reduced to NADH, allowing the quantification of GABA transamination by spectrophotometric recording at 340 nm. The increasing in optical density was recorded during the first 2 min of the assay.

2.5. Western Blot Analysis. Liver homogenates and mitochondrial fractions were obtained in RIPA buffer (Sigma-Aldrich, SLM, USA) and subjected to denaturing SDS-PAGE under reducing conditions. Total protein concentrations were determined by the Bradford method and equal amounts (30 μg) were separated on 10% SDS-PAGE, transferred to nitrocellulose membranes, and blocked for 1 h in TBST buffer (20 mM TRIS, pH 7.5; 500 mM NaCl; 0.5% Tween 20) containing 5% nonfat milk. Membranes were then washed and incubated in the presence of mouse anti-GABA-T antibody (Rb mAb to ABAT, ab108249, Abcam, Cambridge, UK) diluted 1/10,000 in TBST overnight at 4°C. As controls, in the case of homogenates, membranes were incubated in the presence of mouse anti-tubulin antibody (ab56676, Abcam, Cambridge, UK) diluted 1/1,000 or in the case of mitochondrial fractions in the presence of rabbit anti-VDAC1/Porin antibody (ab15895, Abcam, Cambridge, UK) diluted 1/1,000. After washing, membranes were incubated with secondary antibodies conjugated to alkaline phosphatase (1/5,000). Bands were revealed using AP conjugate substrate kit (Bio-Rad, CA, USA). Densitometric analysis was performed using the Image Lab Software (v 3.0, Bio-Rad, CA, USA).

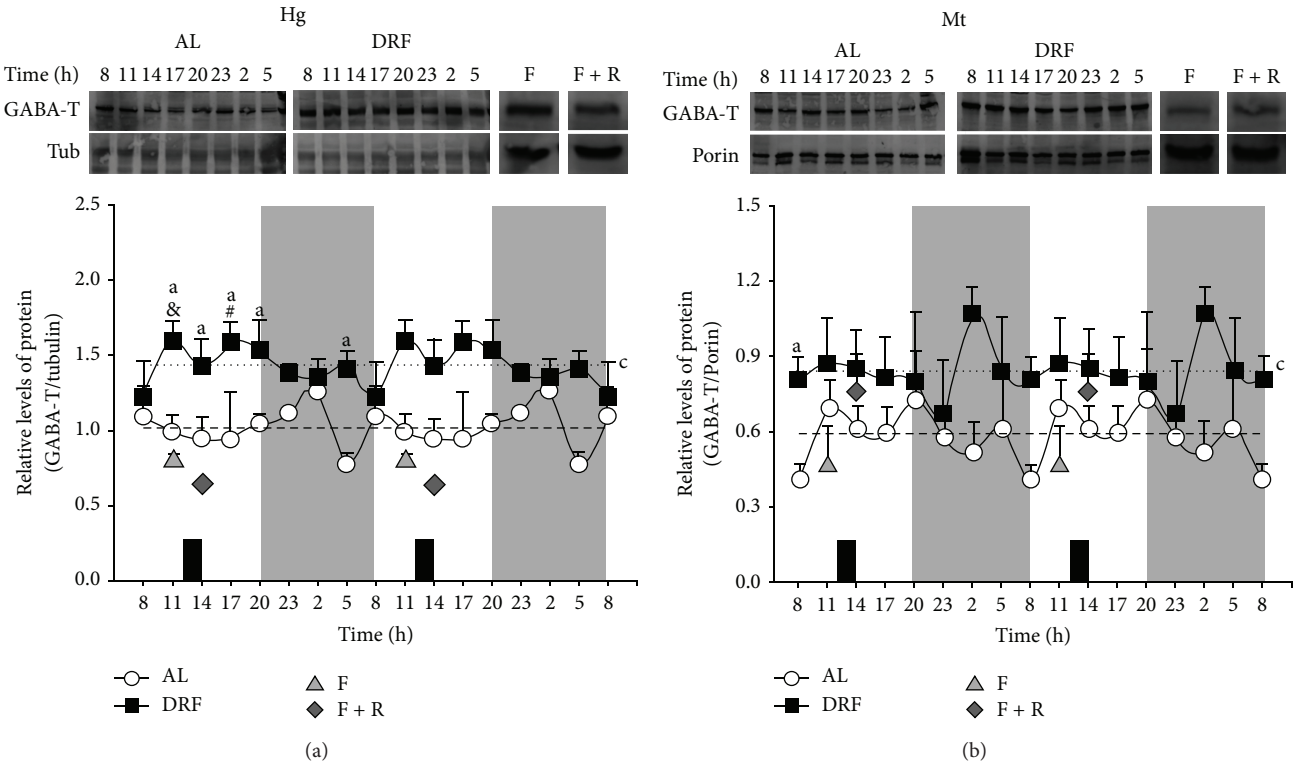

Figure 1: Western blot analysis of 24 h profile of GABA-T protein in liver of AL and DRF rats. Liver homogenates (Hg) (a) and mitochondrial fractions (Mt) (b) were subjected to electrophoresis on 10% SDS-polyacrylamide gels. Data were quantified by densitometry of the bands obtained from homogenates (a) and mitochondrial fractions (b) collected over a 24 h period from the AL and DRF groups and food condition controls, F and F + R. Food availability for the DRF group is indicated by dark boxes (from 12:00 to 14:00 h). Average values are represented as a dashed line for the AL group and as a dotted line for the DRF group. Graphs represent the mean ± SEM of 4 rats per time point. Significant differences ($P < 0.05$) are indicated as follows: a: DRF versus AL by two-way ANOVA and post hoc Bonferroni test; c: mean of DRF versus mean of AL by Student's t-test for both homogenate and mitochondrial fraction; for homogenates only: &, DRF versus F at 11:00; #, DRF versus F + R at 14:00, both by the Student's t-test.

Table 1: Chronobiological analysis of liver GABA-T parameters: mRNA, protein amount, and activity.

	GABA-T mRNA		GABA-T protein				GABA-T activity			
			Hg		Mt		Hg		Mt	
	AL	DRF	AL	DRF	AL	DRF	AL	DRF	AL	DRF
Rhythm (%)	—	—	—	—	—	—	—	54.8	40.3	38.4
Mesor	0.9	0.8	1.1	1.5	0.7	0.9	5.2	5.4	2.4	2.0
Amplitude	0.3	—	—	—	—	—	—	1.55	0.48	0.50
Acrophase (h:min)	7:40/15:15/22:50	—	—	—	—	—	—	9:56	5:56	4:14
Period	8 h	—	—	—	—	—	—	24 h	24 h	24 h

Chronos-Fit analysis was performed to evaluate rhythmicity for GABA-T parameters in liver. Acrophases in GABA-T mRNA from AL group were repeated each 7 h with 40 min. Hg: liver homogenate, Mt: mitochondrial fraction, AL: ad libitum, and DRF: daytime restricted feeding. (—) means that no rhythmic pattern was detected.

2.6. RT-qPCR Amplifications. GABA-T gene expression was evaluated by isolating total RNA from liver tissues (20–30 mg) using the SV Total RNA Isolation System (Promega, WI, USA). The amount and quality of RNA were estimated spectrophotometrically at 260 and 280 nm, and a constant amount of RNA (2 μg) was reverse transcribed using SuperScript III Reverse Transcriptase, Oligo (dT) 12–18 Primer, RNaseOUT Recombinant Ribonuclease Inhibitor, and dNTP Set PCR Grade (Invitrogen, CA, USA). Amplification was performed in triplicate in the CFX96TM Real-Time PCR Detection System (Bio-Rad, CA, USA). Primers used for qPCR amplifications were synthesized by Sigma-Aldrich Co. (MO, USA), and the corresponding sequences were, for GABA-T (GenBank BC081787.1), forward 5′-TTCCGGAAGCTGAGAGACAT-3′ and reverse 5′-AGTCTGAACCTCGTCCACCA-3′ and, for ribosomal protein S18 (Rps18) (GenBank BC126072.1) used as housekeeping gene, forward 5′-TTCAGCACATCCTGC-GAGTA-3′ and reverse 5′-TTGGTGAGGTCAATGTCTGC-3′. Amplifications were carried out with Maxima SYBR

Green qPCR Master Mix (Thermo Fisher Scientific, MA USA) in a 10 μL final reaction volume containing cDNA (1/100) and 0.5 μM of each of the primer pairs in SYBR Green Master Mix, according to the following protocol: activation of Taq DNA polymerase and DNA denaturation at 95°C for 10 min, followed by 40 amplification cycles consisting of 10 s at 95°C, 30 s at 62°C, and 30 s at 72°C. The PCR data were analyzed by the $2^{-\Delta\Delta CT}$ method and cycle thresholds (CT) normalized to the housekeeping gene Rps18 were used to calculate the mRNA levels of GABA-T.

2.7. Data Analysis. Data were classified by group and time and are displayed as mean ± standard error of the mean (SEM). Data were compared using a two-way ANOVA using Fisher's least significant difference (LSD) test for multiple and independent measures, with a factor for group (2 levels) and a factor for time (8 levels). In order to determine significant time effects for each daily sampling profile, a one-way ANOVA was performed for individual groups. The one-way ANOVA was followed by Tukey's post hoc test whereas the two-way ANOVA was followed by a Bonferroni post hoc test with the significance threshold set at $P < 0.05$ for both. The Student's t-test was applied to detect significant differences between DRF rats and the controls of feeding conditions (acute fasting and refeeding) both before and after food access (11:00 h and 14:00 h, resp.). The Student's t-test was also used to identify significant differences ($P < 0.05$) between the 24 h average values of the AL and DRF groups. Rhythmic analysis was performed by Chronos-Fit (v 1.06 developed by P. Zuther, S. Gorbey, and B. Lemmer, 2009) based on a partial Fourier analysis of the data [24]. All statistical analysis was performed with the program STATISTICA, version 4.5 (StatSoft Inc.).

3. Results

All results are double plotted displayed to have a better notion of the rhythmic profiles.

3.1. Liver GABA-T Is Increased by DRF. The amount of GABA-T protein detected by Western blot analysis in the liver homogenate and mitochondrial fraction is shown in Figure 1. GABA-T did not show any rhythmicity in liver homogenate from AL rats (a). DRF rats showed a significant increase in GABA-T protein throughout the 24 h cycle. The average value was ~38% higher in the DRF group than in the AL group (Table 1 and Figure 1(a)). In addition, significant differences (higher levels in DRF than AL rats) were detected at 05:00 h, 11:00 h, 14:00 h, 17:00 h, and 20:00 h. Similar to the AL rats, no rhythmicity was detected in the Western blot signal in the homogenate of the DRF group. The level of GABA-T was responsive to acute 24 h fasting (F group), showing a significant reduction in comparison to the DRF group at 11:00 h. Two hours of feeding after fasting (F + R group) were not enough to restore the low levels of GABA-T associated with the acute fasting condition (a).

Since GABA-T is in an important proportion a mitochondrial enzyme, the amount of this protein was also evaluated by Western blot analysis in the liver mitochondrial fraction in the AL and DRF groups (b). As observed in liver homogenate, GABA-T was significantly increased in the DRF group. However, comparing the calculated average values, the elevation was more moderate (~26%, Table 1). Again, no rhythmicity was detected in either group. A significant difference between both groups was detected at 02:00 h. In contrast to the effect observed in the liver homogenate, neither acute fasting (group F) nor acute fasting followed by 2 h of refeeding (F + R group) modified the amount of GABA-T protein in the mitochondrial fraction. However, as to the controls of acute feeding conditions, there was a significant increase (~85%) in the F + R rats in comparison to the F rats.

3.2. The Activity of Liver GABA-T in the Mitochondrial Fraction Was Modified by DRF. The activity of GABA-T in AL and DRF groups is shown in Figure 2 for the liver homogenate (a) and for the mitochondrial fraction (b). GABA-T activity in the homogenate fluctuated in both groups, with peaks at 23:00 h and 08:00 h in AL and DRF rats, respectively (Table 1). At these times, significant differences were detected between both groups. In contrast, GABA-T activity in the mitochondrial fraction tended to be reduced in the DRF group, and both groups showed rhythmicity. Peak value for AL rats was at 08:00 h and for DRF rats was at 05:00 h (Table 1). A clear sinusoidal pattern was observed in the AL group with the lowest value in the middle of the light phase and the peak at the transition from the dark and to the light period. The DRF group also exhibited a sinusoidal pattern with the lowest value near the end of the light period and the peak 12 h later. However, this pattern was consistent with the lower values of mitochondrial GABA-T activity, especially during the light period.

In both liver homogenate and the mitochondrial fraction, the food condition controls (F and F + R groups) did not show any changes in comparison to the AL and DRF rats at 11:00 h and 14:00 h, respectively.

3.3. mRNA of Liver GABA-T Was Not Rhythmic in the DRF Group. The mRNA for GABA-T was quantified in liver by RT-qPCR in the AL and DRF groups, and the results are shown in Figure 3. AL rats showed rhythmicity in this parameter with 2 larger peaks, one at 17:00 h and the second at 23:00 h, and a minor peak at 08:00 h. There was also a pronounce valley at 20:00 h. Indeed, rhythmic analysis detected an ultradian rhythm with a period of ~8 h (Table 1). DRF rats did not show any rhythmicity. Significant differences between AL and DRF groups were detected at 14:00 h, 17:00 h, and 23:00 h, being higher the values from the AL rats. No significant differences in the expression of GABA-T mRNA were detected between the F and DRF group at 11:00 h as well as between the F + R and DRF group at 14:00 h.

4. Discussion

4.1. Liver GABAergic System. Our data show that under a protocol of daytime restricted feeding (DRF) with the subsequent appearance of the feeding entrained oscillator (FEO) the properties of liver GABA-T are affected and highlight the

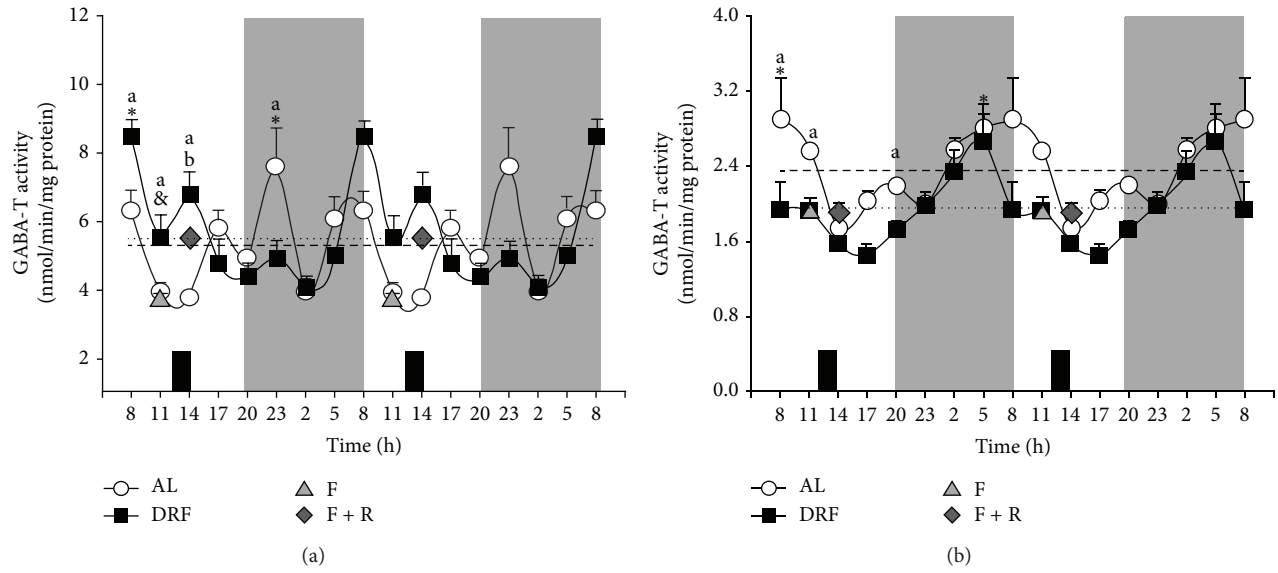

Figure 2: Analysis of 24 h profile of GABA-T activity in the liver of AL and DRF rats. GABA-T activity was measured in both the homogenate (a) and mitochondrial fraction (b) of the livers from AL and DRF rats by a spectrophotometric assay over a 24 h period. Rats were subjected to a 12 h : 12 h regime of light : dark. The shaded zone represents the dark phase. Food availability for RFS group is indicated by dark boxes (from 12:00 to 14:00 h). Controls of food condition are shown (F and F + R). Average values are represented as dashed line for AL group and a dotted line for RFS group. Graphs show the mean ± SEM of 4 rats per time point. Significant differences ($P < 0.05$) are indicated as follows: ∗: DRF versus AL by one-way ANOVA and post hoc Bonferroni test, in both the homogenate and mitochondrial fraction; a: RFS versus AL by two-way ANOVA and post hoc Bonferroni test in the mitochondria fraction only; b: F versus F + R by Student's t-test.

plasticity of the hepatic GABAergic system under a metabolic challenge.

It is well documented that GABA and its metabolizing enzymes are found outside the nervous system and play a role in the cell signaling of several organs and tissues [25]. These tissues express the anabolic and catabolic enzymes for GABA, and measurable levels of this molecule can be detected [7, 12]. It has also been reported that hepatic tissue expresses elements of the GABAergic system, such as specific receptors (GABAR-A and GABAR-B), transporters, and the catabolic enzyme GABA-T [10]. Hepatocytes and other liver cell types are clearly in contact with GABA, which may be produced by the liver itself or may come from the microbial production of the intestinal tract [13, 25]. In this context, it has been suggested that GABA present in hepatic tissue could act as a regulator of the cell cycle and the migration of cancerous hepatocytes [11, 26]. As a signaling molecule, liver GABA must be finely controlled by plasma membrane transporters but, mainly, by its catabolic transformation by GABA-T [27].

4.2. Liver GABA Transaminase. GABA-T is, but not exclusively, a mitochondrial enzyme that requires PLP for its activity. In the liver, it exists as a smaller variant because of proteolytic processing that removes 12–14 amino acids [6]. The pharmacological inhibition of GABA-T has been explored for several years, motivated by attempts to find an effective antiepileptic drug [28]; however, not much information has been reported regarding its transcriptional regulation or the modulation of its activity by covalent modifications.

Our results indicate that liver GABA-T activity, mainly in the mitochondrial fraction, and the level of GABA-T mRNA in AL groups show daily fluctuations. Previously, our group reported that the mitochondrial yield after cellular fractionation did not change by the DRF protocol [17]. The data also show that the DRF protocol affected the properties of hepatic GABA-T at different levels. (1) The elevated levels of this protein enzyme in the liver homogenate and mitochondrial fraction (Figure 1) did not correlate with the corresponding levels of mRNA (Figure 3). A possible explanation is that the restricted feeding schedule promoted an increased stability of GABA-T or an increment in its translational rate. (2) The higher amount in the presence of GABA-T did not correlate with the GABA-T activity measured in liver homogenate and the mitochondrial fraction (Figure 2). This lack of correspondence could be explained by the existence of a negative regulator of GABA-T activity, such as a covalent modification or some other type of posttranslational processing. We have not yet found any reports of phosphorylation, acetylation, methylation, or other modulatory modifications of GABA-T activity. However, these modifications in GABA-T properties promoted by the protocol of DRF/FEO expression can be considered as a metabolic adaptation based on the biochemical plasticity of this enzymatic system.

4.3. GABA-T under Food Synchronization/Food Entrainable Oscillator. The changes in the amount and activity of GABA-T associated with the protocol of daytime restricted feeding are part of an extensive set of metabolic and physiological adaptations that occur in the liver and other organs when

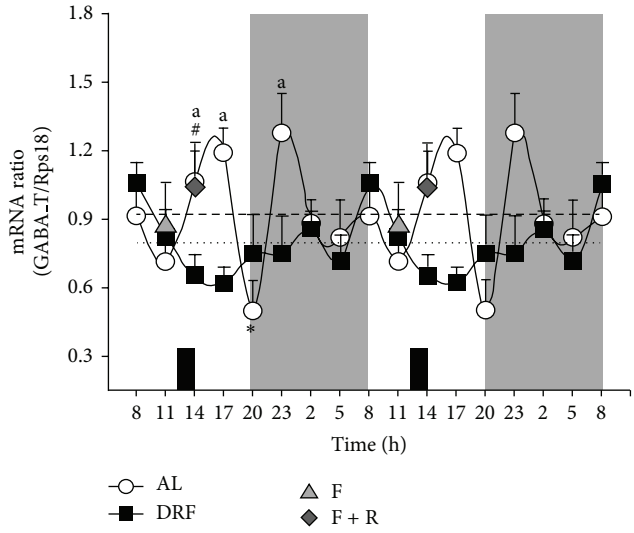

Figure 3: Analysis of the 24 h profile of relative mRNA expression of GABA-T in the liver of rats under AL and DRF conditions. Relative mRNA levels were determined by RT-qPCR and normalized to Rps18 expression. The shaded zone represents the dark phase. Food availability for DRF group is indicated by dark boxes (from 12:00 to 14:00 h). Graphs show the mean ± SEM of 6 to 8 rats per time point. Average values are represented as a dashed line for the AL group and a dotted line for DRF group. Significant differences ($P < 0.05$) are indicated as follows: ∗: DRF versus AL by one-way ANOVA and post hoc Bonferroni test, in both the homogenate and mitochondrial fraction; a: RFS versus AL by two-way ANOVA and post hoc Bonferroni test; #: DRF versus F + R at 14:00, by the Student's *t*-test.

the daily rhythmicity is modified by a new organization of the timing system [29, 30]. The synchronization imposed by offering food for only 2–4 h per day is a powerful timing cue that, in some circumstances, overrules the control of the master pacemaker, the SCN [31]. This situation elicits food anticipatory activity as well as the expression of a biological clock (the FEO) that is independent of the SCN. The anatomical localization of the FEO is unknown, but the hypothesis guiding our research is that it is an emergent oscillator distributed among hypothalamic/midbrain nuclei that control food intake and peripheral organs such as liver, adrenals, stomach, and others important for nutrient processing [15, 32].

It is in the liver where the influence of the FEO is most evident. The liver plays central roles in both the processing of nutrients arriving from the duodenal tract and the modulating of the hunger-satiety cycle [33]. This fact is especially relevant during DRF because of the marked hyperphagia after the 2 h of food access. Indeed, the intense arrival of nutrients during the restricted feeding could be a factor in the daily entrainment showed by the liver [34].

In previous reports, we have shown that DRF/FEO expression strongly modifies the metabolic status of the liver mitochondria, promoting a more oxidized state and increasing the synthesis of ATP [17, 35]. In addition, DRF/FEO expression is associated with an elevation of the malate-aspartate shuttle activity [17]. Together these data indicate that liver mitochondria are responsive to the adaptations associated with FEO expression, as an example of the plasticity shown by the timing system during the metabolic adaptations associated with restricted feeding schedules. This is of particular interest to the present project since GABA-T is mostly a mitochondrial enzyme.

4.4. Rheostatic Adaptation. The exact molecular mechanisms that underlie the adaptive modifications of liver physiology during expression of the FEO and in response to the DRF protocol are not known. However, an initial rationale towards the identification of this sequence of events is to postulate that synchronizing circadian physiology by limited food access has an impact on the reciprocal regulation between energetic metabolic networks and the cellular timing system [36, 37]. During DRF/FEO expression, the connection between the molecular circadian clock and the metabolic activities has been thought to adopt a new relationship that is different from that in the control condition of *ad libitum* feeding. This new interaction has the characteristics of an emergent property, since it is not observed in the *ad libitum* condition or in the control groups of acute fasting and acute fasting followed by refeeding. For example, the increased amount GABA-T protein promoted by the protocol of DRF/FEO expression and detected by Western blot analysis (Figure 1) is unique and is observed neither in the AL group nor in the acute control. The same stands for the augmented GABA-T activity in liver homogenate and the loss of rhythmicity in GABA-T mRNA. Again, all these changes can be considered as part of the plastic adaptations that are present in the liver during the expression of the FEO.

One way to consider the emergence of new properties in biological systems is the concept of rheostasis [38], which is a term used in the theory of physiological control to describe regulation around shifting set points. In contrast to homeostasis, rheostasis triggers associations in situations with potentially adjustable settings [32]. In this context, expression of the FEO could involve a novel rheostatic adaptation in conditions in which two contradictory environmental temporal clues, light-dark cycle and DRF, are coexisting [39].

5. Conclusions

Biochemical properties of liver GABA-T were modified by the DRF protocol. An explanation for these findings should consider the coincidence of the FEO expression with a functional light-driven SCN. In addition, GABA-T regulation could be responding to the intense arrival of nutrients during the 2 h of food access, in the context of restricted feeding schedules. The data raise the possibility that alterations in the hepatic GABAergic system could be among the metabolic and physiological adaptions that occur in the liver during expression of the FEO. This possibility needs further exploration.

Conflict of Interests

The authors declare that there is no conflict of interests regarding the publication of this paper.

Authors' Contribution

Dalia De Ita-Pérez, Isabel Méndez, and Olivia Vázquez-Martínez contributed equally to this project.

Acknowledgments

The authors wish to thank Dr. Dorothy Pless for reviewing the English of this paper and L.N. Fernando López Barrera for his help in preparing the figures. This study was supported by CONACyT (project 129–511) and DGAPA (projects IN202412, MDM, and IA200713, IM) from PAPIIT, UNAM, México.

References

[1] P. K. Mehta, T. I. Hale, and P. Christen, "Aminotransferases: demonstration of homology and division into evolutionary subgroups," *European Journal of Biochemistry*, vol. 214, no. 2, pp. 549–561, 1993.

[2] N. Bouché, B. Lacombe, and H. Fromm, "GABA signaling: a conserved and ubiquitous mechanism," *Trends in Cell Biology*, vol. 13, no. 12, pp. 607–610, 2003.

[3] D. J. Garry, H. D. Coulter, and T. J. McIntee, "Immunoreactive GABA transaminase within the pancreatic islet is localized in mitochondria of the B-cell," *Journal of Histochemistry and Cytochemistry*, vol. 35, no. 8, pp. 831–836, 1987.

[4] P. Storici, G. Capitani, D. de Biase et al., "Crystal structure of GABA-aminotransferase, a target for antiepileptic drug therapy," *Biochemistry*, vol. 38, no. 27, pp. 8628–8634, 1999.

[5] P. Storici, D. De Biase, F. Bossa et al., "Structures of γ-aminobutyric acid (GABA) aminotransferase, a pyridoxal 5′-phosphate, and [2Fe-2S] cluster-containing enzyme, complexed with γ-ethynyl-GABA and with the antiepilepsy drug vigabatrin," *Journal of Biological Chemistry*, vol. 279, no. 1, pp. 363–373, 2004.

[6] Y. Kontani, S. F. Sakata, K. Matsuda, T. Ohyama, K. Sano, and N. Tamaki, "The mature size of rat 4-aminobutyrate aminotransferase is different in liver and brain," *European Journal of Biochemistry*, vol. 264, no. 1, pp. 218–222, 1999.

[7] I. K. Franklin and C. B. Wollheim, "GABA in the endocrine pancreas: its putative role as an islet cell paracrine-signalling molecule," *Journal of General Physiology*, vol. 123, no. 3, pp. 185–190, 2004.

[8] A. Gladkevich, J. Korf, V. P. Hakobyan, and K. V. Melkonyan, "The peripheral GABAergic system as a target in endocrine disorders," *Autonomic Neuroscience: Basic and Clinical*, vol. 124, no. 1-2, pp. 1–8, 2006.

[9] R. Erlitzki, Y. Gong, M. Zhang, and G. Minuk, "Identification of γ-aminobutyric acid receptor subunit types in human and rat liver," *The American Journal of Physiology: Gastrointestinal and Liver Physiology*, vol. 279, no. 4, pp. G733–G739, 2000.

[10] G. Y. Minuk, "Gamma-aminobutyric acid and the liver," *Digestive Diseases*, vol. 11, no. 1, pp. 45–54, 1993.

[11] Y. H. Li, Y. D. Liu, Y. D. Li et al., "GABA stimulates human hepatocellular carcinoma growth through overexpressed GABAA receptor theta subunit," *World Journal of Gastroenterology*, vol. 18, no. 21, pp. 2704–2711, 2012.

[12] J. Y. Wu, L. G. Moss, and O. Chude, "Distribution and tissue specificity of 4-aminobutyrate-2-oxoglutarate aminotransferase," *Neurochemical Research*, vol. 3, no. 2, pp. 207–219, 1978.

[13] R. Dhakal, V. K. Bajpai, and K. H. Baek, "Production of gaba (gamma-Aminobutyric acid) by microorganisms: a review," *Brazilian Journal of Microbiology*, vol. 43, no. 4, pp. 1230–1241, 2012.

[14] F. K. Stephan, "The "other" circadian system: food as a zeitgeber," *Journal of Biological Rhythms*, vol. 17, no. 4, pp. 284–292, 2002.

[15] B. T. S. Carneiro and J. F. Araujo, "The food-entrainable oscillator: a network of interconnected brain structures entrained by humoral signals?" *Chronobiology International*, vol. 26, no. 7, pp. 1273–1289, 2009.

[16] R. E. Mistlberger, "Neurobiology of food anticipatory circadian rhythms," *Physiology and Behavior*, vol. 104, no. 4, pp. 535–545, 2011.

[17] A. Báez-Ruiz, C. Escobar, R. Aguilar-Roblero, O. Vázquez-Martínez, and M. Díaz-Muñoz, "Metabolic adaptations of liver mitochondria during restricted feeding schedules," *The American Journal of Physiology: Gastrointestinal and Liver Physiology*, vol. 289, no. 6, pp. G1015–G1023, 2005.

[18] C. Molina-Aguilar, J. Pérez-Sánchez, O. Vázquez-Martínez, J. Rivera-Zavala, and M. Díaz-Muñoz, "Restricted food access during the daytime modifies the 24-h rhythmicity of apoptosis and cellular duplication in rat liver," *Biological Rhythm Research*, vol. 43, no. 1, pp. 25–37, 2012.

[19] F. Portaluppi, Y. Touitou, and M. H. Smolensky, "Ethical and methodological standards for laboratory and medical biological rhythm research," *Chronobiology International*, vol. 25, no. 6, pp. 999–1016, 2008.

[20] M. Ángeles-Castellanos, J. Mendoza, M. Díaz-Muñoz, and C. Escobar, "Food entrainment modifies the c-Fos expression pattern in brain stem nuclei of rats," *The American Journal of Physiology: Regulatory Integrative and Comparative Physiology*, vol. 288, no. 3, pp. R678–R684, 2005.

[21] I. Aguilar-Delfín, F. López-Barrera, and R. Hernández-Muñoz, "Selective enhancement of lipid peroxidation in plasma membrane in two experimental models of liver regeneration: partial hepatectomy and acute CC14administration," *Hepatology*, vol. 24, no. 3, pp. 657–662, 1996.

[22] M. M. Bradford, "A rapid and sensitive method for the quantitation of microgram quantities of protein utilizing the principle of protein dye binding," *Analytical Biochemistry*, vol. 72, no. 1-2, pp. 248–254, 1976.

[23] M. J. Jung, B. Lippert, and B. W. Metcalf, "The effect of 4 amino hex 5 ynoic acid (γ acetylenic GABA, γ ethynyl GABA) a catalytic inhibitor of GABA transaminase, on brain GABA metabolism in vivo," *Journal of Neurochemistry*, vol. 28, no. 4, pp. 717–723, 1977.

[24] P. Zuther, S. Gorbey, and B. Lemmer, "Chronos-Fit v 1. 06," 2009, http://www.ma.uni-heidelberg.de/inst/phar/lehre/chrono.html.

[25] B. E. Faulkner-Jones, D. S. Cram, J. Kun, and L. C. Harrison, "Localization and quantitation of expression of two glutamate decarboxylase genes in pancreatic β-cells and other peripheral tissues of mouse and rat," *Endocrinology*, vol. 133, no. 6, pp. 2962–2972, 1993.

[26] C. Lodewyks, J. Rodriguez, J. Yan et al., "GABA-B receptor activation inhibits the in vitro migration of malignant hepatocytes," *Canadian Journal of Physiology and Pharmacology*, vol. 89, no. 6, pp. 393–400, 2011.

[27] Y. Zhou, S. Holmseth, C. Guo et al., "Deletion of the gamma-aminobutyric acid transporter 2 (GAT2 and SLC6A13) gene

in mice leads to changes in liver and brain taurine contents," *Journal of Biological Chemistry*, vol. 287, no. 42, pp. 35733–35746, 2012.

[28] D. M. Treiman, "GABAergic mechanisms in epilepsy," *Epilepsia*, vol. 42, 3, pp. 8–12, 2001.

[29] C. Dibner, U. Schibler, and U. Albrecht, "The mammalian circadian timing system: organization and coordination of central and peripheral clocks," *Annual Review of Physiology*, vol. 72, pp. 517–549, 2009.

[30] I. Schmutz, U. Albrecht, and J. A. Ripperger, "The role of clock genes and rhythmicity in the liver," *Molecular and Cellular Endocrinology*, vol. 349, no. 1, pp. 38–44, 2012.

[31] C. A. Feillet, U. Albrecht, and E. Challet, "Feeding time for the brain: a matter of clocks," *Journal of Physiology Paris*, vol. 100, no. 5-6, pp. 252–260, 2006.

[32] R. Aguilar-roblero and M. Díaz-muñoz, "Chronostatic adaptations in the liver to restricted feeding: the FEO as an emergent oscillator," *Sleep and Biological Rhythms*, vol. 8, no. 1, pp. 9–17, 2010.

[33] P. Magni, E. Dozio, M. Ruscica et al., "Feeding behavior in mammals including humans," *Annals of the New York Academy of Sciences*, vol. 1163, pp. 221–232, 2009.

[34] J. Mendoza, "Circadian clocks: setting time by food," *Journal of Neuroendocrinology*, vol. 19, no. 2, pp. 127–137, 2007.

[35] M. Díaz-Muñoz, O. Vázquez-Martínez, R. Aguilar-Roblero, and C. Escobar, "Anticipatory changes in liver metabolism and entrainment of insulin, glucagon, and corticosterone in food-restricted rats," *The American Journal of Physiology: Regulatory Integrative and Comparative Physiology*, vol. 279, no. 6, pp. R2048–R2056, 2000.

[36] R. Buijs, R. Salgado, E. Sabath, and C. Escobar, "Peripheral circadian oscillators: time and food," *Progress in MolecularBiology and Translational Sciences*, vol. 119, pp. 83–103, 2013.

[37] U. Albrecht, "Timing to perfection: the biology of central and peripheral circadian clocks," *Neuron*, vol. 74, no. 2, pp. 246–260, 2012.

[38] N. Mrosovsky, *Rheostasis: the Physiology of Change*, Oxord University Press, 1990.

[39] B. Kornmann, O. Schaad, H. Bujard, J. S. Takahashi, and U. Schibler, "System-driven and oscillator-dependent circadian transcription in mice with a conditionally active liver clock," *PLoS Biology*, vol. 5, no. 2, article e34, 2007.

Hindawi Publishing Corporation
BioMed Research International
Volume 2014, Article ID 930308, 11 pages
http://dx.doi.org/10.1155/2014/930308

Research Article

Developmental Stage-Specific Regulation of the Circadian Clock by Temperature in Zebrafish

Kajori Lahiri,[1,2] Nadine Froehlich,[1] Andreas Heyd,[3] Nicholas S. Foulkes,[1] and Daniela Vallone[1]

[1] *Institute of Toxicology and Genetics, Karlsruhe Institute of Technology, Hermann-von-Helmholtz-Platz 1, 76344 Eggenstein-Leopoldshafen, Germany*
[2] *Institute of Functional Interfaces, Karlsruhe Institute of Technology, Hermann-von-Helmholtz-Platz 1, 76344 Eggenstein-Leopoldshafen, Germany*
[3] *Tuebingen Hearing Research Centre, Section Physiological Acoustics and Communication, Department of Otolaryngology, Head and Neck Surgery, University of Tuebingen, 72076 Tuebingen, Germany*

Correspondence should be addressed to Nicholas S. Foulkes; nicholas.foulkes@kit.edu
and Daniela Vallone; daniela.vallone@kit.edu

Received 19 December 2013; Accepted 10 February 2014; Published 27 March 2014

Academic Editor: Yoav Gothilf

The circadian clock enables animals to adapt their physiology and behaviour in anticipation of the day-night cycle. Light and temperature represent two key environmental timing cues (zeitgebers) able to reset this mechanism and so maintain its synchronization with the environmental cycle. One key challenge is to unravel how the regulation of the clock by zeitgebers matures during early development. The zebrafish is an ideal model for studying circadian clock ontogeny since the process of development occurs *ex utero* in an optically transparent chorion and many tools are available for genetic analysis. However, the role played by temperature in regulating the clock during zebrafish development is poorly understood. Here, we have established a clock-regulated luciferase reporter transgenic zebrafish line (Tg (−3.1) *per1b*::luc) to study the effects of temperature on clock entrainment. We reveal that under complete darkness, from an early developmental stage onwards (48 to 72 hpf), exposure to temperature cycles is a prerequisite for the establishment of self-sustaining rhythms of *zfper1b*, *zfaanat2*, and *zfirbp* expression and also for circadian cell cycle rhythms. Furthermore, we show that following the 5–9 somite stage, the expression of *zfper1b* is regulated by acute temperature shifts.

1. Introduction

Most animals and plants adjust their physiology and behaviour according to the time of the day. These changes represent adaptations to regular environmental changes that result directly or indirectly from the rotation of our earth on its axis. These biological rhythms persist even under constant conditions and are controlled by a highly conserved endogenous clock or pacemaker [1]. The period length of the clock-generated rhythms is not precisely 24 h and so they are termed circadian (circa = around, diem = one day). Daily resetting of the clock by environmental signals such as changes in light, temperature, and nutrient availability (so called "zeitgebers": time givers) is therefore essential to ensure synchronization with the environment [2]. At its simplest level, the clock can be considered to be composed of three parts: a central, cell autonomous pacemaker that generates the circadian rhythm; an input pathway whereby zeitgebers are perceived and adjust the phase of the pacemaker; and finally an output pathway through which the pacemaker regulates a diversity of physiological processes. The basic organization of the central clock mechanism itself appears to be highly conserved through evolution. Many clock components represent transcriptional regulators that are organized in transcription-translation feedback loops. Characteristic delays in certain steps of this mechanism confer the relatively long (24 hours) duration of one cycle [3].

Historically, most attention has been focused on how light regulates the circadian clock and the description of the light input pathway. However, temperature also has a profound effect on circadian clock function. Daily temperature cycles as well as acute shifts of temperature have been well documented to set the phase of the clock rhythm [4]. Furthermore, one of the most fundamental properties of the clock is that the period length of its rhythm remains relatively constant over a range of temperatures, so-called "temperature compensation" [4, 5]. Outside the range of temperature compensation, the clock characteristically arrests at a certain phase [6, 7]. The physiological temperature range for rhythmicity lies well within the temperature range permissive for growth. The molecular basis of these effects of temperature has come primarily from studies of ectothermic organisms including *Neurospora*, lizards, and *Drosophila* [8–11]. Fish have proved to be ideally suited to study the specific effects of temperature cycles on the circadian clock [12, 13]. Although in endothermic organisms temperature changes have little influence on the central pacemaker, fluctuations in body temperature appear to synchronize and thereby sustain circadian rhythms in peripheral tissues [14–16].

The zebrafish naturally inhabits shallow water habitats where it is likely to experience daily changes in water temperature. Using this species as a model, we have previously explored the molecular basis of temperature compensation as well as entrainment of the circadian clock by small temperature shifts [17]. We revealed that the amplitude of clock gene cycling expression in zebrafish is tightly dependent on the ambient temperature. Furthermore, small temperature shifts result in acute changes in the mRNA expression of a subset of clock genes. Thus, in the case of zebrafish peripheral tissues, changes in clock gene transcription appear to contribute to the response of the clock to temperature changes.

When during development does the circadian clock start to function? When is rhythmic circadian clock gene expression first detected? The zebrafish is an ideal model system to understand circadian clock ontogeny since the process of development occurs *ex utero* in an optically transparent chorion and many tools for functional analysis are available. In a study using a zebrafish *per3*-luciferase transgenic line, bioluminescence rhythms were first detected in larvae at 4-5 days postfertilization (dpf) [18]. Other studies documenting the appearance of key clock outputs such as circadian rhythms of S-phase and pineal production of melatonin have revealed the emergence of rhythms from 24 to 36 hours postfertilization (hpf) [19–22]. In all cases, the presence of an LD cycle or a single transition between dark and light from 24 hpf is a prerequisite for the emergence of clock rhythmicity. A detailed study of rhythmic clock gene expression in developing embryos revealed that clock gene expression rhythms are detected very early during development at the single cell level; however, these cell clocks are asynchronous. The effect of exposure to LD cycles is to synchronize the single cell clocks [23].

The role played by temperature in clock entrainment during early zebrafish development is relatively poorly understood. We have established a clock-regulated luciferase reporter transgenic line (Tg (−3.1) *per1b*::luc) and then used this as a model to explore the origins of temperature entrainment in detail.

2. Materials and Methods

2.1. Fish Care, Treatment, and Ethical Statements. The zebrafish Tuebingen strain was raised and bred according to standard procedures [24] in a recirculating water system under 14 hours light and 10 hours dark cycles at 28°C and fed twice per day.

All zebrafish husbandry and experimental procedures were performed in accordance with the German animal protection standards (Animal Protection Law, BGBl. I, 1934 (2010)) and were approved by Local Animal-Protection Committee, Regierungspräsidium Karlsruhe, Germany (License number BrdU treatments Az.:35-9185.81/G-130/12 and general license for fish maintenance and breeding Az.:35-9185.64).

2.2. Establishment of the Tg (−3.1) per1b::luc Transgenic Line. Microinjections for the establishment of the transgenic line were made at the one cell stage as described [24]. Embryos were injected with the pCMV-I-Sce I expression vector encoding a modified I-Sce I meganuclease (276 amino acids) [25] together with the pBluescript *Per1b-luc*-I-SceI plasmid (containing a 3.1kb fragment of the *zfper1b (per4)* promoter [26] cloned upstream of a luciferase reporter). The latter plasmid contains two I-SceI recognition sites for the meganuclease. Embryos were screened for bioluminescence by raising them from 1 to 6 dpf under LD (12 h : 12 h) cycles and then transferring them to 96-multiwell plates in the presence of 0.5 mM beetle luciferin potassium salt solution (Promega) as described elsewhere [27]. Counts were measured on a Perkin Elmer luminescence counter (VICTOR Light 1420) during the first half of the day when *zfper1b* expression was predicted to be at its highest [26]. Positive germline transmitting founders were outcrossed and heterozygous animals were raised.

2.3. Temperature and Lighting Conditions. All the experiments were performed under controlled lighting and temperature conditions. The precise conditions for each experiment are indicated either in the corresponding results or figure legends sections. For temperature cycle experiments, larvae maintained in 96-well plates or in 25 cm^2 flasks were submerged in a 60-liter water bath with circulating heating and cooling units (Lauda, Lauda-Königshofen, Germany) maintained in complete darkness. Temperature cycles were generated by controlling the heating and cooling units using Wintherm plus software (Lauda). During the cold/warm phase transition periods, temperature changes of 1°C were set to occur over 15 minutes. For light/dark cycle experiments, larvae in 96-well plates or in flasks were submerged in a 60-liter thermostat-controlled water bath illuminated with a tungsten light source (20 $\mu W/cm^2$).

2.4. Real-Time Bioluminescence Assay. For all experiments, single embryos were aliquoted into individual wells of a 96-multiwell plate (Nunc) in E3 media (without Methylene Blue) supplemented with 0.5 mM beetle luciferin, potassium salt solution (Promega) and the plate was then sealed using an adhesive "Top Seal" sealing sheet (Packard). Plates were then subjected to different temperature or lighting conditions and bioluminescence from whole embryos and larvae was assayed using a Packard Top-count NXT scintillation counter (2-detector model, Packard) or an EnVision multilabel counter (Perkin Elmer). Bioluminescence data was analyzed using the Import and Analysis Macro (I&A, Plautz and Kay, Scripps) for Microsoft Excel or CHRONO software [28].

2.5. RNA Extraction, RNAse Protection Assays (RPA), and Quantitative Real-Time PCR (qRT-PCR). Total RNA samples were extracted from whole larvae using Trizol RNA isolation reagent (GIBCO-BRL) according to the manufacturer's instructions. RNAse protection assays (RPA) were performed as previously described [26]. The riboprobes for *zfper1b (per4), zfirbp*, and the loading control, *zfβ-actin*, have been described previously [26, 29]. Autoradiographic images were quantified with the aid of Scion Image (NIH) software. The relative expression levels (percentage) are plotted on the y-axis. *β-actin* levels were used to standardize the results. The highest band intensity in each experiment was arbitrarily defined as 100% and then all other values were expressed as a percentage of this value. All experiments were performed in triplicate and error bars denote the standard deviation.

Quantitative Real-Time RT-PCR (qRTPCR) analysis was performed using a StepOnePlus Real-Time RT-PCR System (Applied Biosystems) and SYBR Green I fluorescent dye (Qiagen). Relative expression levels were normalized using *β-actin*. The relative levels of each mRNA were calculated using the $2^{-\Delta\Delta CT}$ method. For *zfper1b* the primer sequences used were F: CCGTCAGTTTCGCTTTTCTC and R: ATGTGCAGGCTGTAGATCCC, while for *zfβ-actin* the primer sequences were F: GCCTGACGGACAGGTCAT and R: ACCGCAAGATTCCATACCC.

2.6. BrdU Incorporation Assay. Larvae were incubated for 15 minutes in 10 mM BrdU fish water solution at different time points during a temperature or light/dark cycle and fixed in 4% PAF in PBS.

The anti-BrdU (1 : 200 Acris BM6048) and the alkaline phosphatase anti-mouse (1 : 500 Vector AP 2000) antibodies were used as first and secondary antibodies, respectively. Staining and data analysis for BrdU incorporation in the skin were carried out as described previously [30].

2.7. Whole-Mount In Situ Hybridization. Larvae previously exposed to temperature or light cycles were fixed in 4% paraformaldehyde in PBS at different time points during 24 hours. *In situ* hybridization was carried out as previously described [31] using the *zfaanat2* probe [20] that was labeled with digoxigenin RNA-labeling mix (Roche).

2.8. Statistical Analysis. Data were analyzed by one-way or two-way analysis of variance (ANOVA) followed by Bonferroni's multiple comparison tests using the GraphPad Prism 4.0 for Windows (Graph Pad Software, http://www.graphpad.com/). Two-way ANOVA were performed using SPSS v 16.0 for Windows (IBM, USA). Cosinor analyses were performed using COSINOR v3.0.2 software (Professor Antoni Diez-Noguera, University of Barcelona). All the results were expressed as mean +/− SEM. $P < 0.05$ was considered statistically significant.

3. Results

3.1. Establishment and Characterization of the Zebrafish Tg (−3.1) per1b::luc Transgenic Line. Zebrafish embryos were injected with the *pBPer1b-luc-I-SceI* construct containing a 3.1kb fragment of the *zfper1b* promoter cloned upstream of a firefly luciferase reporter gene flanked by two I-SceI recognition sites (Figure S1(A)) (see Supplementary Material available online at http://dx.doi.org/10.1155/2014/930308). This construct was coinjected with a plasmid expressing the I-SceI meganuclease enzyme (Figure S1(B)). Out of 280 luciferase positive embryos screened for germline transmission, 3 bioluminescence-positive offspring were obtained. From these we established one line: Tg (−3.1) *per1b*::luc. We firstly analyzed the profile of bioluminescence expression of entire transgenic embryos exposed to light/dark cycles (LD: 12 hours light/12 hours dark) during the first week of development (Figure 1). A significant daily rhythm of bioluminescence was already visible from 2 dpf (days-post-fertilization) (Figure 1(a)). A one-way ANOVA ($P < 0.0001$) followed by a Cosinor analysis of the mean profile of the Tg (−3.1) *per1b*::luc embryos showed the presence of significant periodic oscillations ($P < 0.00001$), although during the first two days of development some variability between individual embryos was observed in the rhythm amplitude and in the precise timing of peaks of expression (22.8% < robustness > 54.9%; 23.8 < period > 25.1 and ZT 2.34 < peak < ZT 3.49). As predicted for expression of the core clock element *zfper1b*, the light entrained bioluminescence rhythm of the Tg (−3.1) *per1b*::luc larvae persisted after transfer to constant darkness (DD) (Figure 1(b)) showing that changes in luciferase reporter expression were not simply driven by light (one-way ANOVA $P < 0.0001$ to test for the time effect followed by Cosinor analysis $P < 0.000001$ to test for periodic oscillation). Furthermore, consistent with previous reports, raising the transgenic larvae in the complete absence of light (DD) resulted in no significant bioluminescence oscillation (Figure 1(c) and $P > 0.05$ for Cosinor analysis), although a significant time effect was observed at 2 and 5 dpf (one-way ANOVA $P < 0.001$ for the time effect). Changes in the basal level of expression of bioluminescence observed at 2 dpf and between 4 and 5 dpf most likely reflect changes in basal expression of *zfper1b* associated with embryonic development.

To validate our transgenic line, we verified that the bioluminescence rhythm of the Tg (−3.1) *per1b*::luc line measured under LD cycles matched the endogenous mRNA expression

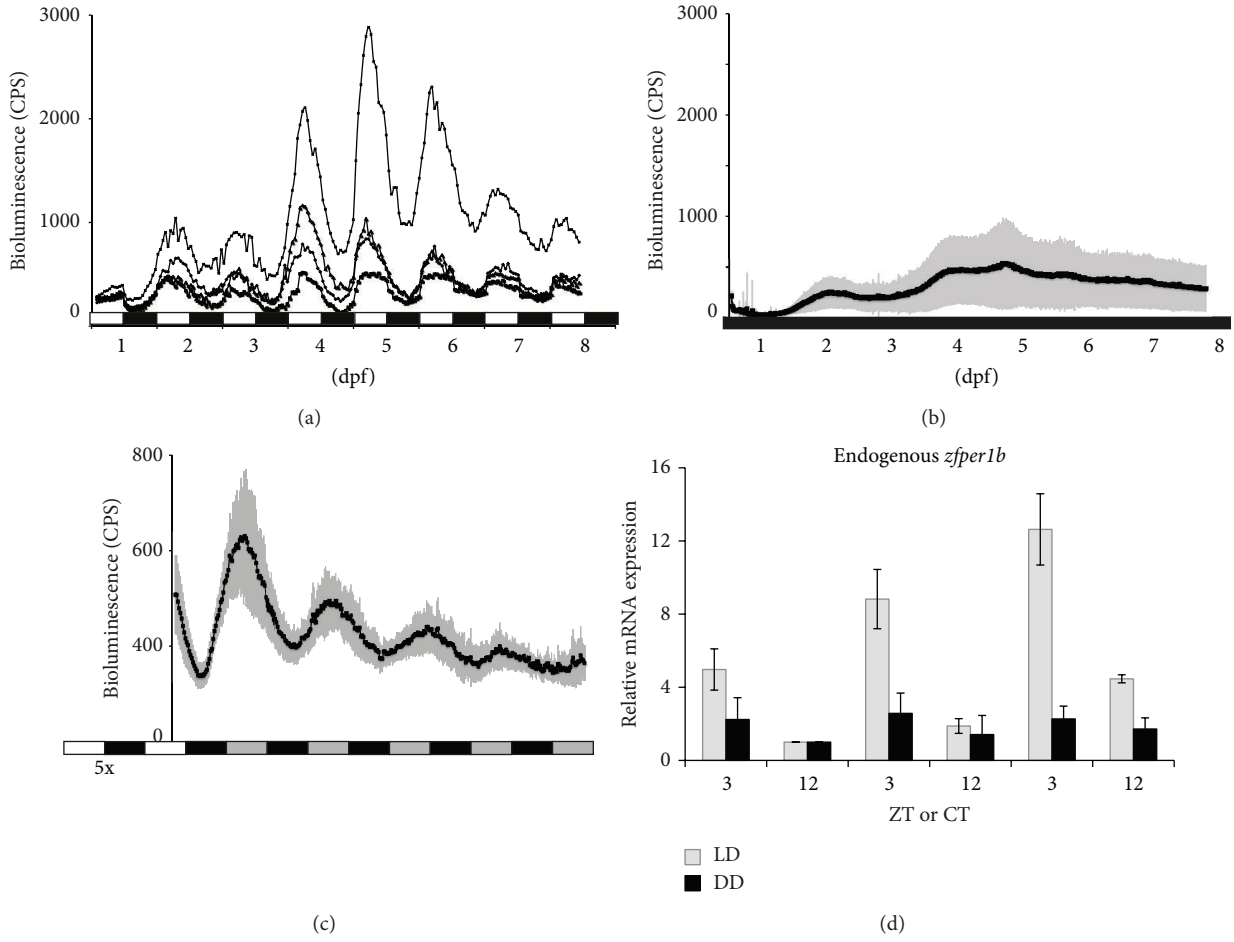

Figure 1: Characterization of the zebrafish Tg (−3.1) *per1b*::luc transgenic line. (a) Bioluminescence in single Tg (−3.1) *per1b*::luc transgenic embryos during development from 3 hrs postfertilization and under light/dark cycles (12 : 12 at 25°C). Traces of 4 representative animals are shown. Below, white and black horizontal bars indicate the duration of the 12 hours light (white) and 12 hours dark (black) periods of the LD cycles. (b) Mean values of bioluminescence expression profiles from transgenic larvae entrained for 5 days in LD cycles at 25°C and then monitored in constant darkness (DD) and constant temperature (25°C). Below, white, grey, and black horizontal bars represent the 12 hours light, subjective day and dark (or subjective night) periods, respectively. Before transfer to constant darkness, the embryos were previously exposed to 5 LD cycles (5×). (c) Mean of bioluminescence expression profiles from transgenic larvae raised for 8 days in DD conditions (black horizontal bar). (d) Peak (ZT3) and trough (ZT12) values of endogenous rhythmic *zfper1b* expression in embryos raised under DD (black vertical bars) or LD (grey vertical bars) cycles from 2 to 4 dpf. The expression levels are represented as fold induction values with respect to the lowest value for each set of samples (ZT12 of the second day for both sets). Each time point represents a pool with a minimum of $n = 20$ larvae.

pattern of the *zfper1b* gene assayed in whole larval RNA extracts (Figure 1(d)). We observed a significant daily oscillation of endogenous *zfper1b* expression from 2 dpf with peak points around ZT3 and trough points around ZT12 (one-way ANOVA $P < 0.001$ for the time effect, $P < 0.0001$ followed by Cosinor analysis, and $P < 0.000001$ for periodic oscillation). Thus, we have established an *in vivo* model that accurately reports endogenous clock gene expression and thereby can facilitate the study of clock function during early development.

3.2. Clock Entrainment by Temperature Cycles in Developing Zebrafish Embryos. Many previous reports have documented that temperature changes can serve as an efficient zeitgeber for the fish circadian clock [12, 13, 17]. Can temperature cycles entrain the clock in developing zebrafish embryos? To address this question, we raised Tg (−3.1) *per1b*::luc embryos under 4°C temperature cycles (23°C–27°C) in constant darkness from 1 dpf for 5 days and then we monitored bioluminescence at a constant 25°C (Figure 2(a)). We observed robust circadian rhythms of bioluminescence which dampened progressively during the assay period (5–9 dpf) ($P < 0.000001$ for periodic oscillation with free running period tau = 25.1; one-way ANOVA $P < 0.001$ for the time effect).

3.3. Clock-Regulated Outputs Entrained by Temperature Cycles during Zebrafish Development. The circadian clock directs a wide variety of output pathways. We have previously

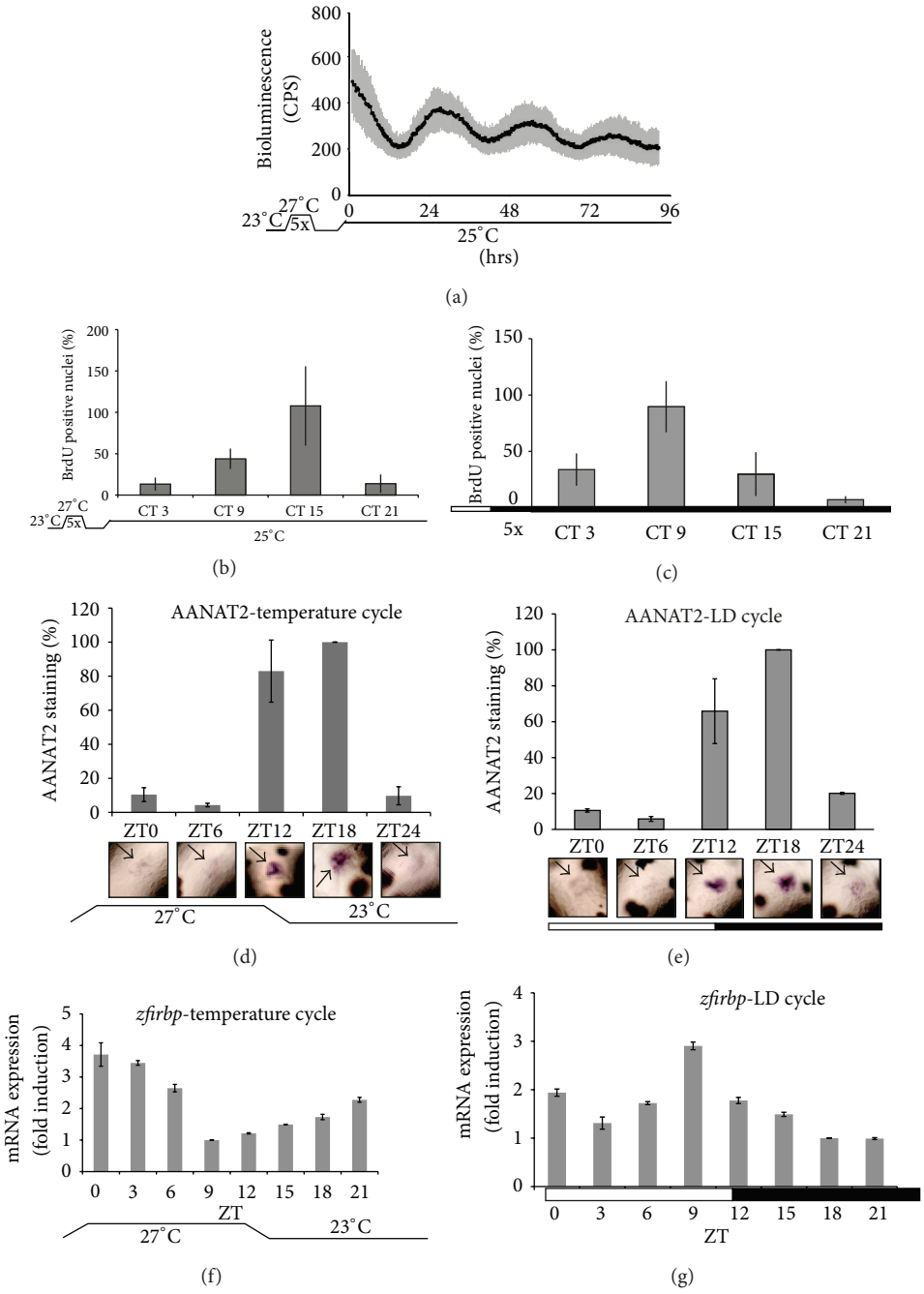

Figure 2: Clock entrainment by temperature cycles in developing zebrafish embryos. (a) Mean values of bioluminescence expression profiles from transgenic larvae entrained for 5 days under 4°C temperature cycles (23–27°C) in constant darkness and then monitored at a constant temperature of 25°C. ((b)-(c)) Whole-mount staining for BrdU incorporation in skin cells of larvae previously entrained by 5× temperature (b) and 5× LD (c) cycles and then sampled during the first day after transfer to constant conditions (darkness and 25°C). The number of BrdU positive nuclei (S-phase nuclei), normalized as percentage (%) of the highest experimental value, is plotted on the *y*-axis. ((d)-(e)) Rhythmic expression of the circadian clock-regulated *zfaanat2* gene in 5 dpf zebrafish larvae under 4°C temperature (d) or light/dark (e) cycles. In each panel, representative *zfaanat2 in situ* hybridization images and quantification graphs from independent experiments (each time point included a minimum of 20 larvae) are shown. On the *y*-axis, expression levels are expressed as % of the highest level measured in each set. Black arrows indicate the position of the *zfaanat2* mRNA signal in the pineal gland. ((f)-(g)) Quantification of the RNAse protection analysis of *zfirbp* expression in whole larva mRNA extracts in larvae entrained under 5× temperature (f) or 5× LD (g) cycles. In each panel, the *x*-axes indicate the times of measurement (hrs), the circadian (CT), or the zeitgeber (ZT) times. On the *y*-axis, expression levels are expressed as fold induction compared to the lowest level measured in the set. In each panel, points are plotted as the means of three independent experiments ± SEM. The black horizontal lines beneath panels (a) and (b) indicate constant temperature while the temperature cycles in panels (a), (b), (d), and (f) are indicated. Black and white bars beneath panels (c), (e), and (g) indicate the dark and light periods of the lighting regimes, respectively.

implicated both the circadian clock and light in the control of cell cycle timing in zebrafish [30, 32]. We wished to test whether temperature cycles, in the absence of light, would also entrain cell cycle rhythms in zebrafish embryos. Temperature itself affects the rate of cell division and other biochemical processes. In order to avoid the complicating effect of temperature driven changes in cell cycle progression we tested the timing of cell cycle in free running conditions at a constant temperature following a period of temperature cycle entrainment. Therefore, we entrained zebrafish larvae by exposure to a 4°C and 24 hours temperature cycle (27°C–23°C) from 1 to 5 dpf and then shifted them to a constant temperature of 25°C for assay. In parallel, as a control, larvae were raised until 5 dpf under LD cycles and then shifted to DD conditions. Both sets of 6 dpf larvae were BrdU labelled for 15 minutes at different circadian time points (CT 3, 9, 15, and 21) and then stained for the presence of BrdU positive (S-phase) nuclei. Positive skin cell nuclei were counted between the posterior tip of the swim bladder and the anus as previously described [30]. Both sets of larvae showed a circadian rhythm in the number of S phase-positive nuclei (Figures 2(b) and 2(c)) with a peak around CT 15 or CT 9 for larvae under temperature or light cycles, respectively (Figures 2(b) and 2(c)) (one-way ANOVA $P < 0.0001$ for the time effect followed by $P < 0.0001$ for periodic oscillation for both temperature and light zeitgebers). Thus, entrainment of the clock by temperature cycles as well as LD cycles results in circadian cell cycle rhythms in developing larvae.

We next examined whether entrainment by temperature cycles could also establish a clock-regulated rhythm of melatonin synthesis. We examined the expression of *zfaanat2* mRNA in the pineal gland, which encodes the rate-limiting enzyme in melatonin biosynthesis [33, 34]. Embryos were raised from 1 to 5 dpf in 4°C temperature cycles in the absence of light and control siblings were raised under LD cycles at a constant temperature. The expression of *zfaanat2* mRNA was detected in the pineal gland of both sets of larvae. In the temperature cycle larvae (Figure 2(d)), *zfaanat2* expression cycles in a circadian fashion with high expression levels during the transition from warm to cold (ZT12 and ZT18) and low levels during the transition from cold to warm temperatures (ZT0/24 and ZT6) (one-way ANOVA $P < 0.001$ for the time effect followed by $P < 0.0001$ for periodic oscillation). In the LD set, high expression levels are observed during the day-night transition (ZT 12 and ZT 18) and low to undetectable levels during the night-day transition (ZT 0/24 and ZT 6), consistent with previous reports [20] (Figure 2(e)) (one-way ANOVA $P < 0.001$ for the time effect followed by $P < 0.0001$ for periodic oscillation). Thus, in the absence of light, rhythmic *zfaanat2* expression can be established by exposure to a temperature cycle.

Finally, we examined the expression of interphotoreceptor retinoid-binding protein (*zfirbp*) mRNA in whole body RNA extracts prepared from our larvae raised under 4°C temperature cycles compared with LD cycles (Figures 2(f) and 2(g)). Consistent with previous reports documenting *zfirbp* expression in the retina and pineal gland [23], in LD larvae (Figure 2(g)) we revealed a rhythmic expression profile with a peak of expression during the light phase (peak ZT 9) (one-way ANOVA $P < 0.0001$ for the time effect followed by $P < 0.0001$ for periodic oscillation). In larvae entrained by temperature cycles, we also observed rhythmic expression of *zfirbp*. The highest expression was detected at the transition between the cold and warm phases (Figure 2(f)) (one-way ANOVA $P < 0.0001$ for the time effect followed by $P < 0.0001$ for periodic oscillation). Thus, in photoreceptive structures, temperature cycles can substitute for LD cycles to entrain rhythmic expression of clock output genes.

3.4. Clock Entrainment by Temperature Cycles Is Dependent on the Developmental Stage. When during development are temperature cycles able to entrain the circadian clock? To tackle this question, we used our clock reporter transgenic line. Tg (−3.1) *per1b*::luc embryos from 1 hour postfertilization (1hpf) were subjected to 1, 2, or 3 temperature cycles (23°C–27°C) in the absence of light. Then the larvae were tested in a bioluminescence assay at a constant temperature. Pools of transgenic larvae raised either under 1 or 2 temperature cycles showed a mean bioluminescence profile closely resembling that observed for larvae raised under constant temperature and darkness conditions (Figures 3(a) and 3(b) and compare with Figure 1(c)) with peaks of expression observed on the 2nd and on the 4th-5th day but with a complete lack of *circa* 24 hours periodicity. Interestingly, a small subset (*circa* 10%) of individual larvae under these conditions did exhibit cycling reporter expression although with different phases and amplitudes. In contrast, in the majority of embryos exposed to 3 temperature cycles, a robust circadian rhythm of bioluminescence was established (Figure 3(c)). We next questioned whether it is the number of temperature cycles experienced that synchronizes the clock *in vivo* or whether only at a particular developmental stage are the larvae responsive to temperature signals. Thus, to address this question we raised embryos under constant temperature and constant darkness and then exposed them to a single temperature cycle at 3 dpf before immediately assaying bioluminescence under constant conditions (Figure 3(d)). Interestingly, one temperature cycle delivered at 3 dpf results in circadian cycling comparable to that induced by exposure to 3 consecutive temperature cycles. This result indicates that the developmental stage is an important factor in defining the sensitivity of the circadian clock to entrainment by temperature cycles.

3.5. An Acute Temperature Shift Regulates Clock Gene Expression during Early Development from the 5–9 Somites Stage. Previous studies have implicated differential maturation of elements of the circadian clock during early embryonic development. Is there evidence of temperature-dependent clock gene expression prior to the entrainment of the clock by temperature? We have previously reported a rapid response of *zfper1b* transcription to acute temperature shifts in the Pac-2 cell line. A rapid temperature decrease results in sustained induction, while a temperature increase leads to a significant downregulation of *zfper1b* expression [17]. We wished to test at which stage of development this temperature-induced change in *zfper1b* expression is first detected. We raised

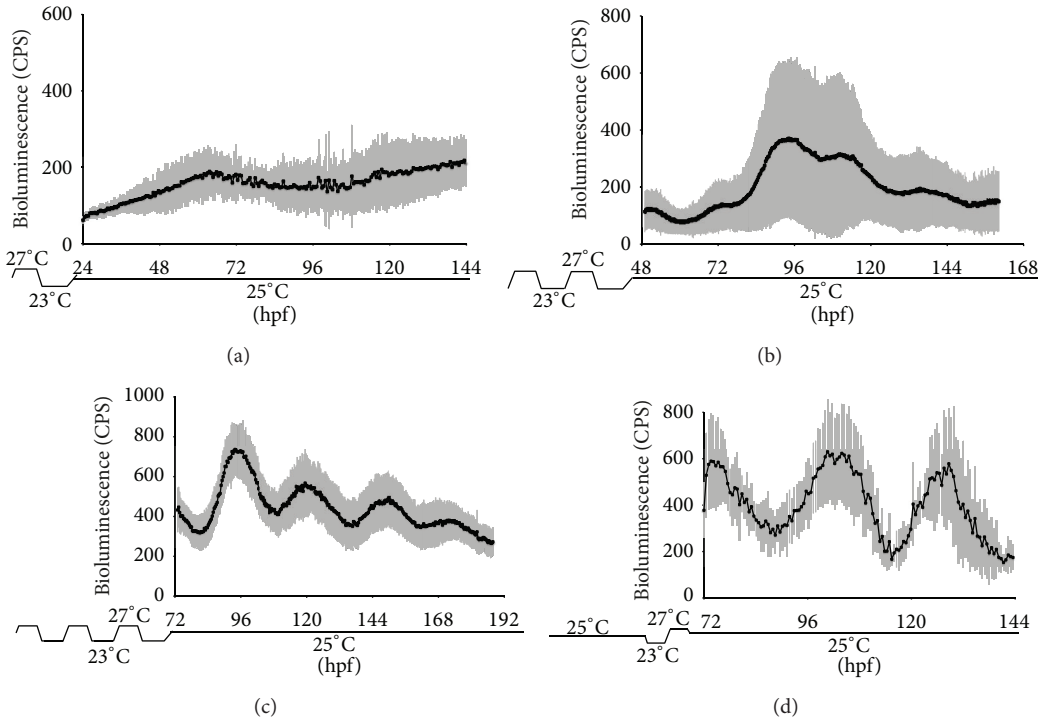

Figure 3: Clock entrainment by temperature cycles is dependent on the developmental stage. ((a)–(c)) Mean values of bioluminescence profiles of transgenic embryos raised under 4°C temperature cycles (23–27°C) for (a) 1 day (0–24 hpf), (b) 2 days (24–48 hpf), or (c) 3 days (48–72 hpf) and then monitored for 5 days at a constant 25°C. (d) Mean values of bioluminescence profiles of transgenic embryos raised at a constant 25°C for the first two days of development (0–48 hpf) and then subjected to a single 4°C temperature cycle (23–27°C) during the third day (48–72 hpf) before monitoring for three days at 25°C. In each panel, standard deviation of bioluminescence measurements between animals is plotted as grey vertical lines above each point. Each panel shows the mean values of 96 larvae (1 × 96 multiwell plate).

embryos immediately after fertilization in constant darkness at 29°C until different defined stages during early development. We then subjected them to a single temperature shift to 23.5°C for 4 hours before immediately sacrificing them for RNA extraction and assay of *zfper1b* mRNA levels (Figure 4). The *zfper1b* transcript is clearly maternally inherited, being detected before the onset of zygotic transcription. Subsequently, during the initial stages of development starting from the early cell stage to shield stage, the expression levels of *zfper1b* slowly decreased and did not show any significant response to the temperature shift (Figure 4(c)). Starting from the 5–9 somites stage the expression levels of *zfper1b* started to increase significantly (blue trace and one-way ANOVA $P < 0.001$) following the temperature shift when compared to control embryos maintained for the entire experiment at 29°C (black trace). These results indicate that following the 5–9 somites stage of development, the expression of key core clock elements becomes responsive to temperature changes.

4. Discussion

The zebrafish represents a valuable vertebrate model for studying the origins and regulation of circadian clock function during embryonic development. Such studies are technically more difficult to perform and interpret in placental mammals such as the mouse. Furthermore, the use of bioluminescent clock reporters has been extensively employed for noninvasive analysis of the clock in a broad range of model species. The use of such an *in vivo* luciferase assay to monitor gene expression has allowed us to measure circadian clock gene expression in individual embryos and larvae. One of the surprising results has been the considerable interindividual variability in rhythm amplitude, basal expression levels, and also the general expression profile. For these reasons, we have expressed results as the mean of individual traces from between 62 and 79 individuals. This variability from embryo to embryo might reflect real differences at the level of gene expression regulation and signal transduction—which are not reflected by differences at the morphological level. It is tempting to speculate that such differences, if maintained during development, might ultimately confer different circadian clock properties on individual fish.

Our results have revealed several properties of the developing circadian clock mechanism. Firstly, in the absence of entraining signals such as light or temperature cycles, most larvae show a normal morphological development and fail to establish overt circadian rhythms. Thus our results agree with previous studies addressing this issue [18, 20–23] and disagree with one early report claiming maternal inheritance of the circadian clock [35]. However, our results have shown

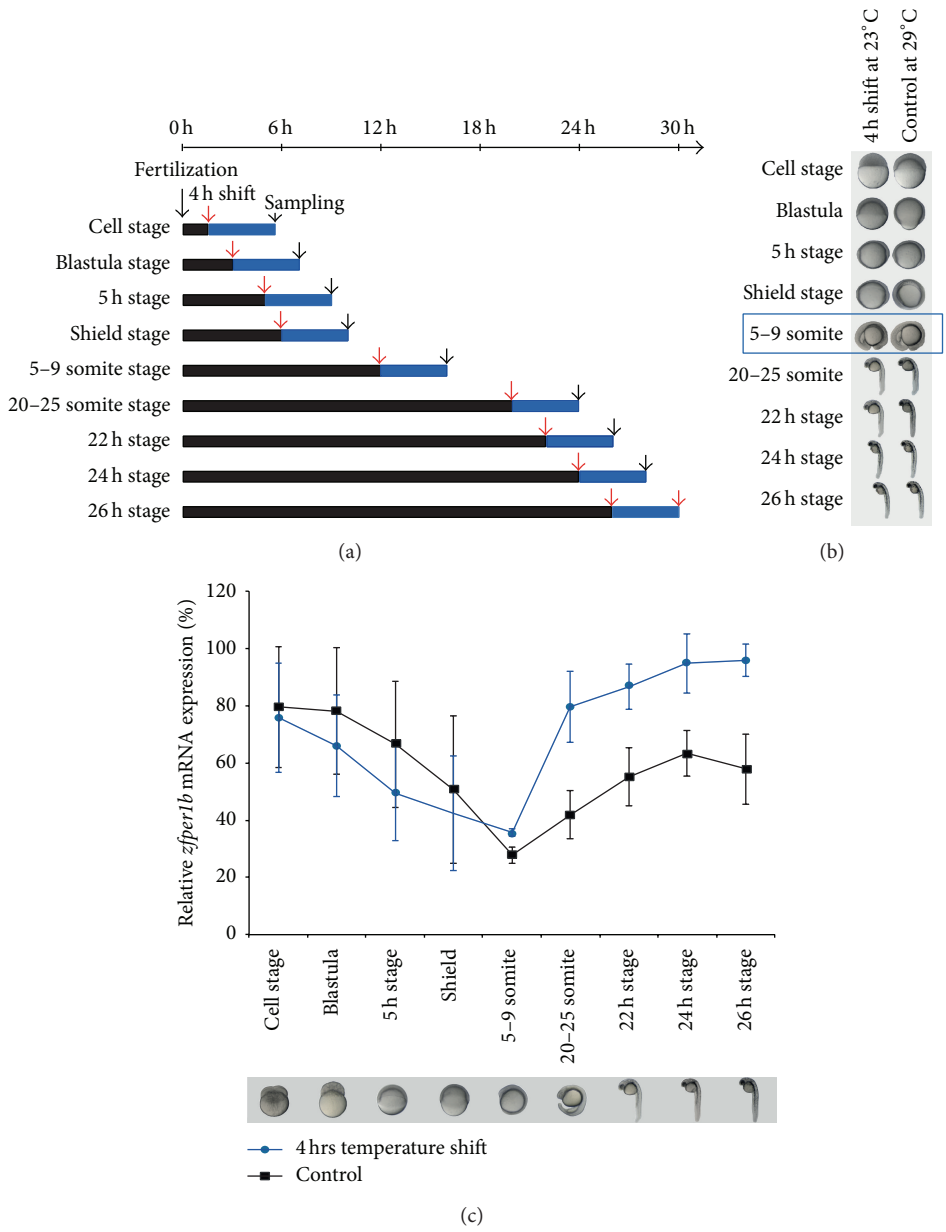

FIGURE 4: Acute temperature shift regulates *zfper1b* expression during early development. (a) Schematic representation of the experimental design. After fertilization, embryos were raised under a constant 29°C and at different developmental stages were acutely shifted for 4 h to 23.5°C (red arrows) (circa 20 embryos for each experimental group). Then mRNA from temperature shifted groups and a control group maintained at a constant 29°C were isolated (black arrows). (b) Images of embryos raised at 29°C (control) or 4 hrs after a temperature shift applied at different developmental stages. The developmental stage where the temperature shift induced *zfper1b* expression is indicated by a blue box. (c) Expression level of *zfper1b* measured in the different groups of embryos by qRT-PCR (control in black and temperature shift groups in blue).

that *zfper1b* gene expression is not constant during the development of larvae under constant conditions. The *zfper1b* expression level gradually increases from fertilization until a first peak at 2 dpf and then subsequently a second peak at circa 4-5 dpf (25°C) corresponding to the hatching time. It is tempting to speculate that these changes in expression reflect key developmental events.

Exposure to temperature cycles during the first 2 days of development fails to establish a circadian rhythm. This contrasts with the situation in zebrafish Pac-2 cells, where a single temperature cycle is sufficient to establish robust rhythms of clock gene expression [17]. One could speculate that the lack of response of the embryonic clock to 2 cycles of entrainment might reflect incompatibility with the high levels of cell proliferation or low levels of cell differentiation that characterizes this developmental period. The finding that the phase of the circadian clock is faithfully inherited when daughter cells divide and that cell cycle progression

does not appear to interfere with the clock [36] would tend to argue against high levels of cell proliferation being responsible for the lack of entrainment during the first 2 days. However these reports have been made with cultured differentiated cells. It therefore remains to be tested whether the same applies for embryonic cells *in vivo*. Alternatively, expression of certain clock components or key elements of temperature sensing signal transduction pathways may not yet have matured prior to the second day of development. When larvae are raised under constant conditions, the third day of development immediately follows the first peak of period gene expression, again suggesting that this may reflect a landmark in the establishment of the clock at the whole animal level. Interestingly, a single temperature shift delivered during the first 12 hours of development was previously reported to elicit circadian rhythms of endogenous *zfper1* mRNA expression [23]. Differences between this report and our findings may result from the fact that our transgenic assay specifically reports changes in transcription while assays of endogenous mRNA levels may also reflect regulated mRNA stability. Thus, potentially temperature shifts may regulate gene expression at multiple levels.

Interestingly, previous studies have reported that single light/dark transitions as early as 24 hpf are sufficient to initiate circadian clock rhythmicity in the pineal gland [22]. However, our results that are based on clock gene expression at the whole animal level suggest a much later maturation of temperature cycle entrainment. This may reflect a real difference in the developmental appearance of clock entrainment by these two zeitgebers. Alternatively, there may be tissue specific differences in the maturation of circadian clock entrainment mechanisms. Our results differ from the previously published data for the *per3*-luc transgenic line [18], where fish exhibited circadian rhythms of bioluminescence only when subjected to more than 4xLD cycles. This may indicate that expression of the *zfper3* and *zfper1b* genes differs during development. In this regard, there is already evidence that the spatiotemporal expression pattern of *zfper2* and *zfper3* differs [37], suggesting differential roles for clock gene family members during the development of various tissues. This may point to cell type-specific roles for the clock or alternatively noncircadian clock functions for certain clock genes.

Our laboratory has previously demonstrated that the circadian clock regulates the timing of S-phase of the cell cycle [30, 32]. Here we have demonstrated that S-phase rhythms are also observed in larvae that have been exposed to a temperature cycle and then transferred to constant temperature. An apparent phase difference between the LD and temperature cycle-entrained cell cycle rhythms may reflect differences in the timing of how light/dark and high-low temperature transitions affect the core clock and, in turn, the cell cycle control machinery. Temperature cycle entrainment of cell cycle rhythms reinforces the idea that these are not purely light-driven but represent a circadian clock output. The cell cycle in most vertebrate species is not a temperature compensated process and so the temperature itself can influence its rate of progress. Given that the clock represents a temperature compensated mechanism, the coupling of temperatures cycles, clock entrainment, and the timing of the cell cycle may represent a mechanism to constrain the rate of cell proliferation under different environmental temperature conditions and thereby control the rate of development. Indeed, recent studies have revealed a strong impact of exposure to temperature as well as light cycles on the timing of hatching as well as the subsequent larval performance in zebrafish [38, 39].

Our results have revealed that circadian rhythms of *zfaanat2* expression, in the photoreceptive pineal gland, can also mature during development in the complete absence of light, upon exposure to temperature cycles. We have also revealed that temperature cycles result in the establishment of rhythmic *zfirbp* expression in larvae. The function of IRBP seems to be linked with the visual cycle trafficking of 11-*cis* retinal and all-*trans* retinol between the photoreceptors and the retinal epithelium. The *irbp* gene is expressed early during rodent retinal development and is upregulated before the expression of opsins [40]. The temporal and spatial expression patterns of the *zfirbp* gene in zebrafish are consistent with a role in retinal development and suggest coordination of retinal pigment epithelium and photoreceptor differentiation [41]. There has been so far no evidence that temperature can play a role in the regulation of expression of this gene.

5. Conclusions

Together, our results document a developmental maturation of the clock's response to temperature and set the stage for future work aimed at exploring how much the mechanisms of entrainment via temperature cycles and LD cycles are comparable.

Conflict of Interests

The authors declare that there is no conflict of interests regarding the publication of this paper.

Authors' Contribution

Kajori Lahiri and Nadine Froehlich contributed equally to this work.

Acknowledgments

This research was funded by the Karlsruhe Institute of Technology (KIT, Germany) through the Helmholtz funding programme: BioInterfaces; the European Union (ZF-HEALTH Project GA no.: 242048-2); and by the Max Planck Society (Germany) and the CNRS (France). We acknowledge support by the Deutsche Forschungsgemeinschaft and the open access publishing fund of Karlsruhe Institute of Technology. The authors thank Mareike Rastetter, Thomas Baumgärtner, Nadeshda Wolf, Natalja Kusminski, and Nadine Eschen for excellent technical assistance. The authors are grateful to Cristina Santoriello, Srinivas Babu Gondi, Cristina Pagano, Felix Loosli, and Ines Cuesta for help, support, and constructive discussions. The authors also thank Philippe Beaufils,

Sophie Chabanis-Davidson, and the practical students from the European School Karlsruhe for technical help.

References

[1] C. S. Pittendrigh, "Circadian rhythms and the circadian organization of living systems," *Cold Spring Harbor Symposia on Quantitative Biology*, vol. 25, pp. 159–184, 1960.

[2] C. S. Pittendrigh, "Temporal organization: reflections of a Darwinian clock-watcher," *Annual Review of Physiology*, vol. 55, pp. 16–54, 1993.

[3] K. Wager-Smith and S. A. Kay, "Circadian rhythm genetics: from flies to mice to humans," *Nature Genetics*, vol. 26, no. 1, pp. 23–27, 2000.

[4] B. M. Sweeney and J. W. Hastings, "Effects of temperature upon diurnal rhythms," *Cold Spring Harbor Symposia on Quantitative Biology*, vol. 25, pp. 87–104, 1960.

[5] C. S. Pittendrigh, "On temperature independence in the clock system controlling emergence time in drosophila," *The Proceedings of the National Academy of Sciences of the United States*, vol. 40, pp. 1018–1029, 1954.

[6] Y. Liu, N. Y. Garceau, J. J. Loros, and J. C. Dunlap, "Thermally regulated translational control of FRQ mediates aspects of temperature responses in the Neurospora circadian clock," *Cell*, vol. 89, no. 3, pp. 477–486, 1997.

[7] S. Martino-Catt and D. R. Ort, "Low temperature interrupts circadian regulation of transcriptional activity in chilling-sensitive plants," *Proceedings of the National Academy of Sciences of the United States of America*, vol. 89, no. 9, pp. 3731–3735, 1992.

[8] W. F. Zimmerman, C. S. Pittendrigh, and T. Pavlidis, "Temperature compensation of the circadian oscillation in Drosophila pseudoobscura and its entrainment by temperature cycles," *Journal of Insect Physiology*, vol. 14, no. 5, pp. 669–684, 1968.

[9] H. Underwood and M. Calaban, "Pineal melatonin rhythms in the lizard Anolis carolinensis: I. Response to light and temperature cycles," *Journal of Biological Rhythms*, vol. 2, no. 3, pp. 179–193, 1987.

[10] C. D. Francis and M. L. Sargent, "Effects of temperature perturbations on circadian conidiation in neurospora," *Plant Physiology*, vol. 64, pp. 1000–1004, 1979.

[11] Y. Liu, M. Merrow, J. J. Loros, and J. C. Dunlap, "How temperature changes reset a circadian oscillator," *Science*, vol. 281, no. 5378, pp. 825–829, 1998.

[12] J. Falcon, V. Bolliet, J. P. Ravault, D. Chesneau, M. A. Ali, and J. P. Collin, "Rhythmic secretion of melatonin by the superfused pike pineal organ: thermo- and photoperiod interaction," *Neuroendocrinology*, vol. 60, no. 5, pp. 535–543, 1994.

[13] A. Zachmann, S. C. M. Knijff, V. Bolliet, and M. A. Ali, "Effects of temperature cycles and photoperiod on rhythmic melatonin secretion from the pineal organ of a teleost (Catostomus commersoni) in vitro," *Neuroendocrinology Letters*, vol. 13, no. 5, pp. 325–330, 1991.

[14] S. A. Brown, G. Zumbrunn, F. Fleury-Olela, N. Preitner, and U. Schibler, "Rhythms of mammalian body temperature can sustain peripheral circadian clocks," *Current Biology*, vol. 12, no. 18, pp. 1574–1583, 2002.

[15] E. D. Buhr, S.-H. Yoo, and J. S. Takahashi, "Temperature as a universal resetting cue for mammalian circadian oscillators," *Science*, vol. 330, no. 6002, pp. 379–385, 2010.

[16] J. Morf and U. Schibler, "Body temperature cycles: gatekeepers of circadian clocks," *Cell Cycle*, vol. 12, pp. 539–540, 2013.

[17] K. Lahiri, D. Vallone, S. B. Gondi, C. Santoriello, T. Dickmeis, and N. S. Foulkes, "Temperature regulates transcription in the Zebrafish circadian clock," *PLoS Biology*, vol. 3, no. 11, article e351, 2005.

[18] M. Kaneko and G. M. Cahill, "Light-dependent development of circadian gene expression in transgenic Zebrafish," *PLoS Biology*, vol. 3, no. 2, p. e34, 2005.

[19] J. Falcón, Y. Gothilf, S. L. Coon, G. Boeuf, and D. C. Klein, "Genetic, temporal and developmental differences between melatonin rhythm generating systems in the teleost fish pineal organ and retina," *Journal of Neuroendocrinology*, vol. 15, no. 4, pp. 378–382, 2003.

[20] Y. Gothilf, S. L. Coon, R. Toyama, A. Chitnis, M. A. A. Namboodiri, and D. C. Klein, "Zebrafish serotonin N-acetyltransferase-2: marker for development of pineal photoreceptors and circadian clock function," *Endocrinology*, vol. 140, no. 10, pp. 4895–4903, 1999.

[21] N. Kazimi and G. M. Cahill, "Development of a circadian melatonin rhythm in embryonic Zebrafish," *Developmental Brain Research*, vol. 117, no. 1, pp. 47–52, 1999.

[22] R. Vuilleumier, L. Besseau, G. Boeuf et al., "Starting the Zebrafish pineal circadian clock with a single photic transition," *Endocrinology*, vol. 147, no. 5, pp. 2273–2279, 2006.

[23] M. P. S. Dekens and D. Whitmore, "Autonomous onset of the circadian clock in the Zebrafish embryo," *EMBO Journal*, vol. 27, no. 20, pp. 2757–2765, 2008.

[24] C. N. Dahm -VaR, Ed., *Editor Zebrafish Practical Approach*, Oxford Oxford University Press, 2002.

[25] P. Rouet, F. Smih, and M. Jasin, "Expression of a site-specific endonuclease stimulates homologous recombination in mammalian cells," *Proceedings of the National Academy of Sciences of the United States of America*, vol. 91, no. 13, pp. 6064–6068, 1994.

[26] D. Vallone, S. B. Gondi, D. Whitmore, and N. S. Foulkes, "E-box function in a period gene repressed by light," *Proceedings of the National Academy of Sciences of the United States of America*, vol. 101, no. 12, pp. 4106–4111, 2004.

[27] D. Vallone, C. Santoriello, S. B. Gondi, and N. S. Foulkes, "Basic protocols for Zebrafish cell lines: maintenance and transfection," *Methods in Molecular Biology*, vol. 362, pp. 429–441, 2007.

[28] T. Roenneberg and W. Taylor, "Automated recordings of bioluminescence with special reference to the analysis of circadian rhythms," *Methods in Enzymology*, vol. 305, pp. 104–119, 2000.

[29] D. Whitmore, N. S. Foulkes, U. Strähle, and P. Sassone-Corsi, "Zebrafish Clock rhythmic expression reveals independent peripheral circadian oscillators," *Nature Neuroscience*, vol. 1, no. 8, pp. 701–707, 1998.

[30] M. P. S. Dekens, C. Santoriello, D. Vallone, G. Grassi, D. Whitmore, and N. S. Foulkes, "Light regulates the cell cycle in Zebrafish," *Current Biology*, vol. 13, no. 23, pp. 2051–2057, 2003.

[31] T. Dickmeis, K. Lahiri, G. Nica et al., "Glucocorticoids play a key role in circadian cell cycle rhythms," *PLoS Biology*, vol. 5, no. 4, article e78, 2007.

[32] M. L. Idda, E. Kage, J. F. Lopez-Olmeda, P. Mracek, N. S. Foulkes, and D. Vallone, "Circadian timing of injury-induced cell proliferation in Zebrafish," *PLoS ONE*, vol. 7, no. 3, Article ID e34203, 2012.

[33] S. L. Coon, V. Bégay, D. Deurloo, J. Falcón, and D. C. Klein, "Two arylalkylamine N-acetyltransferase genes mediate melatonin synthesis in fish," *The Journal of Biological Chemistry*, vol. 274, no. 13, pp. 9076–9082, 1999.

[34] D. C. Klein, S. L. Coon, P. H. Roseboom et al., "The melatonin rhythm-generating enzyme: molecular regulation of serotonin n-acetyltransferase in the pineal gland," *Recent Progress in Hormone Research*, vol. 52, pp. 307–357, 1997.

[35] F. Delaunay, C. Thisse, O. Marchand, V. Laudet, and B. Thisse, "An inherited functional circadian clock in Zebrafish embryos," *Science*, vol. 289, no. 5477, pp. 297–300, 2000.

[36] E. Nagoshi, C. Saini, C. Bauer, T. Laroche, F. Naef, and U. Schibler, "Circadian gene expression in individual fibroblasts: cell-autonomous and self-sustained oscillators pass time to daughter cells," *Cell*, vol. 119, no. 5, pp. 693–705, 2004.

[37] F. Delaunay, C. Thisse, B. Thisse, and V. Laudet, "Differential regulation of period 2 and period 3 expression during development of the Zebrafish circadian clock," *Gene Expression Patterns*, vol. 3, no. 3, pp. 319–324, 2003.

[38] N. Villamizar, B. Blanco-Vives, C. Oliveira et al., "Circadian rhythms of embryonic development and hatching in fish: a comparative study of Zebrafish (diurnal), Senegalese sole (nocturnal), and Somalian cavefish (blind)," *Chronobiology International*, vol. 30, no. 7, pp. 889–900, 2013.

[39] N. Villamizar, L. Ribas, F. Piferrer, L. M. Vera, and F. J. Sanchez-Vazquez, "Impact of daily thermocycles on hatching rhythms, larval performance and sex differentiation of Zebrafish," *PLoS ONE*, vol. 7, Article ID e52153, 2012.

[40] G. I. Liou, M. Wang, and S. Matragoon, "Timing of interphotoreceptor retinoid-binding protein (IRBP) gene expression and hypomethylation in developing mouse retina," *Developmental Biology*, vol. 161, no. 2, pp. 345–356, 1994.

[41] D. L. Stenkamp, L. L. Cunningham, P. A. Raymond, and F. Gonzalez-Fernandez, "Novel expression pattern of interphotoreceptor retinoid-binding protein (IRBP) in the adult and developing Zebrafish retina and RPE," *Molecular Vision*, vol. 4, p. 26, 1998.

Hindawi Publishing Corporation
BioMed Research International
Volume 2014, Article ID 868567, 7 pages
http://dx.doi.org/10.1155/2014/868567

Research Article

Neuropeptide Y in the Adult and Fetal Human Pineal Gland

Morten Møller,[1] Pansiri Phansuwan-Pujito,[2] and Corin Badiu[3]

[1] *Department of Neuroscience and Pharmacology, Laboratory of Neuropsychiatry, University of Copenhagen, 2100 Copenhagen, Denmark*
[2] *Department of Anatomy, Faculty of Medicine, Srinakharinwirot University, Bangkok 10110, Thailand*
[3] *National Institute of Endocrinology, "C. Davila" University of Medicine and Pharmacy, 050474 Bucharest, Romania*

Correspondence should be addressed to Morten Møller; morm@sund.ku.dk

Received 16 December 2013; Accepted 10 February 2014; Published 17 March 2014

Academic Editor: Yoav Gothilf

Neuropeptide Y was isolated from the porcine brain in 1982 and shown to be colocalized with noradrenaline in sympathetic nerve terminals. The peptide has been demonstrated to be present in sympathetic nerve fibers innervating the pineal gland in many mammalian species. In this investigation, we show by use of immunohistochemistry that neuropeptide Y is present in nerve fibers of the adult human pineal gland. The fibers are classical neuropeptidergic fibers endowed with large *boutons en passage* and primarily located in a perifollicular position with some fibers entering the pineal parenchyma inside the follicle. The distance from the immunoreactive terminals to the pinealocytes indicates a modulatory function of neuropeptide Y for pineal physiology. Some of the immunoreactive fibers might originate from neurons located in the brain and be a part of the central innervation of the pineal gland. In a series of human fetuses, neuropeptide Y-containing nerve fibers was present and could be detected as early as in the pineal of four- to five-month-old fetuses. This early innervation of the human pineal is different from most rodents, where the innervation starts postnatally.

1. Introduction

The pineal gland of mammals is an endocrine gland secreting the hormone melatonin with a circadian rhythm exhibiting a zenith during the night time [1, 2]. The synthesis of melatonin is regulated by a dense network of sympathetic nerve fibers originating from perikarya located in the autonomic superior cervical ganglia [3, 4]. Most of these sympathetic nerve fibers do also costore neuropeptide Y (NPY).

NPY was originally isolated from the porcine hypothalamus [5] and later found to be colocalized with noradrenaline in most sympathetic fibers [6] including the nerve fibers innervating the rat pineal gland [6–10].

The sequence of the NPY gene encodes a pre-pro NPY, a precursor peptide of 97 amino acids, which is cleaved into the pro-NPY, a 69-aa peptide [11]. The pro-NPY molecule is post-translationally processed by a single cleavage to neuropeptide Y (NPY) and a C-terminal peptide of NPY (CPON). NPY is Cterminally amidated, and the amidation is essential for binding of NPY to its corresponding receptors [12].

A few of the NPYergic nerve fibers innervating especially the rostral part of the rat pineal gland do not originate from perikarya in the superior cervical ganglia [8, 9, 12, 13]. Thus, some NPY-containing nerve fibers remain in the gland after bilateral superior cervical ganglionectomy [12] and these fibers might originate from neurons located in the brain itself (pineal central innervations). Ultrastructural analysis using immunocytochemistry has shown NPY to be confined in the large dense core granules in the sympathetic nerve terminals [12].

The NPYergic innervation of the mammalian pineal has later been confirmed in numerous mammalian species, for example, cotton rat [14], Golden hamster [15], European hamster [16], guinea pig [17], gerbil [13], mink [18], chinchilla [19], tree shrew [20], brown bat [21], sheep [22, 23], cat [24], pig [25, 26], cow [27, 28], and monkey [29].

Release of noradrenaline in the pineal gland starts a biochemical cascade, which includes binding of the transmitter to beta-adrenergic receptors and initiation of the cAMP second messenger system, which has been thoroughly

described [30]. However, what happens after release of NPY in the pineal gland is still a matter of discussion.

Melatonin is also synthesized in and secreted from the human pineal gland [31] and removal of the sympathetic input to the gland inhibits the elevated night time excretion of the hormone [32]. There has been a single report on the presence of a few NPY-immunoreactive fibers in the human pineal gland [33]. We have in this investigation performed a detailed study of the presence of the NPYergic innervations in adult human pineal obtained at autopsy and included a series of human fetal pineal gland obtained by caesarian sections. We show the presence of dense NPYergic innervations in adult pineal gland. An NPYergic innervation is also present in human fetal pineals where the first immunoreactive nerve fibers were observed in the 4th fetal month.

2. Materials and Methods

2.1. Antisera and Peptides. The primary Rabbit antisera against NPY used in the present investigation (numbers 8182 and 337) have been characterized previously [34, 35]. Antisera against the C-terminal flanking peptide of NPY (CPON) were purchased from Cambridge Research Biochemical (Cheshire, UK).

Biotinylated swine antirabbit IgG was obtained from Dako, Glostrup, Copenhagen (number E353). The ABC-streptavidin-horseradish peroxidase complex was obtained from Vector, Burlingame, CA, USA. (Vectastain Elite ABC kit, number PK-6100)

2.2. Adult Human Pineal Gland. A series of human pineal glands of both sexes were obtained from hospital autopsies. The age varied from 6 to 82 years. The postmortem time before fixation varied from 12 to 36 hours.

The brains were removed and the epithalamic area was dissected from the brain and immersed in cold (4°C) 4% paraformaldehyde in 0.1 M phosphate buffer (pH 7.4) for 5 days. The tissue blocks were then infiltrated with a solution of 30% sucrose in phosphate buffered saline (PBS) for 3 days and 18 μm or 40 μm thick serial cryostat sections were cut into sagittal and coronal planes. The 40 μm thick sections were transferred to PBS at 4°C. The 18 μm thick sections were placed on gelatinized glass slides.

2.3. Human Fetal Brains. The material examined was obtained from legal abortions and consisted of pineal glands from human fetuses of both sexes. The gestational ages were from 2.5 months (9 weeks) to 6 months (24 weeks). The postmortem interval preceding fixations varied, but in most cases the brains were immersed in cold (4°C) 4% paraformaldehyde in 0.1 M phosphate buffer (pH 7.4) for less than 30 minutes after removal from the uterus. Two extensive sagittal cuts were made in each hemisphere to ensure good penetration of the fixative into the brain ventricular system. The brains were cryoprotected in 30% sucrose as described above, frozen in crushed CO_2, and cut into sagittal or coronal, 18 μm thick, cryostat sections.

2.4. Immunohistochemistry. The sections were processed for immunohistochemistry by the use of the streptavidin enzyme histochemical technique. The 40 μm thick sections were reacted as free floating sections and the 18 μm thick sections were reacted on the glass slides in a humid chamber. The sections were rinsed twice for 5 min in PBS and pretreated in 1% H_2O_2 in PBS for 10 min. They were then incubated for 20 min in a 4% swine serum solution in PBS containing 0.3% Triton X-100 and 1% bovine serum albumin. This was followed by incubation in the primary antiserum for 24 h at 4°C. The dilutions were as follows: NPY (antisera numbers 337 and 8182), 1 : 1,000; CPON, 1 : 2,000. The sections were then washed in PBS to which 0.25% bovine serum albumin and 0.1% Triton X-100 were added (PBS-BT) for 3 × 10 min followed by incubation with the biotinylated swine anti-rabbit IgG, diluted 1 : 400 in PBS-BT, for 60 min at room temperature. They were next washed for 3 × 10 min in KPBS-BT and finally incubated for 60 min at room temperature in an ABC-streptavidin-horseradish peroxidase complex 1 : 500 in PBS-BT. After washing in KPBS-BT for 10 min, in KPBS alone for 10 min, and in 50 mM Tris/HCl buffer (pH 7.6) for 10 min, the sections were reacted for peroxidase activity by incubation with a solution of 1.25 mg/L diaminobenzidine (DAB) in 0.05 M Tris/HCl-buffer (pH 7.6) and 0.003% H_2O_2 for 20 min. After washing for 2 × 5 min in distilled water, the sections were mounted on gelatinized glass slides, dried, dehydrated in a series of ethanols, and embedded in Depex. Some adjacent sections were counterstained in thionine after the DAB reaction.

Absorption controls were done by substituting the primary antisera with antisera preabsorbed for 48 hr with the specific antigen (100 μg/mL diluted antiserum) at 4°C.

3. Results

3.1. Adult Human Pineal Glands. The adult human pineal is located on the dorsal part of the brain stem at the mesodiencephalic border connected to the epithalamic area with a short broad stalk (Figure 1(a)). The gland varies in size and often develops calcifications in adult; it is about 12 mm height, 7 mm in width, and about 6 mm in anterior-posterior direction. The third ventricle makes an evagination; the pineal recess into the stalk and separates the rostral habenular area from the posterior commissure caudal to the gland.

The pineal parenchyma, consisting of pinealocytes, interstitial cells, phagocytes, and capillaries, is arranged into large folliculi separated by septae of connective tissue and blood vessels.

Numerous NPY-immunoreactive nerve fibers endowed with large *boutons en passage* were present in a perifollicular position (Figures 2(a) and 2(b)). Some of the immunoreactive nerve fibers penetrated into the follicle itself, but a dense innervation of the follicle itself was not present.

Several immunoreactive nerve fibers were present in the pineal stalk and some of these immunoreactive nerve fibers entered the rostral part of the pineal gland.

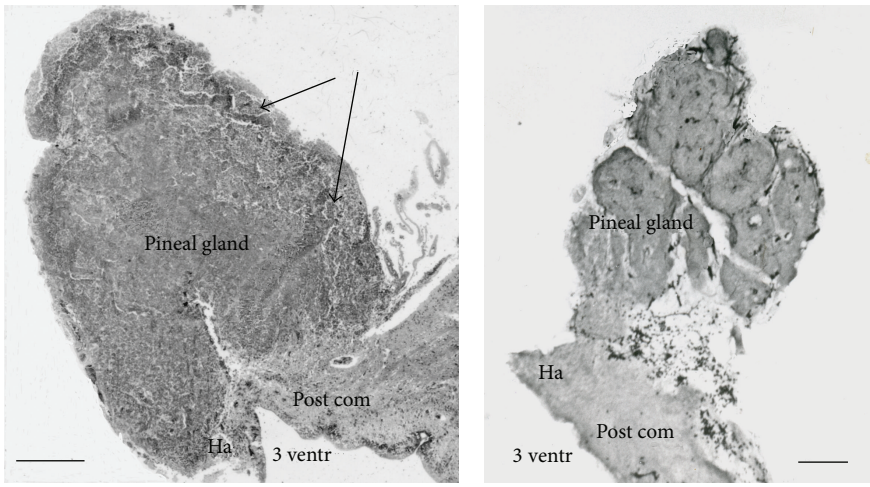

(a) (b)

Figure 1: (a) Sagittal section of a human pineal gland of a young adult obtained at autopsy. The pineal recess is seen below the gland and some pial tissue is located caudal to the gland. Note the follicular appearance of the pineal parenchyma (arrows). Bar = 1 mm. (b) Sagittal section of a 7-month-old human fetus. Note the follicular appearance of the parenchyma. Bar = 250 μm. Ha: habenula, Post com: posterior commissure, and 3 ventr: third ventricle.

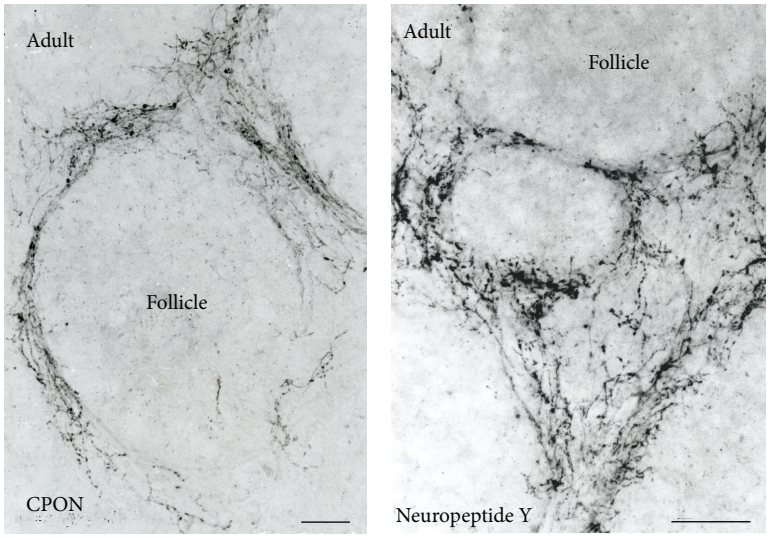

(a) (b)

Figure 2: (a) and (b) Photomicrographs of parts of the adult human pineal gland obtained at autopsy, which have been immunoreacted for CPON (a) and NPY (b). Note in both pineals the perifollicular location of NPY-immunoreactive nerve fibres with large *boutons en passage*. Several of the nerve fibres penetrate into the follicle. Bars = 250 μm ((a) and (b)).

3.2. Fetal Pineal Glands. The human fetal pineal gland develops in the second month of gestation as an evagination of the ependyma covering the third ventricle at the diencephalic-mesencephalic border [36, 37]. The cell proliferation of the ependymal cells gives rise toto an anterior- and posterior "anlage" (lobe) which later are merging. In the third gestational month, the pineal is macroscopically visible (Figure 3). The follicular appearance of the pineal parenchyma is clearly visible (Figure 1(b)).

The NPYergic innervation of the fetal pineal with gestational ages of 6 to 7 months was quite dense (Figure 4(a)). The number of NPYergic immunoreactive nerve fibers declined in the 5-month-old fetuses (Figure 4(b)), and in the 4th gestational month only few and thin immunoreactive fibers were observed. In our series, we did not stain immunoreactive nerve fibers in fetuses younger than 4th gestational month.

There was a clear relationship between the postmortem time of the tissue before fixation and the immunoreactivity

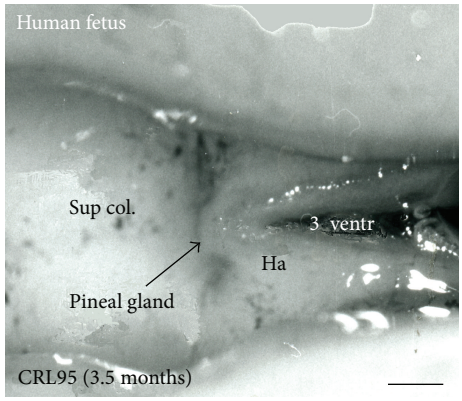

Figure 3: Superior (dorsal) view of the diencephalic-mesencephalic area of a 3.5-month-old human fetus. The third ventricle (3 ventr) without pial covering is seen to the right in the micrograph. The small pineal gland is a small protuberance (arrow) and merging via the broad stalk with the habenula (Ha). Sup col.: superior colliculus. Bar = 2 mm.

of the nerve fibers in the tissue sections. The morphological best fibers were obtained in the pineals which were fixed with the shortest time delay.

4. Discussion

We show in this paper dense NPYergic innervations of both the adult and fetal human pineal glands with classical neuropeptidergic nerve fibers endowed with large *boutons en passage*. The prominent perifollicular distribution of the nerve fibers in the human is different from the distribution seen in several other rodent and nonrodent species, where many of the NPYergic nerve fibers penetrate into the pineal parenchyma between the pinealocytes. Due to the delay caused by the diffusion distance from the perifollicular terminals to the pinealocytes, this might indicate a modulatory function for NPY in human pineal biochemistry. The majority of the NPYergic nerve fibers are probably originating from sympathetic nerve fibers in the superior cervical ganglion. However, the evidence of a sympathetic innervation of the human pineal gland is indirect because a superior cervical ganglionectomy in humans has never been performed. However, in tetraplegic patients, with total transverse lesions of the cervical spinal cord, the night time elevation of plasma melatonin is abolished [38–41]. This indicates that intact nerve fibers in the cervical parts of the spinal cord are a prerequisite for the presence of a circadian rhythm of melatonin secretion. Further, transection of the sympathetic trunk at the level of the second thoracic ganglion in patients to prevent hyperhidrosis abolishes the night time elevation of melatonin secretion in the majority of these patients [32].

The current study also showed many NPYergic nerve fibers in pineal stalk of both the adult and fetal pineals and might indicate the presence of NPYergic nerve fibers innervating of the human pineal from the brain via the pineal stalk. Such a central pineal innervation in mammals has been a matter of controversy. Early studies in humans described the presence of silver stained nerve fibers penetrating into the pineal gland via the stalk from the habenular and posterior commissures [42]. However, in later studies of the rat it was suggested that these fibers looped in the rostral part of the pineal and returned to the brain without making functional contacts [43]. Contrarily, lesions of the habenular area in the rat resulted in anterograde degenerating nerve fibers in the pineal gland [44]. Later, retro- and anterograde *in vivo* tracings of fibers innervating the pineal gland showed the origin of these central fibers to be located in the paraventricular nucleus [45] as well as in neurons located in the lateral geniculate body of the thalamus [46, 47]. In rodents, the intergeniculate leaflet of the lateral geniculate body contains NPYergic neurons, which projects to the SCN and is responsible for a nonphotic regulation of the endogenous clock [48]. It is possible that some NPYergic neurons in the intergeniculate leaflet also project to the pineal gland.

A parasympathetic innervation of the pineal gland is also present [49, 50]. NPY also been found to be colocalized with acetylcholine in parasympathetic ganglia known to project to the pineal gland [51]. Therefore, the parasympathetic system might contribute to the pineal NPYergic innervation.

The physiological function of NPY in the pineal gland is not clear. There is no direct stimulatory effect of NPY on the secretion of melatonin in cultures, but NPY has an indirect effect by inhibiting the stimulatory effect of noradrenaline on melatonin release [52, 53]. The effect of NPY on the noradrenergic transmission is probably transmitted via inhibitory G-proteins in the membrane reducing the activity of adenylate cyclase in the target cells [54, 55]. The cells possessing receptors for NPY in the pineal gland have not been determined, but specific binding sites have been demonstrated in suspensions of cultured pineal cells [52], indicating that postsynaptic receptors are present in the pineal gland. Further evidence has shown that the NPY binding site is of the Y1 subtype [53], which is supported by reverse-transcriptase polymerase chain reaction studies, showing that only Y1 mRNA, and not any of the other subtypes (Y2, Y4, or Y5) was expressed [56].

The detection of weakly stained NPYergic fibers in four-month-old fetal pineal is in accord with studies on NPY in other regions of the brain, demonstrating that NPY can be detected around the 4th fetal month and that the number of NPYergic neurons increases with fetal age [57]. In a study of human fetal spinal cords NPY-immunoreactive neurons were found in the dorsal horn as early as 10 weeks of fetal age [58].

From the physiological point of view there are indications in the European hamster *(Cricetus cricetus)* that NPY might control annual rhythms. Thus, the number of NPYergic intrapineal nerve fibers exhibits an annual rhythm with a zenith in midwinter [16]. At midwinter 5-methoxytryptophol starts to exhibit a nycthemeral rhythm and the activity of hydroxyindole-O-methyltransferase (HIOMT), a key enzyme in the synthesis of melatonin, is significantly increased [59]. In the rat, NPY stimulates HIOMT activity [60]. If NPY also stimulates HIOMT in the European hamster, NPY might be directly involved in the annual regulation of the pineal gland in this species.

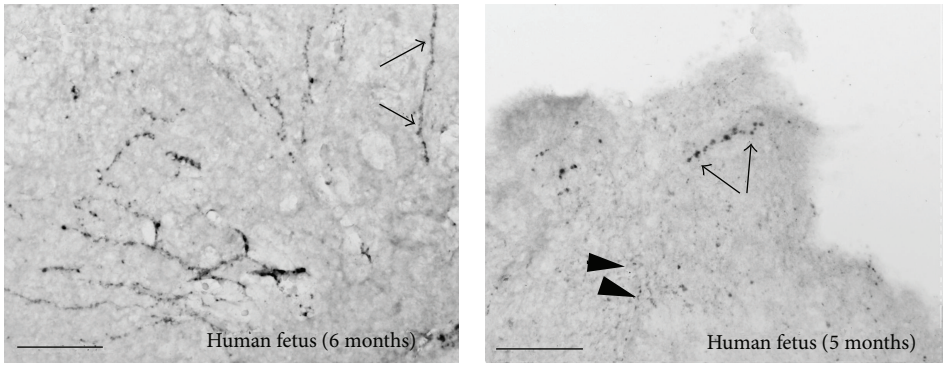

(a) (b)

Figure 4: Photomicrographs of parts of human fetal pineal glands reacted immunohistochemically for neuropeptide Y. (a) Pineal gland from 6-month-old fetus. Arrows mark a long NPY-immunoreactive nerve fiber with large *boutons en passage*. (b) Pineal gland from 5-month-old fetus. Arrows mark an immunoreactive nerve fiber with large *boutons en passage*. Arrow heads point toward smaller immunoreactive boutons. Bar = 200 μm.

In summary, this paper shows the presence of dense innervations of the human pineal gland with classical neuropeptidergic NPY-immunoreactive nerve fibers. The NPY-ergic innervation of the human pineal gland starts in fetal life at about the 4th month of gestation.

Conflict of Interests

The authors declare that there is no conflict of interests regarding the publication of this paper.

Acknowledgments

This study was supported by the Lundbeck Foundation and the Novo Nordisk Foundation to Morten Møller and the Research fund of Srinakharinwirot University to P. Phansuwan-Pujito.

References

[1] R. J. Reiter, "Pineal melatonin: cell biology of its synthesis and of its physiological interactions," *Endocrine Reviews*, vol. 12, no. 2, pp. 151–180, 1991.

[2] J. H. Stehle, C. von Gall, and H.-W. Korf, "Melatonin: a clock-output, a clock-input," *Journal of Neuroendocrinology*, vol. 15, no. 4, pp. 383–389, 2003.

[3] R. Y. Moore and D. C. Klein, "Visual pathways and the central neural control of a circadian rhythm in pineal serotonin N acetyltransferase activity," *Brain Research*, vol. 71, no. 1, pp. 17–33, 1974.

[4] M. Møller and F. M. Baeres, "The anatomy and innervation of the mammalian pineal gland," *Cell and Tissue Research*, vol. 309, no. 1, pp. 139–150, 2002.

[5] K. Tatemoto, M. Carlquist, and V. Mutt, "Neuropeptide Y-a novel brain peptide with structural similarities to peptide YY and pancreatic polypeptide," *Nature*, vol. 296, no. 5858, pp. 659–660, 1982.

[6] F. Schon, J. M. Allen, and J. C. Yeats, "Neuropeptide Y innervation of the rodent pineal gland and cerebral blood vessels," *Neuroscience Letters*, vol. 57, no. 1, pp. 65–71, 1985.

[7] J. M. Lundberg, L. Terenius, and T. Hokfelt, "Neuropeptide Y (NPY)-like immunoreactivity in peripheral noradrenergic neurons and effects of NPY on sympathetic function," *Acta Physiologica Scandinavica*, vol. 116, no. 4, pp. 477–480, 1982.

[8] S. Reuss and R. Y. Moore, "Neuropeptide Y-containing neurons in the rat superior cervical ganglion: projections to the pineal gland," *Journal of Pineal Research*, vol. 6, no. 4, pp. 307–316, 1989.

[9] R. E. Zigmond and Y. Sun, "Regulation of neuropeptide expression in sympathetic neurons. Paracrine and retrograde influences," *Annals of the New York Academy of Sciences*, vol. 814, pp. 181–197, 1997.

[10] E. Zhang, J. D. Mikkelsen, and M. Møller, "Tyrosine hydroxylase- and neuropeptide Y-immunoreactive nerve fibers in the pineal complex of untreated rats and rats following removal of the superior cercical ganglia," *Cell and Tissue Research*, vol. 265, no. 1, pp. 63–71, 1991.

[11] J. D. Mikkelsen and M. M. T. O'Hare, "An immunohistochemical and chromatographic analysis of the distribution and processing of proneuropeptide Y in the rat suprachiasmatic nucleus," *Peptides*, vol. 12, no. 1, pp. 177–185, 1991.

[12] J. D. Mikkelsen and M. Møller, "Neuropeptide Y in the mammalian pineal gland," *Microscopy Research and Technique*, vol. 46, no. 4-5, pp. 239–256, 1999.

[13] Y. Shiotani, M. Yamano, and S. Shiosaka, "Distribution and origins of substance P (SP)-, calcitonin gene-related peptide (CGRP)-, vasoactive intestinal polypeptide (VIP)- and neuropeptide Y (NPY)-containing nerve fibers in the pineal gland of gerbils," *Neuroscience Letters*, vol. 70, no. 2, pp. 187–192, 1986.

[14] S. Matsushima, Y. Sakai, Y. Hira, Y. Oomori, and S. Daikoku, "Immunohistochemical studies on sympathetic and non-sympathetic nerve fibers and neuronal cell bodies in the pineal gland of cotton rats, Sigmodon hispidus," *Archives of Histology and Cytology*, vol. 57, no. 1, pp. 47–58, 1994.

[15] H. Schröder, "Neuropeptide Y (NPY)-like immunoreactivity in peripheral and central nerve fibres of the golden hamster (Mesocricetus auratus) with special respect to pineal gland innervation," *Histochemistry*, vol. 85, no. 4, pp. 321–325, 1986.

[16] M. Møller, M. Masson-Pévet, and P. Pévet, "Annual variations of the NPYergic innervation of the pineal gland in the European

hamster (Cricetus cricetus): a quantitative immunohistochemical study," *Cell and Tissue Research*, vol. 291, no. 3, pp. 423–431, 1998.

[17] H. Schroder and L. Vollrath, "Neuropeptide Y (NPY)-like immunoreactivity in the guinea pig pineal organ," *Neuroscience Letters*, vol. 63, no. 3, pp. 285–289, 1986.

[18] M. Møller, J. D. Mikkelsen, and L. Martinet, "Innervation of the mink pineal gland with neuropeptide Y (NPY)-containing nerve fibers. An experimental immunohistochemical study," *Cell and Tissue Research*, vol. 261, no. 3, pp. 477–483, 1990.

[19] M. Nowicki, J. Wojtkiewicz, B. Seremak et al., "Specific distribution pattern of nerve fibers containing catecholamine-synthesizing enzymes, neropeptide Y (NPY) and C-terminal flanking peptide of NPY (CPON) in the pineal gland of the chinchilla (Chinchilla laniger)—an immunohistochemical study," *Folia Histochemica et Cytobiologica*, vol. 41, no. 4, pp. 193–200, 2003.

[20] M. Kado, A. Yoshida, Y. Hira, Y. Sakai, and S. Matsushima, "Light and electron microscopic immunocytochemical study on the innervation of the pineal gland of the tree shrew (Tupaia glis), with special reference to peptidergic synaptic junctions with pinealocytes," *Brain Research*, vol. 842, no. 2, pp. 359–375, 1999.

[21] L. K. Laemle and J. R. Cotter, "Neuropeptide Y-like immunoreactivity in the diencephalon of the little brown bat (Myotis lucifugus): localized variations with physiological state," *Journal of Comparative Neurology*, vol. 316, no. 4, pp. 447–458, 1992.

[22] L. M. Williams, P. J. Morgan, G. Pelletier, G. I. Riddoch, W. Lawson, and G. R. Davidson, "Neuropeptide Y (NPY) innervation of the ovine pineal gland," *Journal of Pineal Research*, vol. 7, no. 4, pp. 345–353, 1989.

[23] B. Cozzi, J. D. Mikkelsen, J.-P. Ravault, and M. Møller, "Neuropeptide Y (NPY) and C-flanking peptide of NPY in the pineal gland of normal and ganglionectomized sheep," *Journal of Comparative Neurology*, vol. 316, no. 2, pp. 238–250, 1992.

[24] M. Møller, P. Phansuwan-Pujito, S. Pramaulkijja, N. Kotchabhakdi, and P. Govitrapong, "Innervation of the cat pineal gland by neuropeptide Y-immunoreactive nerve fibers: an experimental immunohistochemical study," *Cell and Tissue Research*, vol. 276, no. 3, pp. 545–550, 1994.

[25] B. Przybylska-Gornowicz, B. Lewczuk, and M. Møller, "Demonstration of nerve fibers containing the C-terminal flanking peptide of neuropeptide Y (CPON) in the pig pineal gland (Sus domesticus): an immunocytochemical study by light and electron microscopy," *Anatomical Record*, vol. 248, no. 4, pp. 576–782, 1997.

[26] M. Bulc, B. Lewczuk, M. Prusik, and J. Całka, "The foetal pig pineal gland is richly innervated by nerve fibres containing catecholamine-synthesizing enzymes, neuropeptide Y (NPY) and C-terminal flanking peptide of NPY, but it does not secrete melatonin," *Histolology Histopathology*, vol. 28, no. 5, pp. 633–646, 2013.

[27] P. Phansuwan-Pujito, S. Pramaulkijja, P. Govitrapong, and M. Møller, "An immunohistochemical study of neuropeptide Y in the bovine pineal gland," *Journal of Pineal Research*, vol. 15, no. 1, pp. 53–58, 1993.

[28] S. Regodón and V. Roncero, "Embryonic development of the bovine pineal gland (Bos taurus) during prenatal life (30 to 135 days of gestation)," *Histology and Histopathology*, vol. 20, no. 4, pp. 1093–1103, 2005.

[29] J. D. Mikkelsen and G. Mick, "Neuropeptide Y-immunoreactive nerve fibres in the pineal gland of the macaque (*Macaca fascicularis*)," *Journal of Neuroendocrinology*, vol. 4, no. 6, pp. 681–688, 1992.

[30] E. Maronde, M. Pfeffer, C. Von Gall et al., "Signal transduction in the rodent pineal organ: from the membrane to the nucleus," *Advances in Experimental Medicine and Biology*, vol. 460, pp. 109–131, 1999.

[31] K. Ackermann and J. H. Stehle, "Melatonin synthesis in the human pineal gland: advantages, implications, and difficulties," *Chronobiology International*, vol. 23, no. 1-2, pp. 369–379, 2006.

[32] M. Møller, O. Osgaard, and M. Grønbech-Jensen, "Influence of sympathectomy in humans on the rhythmicity of 6-sulphatoxymelatonin urinary excretion," *Molecular and Cellular Endocrinology*, vol. 252, no. 1-2, pp. 40–45, 2006.

[33] R. Y. Moore and P. Sibony, "Enkephalin-like immunoreactivity in neurons in the human pineal gland," *Brain Research*, vol. 457, no. 2, pp. 395–398, 1988.

[34] J. D. Mikkelsen, P. J. Larsen, C. Kruse-Larsen, M. M. T. O'Hare, and T. W. Schwartz, "Immunohistochemical and chromatographic identification of peptides derived from proneuropeptide Y in the human frontal cortex," *Brain Research Bulletin*, vol. 31, no. 3-4, pp. 415–425, 1993.

[35] J. D. Mikkelsen and M. M. O'Hare, "An immunohistochemical and chromatographic analysis of the distribution and processing of proneuropeptide Y in the rat suprachiasmatic nucleus," *Peptides*, vol. 12, no. 1, pp. 177–185, 1991.

[36] R. O'Rahilly, "The development of the epiphysis cerebri and the subcommissural complex in staged human embryos," *Anatatomical Record*, vol. 160, pp. 488–489, 1968.

[37] M. Møller, "The ultrastructure of the human fetal pineal gland. I. Cell types and blood vessels," *Cell and Tissue Research*, vol. 152, no. 1, pp. 13–30, 1974.

[38] L. W. Kneisley, M. A. Moskowitz, and H. G. Lynch, "Cervical spinal cord lesions disrupt the rhythm in human melatonin excretion," *Journal of Neural Transmission*, vol. 252, supplement 13, pp. 311–323, 1978.

[39] Y. Li, D. H. Jiang, M. L. Wang, D. R. Jiao, and S. F. Pang, "Rhythms of serum melatonin in patients with spinal lesions at the cervical, thoracic or lumbar region," *Clinical Endocrinology*, vol. 30, no. 1, pp. 47–56, 1989.

[40] J. M. Zeitzer, N. T. Ayas, S. A. Shea, R. Brown, and C. A. Czeisler, "Absence of detectable melatonin and preservation of cortisol and thyrotropin rhythms in tetraplegia," *Journal of Clinical Endocrinology and Metabolism*, vol. 85, no. 6, pp. 2189–2196, 2000.

[41] J. M. Zeitzer, N. T. Ayas, A. D. Wu, C. A. Czeisler, and R. Brown, "Bilateral oculosympathetic paresis associated with loss of nocturnal melatonin secretion in patients with spinal cord injury," *Journal of Spinal Cord Medicine*, vol. 28, no. 1, pp. 55–59, 2005.

[42] K. Scharenberg and L. Liss, "The histologic structure of the human pineal body," *Progress in Brain Research C*, vol. 10, pp. 193–217, 1965.

[43] J. A. Kappers, "The development, topographical relations and innervation of the epiphysis cerebri in the albino rat," *Zeitschrift für Zellforschung und Mikroskopische Anatomie*, vol. 52, no. 2, pp. 163–215, 1960.

[44] O. K. Rønnekleiv and M. Møller, "Brain-pineal nervous connections in the rat: an ultrastructure study following habenular lesion," *Experimental Brain Research*, vol. 37, no. 3, pp. 551–562, 1979.

[45] H. W. Korf and U. Wagner, "Evidence for a nervous connection between the brain and the pineal organ in the guinea pig," *Cell and Tissue Research*, vol. 209, no. 3, pp. 505–510, 1980.

[46] M. Møller and H. W. Korf, "The origin of central pinealopetal nerve fibers in the mongolian gerbil as demonstrated by the retrograde transport of horseradish peroxidase," *Cell and Tissue Research*, vol. 230, no. 2, pp. 273–287, 1983.

[47] J. D. Mikkelson, B. Cozzi, and M. Møller, "Efferent projections from the lateral geniculate nucleus to the pineal complex of the Mongolian gerbil (Meriones unguiculatus)," *Cell and Tissue Research*, vol. 264, no. 1, pp. 95–102, 1991.

[48] D. Janik, J. D. Mikkelsen, and N. Mrosovsky, "Cellular colocalization of Fos and neuropeptide Y in the intergeniculate leaflet after nonphotic phase-shifting events," *Brain Research*, vol. 698, no. 1-2, pp. 137–145, 1995.

[49] G. C. Kenny, "The innervation of the mammaliam pineal body. (A comparative study)," *Proceedings of the Australian Association of Neurologists*, vol. 3, pp. 133–140, 1965.

[50] H. J. Romijn, "Structure and innervation of the pineal gland of the rabbit, Oryctolagus cuniculus (L.). III. An electron microscopic investigation of the innervation," *Cell and Tissue Research*, vol. 157, no. 1, pp. 25–51, 1975.

[51] G. G. Leblanc, B. A. Trimmer, and S. C. Landis, "Neuropeptide Y-like immunoreactivity in rat cranial parasympathetic neurons: coexistence with vasoactive intestinal peptide and choline acetyltransferase," *Proceedings of the National Academy of Sciences of the United States of America*, vol. 84, no. 10, pp. 3511–3515, 1987.

[52] J. Olcese, "Neuropeptide Y: an endogenous inhibitor of norepinephrine-stimulated melatonin secretion in the rat pineal gland," *Journal of Neurochemistry*, vol. 57, no. 3, pp. 943–947, 1991.

[53] V. Simonneaux, A. Ouichou, C. Craft, and P. Pévet, "Presynaptic and postsynaptic effects of neuropeptide Y in the rat pineal gland," *Journal of Neurochemistry*, vol. 62, no. 6, pp. 2464–2471, 1994.

[54] B. B. Fredholm, I. Jansen, and L. Edvinsson, "Neuropeptide Y is a potent inhibitor of cyclic AMP accumulation in feline cerebral blood vessels," *Acta Physiologica Scandinavica*, vol. 124, no. 3, pp. 467–469, 1985.

[55] S. Kassis, M. Olasmaa, L. Terenius, and P. H. Fishman, "Neuropeptide Y inhibits cardiac adenylate cyclase through a pertussis toxin-sensitive G protein," *Journal of Biological Chemistry*, vol. 262, no. 8, pp. 3429–3431, 1987.

[56] J. D. Mikkelsen, F. Hauser, and J. Olcese, "Neuropeptide Y (NPY) and NPY receptors in the rat pineal gland," *Advances in Experimental Medicine and Biology*, vol. 460, pp. 95–107, 1999.

[57] S. M. Wai, P. M. Kindler, E. T. K. Lam, A. Zhang, and D. T. Yew, "Distribution of neuropeptide Y-immunoreactive neurons in the human brainstem, cerebellum, and cortex during development," *Cellular and Molecular Neurobiology*, vol. 24, no. 5, pp. 667–684, 2004.

[58] W. Z. Shen, "Distribution of neuropeptide Y in the developing human spinal cord," *Neuroscience*, vol. 62, no. 1, pp. 251–256, 1994.

[59] C. Ribelayga, P. Pévet, and V. Simonneaux, "Possible involvement of neuropeptide Y in the seasonal control of hydroxyindole-O-methyltransferase activity in the pineal gland of the European hamster (Cricetus cricetus)," *Brain Research*, vol. 801, no. 1-2, pp. 137–142, 1998.

[60] C. Ribelayga, P. Pévet, and V. Simonneaux, "Adrenergic and peptidergic regulations of hydroxyindole-O-methyltransferase activity in rat pineal gland," *Brain Research*, vol. 777, no. 1-2, pp. 247–250, 1997.